BLOOD VESSEL GROWTH IN PRIMATE RETINAL DEVELOPMENT: RELATIONSHIP OF RETINAL MATURATION WITH CHORIOCAPILLARIS GROWTH AND A ROLE FOR TGF-ß IN THE RETINA

Marie Alexandra Allende

A thesis submitted in fulfilment of the requirements for the degree of
Doctor of Philosophy,
Department of Clinical Ophthalmology and Save Sight Institute,
University of Sydney
2008

DECLARATION

I hereby declare that this thesis is my own work, except where due acknowledgement is stated below and in the thesis text. To the best of my knowledge, this thesis contains no material previously published or written by another person, nor material which to a substantial extent has been accepted for the award of any other degree or diploma of a university or other institute of higher learning. All experiments described in this thesis were performed in the Save Sight Institute laboratories, University of Sydney, located at the Sydney Eye Hospital Campus, between 2002 and 2006. Real-time PCR was conducted in the Biological Sciences Department in the Australian National University, Canberra. Statistical analysis and interpretation of repeated measures including ANOVA was generously carried out by Dr Jan Provis at the Australian National University, Canberra.

Alexandra Allende

March, 2008

“When you employ the microscope, shake off all prejudice, nor harbour any favourite opinions: for if you do, ‘tis not unlikely fancy will betray you into error, and make you think you see what you would wish to see. Remember that truth alone is the matter you search after; and if you have been mistaken, let not vanity seduce you to persist in your mistake.”

From *The Microscope Made Easy* by Henry Baker (1742)

“Not what man knows but what man feels, concerns art. All else is science.”

(Bernard Berenson, 1897)

ACKNOWLEDGEMENTS

Many thanks to Michele whose relentless generosity, warm heartedness and willingness to help have meant that almost any obstacle could be surmounted, especially with a corny joke thrown in the mix and a few snacks. Despite the many demands by many people and a strong work ethic, amidst disputed claims of procrastination Michele always made time for you and encouraged a balanced lifestyle. Her passion for science and research amidst political and bureaucratic pressures is inspiring, professional and demonstrates what a treasure in academia she is. A cup of tea and some lollies have a tendency to fix almost everything.

A big thank you must go to Jan whose positive outlook, non-stressful attitude and long distance mentoring was greatly appreciated. She's a role model to all women by being practical, professional, intelligent, patient, funny, happy and fit. Also thanks to Riccardo whose enthusiasm and determination despite multiple experimental hitches helped enormously in the molecular biology section. His devotion to science sprinkled with conversational controversies was amusing and interesting. Thank you to Phillip for shedding light on the philosophy of a PhD and for initiating the journey by introducing the possibility of research at a time I was deciding about what to do next.

Lots of thanks to Richard for not getting upset with unexpected lab outcomes, providing advice on statistical analyses, being helpful with all lab issues and for smiling more often than not. Thanks to Sharon whose artistic merits, sensible approach and neat writing provided lofty benchmarks in our lab, to Yong Juan for her cuteness and English language interpretations that livened up every lab session, to Ken for his interesting stories, cultural enlightenment, kooky mishaps and obsessions and to Goff, Li, Marina and Martin for their moral support and chit chats.

Thanks to personnel at the Prince of Wales Hospital Department of Endocrinology for co-ordinating the donor program, particularly Georgia and all donors for making tissues available for research and to the staff at the Save Sight Institute and Eye Bank including Professor Bilson, Raj and

Meidong for providing laboratory facilities and tissue to conduct quality research.

Thank you to the NHMRC for a scholarship at a time when financial assistance was extremely helpful.

Thanks to Anna, Karen, Chris, Geraldine, Kamani, Rachel and Paul.

Above all a big thanks to mum, the ultimate patient human being, dad, who instigated an intellectual curiosity from early on, Gas, whom it's easy and enjoyable spending time with, and my late gran, greatly adaptable and stubborn with a lot of common sense, whom altogether have provided a stable supportive framework, welcomed distractions and a constant reminder of what is important in life.

ABSTRACT

Background: The development of the blood supply in the primate retina has been extensively studied; however the relationship of the differentiating retina to the choroidal blood supply is less well known. The interaction of astrocytes and vascular endothelial cells promotes the development of the retinal vasculature from 14 weeks' gestation (WG). Initially, astrocytes lead the developing capillaries from the optic nerve towards the macular area. However, neither astrocytes nor endothelial cells enter a prescribed avascular area, within which the fovea later forms. This may be attributed to expression of a factor that inhibits astrocyte and endothelial cell proliferation in the fovea. A factor found in the CNS that is already known to have these effects is transforming growth factor-β (TGF-β).

Aims: This thesis investigated the relationship between retinal maturation and choroidal blood vessel supply and the possible role for TGF-β as an antiangiogenic factor in maintaining an avascular fovea during primate retinal development.

Methods: Human eyes between 11 WG and 40 years were obtained with ethical approval from Prince of Wales Hospital and the NSW Lions Eye Bank and fixed and sectioned for histological procedures or prepared for polymerase chain reaction (PCR). Macaque eyes from foetal day (fd) 64 to postnatal 11years (p11y) were obtained from Bogor Agriculture University, Indonesia with the approval of the Ethics Committee of the University of Washington, Seattle, USA. Macaque eyes were also fixed and sectioned for immunohistochemistry and *in situ* hybridisation.

RNA was extracted from human foetal retinas and used for RTPCR (Reverse Transcriptase PCR), QPCR (Quantitative PCR) and preparation of riboprobes. PCR products were analysed using both restriction digest and sequencing. RTPCR was used to identify TGF-β1, TGF-β2 and TGF-β3 in the developing human and in the developing and adult macaque retinas whilst QPCR was used to quantify the TGF-β isoforms in central compared to peripheral retina and in foetal compared to adult retina.

In situ hybridisation was performed according to a standard protocol and visualised using Roche HNPP Fast Red detection set with designed riboprobes for TGF-β1, TGF-β2 and TGF-β3 (DIG RNA labelling kit). Some sections were counterstained with vimentin antibody.

Immunohistochemistry was performed on human retina and choroid sections using antibodies to CD34 and Ki67 and on human and macaque retina using antibodies to synaptophysin, vimentin, GFAP, calbindin, S-opsin, RG-opsin, rhodopsin, TGF-β1, TGF-β2, TGF-β3 and their receptors TβRI and TβRII. Sections of the retina were imaged and analysed using either a Leica Confocal microscope and TCSNT software or Zeiss Confocal microscope and LSM 5 Pascal software. Data from the human retina and choroid sections corresponding to different regions (foveal, parafoveal nasal, parafoveal temporal, nasal and temporal) was collected to measure the number of Ki-67 immunolabelled mitotic endothelial cells and the area of CD34 immunolabelled choriocapillaris using Adobe Photoshop version 5.0.2, NIH software version 1.62 (measurement macros) and Excel. In the human and macaque sections the intensity of TGF-β protein and mRNA expression was captured from different regions of the retina (foveal, parafoveal nasal, parafoveal temporal, nasal, temporal, nasal to disc) to compile montages. Montages were then re-imported into LSM 5 Pascal software to measure the optical density across each montage along the ganglion cell layer, outer neuroblastic zone and photoreceptor layer collecting data in Excel for graphical representation. In addition to the montages, individual sections were assessed for co-localisation of TGF-β and TβR to various retinal cell types.

Results: Analyses of choriocapillaris area and endothelial cell (EC) proliferation were able to demonstrate that the area of choriocapillaris endothelium is greater in the foveal region at all ages (14-18.5WG), that the rate of choriocapillaris EC proliferation declines dramatically over this same period and that the lowest rates of EC proliferation are at the incipient fovea. Most importantly these findings indicate that EC proliferation in the choriocapillaris does not appear to be promoted by increased metabolic activity in central retinal neurons which are more developed with higher

oxygen and nutrient demands, which is the mechanism widely thought to regulate development of the retinal vasculature.

PCR showed all TGF-β isoforms to be present in the human developing and adult retina. QPCR revealed that TGF-β2 was the most predominant isoform, followed by TGF-β3 with very small amounts of TGF-β1 seen. The isoforms were more abundant in developing rather than adult retina and in central rather than peripheral retina. Studies of the distribution of TGF-β protein and mRNA using immunohistochemistry and *in situ* hybridisation confirmed the low levels of TGF-β1 protein and mRNA observed in QPCR and demonstrated distinct centroperipheral gradients in the photoreceptor layer for TGF-β2 and TGF-β3. Relative high amounts of TGF-β in the fovea could affect vascular patterning due to TβRI seen in astrocytes which lead the blood vessels at the foveal rim at the level of the ganglion cell plexus. TGF-β2 and TGF-β3 expression is detected before formation of the foveal avascular zone (FAZ) at fd64 (~15WG) - fd73 (~17WG) with levels peaking in the foveal region at fd105 (~25WG) by the time the FAZ forms.

Conclusions: This thesis has shown that EC proliferation in the choriocapillaris does not appear to be promoted by increased metabolic activity in central retinal neurons as reduced rates of EC proliferation in the 'foveal' chorioretinal location were observed at all ages studied between 14 and 18.5WG. The findings suggest that mechanisms regulating proliferation and growth of the choroidal vasculature are independent of differentiation in the neural retina and are therefore different to those governing the formation of the retinal vasculature.

All TGF-β isoforms are expressed in developing and adult human and macaque retina with TGF-β2 being the predominant isoform. TGF-β isoforms are more abundant in central compared to peripheral retina and in developing compared to adult retina. Centro-peripheral gradients of TGF-β2 and TGF-β3 across the photoreceptor layer and TβRI on astrocytes support the presence of TGF-β in the fovea as an antiproliferative and antiangiogenic factor by helping to define the FAZ early in development, well before 23-25 WG in humans and before fd100 in macaques.

PUBLICATIONS

Papers and Abstracts

Allende M.A., Madigan M.C and Provis J.M. **Endothelial Cell Proliferation in the Choriocapillaris During Human Retinal Differentiation** *Br J Ophthalmol* 2006; 90: 1046-1051

Allende M.A., Natoli R and Provis J.M. **TGF ß in Developing Primate Foetal Retina** *Mechanisms of Devpt* 2005 122: Abstract S85

Allende M.A. **Transforming Growth Factor ß in Human Foetal Eye** *Invest Ophthalmol Vis Sci* 2004 45:E-Abstract 3544

Allende M.A. and Provis J.M **Development of the Choriocapillaris in Human Foetal Retina** *Invest Ophthalmol Vis Sci* 2003 44:E-Abstract 644

CONFERENCE PRESENTATIONS

Transforming Growth Factor –ß in Developing Primate Foetal Retina

2005 International Society of Developmental Biologists Congress, Sydney

2005 European Vision and Eye Research Conference, Vilamoura, Portugal

2005 RANZCO, Hobart

2005 Australian Visual Sciences Meeting, Melbourne

Transforming Growth Factor –ß in Human Foetal Retina

2004 International Congress of Eye Research, Sydney

2004 Association for Research in Vision and Ophthalmology, Fort Lauderdale, USA

Development of the Human Choriocapillaris

2003 Association for Research in Vision and Ophthalmology, Fort Lauderdale, USA

Transforming Growth Factor –ß in Human Foetal Eye

2003 Australian Visual Sciences Meeting, Melbourne

Development of the Human Choriocapillaris

2002 Australian Visual Sciences Meeting, Sydney

TABLE OF CONTENTS

LIST OF FIGURES

LIST OF TABLES

ABBREVIATIONS

aFGF – acidic fibroblast growth factor
ALK – activin receptor-like kinase
AMD – age-related macular degeneration
Bcl-2 – anti-apoptotic factor
BDNF – brain-derived neurotrophic factor
bFGF – basic fibroblast growth factor
BM – basement membrane
BMP – bone morphogenetic protein
bp – base pairs
BRB – blood-retinal barrier
BREC – bovine retinal endothelial cells
CNS – central nervous system
CRALBP – cellular retinaldehyde binding protein
DIG – digoxigenin
DINL – deep inner nuclear layer plexus
DNA – deoxyribonucleic acid
dpc – days post conception
Dpp – decepentaplegic
DR – diabetic retinopathy
DVR – vegetal 1 related group
EC – endothelial cell
ECM – extracellular matrix
EGF – epidermal growth factor
ELISA – enzyme linked immunosorbent assay
ELM – external limiting membrane
EM – electron microscope
FAZ – foveal avascular zone
fd – foetal day/s
FGF – fibroblast growth factor
FOH – fibres of Henle
GCL – ganglion cell layer
GCP – ganglion cell layer plexus
GDNF – glial cell line-derived neurotrophic factor
GFAP – glial fibrillary acidic protein

h – hour/s
HIF – hypoxia inducible factor
IGF – insulin-like growth factor
IL – interleukin
ILM – inner limiting membrane
INL – inner nuclear layer
IPL – inner plexiform layer
IPM – interphotoreceptor matrix
IR – immunoreactive
IS – inner segments
kDa – kilo Dalton
LAP – latency associated peptide
LGN – lateral geniculate nucleus
LIF – leukemia inhibitory factor
LLC – large latent complex
LM – light microscope
LTBP – latent TGF-β binding protein
LTGF-β – latent TGF-β
MAPK – mitogen activated protein kinase
MCM – Müller cell conditioned medium
MD – median values
min – minute/s
ml – millilitre/s
MMP – matrix metalloproteinase
Mo – month/s
mRNA – messenger RNA
MW – molecular weight
NFL – nerve fibre layer
NGF – nerve growth factor
NMDA – N-methyl-D-aspartate
OD – optical density
ON – optic nerve
ONL – outer nuclear layer
OPL – outer plexiform layer
OS – outer segments
P – postnatal
PBS – phosphate buffered saline
PCD – programmed cell death

PCR – polymerase chain reaction

PDGF/a – platelet-derived growth factor

PDGFRα – platelet derived growth factor receptor α

PEDF – pigment epithelium-derived factor

PR – photoreceptor layer

QPCR – quantitative polymerase chain reaction

RNA – ribonucleic acid

ROP – retinopathy of prematurity

RPC – retinal progenitor cell

RPE – retinal pigmented epithelium

RT – room temperature

RTPCR – reverse transcriptase-polymerase chain reaction

SARA – Smad anchor for receptor activation

SD – standard deviation

SEM – standard error measurement

SINL – superficial inner nuclear layer plexus

SLC – small latent complex

TβR – transforming growth factor β receptor

TIMP – tissue inhibitors of metalloproteinase

TNF – tumor necrosis factor

TSP-1 – thrombospondin-1

TUNEL – terminal dUTP nick end labelling

TGF-β – transforming growth factor β

VEGF/VEGFR – vascular endothelial growth factor/ VEGF receptor

WG – weeks' gestation

Wk – week/s

Y – year/s

CHAPTER 1 – INTRODUCTION

INTRODUCTION

1.1 DEVELOPMENT AND STRUCTURE OF THE HUMAN RETINA AND CHOROID

1.1.1 OVERVIEW OF OCULAR DEVELOPMENT

Prenatal development can be divided into three stages; embryogenesis (0-3 weeks' gestation (WG)), organogenesis (4-8WG) and differentiation (9WG – birth). Only aspects of development pertinent to retinal and choroidal development are summarised here.

Eye formation is first evident at the beginning of the fourth week of development. This is where at the anterior end of the neural tube, optic sulci appear that later form optic vesicles (O'Rahilly, 1975).

The optic vesicles form the optic cups between 5 and 6WG. The inner thicker layer of the optic cup becomes the sensory retina, the outer thinner layer forms the retinal pigmented epithelium (RPE) and the surrounding mesenchyme gives rise to endothelial blood spaces that form the choriocapillaris and the sclera. The optic fissure along the inferior cup allows the hyaloid artery and vein, which branch off the ophthalmic artery and vein, to supply the inner optic cup layer, lens and mesenchyme. When the optic stalk fuses, the optic nerve is formed and the enclosed blood vessels now form the central retinal artery and vein (Moore, 1988; O'Rahilly, 1975; Mann, 1964; Duke-Elder, 1963) (Figure 1.1 and 1.2).

Most ocular structures develop and mature after 9WG, except for the macula that continues to differentiate after birth (Hendrickson & Yuodelis, 1984). Mesodermal cells invade the optic cup by the end of the first month of gestation and differentiate into the hyaloid artery and its branches occupying most of the vitreal space between the lens and neural retina. The hyaloid system begins to atrophy in the fourth month of gestation and blood flow stops in the seventh month (Jakobiec, 1982). The hyaloid system is fully developed at 9 WG, then regresses uniformly to completely disappear by birth (Saint-Geniez & D'Amore, 2004; Zhu *et al.*, 2000a).

In general, development of the eye is organised by secreted signalling molecules that belong to several gene families. Hedgehog (Shh), wingless (Wnt), transforming growth factor-β (TGF-β), bone morphogenetic proteins (BMP) and fibroblast growth factor (FGF) families help activate specific intracellular cascades that control gene transcription. Growth factors modulate the migration, proliferation and differentiation of embryonic cells. For example, the generation of the optic stalk and the optic vesicle is under the influence of signals from Shh and TGF-β families (Esteve & Bovolenta, 2005; Yang, 2004); TGF-β and FGF signalling act antagonistically to separate the RPE and neural retina from the optic vesicle; Shh and BMP control the dorsal ventral polarity of the optic cup together with Vax and Tbx5 transcription factors (Yang, 2004; Martinez-Morales *et al.*, 2004; Golz *et al*., 2008), and Shh has been implicated in the propagation of retinal differentiation in vertebrates (Zhang & Yang, 2001). TGF-β also has a specific role in directing the migration and development of cranial neural crest cells (Tripathi, 1991) and FGF has been described as part of a 'signalling centre' that coordinates and initiates retinal differentiation (Martinez-Morales *et al.*, 2005).

FIGURE 1.1 Early eye development. **A.** Cranial end of 22 day old embryo showing first indication of eye development. Neural folds are not yet fused to form the primary brain vesicles. **B.** Transverse section through an optic sulcus. **C.** Schematic drawing of the forebrain at 28 days, with its covering layers of mesoderm and surface ectoderm. **D, F and H**. Schematic sections of the developing eye illustrating successive stages in the development of the optic cup and the lens vesicle. **E.** Lateral view of 32 day embryo showing external appearance of the optic cup. **G.** Transverse section through the optic stalk, showing the optic fissure and its contents. The edges of the optic fissure grow together and fuse, thereby completing the optic cup and enclosing the central artery and vein of the retina in the cup and optic nerve. (Adapted from figure 19-1, Moore, 1988).

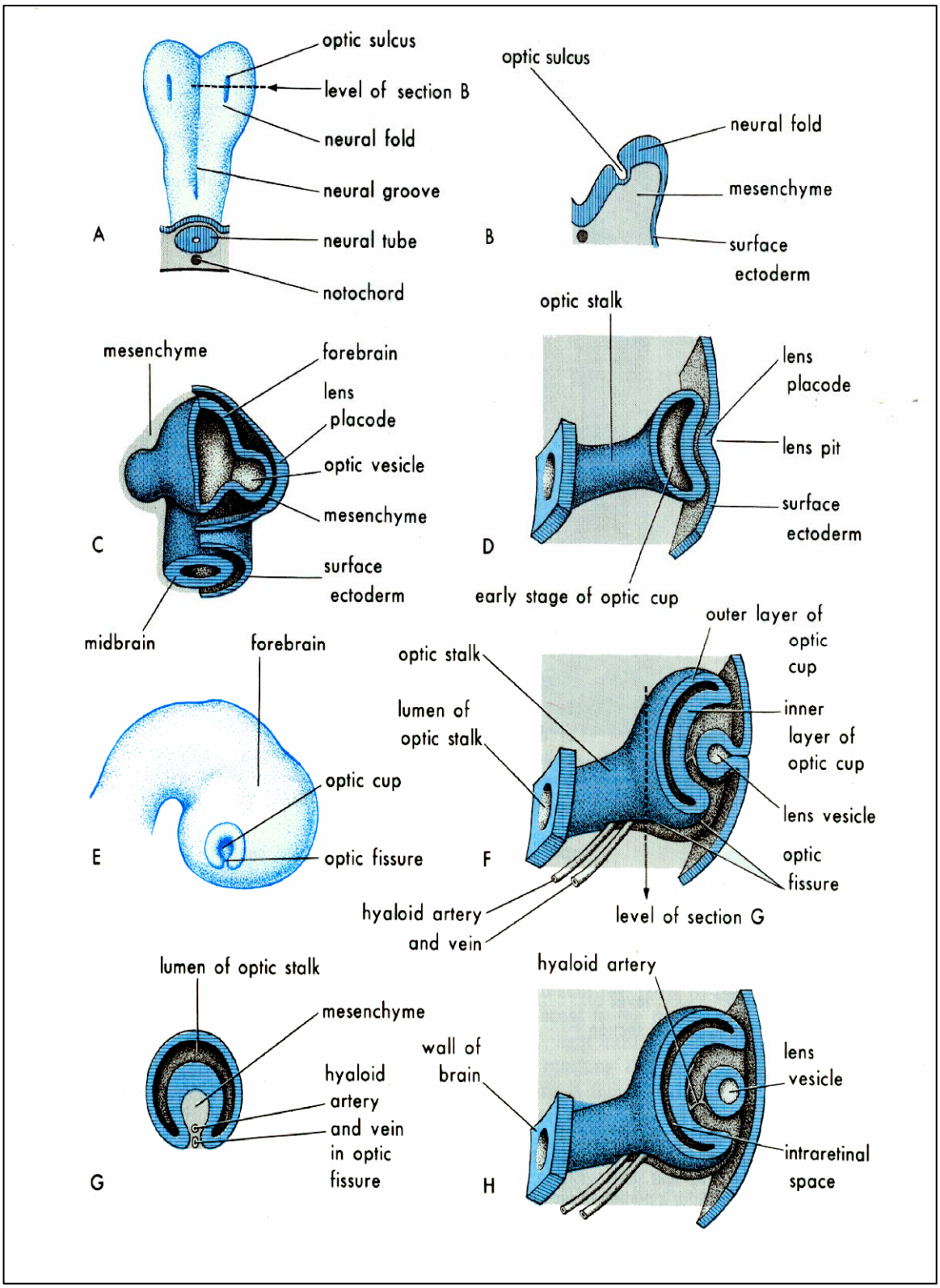
optic sulcus
level of section B
neural fold
neural groove
neural tube
notochord
A
optic sulcus
neural fold
mesenchyme
surface ectoderm
B
mesenchyme
forebrain
lens placode
optic vesicle
mesenchyme
surface ectoderm
midbrain
C
optic stalk
lens placode
lens pit
surface ectoderm
early stage of optic cup
D
forebrain
optic cup
optic fissure
E
optic stalk
lumen of optic stalk
outer layer of optic cup
inner layer of optic cup
lens vesicle
optic fissure
hyaloid artery and vein
level of section G
F
lumen of optic stalk
mesenchyme
hyaloid artery and vein in optic fissure
G
hyaloid artery
wall of brain
lens vesicle
intraretinal space
H

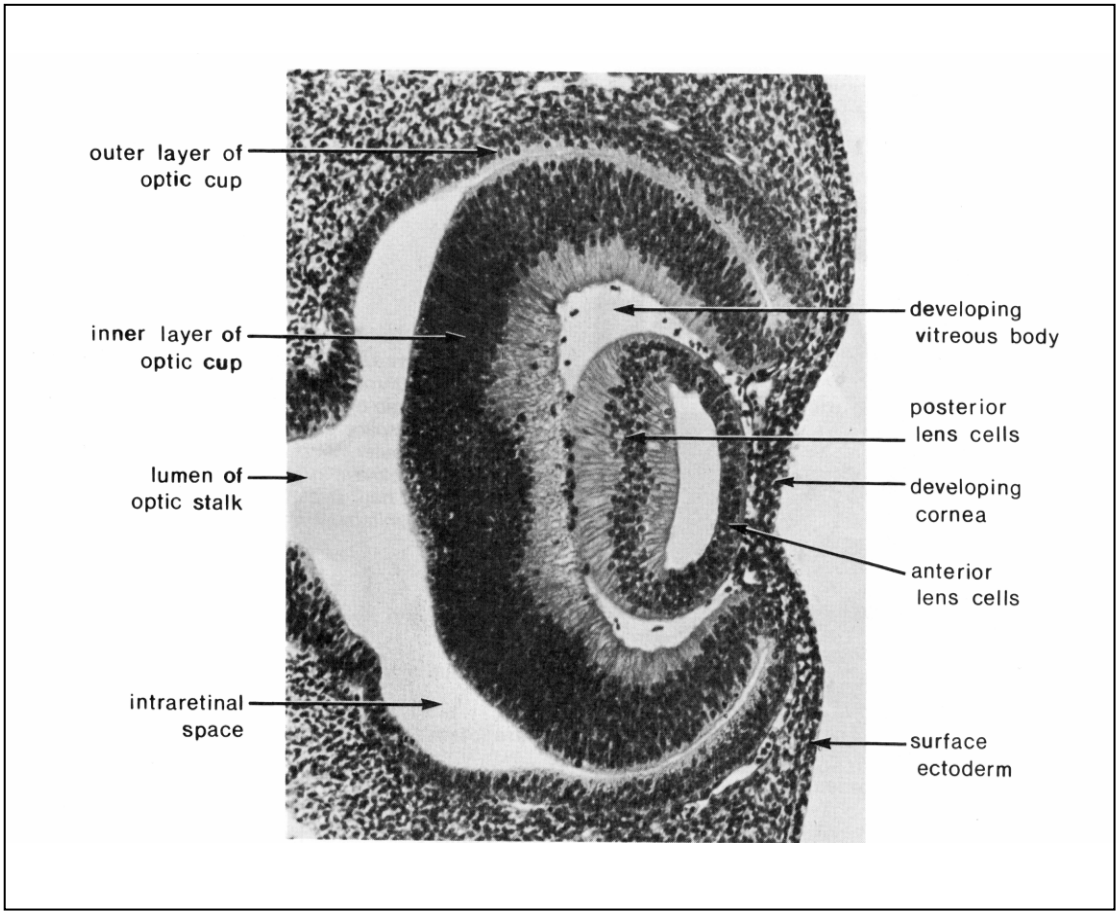

FIGURE 1.2 Sagittal section through the developing eye of a 41 day old embryo. The intraretinal space of the optic cup represents the cavity of the original optic vesicle (200x magnification). (Adapted from figure 19-3 Moore, 1988).

1.1.1 THE CHOROID

Structure

The choroid consists of layers of blood vessels in loose stroma extending from the *ora serrata* anteriorly to the optic nerve posteriorly forming the posterior part of the uveal tract that provides a vascular supply to the outer retina. The innermost vascular layer of the choroid is the choriocapillaris, comprising a highly permeable capillary network.

The choriocapillaris has an afferent supply from three sources: mainly short posterior ciliary vessels that come from around the optic disc, branching as they pass anteriorly into the choroid; recurrent branches of long ciliary vessels as they pass back from the ora region to supply the choroid up to the equator and branches of the anterior ciliary arteries, which pass back from the ciliary muscle to enter the choriocapillaris. There are extensive anastomoses, with venous return via the vortex veins (Hogan, 1971).

Development

Development of the choroid was the subject of several early studies, first described by Hovius in 1702 when the term ‘choroid’ was derived from the Greek work for “membrane” and “form” (Ryan, 2001). Leber (1903) dissected the choroid and Versari (1910) injected Prussian blue into human choroidal vessels. Further histological studies were carried out by Mann (1928; 1964), Duke-Elder and Cook (1963), Hogan, Alvarado and Weddell (1971) including electron microscope (EM) analyses in the chick (Francois *et al.*, 1963) and rat (Braekevelt & Hollenberg, 1970; Leeson, 1968). The most detailed light microscope (LM) studies of the human choroid were done by Heimann (1970, 1972, 1974) along with EM observations of the developing choroid in the primate *Macaca mulatta* done by Ozanics (1978); and in the human by Mund (1972), Sellheyer and Spitznas (1988) and Sellheyer (1990).

Recent studies have concentrated on choroidal neovascularisation using immunohistochemistry, *in situ* hybridisation, cell culture, ultrasonography and gene therapy. These have shed light on functional choroid development that

is observed in diseases such as age related macular degeneration and diabetic retinopathy with experiments done in mice (Rousseau *et al.*, 2003; Zhao & Overbeek, 1999; Zhao & Overbeek, 2001b; Rousseau *et al.*, 2000; Neuhardt *et al.*, 1999), in rats (Steinle *et al.,* 2002; Shi *et al.*, 2004; Yi *et al.*, 1998), in chicks (Nickla *et al.*, 1998), in bovine (Sakamoto *et al.*, 1995; Morse *et al.*, 1989), and in humans (Steinle & Smith, 2002; Steinle *et al.*, 2005). For example, chronic sympathetic denervation of the adult rat results in increased thickness of the choroid and vascular luminal area with increased numbers of choroidal small venules (Steinle *et al.,* 2002). This suggests that sympathetic innervation is important in maintaining ocular vascularity and that chronic loss of sympathetic activity may contribute to abnormal vascular proliferation in diseases such as age related macular degeneration.

The mesenchyme surrounding the optic cup forms vascular channels from 29 days' gestation that surround the optic vesicle (Ozanics *et al.*, 1978). Other choroidal cells, including stromal cells, melanocytes and pericytes are derived from neural crest cells (Etchevers *et al.*, 2001). Closed endothelial channels first display slit-like lumina and then expand around the optic vesicle to form a vascular plexus (Sellheyer, 1990).

The RPE forms the outer blood-retinal barrier (BRB) between the neural retina and the choroid by the second month, and is surrounded by a primitive choriocapillaris, fed by branches of short and long posterior ciliary arteries (Figure 1.3). By 9WG, numerous fenestrations are seen in the choriocapillaris endothelial cells, juxtaposed to Bruch's membrane (Sellheyer, 1990; Sellheyer & Spitznas, 1988). These fenestrations contribute to the permeability of the choriocapillaris, with subsequent diffusion of oxygen and nutrients to the RPE and outer retina. The RPE is essential for the development of the choroid as growth factors released by the RPE such as FGF-2, VEGF and FGF-9 are involved in endothelial cell proliferation and differentiation (Zhao & Overbeek, 2001b; Sakamoto *et al.*, 1995). The larger, outer vessels of the choroid form a predominantly venous layer (Haller's layer) in the fourth month. In the fifth month, Sattler's layer, mostly medium sized arterial vessels, is formed between the choriocapillaris and Haller's layer, but doesn't reach the ciliary body until the sixth month (Figure 1.4). Anastomoses of vessels in the ciliary body are not complete until eight

months' gestation (Heimann, 1972). Pigmentation of the choroid begins at the optic disc and extends anteriorly to the *ora serrata* to be completed by 9 months (Mund *et al.*, 1972).

Physiology

The choroidal circulation has one of the highest rates of blood flow in the human body. Per gram of tissue, the choroid has four times more blood flow than the renal cortex (Ryan, 2001). The choroidal blood supply, present in all mammalian species, is responsible for providing nutrients and oxygen to the retina.

The retinal vasculature has evolved to supply the inner retina in many species where the retina is thick (>150μm) and the underlying choroidal circulation is unable to meet the metabolic demands (Buttery *et al.*, 1991).

Early studies claimed that the choriocapillaris was thickest at the submacular region even though the macular vessels' diameter approximates 20μm and other choroidal vessels range from 18-50μm diameter (Leber, 1903 cited in Hogan, 1971). In the central retina the choroid is thickest, with reduced intervascular space to be able to meet higher metabolic demands of the retina due to high density of cones present and lack of retinal vasculature (Fryczkowski & Sherman, 1988). In central fovea (the foveola), oxygen diffuses approximately 100μm from the choriocapillaris to supply inner segments of foveal cones. In the rest of the retina, oxygen from the choroid diffuses 50-60μm but the presence of deep retinal vessels ensures oxygen diffusion from these vessels from 50μm in the periphery to 100μm in the parafoveal region (Ahmed *et al.*, 1993). This anatomical specialisation occurs early in the choroidal blood supply of this area, differentiating before the macula itself as all the temporal short posterior ciliary arteries enter the eyeball in the macular region with one of these sending 2-3 branches into the submacular zone (Hayreh, 1974). In contrast, no central vessels were found when the lobular structure of the choroid was studied, instead lobules were identified throughout the eye, except for the area located beneath the macula where arterial and venular channels appeared to be freely interconnected. This region has an abundant arterial supply with arteriolar openings outnumbering venular openings by 3:1 (Fryczkowski *et al.*, 1991).

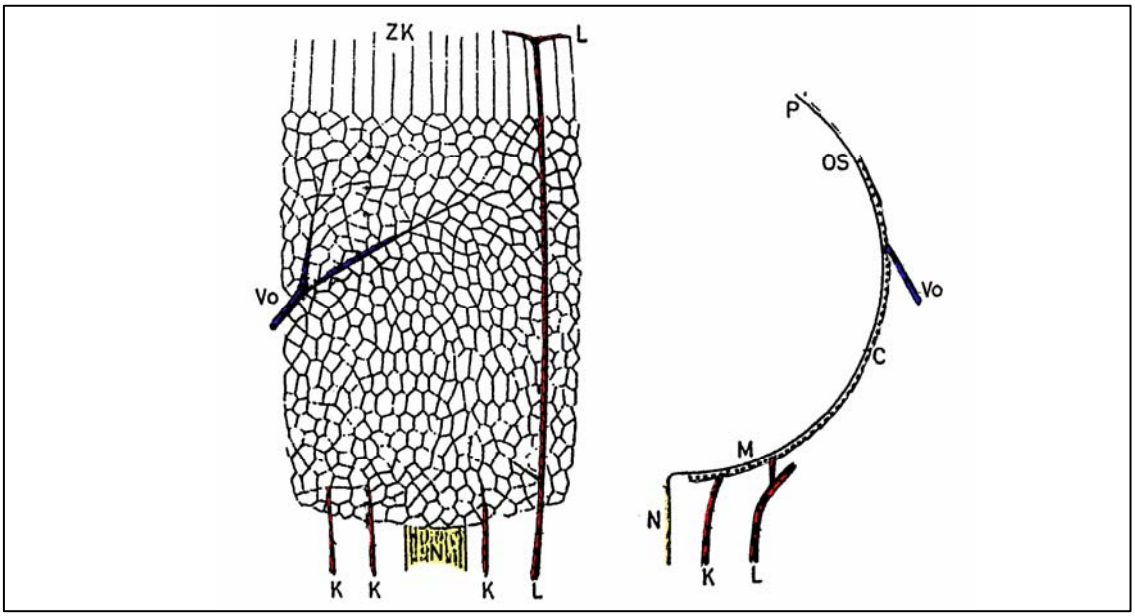

FIGURE 1.3 Choroidal vasculature at 9WG where K: short posterior ciliary arteries; L: long posterior ciliary arteries; N: optic nerve; Vo: vortex vein; ZK: level of what will become the ciliary body; M: region that will become macular zone; C: choriocapillaris; OS: region that will become ora and P: pigment epithelium. (Adapted from Heimann, 1972).

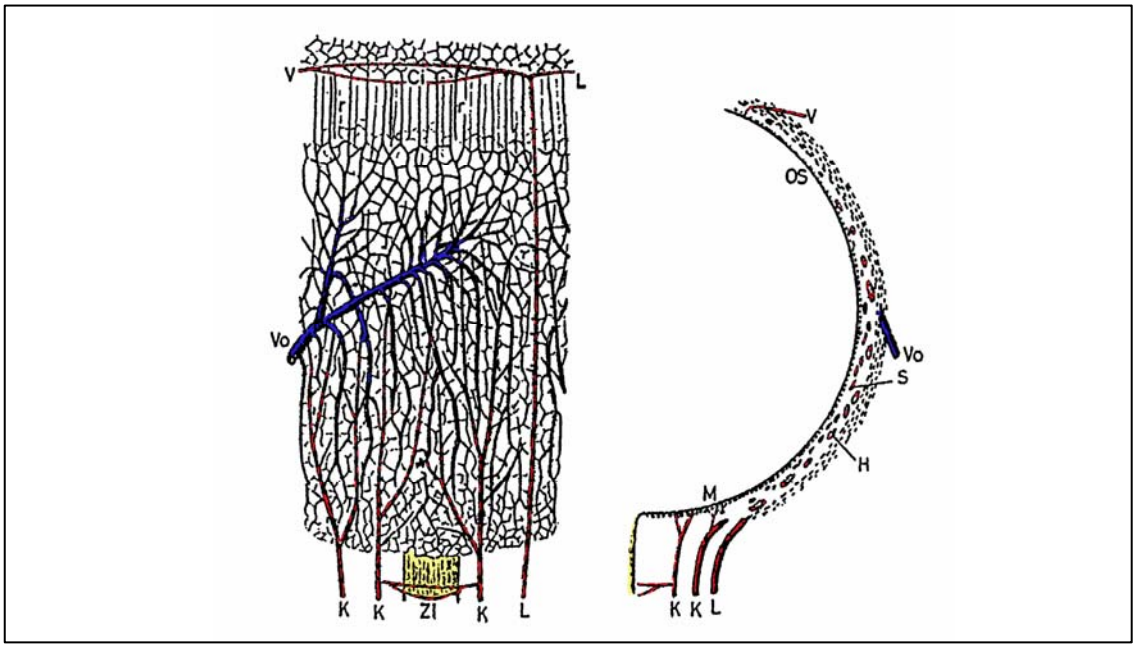

FIGURE 1.4 Choroidal vasculature at 25WG where K: short posterior ciliary arteries; L: long posterior ciliary arteries; ZI: circle of Haller-Zinn; Vo: vortex vein; V: anterior ciliary artery; Ci: major arterial circle of the iris; R: recurrent branches; M: region that will become macular zone; OS: ora serrata; H: Haller's layer and S: Sattler's layer. (Adapted from Heimann, 1972).

1.1.2 THE RETINA

Structure

The neural retina extends from the *ora serrata* anteriorly to the optic disc posteriorly. The posterior primate retina has a 1-2mm yellow depression - the *macula lutea* (Latin “yellow spot”) - with a central area, the *fovea centralis* (Latin “central pit”), that is responsible for maximal visual acuity. It is this feature that distinguishes the primate retina from other mammalian retina.

The retina comprises ten layers: RPE, photoreceptor layer of rods and cones (consisting of inner (IS) and outer segments (OS)), external limiting membrane (ELM), outer nuclear layer (ONL), outer plexiform layer (OPL), inner nuclear layer (INL), inner plexiform layer (IPL), ganglion cell layer (GCL), nerve fibre layer (NFL) and internal limiting membrane (ILM) (Figure 1.5).

In the fovea, the only layers present are the RPE, the cone photoreceptor layer, the external limiting membrane, the outer nuclear layer with cone cell nuclei, the inner fibres of the photoreceptors (known as fibres of Henle (FOH) in cones) and the internal limiting membrane.

Outside the fovea, the retina has three neuronal and two synaptic layers. The primary neurons, the photoreceptors synapse at the OPL onto bipolar and horizontal neurons in the INL, then the bipolar cells and amacrine cells in the INL synapse onto the ganglion cells at the IPL (Figure 1.6). Three types of non neuronal glial cell are found in the human retina; Müller cells, astrocytes and microglia.

Photoreceptors comprise of cones, responsible for photopic high acuity colour vision, and rods, responsible for scotopic vision and detection of movement.

Bipolar cells are second order neurons in the visual circuitry (Kolb *et al.*, 1992; Boycott & Wassle, 1991) and horizontal cells modulate visual information from the photoreceptors via a network of fibres that integrates activity of the photoreceptor cells horizontally. The concentration of horizontal

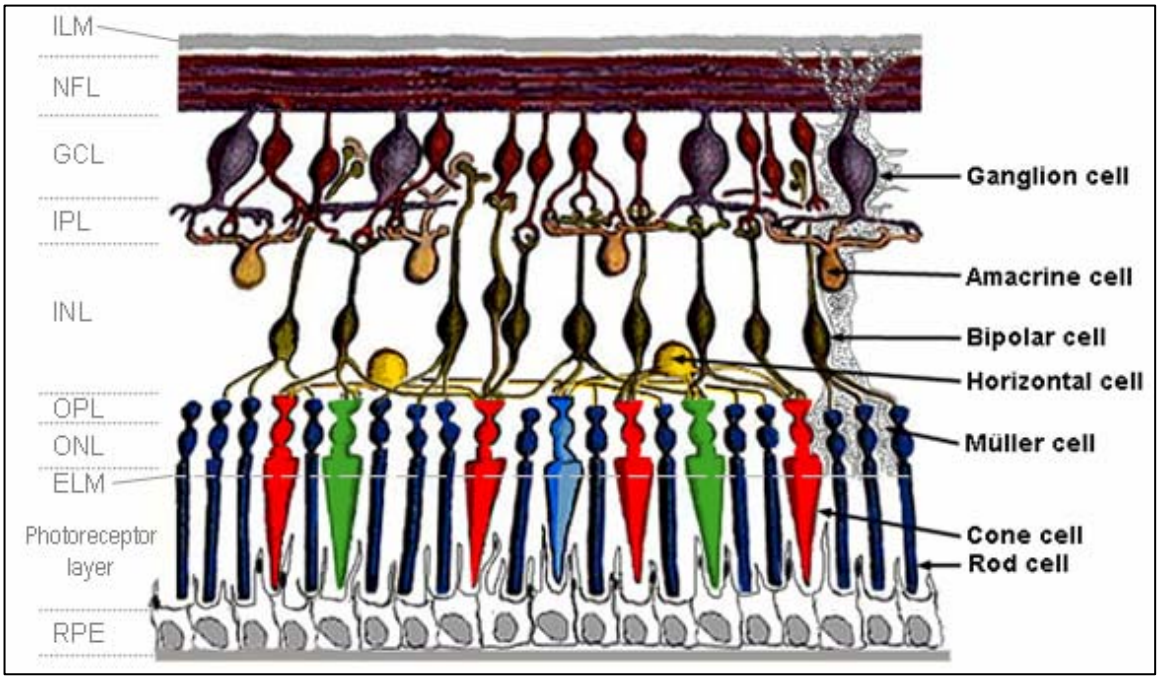

FIGURE 1.5 Schematic diagram of architecture of the retina showing its layers and corresponding cells. ILM: internal limiting membrane, NFL: nerve fibre layer, GCL: ganglion cell layer, IPL: inner plexiform layer, INL: inner nuclear layer, OPL: outer plexiform layer, ONL: outer nuclear layer, ELM: external limiting membrane and RPE: retinal pigmented epithelium. Adapted from www.theness.com.

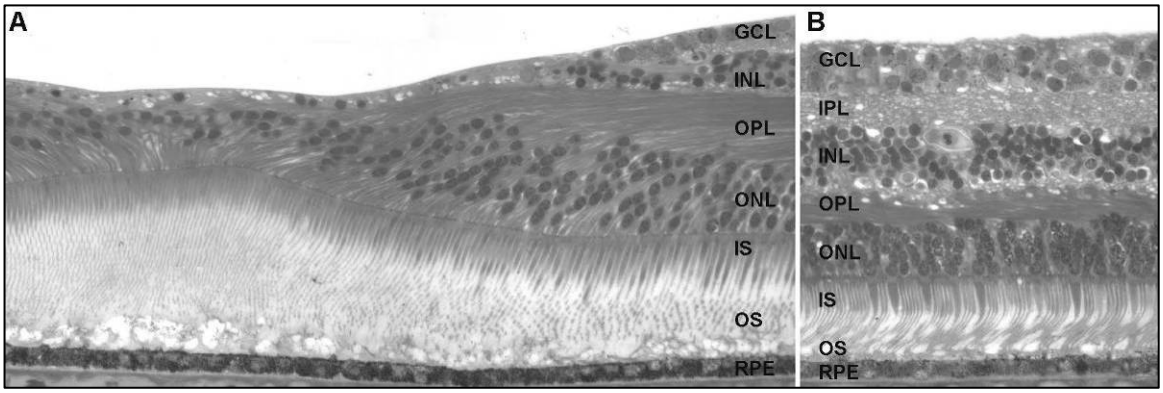

FIGURE 1.6 A. Retinal layers in fovea and parafovea, and **B.** peripheral retina where GCL: ganglion cell layer, IPL: inner plexiform layer, INL: inner nuclear layer, OPL: outer plexiform layer, ONL: outer nuclear layer, photoreceptor layer of rods and cones (consisting of IS: inner and OS: outer segments), RPE: retinal pigmented epithelium. (Adapted from Hendrickson and Provis, 2004).

cells is highest at the fovea and their number decreases towards the periphery (Wassle *et al.*, 2000; Dacey *et al.*, 1996; Kolb *et al.*, 1980; Kolb *et al.*, 1994; Polyak, 1941).

Most amacrine cells produce GABA and glycine which have an inhibitory action on the ganglion cells (Kolb *et al.*, 1992; Crooks & Kolb, 1992). Ganglion cells are the final output neurons of the retina. Like amacrine cells, ganglion cells increase their dendritic tree span with eccentricity from the fovea (Kolb *et al.*, 1981; Boycott & Wassle, 1974). Two major types of ganglion cells M or parasol and P cells which can be further subdivided into P1 or midget and P2 or small bistratified cells are found in the retina (Kolb *et al.*, 1992; Rodieck *et al.*, 1985; Polyak, 1941). Parasol cells project to the magnocellular layers of the lateral geniculate nucleus (LGN), the midget cells project to the parvocellular layers of the LGN (Shapley, 1982) and the bistratified cells project to the koniocellular layers of the LGN (Martin & Perry, 1988). The M pathway is concerned with initial analysis of movement seen whereas the P and K pathways are concerned with analysis of fine structure and colour vision.

Müller cell nuclei are located in the INL, with processes extending between the two limiting membranes. They are the largest of all cells in the retina and have an important role in the orientation, displacement and positioning of the developing neurons as well as providing structural alignment of neuronal elements in developed retina. They express the neural progenitor marker, nestin in both differentiated and undifferentiated human foetal retina, suggesting that they are end stage progenitor cells (Walcott & Provis, 2003). Glutamate transporters on Müller cells are present by 10WG before synaptic vesicle proteins are evident, suggesting a role for Müller cells in shaping synaptogenesis in the developing human retina (Diaz *et al.*, 2007). They are important producers of proangiogenic (VEGF) and antiangiogenic factors (TGF-β, PEDF and TSP-1) that influence blood vessel growth and apoptosis (Eichler *et al.*, 2004). They control retinal homeostasis protecting ionic shifts in neurons and mopping up neural waste products such as carbon dioxide. They also break down glycogen to fuel aerobic metabolism of nerve cells and help recycle neurotransmitters such as glutamate (Reichenbach, 1997).

Astrocytes are derived embryonically from the cells of the neural crest as they migrate into the retina via the optic nerve (Huxlin *et al.*, 1992; Ling & Stone, 1988). They can be divided into fibrous and protoplasmic astrocytes. Fibrous astrocytes have many cytoplasmic processes and are located in the NFL whereas protoplasmic astrocytes have short blunt processes and extend to the IPL (Sigelman, 1982). Astrocytes contact the abluminal aspect of blood vessels, contributing to the inner blood-retinal barrier and they have been shown to accompany the development of the primary retinal plexus in several species but do not present in the avascular fovea (Sandercoe *et al.*, 1999; Provis *et al.*, 1997; Gariano *et al.*, 1996; Chan-Ling & Stone, 1991; Ling *et al.*, 1989; Ling & Stone, 1988; Stone & Dreher, 1987).

Microglia are the immunocompetent cells of the retina, derived from mesodermal invasion of the retina. They are found in the fovea up to 20WG and continue to migrate from the optic nerve head to peripheral retina til 25WG, settling in the mature retina between the NFL and OPL (Provis *et al.*, 1996; Diaz-Araya *et al.*, 1995). They can be stimulated into a macrophagic role by tissue debris which is carried to the vasculature for removal from the retina (Matsubara *et al.*, 1999; Penfold *et al.*, 1993).

Specialisation of the fovea

The '*macula'* refers to a region 5-6 mm in diameter at the posterior pole of the eye that appears as a yellow spot (*macula lutea*) due to the presence of xanthophyll pigments, lutein and zeaxanthin. These pigments are thought to protect the retina from blue light and may even act as antioxidants to protect photoreceptors from dying (Provis *et al.*, 1995; Snodderly, 1995; Kirschfeld, 1982; Wald, 1945). The central 1mm^2 of the macula is known as the *fovea centralis* which is surrounded by the adjacent parafovea and outermost perifovea (Figure 1.7A). The fovea is characterised by a high density of photoreceptors and ganglion cells, an absence of retinal blood vessels and unique neuronal connections (Provis *et al.*, 2005).

The fovea consists of the foveal slope and foveola. The foveal slope at the foveal rim is rod dominant and contains the perifoveal capillary plexus, whose three layers anastomose at the cone dominant base of the foveal slope

forming a vascular ring surrounding the foveola (Provis *et al.*, 2000; Provis, 2001; Provis *et al.*, 2005; Snodderly *et al.*, 1992). The neuronal composition of the foveal slope has a cone connected to a bipolar cell subsequently linked to a midget ganglion cell which supports high visual acuity and colour vision (Hendrickson, 1994; Dacey, 1996; Dacey *et al.*, 1996; Wassle *et al.*, 1994; Polyak, 1941) (Figure 1.7B). The fovea has virtually only cones in its ONL (Hendrickson, 1994; Diaz-Araya & Provis, 1992; Hendrickson & Yuodelis, 1984). The parafovea has a low density of retinal vessels, high density of ganglion cells and below average spatial densities of rods whilst the perifovea has a high cone:rod ratio, high density of retinal vessels and above average cone and ganglion cell densities (Packer *et al*., 1989; Curcio *et al.*, 1990; Provis *et al.*, 2005).

The significance of the avascular zone is that structures such as vessels and blood cells do not deflect incident light, helping to improve visual acuity at this region. As a result of a lack in blood supply other than from the choriocapillaris, this region dense with photoreceptors in primates appears to be associated with the presence of a foveal depression, where the retina is thinner and more readily supplied by the choriocapillaris. The lateral displacement of cells in the pit may indicate an adaptive advantage to reduce metabolic stress by having these cells closer to the retinal blood supply, but how the structure evolved is not known (Provis, 2001).

The fovea is the first part of retina to differentiate where it can be defined as early as 11 WG (Provis *et al.*, 1985).

During the third trimester and continuing until 5-8 years of age, cells within and surrounding the fovea rearrange themselves. Initially the retinal ganglion cells and inner nuclear layer cells move centrifugally away from the foveal centre during the third trimester whilst the cone cells move centripetally forming a domed cone mosaic in the adult retina (Sandercoe *et al.*, 2003; Springer, 1999; Provis *et al.*, 1998; Mann, 1964). The factors that support active migration for these populations of cells are not known. Alternatively, it is possible that instead of migrating, the retinal ganglion cells and inner nuclear cells die, thus reducing their numbers in the fovea whilst the cone cells proliferate thus increasing their population centrally. However, formation

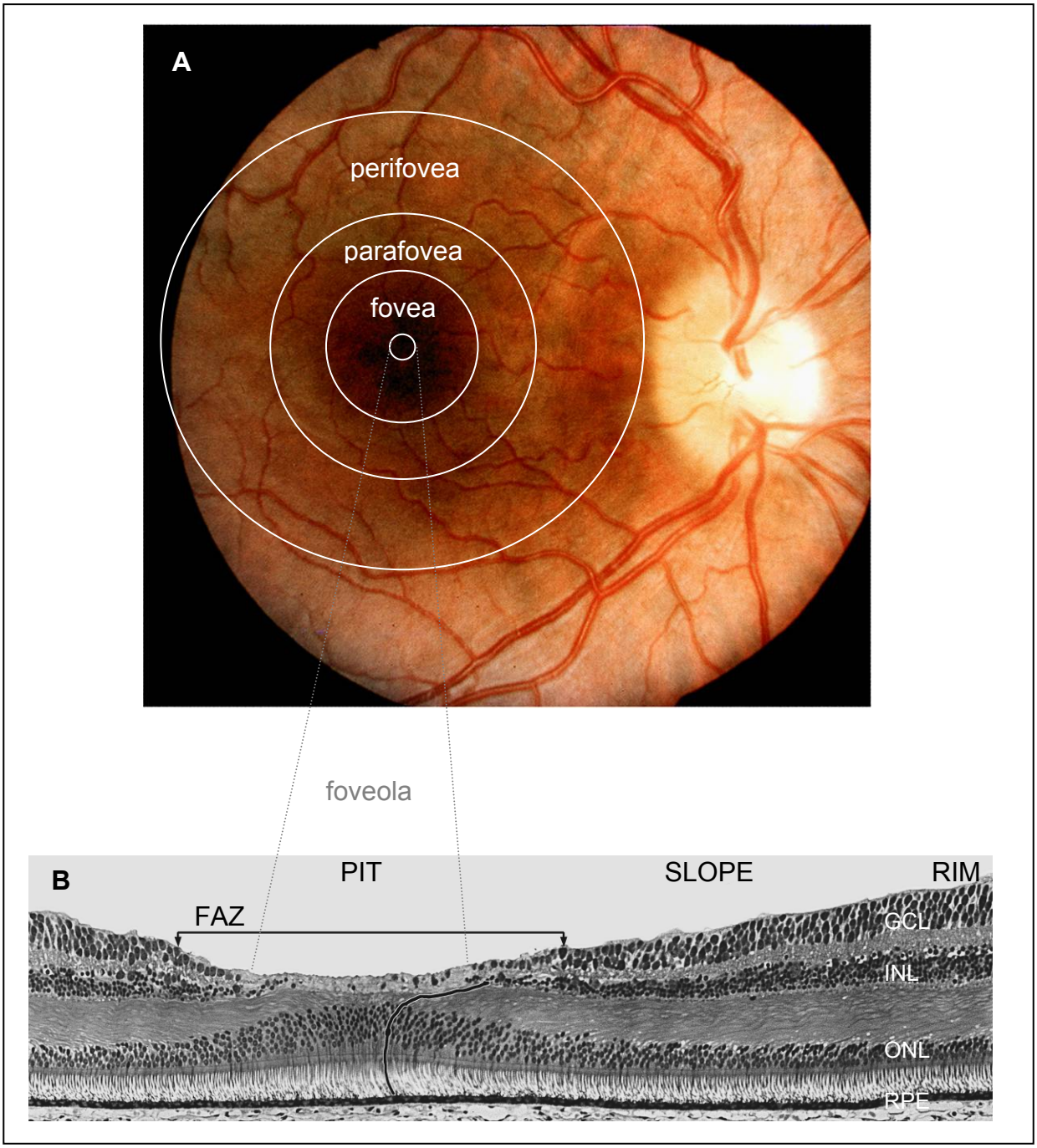

FIGURE 1.7 A. Fundus photograph of the human eye showing anatomical regions of the fundus: the perifovea, parafovea, fovea and foveola (Polyak, 1941). **B.** Transverse section of foveal retina, pit, slope, rim and foveal avascular zone (FAZ, within arrows), with foveola matched with fundus photograph above. Trace shown of laterally displaced synaptic connection made between photoreceptor, bipolar cell and ganglion cell. GCL: ganglion cell layer, INL: inner nuclear layer, ONL: outer nuclear layer, RPE: retinal pigment epithelium. (Adapted from Hendrickson and Provis, 2004).

of the foveal pit occurs without significant evidence of apoptosis or mitosis (Georges *et al.*, 1999; Provis, 1987). Cone photoreceptors are unlikely to be created postnatally, as retinal histogenesis is finished by the beginning of the third trimester (Springer, 1999; La Vail *et al*., 1991).

A third hypothesis of foveal morphogenesis is that development itself weakens the retinal wall allowing it to stretch and causing passive centrifugal movement of inner retinal cells, but the fovea does not appear to stretch significantly as in monkeys where the optic disc-fovea distances do not appear to increase with age (Springer & Hendrickson, 2005; Springer, 1999; Kirby & Steineke, 1996; Robinson, 1991).

During the first half of gestation much of the retina is avascular and the retina derives most of its oxygen by diffusion from the choriocapillaris and hyaloid system. The superior and inferior vascular arcades grow from the optic disc towards the central retina, curving around the fovea without entering the foveal avascular zone (FAZ) (Provis *et al.*, 2000; Gariano *et al.*, 1994). Using engineering models, mechanical experiments have shown that as tissue within an avascular zone is more elastic than the surrounding vascularised retina, if a stretching force is applied, a pit would be formed in the avascular zone (Springer & Hendrickson, 2004a). Following measurements of developing monkey retinas between 68 days postconception (dpc) and adult, it was found that retinal length increased rapidly until 115dpc and then remained unchanged between 115dpc-180dpc. After birth, the retina again grew rapidly for 3 months and then very slowly into adulthood. The onset of pit development overlapped the late foetal stable phase suggesting that the main mechanical factor in commencing pit formation was intraocular pressure rather than retinal growth induced stretch (Springer & Hendrickson, 2004b). After the stable development phase of retinal growth, in the first four months after birth, central retinal stretch forces are thought to remodel the pit and help in packing cones in the fovea. A stretching of the inner retina may generate lift forces as the pit becomes shallower and wider drawing cones centripetally (Springer & Hendrickson, 2005).

The pit may result from hypoxia due to a local absence of retinal vessels, a thickened foveal cone mosaic and insufficient oxygenation from the choroidal

blood supply as photoreceptors can consume high concentrations of oxygen from the choroid-over 90% in the adult (Ahmed *et al.*, 1993; Rodieck, 1988). In species where a retinal vasculature develops it has been proposed that transient hypoxia in the inner layers of the developing retina is induced by increased metabolic activity in maturing retinal neurons and photoreceptors, resulting in the proliferation and migration of retinal endothelial cells, mediated by growth factors (Stone, 1997; Michaelson, 1948) However, the central primate retina – despite being developmentally advanced relative to other regions (Georges *et al.*, 2006; Xiao & Hendrickson, 2000; Bumsted & Hendrickson, 1999; Bumsted *et al.*, 1997; Linberg & Fisher, 1990; Provis & van Driel, 1985) is avascular for a protracted period, and formation of retinal vessels in the central retina is delayed (Provis *et al.*, 2000; Engerman, 1976).

This suggests that other factors are expressed in the central retina which (a) guide developing vessels around the future foveal region, resulting in a longer growth trajectory for vessels in temporal compared with nasal retina, and/or (b) significantly reduce the rates of proliferation and migration of retinal endothelial cells (EC) in central retina, resulting in a slower rate of vessel formation and/or (c) assist in keeping the avascular zone more elastic than the surrounding vascularised retina (Stone *et al.*, 1995; Provis, 2001). TGF-β is one such candidate factor.

Development of the neural retina

The retina develops from the walls of the optic cup, the outer thinner layer forming the RPE and the inner thicker layer forming the neural retina. Retinal differentiation commences centrally, at the posterior pole, and proceeds in a wave-like manner towards the periphery, so that cell division first ceases and differentiation of the retinal laminae first occurs in the central region, at the incipient fovea and progressively in more peripheral regions (Provis & van Driel, 1985; Rapaport & Stone, 1982).

Retinal progenitor cells (RPC) have radial processes and nuclei that migrate along them between the ventricular layer, where cell division occurs and the inner retina where DNA synthesis occurs (Waid & McLoon, 1995). Studies relying on incorporation of labelled thymidine during DNA synthesis prior to the final cell division have indicated that retinal neurons are born in two

phases. The early phase includes ganglion cells, horizontal cells and cone photoreceptors whilst the late phase includes amacrine cells, bipolar cells and rod photoreceptors (Levine & Green, 2004; Walcott & Provis, 2003; Rapaport *et al.*, 1996; Harman & Ferguson, 1994; Harman *et al.*, 1989). Müller cells are thought to be the end-stage differentiation of RPC (Walcott & Provis, 2003).

The incipient foveal region differentiates first, with all retinal layers evident by 11WG (Linberg & Fisher, 1990; Provis & van Driel, 1985). Many of the physiological markers of retinal cells are expressed in central neurons by 14-15 WG including glutamate transporters and S and L/M opsins (Georges *et al.*, 2006; Xiao & Hendrickson, 2000).

Between 14WG and 17WG, the cell population in the ganglion cell layer increases rapidly. The nuclei of the ganglion cells are confined to the ganglion cell layer and the axons are aligned by the Müller cell processes although the precise nature of the signals controlling this have not been defined (Bron, 1997). Ganglion cells send axons to synapse with primary visual nuclei in the brain when they first differentiate (Rakic, 1977). Initially, there is a substantial overproduction of ganglion cells, more than twice the number seen in an adult retina, which is then substantially eliminated between 18WG and 30WG to reach a population range seen in the adult retina (Provis & Penfold, 1988; Provis *et al.*, 1985). The decreased number of cells is accounted for by a period of cell loss due to natural cell death or apoptosis thought to be due to synaptic competition between the ganglion cells for target nuclei (Oppenheim, 1991; Provis *et al.*, 1985).

Immunolabelling of synaptic proteins (Georges *et al.*, 1999; Okada *et al.*, 1994) showed that the first synapses formed are in the primate IPL, followed by those in the OPL, but controversy exists about whether synapses are amacrine or bipolar or both (Crooks *et al.*, 1995; Linberg & Fisher, 1990; van Driel *et al.*, 1990; Nishimura & Rakic, 1987). In the OPL, synaptic development is first evident in the foveal cones at 11WG as synaptic ribbons and clustered vesicles (Linberg & Fisher, 1990). This later spreads across the retina, with horizontal cells seeming to make the first contact with ribbon synapses (Hendrickson, 1996) and with rods appearing to form synapses

later than cones (Okada *et al.*, 1994). At 22WG rod photoreceptors develop cell bodies with inner segments that bulge beyond the external limiting membrane.

Amacrine cells are identifiable at the inner border of the outer neuroblastic layer by 14WG (Rhodes, 1979). At 18WG, the outer region of the cone accumulates mitochondria and polysomes, and the cell membrane involutes to envelop the cilium extending a cytoplasmic process toward the apical region of the retinal pigment epithelial cells. Photoreceptor outer segments differentiate at five months, when multiple infoldings of the plasma membrane develop because of the influence of the ciliary filaments, which parallel the development of the horizontal cells (Springer & Hendrickson, 2004a; Springer & Hendrickson, 2004b; Springer & Hendrickson, 2005; Hendrickson, 1996; Dorn *et al.*, 1995).

Following synaptic formation of the IPL, there is a wave of bipolar cell death starting around 15WG that progresses in a centro-peripheral pattern across the retina during further development suggesting that bipolar apoptosis is associated with onset of synaptogenesis (Georges *et al.*, 1999).

As gestation progresses the area devoid of mitotic activity increases so that by 24WG, dividing cells are present in 62.5% of the retinal surface and are confined to the periphery. By 30WG mitotic activity has ceased completely but the surface area of the retina increases until 3 weeks post birth which is attributed to the growth and maturation of individual cells (Sandercoe *et al.*, 1999; Provis *et al.*, 1985).

Development of the retinal vasculature

a) Mechanisms

Two processes describe the formation of new blood vessels that results in the creation of endothelial lined tubes. When the endothelial cell precursors differentiate from mesoderm forming a primary capillary plexus it is termed vasculogenesis (Pepper, 1997). When the new vessels are formed by sprouting from pre-existing vessels then it is known as angiogenesis (Pepper,

1997). The primary vasculature is thought to be established via vasculogenesis whilst deep capillaries growing from the primary vasculature into the inner layers of the retina or secondary vasculature are formed by angiogenesis (Chan-Ling *et al.*, 2004; Provis, 2001; Sandercoe *et al.*, 1999; Chan-Ling *et al.*, 1990; Ashton, 1970). Spindle shaped vascular precursor cells migrating from the optic disc to the periphery have been thought to be associated with establishment of the primary vasculature but whether they are astrocyte precursor cells or angioblasts remains controversial. Astrocyte precursors may enter the retina ahead of the retinal vessels and be stimulated to differentiate into mature GFAP immunoreactive astrocytes in the presence of invading endothelial cells that produce leukemia inhibitory factor (LIF) (Mi *et al.*, 2001). Astrocytes are associated with the developing vessels, leading them by at least a few hundred microns, producing VEGF (Provis *et al.*, 1997; Gariano *et al.*, 1996; Ling & Stone, 1988). Differentiated astrocytes in advance of the vascular front are sensitive to changes in oxygen and respond to hypoxia by upregulating VEGF expression, which drives endothelial cell proliferation (Provis *et al.*, 1997; Stone, 1997; Aiello *et al.*, 1995; Pierce *et al.*, 1995; Stone *et al.*, 1995). Similarly VEGF expression by Müller cells is thought to regulate development of the deep, secondary vascular plexus (Stone, 1997). Chan-Ling *et al.* have suggested that the vascular precursor cells may be angioblasts rather than immature astrocytes (Chan-Ling *et al.*, 2004). However, an extensive network of astrocytes, that are not GFAP+, have been identified and it is possible that the vascular precursor cells may be microglia instead. Microglia have been recently found to be closely apposed to developing blood vessels (Checchin *et al.*, 2006). The depletion of resident microglia in retinal explants was also found to be associated with reduced developmental vessel growth and density, restored by intravitreal microglial injection (Checchin *et al.*, 2006).

In addition, when the retinal vascular network in mice was labelled using a probe (VEGF receptor 1 and 2) against endothelial cells and angioblasts, this probe failed to label the spindle shaped cells in front of it. These spindle cells were positively stained with a marker for retinal astrocytes (PDGFRα) implying that the immature retinal astrocytes precede the forming retinal vasculature and that the vasculature forms by angiogenesis and not by

angioblasts in vasculogenesis (Fruttiger, 2002). Similarly when retinal astrocytes were blocked, there was a loss of vascular patterning comprising endothelial cells with filopodial extensions that would normally follow the astrocytic template (Dorrell *et al.*, 2002).

The importance of the VEGF and VEGF-receptor system in blood vessel growth has been demonstrated by:

A) Spatiotemporal expression of VEGF and its receptors, which correlates with phases of vasculogenesis and angiogenesis in the embryo and with phases of neovascularisation in the adult (Mandriota *et al.*, 1996; Mustonen & Alitalo, 1995).

B) Mice lacking VEGFR-2, required for endothelial cell differentiation or VEGFR-1, needed for correct vascular assembly, die at early stages in development (Fong *et al.*, 1995; Shalaby *et al.*, 1995).

C) VEGF is the major angiogenic factor in an animal model in ischemia stimulated retinal neovascularisation which was upregulated in retinal endothelial cells, pericytes, RPE cells, ganglion cells and Müller cells (Aiello *et al.*, 1995).

D) VEGF antibodies block tumour angiogenesis and growth (Millauer *et al.*, 1994; Kim *et al.*, 1993).

The regulation of angiogenesis by hypoxia is mediated by the transcriptional regulator, hypoxia inducible factor (HIF-1), which stimulates angiogenesis by activating VEGF gene transcription (Das & McGuire, 2003; Ozaki *et al.*, 1999). Incubation of bovine microvascular and large vessels aortic endothelial cells which express VEGFR-2 but not VEGFR-1, with TGF-β1, results in a marked decrease in VEGFR-2 expression. This down regulation induced by TGF-β1 may be responsible for the inhibitory effect on VEGF, induced in *in vitro* angiogenesis (Mandriota *et al.*, 1996; Pepper *et al.*, 1993). Negative regulators of vascular growth include TGF-β, pigment-epithelium derived factor (PEDF), angiostatin, endostatin, thrombospondin-1 (TSP-1) and MMP (matrix metalloproteinase) inhibitors (TIMPs).

Contact between endothelial cells and pericytes activates TGF-β, which then stabilises vessels by inhibiting endothelial cell proliferation, migration and pericyte differentiation (Antonelli-Orlidge *et al.*, 1989). When VEGF is downregulated TGF-β has been found to be upregulated (Ogata *et al.*, 2001). TGF-β will be described in more detail in Chapter 1.2.

Hypoxia downregulates expression of PEDF and induces expression of VEGF whilst hyperoxia upregulates PEDF whilst downregulating VEGF in a retinoblastoma cell line (Dawson *et al.*, 1999). PEDF has also been shown to reduce corneal neovascularisation and retinal neovascularisation when injected intravitreally (Duh *et al.*, 2002; Dawson *et al.*, 1999).

Angiostatin and endostatin have been shown to suppress new vessel growth (O'Reilly, 1997; O'Reilly *et al.*, 1997; O'Reilly *et al.*, 1994) and TSP-1, secreted by endothelial cells and smooth muscle cells inhibits endothelial cell proliferation, migration and tumour angiogenesis (Tolsma *et al.*, 1997; Majack *et al.*, 1985; McPherson *et al.*, 1981). TIMPs bind the proteinases and inhibit their activity, stopping cell migration and tube formation (Moses *et al.*, 1996).

b) Patterning

The first retinal vessels form at the optic disc at approximately 14 WG and initially grow in a lobular arrangement, each lobule defining the territories of one of the quadrantic arteries of the mature retina (Provis, 2001; Sandercoe *et al.*, 1999; Provis *et al.*, 1997; Ashton, 1970; Patz, 1966; Mann, 1964; Michaelson, 1948; Michaelson *et al.*, 1954). The vessels of the primary vasculature form at the NFL/GCL interface and nasal to the optic disc the superior and inferior lobes merge along the equator at ~20 WG (Provis, 2001). Temporally, the superior and inferior vascular lobes skirt around the foveal region to meet along the equator, peripheral to the foveal region, at ~25 WG and establish the FAZ (Provis, 2001; Provis *et al.*, 2000; Gariano *et al.*, 1994) (Figure 1.8).

The secondary vasculature develops by sprouting from the primary layer, which then crosses the IPL forming a new vascular layer at the IPL/INL interface - the superficial inner nuclear layer plexus (SINL) (Provis, 2001; Gariano *et al.*, 1994). Branches of the SINL then penetrate the INL to form a

layer of vessels at the INL/OPL border - the deep INL plexus (DINL) (Gariano *et al.*, 1994). Analysis of retinal wholemounts and sections suggest that the lobular vessels that skirt around the fovea first form near the optic disc growing on the nasal side first, with the SINL just ahead of the DINL (Provis, 2001; Gariano *et al.*, 1994). Along the horizontal meridian, approximately 1 mm from the optic disc, primary vessels leave the NFL, cross the GCL and continue to grow towards the incipient fovea at the GCL/IPL interface, forming the ganglion cell layer plexus (GCP) (Provis, 2001; Provis *et al.*, 2000). Close to the disc SINL and DINL are present; within a few millimetres GCP and SINL are present whilst closest to the fovea only GCP capillaries are seen (Provis, 2001). The innermost GCP capillaries are established at around foetal day (fd) 100 in the macaque which corresponds to around 24WG in the human but the deep plexus of the perifoveal capillary bed is not complete until birth (Provis, 2001; Provis *et al.*, 2000). At fd105~25WG a ring of vessels and astrocytes surrounds the avascular area where blind ending capillary sprouts are seen (Provis, 2001; Provis *et al.*, 2000). A foveal depression surrounded by the GCP is then noted within the avascular zone with no deep plexus within a millimetre of the fovea until fd142~32WG (Provis, 2001; Provis *et al.*, 2000). Then GCP capillaries contribute to the deep plexus establishing the DINL before the SINL getting as close as 250μm from the foveal centre at fd155~35WG. Anastomosis of the deep plexus with the GCP capillaries occurs in the perinatal period (Provis, 2001; Provis *et al.*, 2000) (Figure 1.9). Astrocytes leading the GCP vessels towards the incipient fovea retreat from it upon formation of the foveal avascular zone (Provis *et al.*, 2000).

The long trajectory of the temporal vessels, combined with a slow growth rate results in the central retina remaining avascular for a much longer period than other parts of the retina (Engerman, 1976). The central fovea is not normally vascularized at any stage of development (Provis *et al.*, 2000; Gariano *et al.*, 1994). This occurs despite the central retina being the most developmentally advanced and having the highest density of cells when compared to other parts of the retina (Provis, 2001; Hendrickson & Yuodelis, 1984) . The slow growth of temporal vessels contrasts with the usual

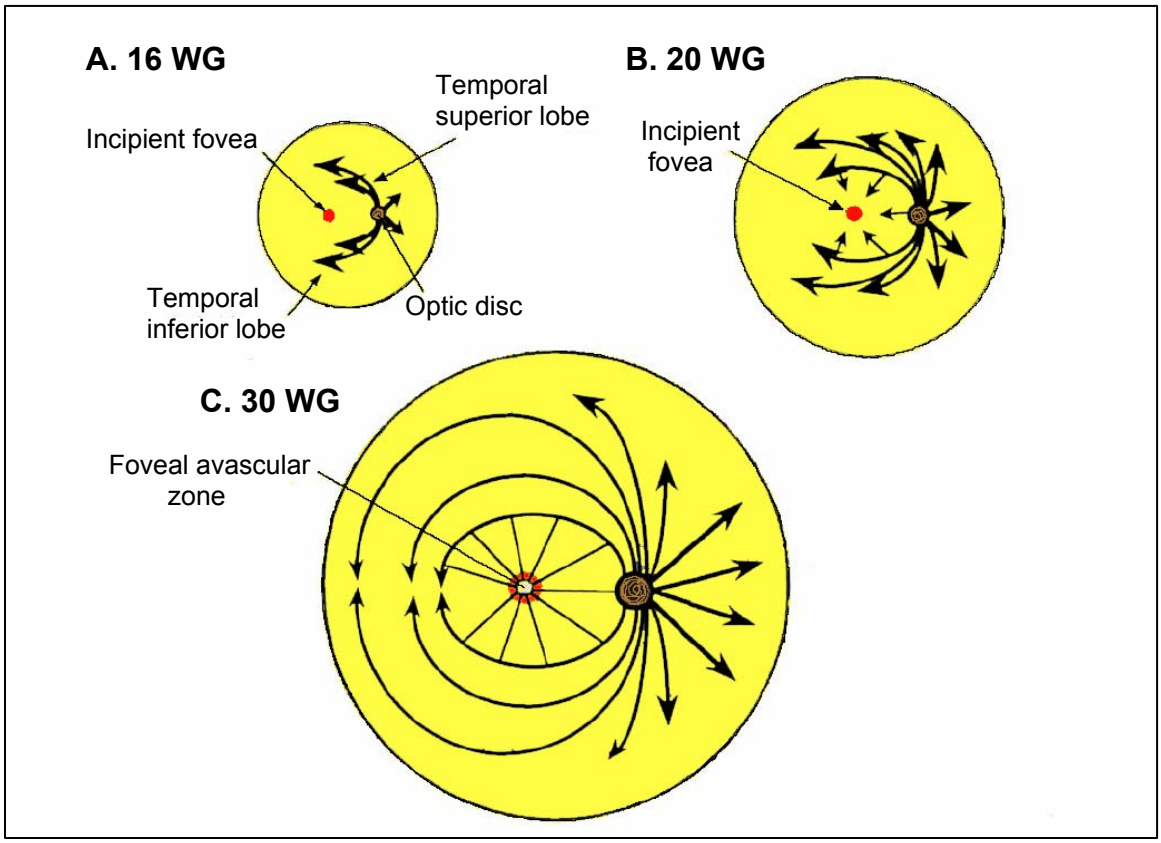

FIGURE 1.8 Retinal wholemounts showing growth patterns of the primary retinal vasculature at various stages of gestation. **A.** The earliest vessels (thick arrows) form four lobes corresponding with each retinal artery. **B.** The temporal lobes skirt around the incipient fovea with small branches from the lobular vessels establishing the ganglion cell layer plexus (GCP small arrows). **C.** GCP vessels anastomose around the fovea defining the foveal avascular zone. (Adapted from Provis, 2001).

mechanism of retinal vascularisation, where endothelial cell growth is thought to be mediated by hypoxia produced by high metabolic demand, such as increased numbers of active photoreceptors, which in turn increase VEGF expression and stimulate angiogenic and vasculogenic vessel development (Provis, 2001; Stone *et al.*, 1999; Stone *et al.*, 1995). Cell proliferation in the vascular complex increases with retinal maturation except when retinas are older than 20WG, where cell proliferation is found to be lowest near the fovea before the time the deep plexus forms (Sandercoe *et al.*, 1999). The diameter of the foetal FAZ is similar to the adult avascular zone, suggesting that remodelling occurs in a dynamic fashion as the foveal pit develops. Because the adult avascular zone outlines the foveal slope, and vessel growth near the fovea is retarded together with reduced cell proliferation, an inhibitory molecule within the foetal fovea potentially marks out the future foveal zone repelling astrocytes, blood vessels and ganglion cell axons from this region (Provis, 2001; Provis *et al.*, 2000).

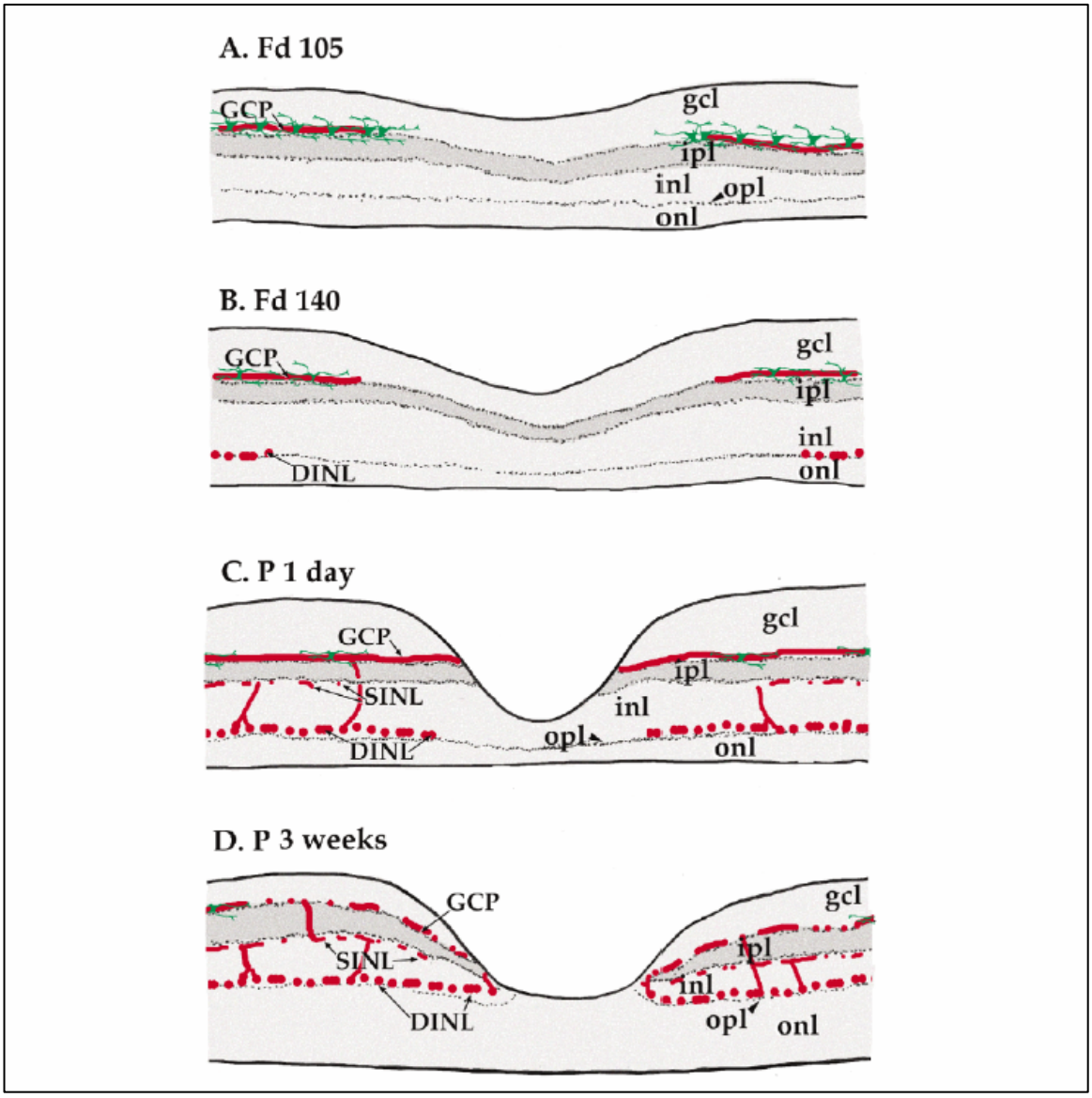

FIGURE 1.9 Stages of formation of the perifoveal capillary plexus in monkey (fd: foetal day and P: postnatal). **A.** GCP vessels (red) define the avascular area lead by astrocytes (green) followed by formation of the foveal depression. **B.** DINL then SINL capillaries approach the developing foveal depression about six weeks after the GCP. **C.** SINL capillaries form in the deep plexus in the perinatal period. **D.** Anastomosis of GCP and deep plexus around the foveal depression in early postnatal period (Provis, 2001).

1.2 THE ROLE OF TRANSFORMING GROWTH FACTOR-β IN RETINAL DEVELOPMENT

Primate retinal development is a highly complex and controlled process that involves expression of several families of growth factors, acting in a tightly regulated spatial and temporal sequence. Earlier studies from this laboratory demonstrated the importance of FGF and VEGF in normal development of cone photoreceptors and retinal vasculature (Cornish *et al.*, 2004c; Cornish *et al.*, 2004b; Cornish *et al.*, 2004a; Cornish *et al.*, 2005; Sandercoe *et al.*, 2003).

As discussed previously (Chapter 1.1), as blood vessels approach the incipient primate fovea, proliferation of endothelial cells and astrocytes is reduced in this region and along the horizontal meridian; the FAZ is also clearly defined before formation of the foveal depression. Taken together with the observation that endothelial cells and astrocytes do not enter the developing fovea at any time during development, these findings suggest that a factor(s) with anti-proliferative, anti-migratory and/or anti-angiogenic properties may be expressed in the incipient foveal region, prior to physical marking of the FAZ by astrocytes and endothelial cells (before 23 to 25WG in humans, and before ~fd100 in monkey).

Previous studies indicate that one potential factor is Transforming Growth Factor-β (TGF-β), and the following section discusses in detail the structure and properties of TGF-β and its receptors in the context of its potential role in the developing human fovea.

The Transforming Growth Factor (TGF)–β family are multifunctional, naturally occurring proteins that regulate cell growth, differentiation, migration and extracellular matrix (ECM) production and play important roles in embryonic development, wound healing, immune responses and vascular development in species from flies and worms to mammals (Duenker, 2005; Shi & Massague, 2003; Govinden & Bhoola, 2003; Schuster & Krieglstein, 2002; Ten Dijke *et al.*, 2002; Mummery, 2001; Zhao and Overbeek, 2001; Bottner *et al.*, 2000; Dunker & Krieglstein, 2000; Patterson & Padgett, 2000;

Massague *et al.*, 2000; Clark & Coker, 1998; Massague, 1998; Lawrence, 1996; Saltis, 1996; Nishida *et al.*, 1995; Cox, 1995; Pasquale *et al.*, 1993).

TGF-β is the prototype of a growing superfamily of peptide growth factors, containing TGF-β isoforms, activin/inhibin family, bone morphogenetic protein (BMP) family, Müllerian inhibiting substance, glial cell derived neurotrophic factor (GDNF), and other factors that are characterised by structural similarities and similar signalling cascades but with functional diversity (Duenker, 2005; Itoh *et al.*, 2000; Massague, 2000; Massague *et al.*, 1990; Roberts & Sporn, 1989). There are seven genetically distinct TGF-β isoforms TGF-β1, TGF-β1.2, TGF-β2, TGF-β2.3, TGF-β3, TGF-β4 and TGF-β5 (Clark & Coker, 1998; Lutty *et al.*, 1991; Roberts *et al.*, 1990a; Rizzino, 1988). Only three isoforms TGF-β1, TGF-β2 and TGF-β3 have been detected in mammals (Pasquale *et al.*, 1993; Roberts *et al.*, 1990a).

The TGF-β isoforms have been widely recognised as a prototype of multifunctional growth factors and master switches in the regulation of key events in development, disease and repair (Bottner *et al.*, 2000; Kingsley, 1994; Wahl, 1992; Roberts *et al.*, 1990a).

The essential role of the TGF-β family in normal development has been demonstrated in studies of TGF-β isoform knockout mice.

In TGF-β1 knockout mice, 50% of animals die in utero and the remainder succumb to uncontrolled inflammation by 3 to 6 weeks post birth (Javelaud & Mauviel, 2004; Clark & Coker, 1998). TGF-β2 deficient mice reveal obvious ocular malformations, including cell migration into the posterior chamber of the eye, hyperplastic retinas and decreased thickness of the corneal stroma (Sanford et al., 1997). TGF-β3 knockout mice do not reveal an eye phenotype, but show defects in palate fusion, heart and lung development (Duenker, 2005; Kaartinen *et al.*, 1997; Cox, 1995; Proetzel *et al.*, 1995). Interestingly, overexpression of TGF-β1 in TGF-β2 null mice rescues the abnormalities in ocular development caused by the deletion of TGF-β2 (Saika, 2005; Zhao & Overbeek, 2001a; Proetzel *et al.*, 1995; Shull & Doetschman, 1994; Kaartinen *et al.*, 1995). These studies clearly demonstrate that all TGF-β isoforms display overlapping spatial and temporal

expression patterns in most tissues, and that ablation of one TGF-β isoform may be compensated for by another isoform resulting in a lack of an obvious phenotype (Duenker, 2005).

1.2.1 STRUCTURE OF TRANSFORMING GROWTH FACTOR-β

TGF-β is part of a growth factor superfamily comprising more than 50 members, which have been grouped according to sequence similarities. This encompasses activins, glial cell line-derived neurotrophic factor (GDNF) sub-family and bone morphogenic proteins (BMP) including the decepentaplegic (Dpp) and the vegetal-1 related group (DVR) (Bottner *et al.*, 2000) (Figure 1.10).

The three mammalian isoforms encoded by the three distinct genes are structurally nearly identical with nine conserved cysteine residues and 76-80% amino acid homology. These are synthesised by many cell types including platelets, macrophages, fibroblasts and tumour cells (Javelaud & Mauviel, 2004), and secreted as latent precursor molecules which need to be activated by changing into the mature form for receptor binding and activation of signalling pathways (Javelaud & Mauviel, 2004; Barcellos-Hoff, 1996). In humans TGF-β1, TGF-β2 and TGF-β3 are located on three different chromosomes, 19q13, 1q41, 14q24 respectively (Govinden & Bhoola, 2003; Roberts, 1998; Cox, 1995; ten Dijke *et al.*, 1988).

The TGF-β molecules consist of 390 to 414 amino acids, and contain an amino-terminal hydrophobic signal peptide region, the 249 residue latency-associated-peptide (LAP) region and the C-terminal, bioactive region that has 112 amino acids per monomer (Javelaud & Mauviel, 2004) (Figure 1.11A). They are characterised by a knot composed of six cysteines that form three intramolecular disulfide bonds - two of which form an eight membered ring, which is traversed by the third cysteine bond that helps stabilise several β-sheet bands (Figure 1.11B). A seventh cysteine makes an intermolecular cysteine bridge that links the two monomers into a functional dimer, providing additional stabilisation due to hydrogen bonds between the monomers (Javelaud & Mauviel, 2004; Bottner *et al.*, 2000; McDonald & Hendrickson, 1993) (Figure 1.11B).

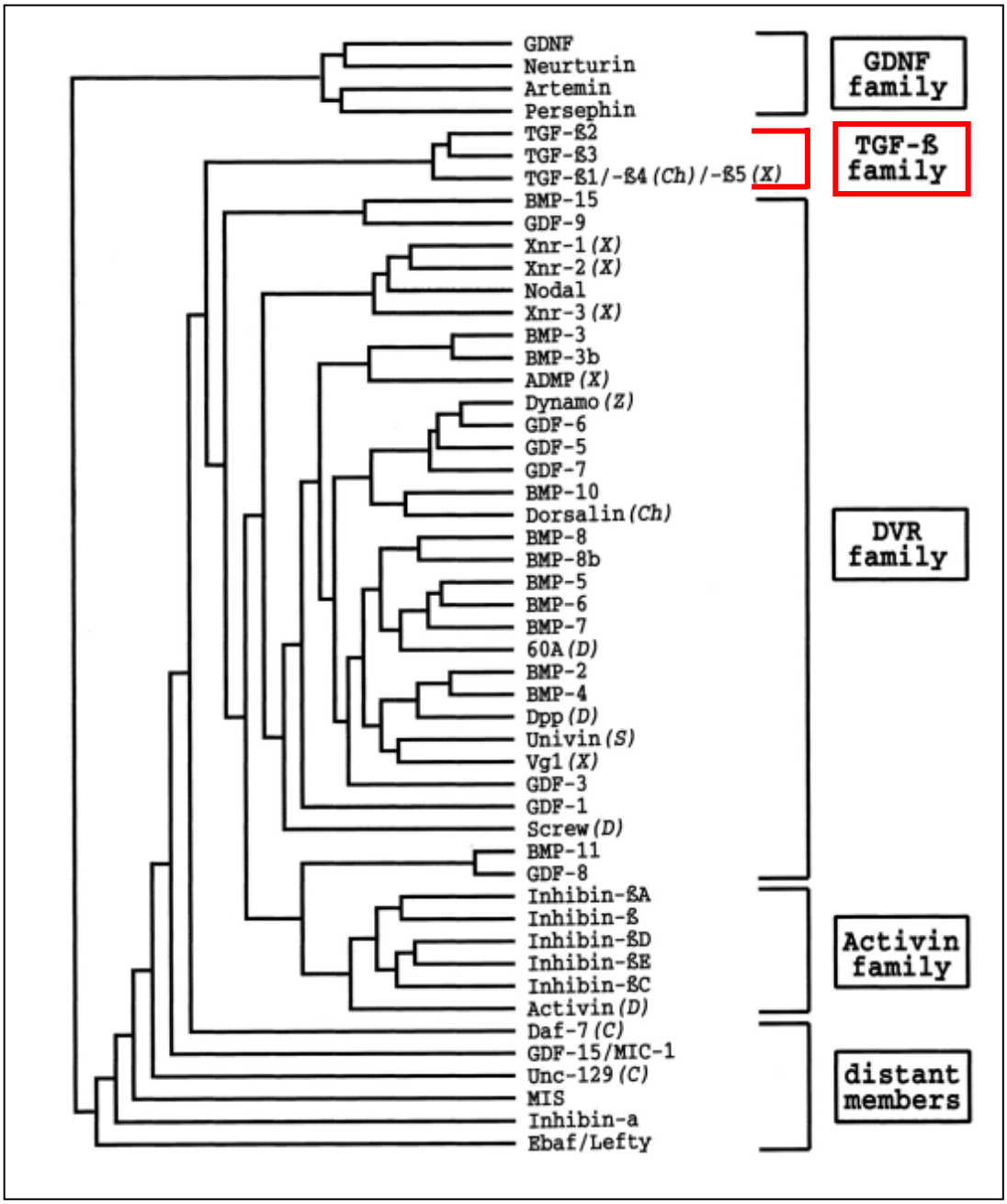

FIGURE 1.10 Dendrogram showing members of the TGF-β superfamily where amino acid sequences of the carboxy terminal domains of various mammalian members of the TGF-β superfamily were compared unless indicated otherwise with (C) C. elegans; (Ch), chicken; (D), Drosophila; (S), Sea urchin; (X), Xenopus; (Z), Zebrafish. (Adapted from figure 1, Bottner et al., 2000).

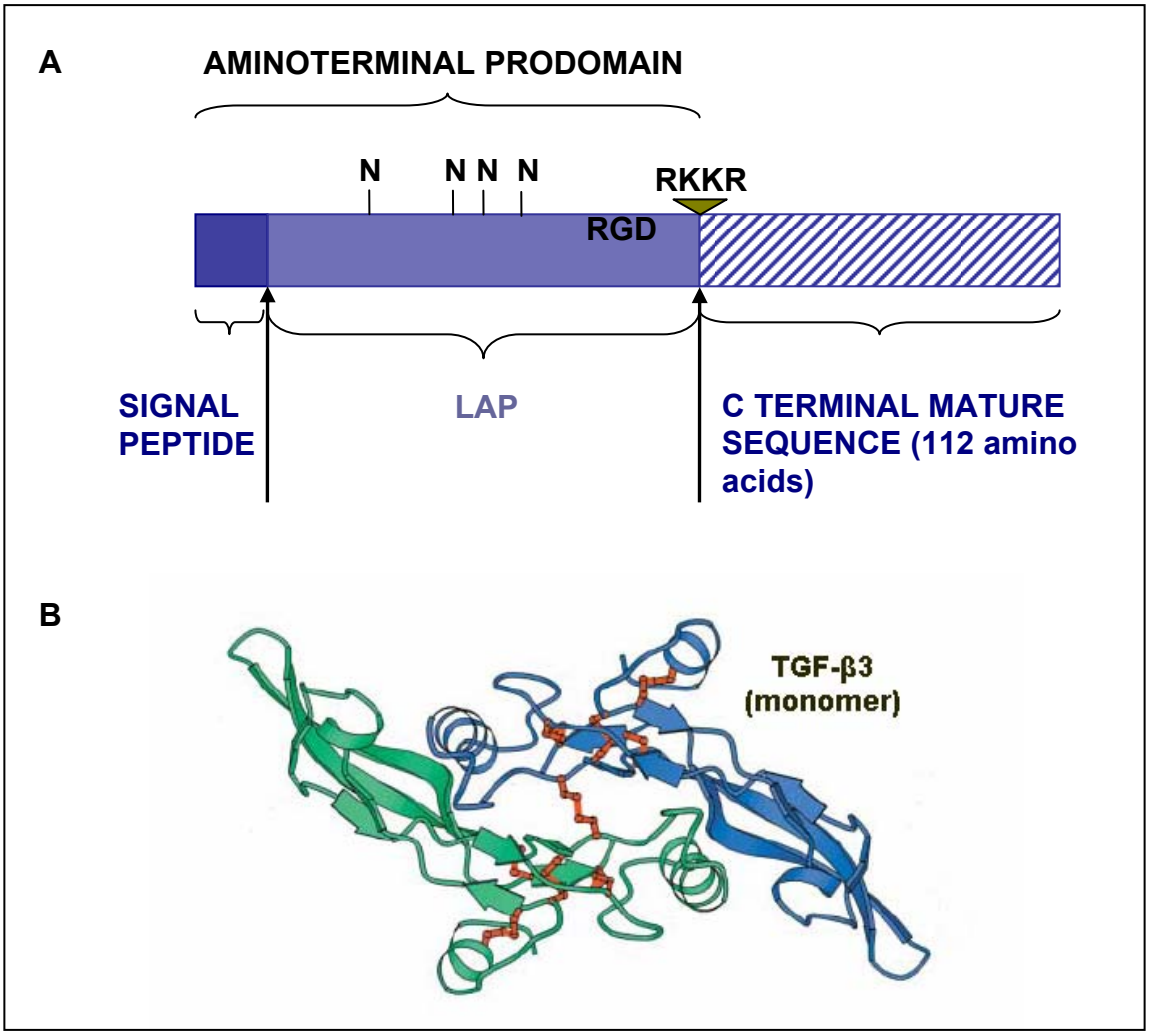

FIGURE 1.11 A. Simplified diagram of the TGF-β molecule**.** The total protein consists of 412 amino acids (aa) where the aminoterminal prodomain = Signal peptide and latency associated protein (LAP), with 4 nitrogen glycosylation sites and the potential fibronectin/vitronectin recognition site RGD. The prodomain is proteolytically cleaved at an RKKR site to release a mature carboxyterminal subunit of 112aa. (Arrows refer to cleavage sites). (Adapted from Cox, 1995). **B.** Structure of representative TGF-β ligand, TGF-β3 (Mittl *et al.*, 1996). The two ligands are coloured blue and green, cysteine side chains and disulfide bonds are represented by the red lines. The two monomers are linked by a disulfide bond. (Adapted from Figure 3A, Shi and Massague, 2003).

The LAP and signal peptide are important in disulfide bond formation, folding and exporting the mature protein (Cox, 1995).The three mammalian isoforms are regulated at the transcriptional level (Govinden & Bhoola, 2003; Roberts, 1998). They are transcribed as TGF-β precursor mRNA, with the 3' region corresponding to the mature TGF-β region and the 5' region corresponding to the latency associated peptide LAP (Nishida *et al.*, 1995; Miyazono *et al.*, 1988).

Mature TGF-β is a 24kDa homodimer that is noncovalently associated with the 80kDa LAP, which together are known as latent TGF-β (LTGF-β). The LAP is required for efficient secretion, preventing binding to ubiquitous cell surface receptors.

The LTGF-β complex may be stored in granules in platelets or secreted by all cells, and can bind to a cell membrane associated mannose-6-phosphate receptor, circulate or bind to the ECM (Govinden & Bhoola, 2003; Clark & Coker, 1998; Munger *et al.*, 1997; Gleizes *et al.*, 1996). Latent TGF-β is usually secreted as a large latent complex (LLC) covalently bound via the LAP region to latent TGF-β binding protein (LTBP) or as a small latent complex (SLC) without LTBP. Newly synthesised TGF-β is released from most cells as the LLC (Govinden & Bhoola, 2003; Munger *et al.*, 1997; Gleizes *et al.*, 1996; Nishida *et al.*, 1995; Olofsson *et al.*, 1992) (Figure 1.12). LTBP1 is involved in the sequestration of LTGF-β in the ECM and in the regulation of its activation in the extracellular environment by ensuring the correct folding, secretion and target of TGF-β (Figure 1.13) (Govinden & Bhoola, 2003; Saharinen & Keski-Oja, 2000; Munger *et al.*, 1997; Gleizes *et al.*, 1996). The LAP confers latency to the complex whereas LTBP1 serves to bind TGF-β to the ECM and enable its proteolytic activation (Govinden & Bhoola, 2003; Gualandris *et al.*, 2000).

Conformational changes of the LTGF-β complex as a result of LAP cleavage by plasmin, thrombin, plasma transglutinases or endoglycosylases, or physical interactions of the LAP with other proteins such as TSP-1, leads to the release and activation of TGF-β (Javelaud & Mauviel, 2004; Zhao & Overbeek, 2001a; Khalil, 1999; Nishida *et al.*, 1995; Lutty *et al.*, 1993; Lyons*et al.*, 1988).

The biological half life of TGF-β is short, ~1hour, and it is rapidly cleared via the action of scavenger molecules such as α-2-macroglobulin (Dennler *et al.*, 2002; Vaughan & Vale, 1993; Wakefield *et al.*, 1990).

1.2.2 TRANSFORMING GROWTH FACTOR-β RECEPTORS

Members of the TGF-β superfamily signal through a family of transmembrane receptor-linked serine/threonine kinases that have a short cysteine-rich extracellular domain, a single transmembrane domain and an intracellular serine/threonine kinase domain via mediators of TGF-β signalling known as Smads (Duenker *et al.*, 2005; Govinden & Bhoola, 2003; Padgett, 1999b; Padgett, 1999a; Heldin *et al.*, 1997; Attisano & Wrana, 1996; Massague, 1996; Massague & Weis-Garcia, 1996; Miyazono *et al.*, 1994). The biological effects of TGF-β are exerted via specific binding interactions involving two distinct membrane bound receptors, types I and II (TβRI and TβRII) (Figure 1.14). A third receptor, type III (TβRIII), has also been identified, with no known signalling function.

The dimeric arrangement of the ligands suggests the formation of a tetrameric complex with TβRI and TβRII (Bottner *et al.*, 2000; Yamashita *et al.*, 1994). The receptor serine/threonine kinase family in the human genome comprises 12 members: 7 type I and 5 type II receptors all dedicated to TGF-β signalling (Shi & Massague, 2003; Manning *et al.*, 2002). TGF-β displays a high affinity for type II receptors and does not interact with the individual type I receptors (Shi & Massague, 2003; Massague, 1998). Initially, the ligand binds tightly to the ectodomain of the type II receptor, which allows subsequent incorporation of the type I receptor, forming a large ligand-receptor complex involving a ligand dimer and four receptor molecules (Duenker, 2005; de Caestecker, 2004; Shi & Massague, 2003; Itoh *et al.*, 2000; Miyazono, 2000; Wrana & Attisano, 2000; Heldin *et al.*, 1997; Cox, 1995; Wrana *et al.*, 1994; Wrana *et al.*, 1992). Structural analysis reveals that binding occurs at the far ends of the elongated ligand dimer where each receptor binds to one monomer of the dimeric TGF-β (Shi & Massague, 2003; Hart *et al.*, 2002). Binding to the extracellular domains of both types of receptors by the dimeric ligand induces close proximity and productive conformation for the intracellular kinase domains of the receptors, facilitating

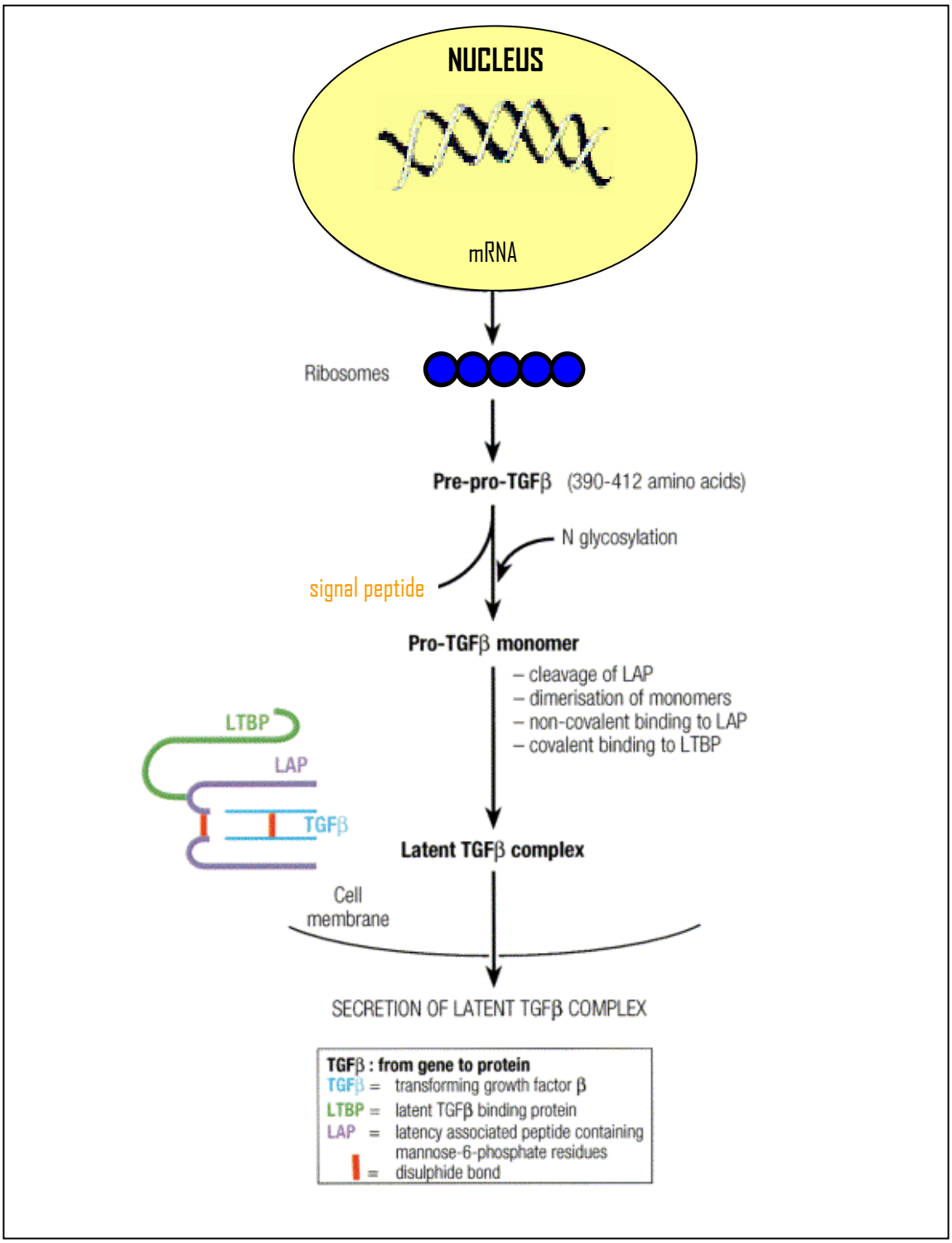

FIGURE 1.12 Synthesis and secretion of TGF-β1 – from gene to released product. Process for TGF-β2 and TGF-β3 isoforms is similar. (Adapted from Clark and Coker, 1998).

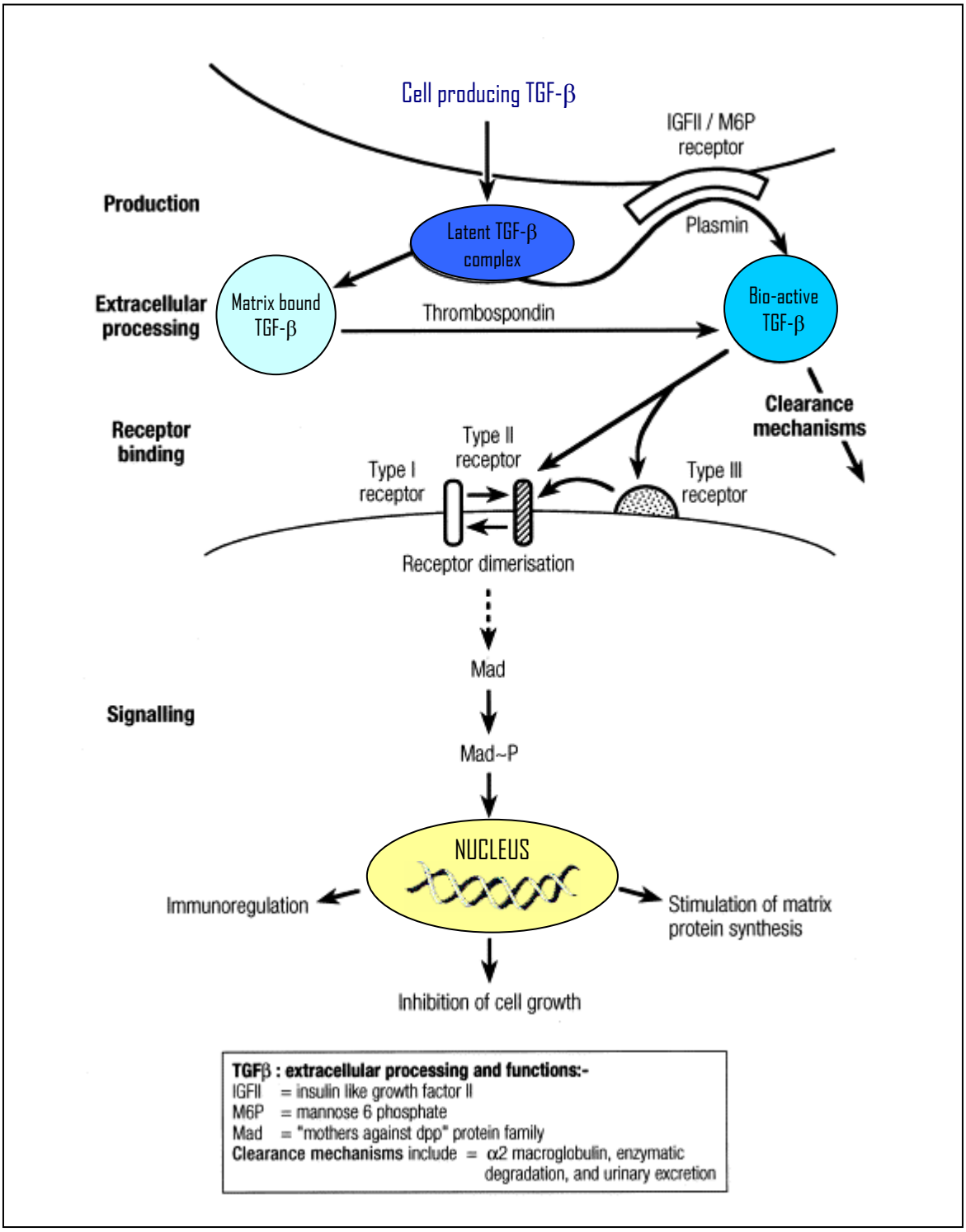

FIGURE 1.13 Diagram showing the extracellular pathway for TGF-β, which is released in the latent form, acts on receptors and is subsequently catabolised. (Adapted from Clark and Coker, 1998).

the phosphorylation and subsequent activation of the type I receptor (Govinden & Bhoola, 2003; Wrana, 1998) (Figure 1.14 and Figure 1.15).
TβRI has a highly conserved sequence known as the “GS” domain, which contains a repetitive glycine-serine motif between transmembrane and kinase domains. TβRII has more distantly related kinase domains (Bottner *et al.*, 2000; Franzen *et al.*, 1995; Wieser *et al.*, 1995). The GS region in TβRI is phosphorylated by TβRII leading to its activation, and is an important regulatory domain for TGF-β signalling (Shi & Massague, 2003; Massague, 1998). TβRII has a large C terminal extension that is rich in serine and threonine (Govinden & Bhoola, 2003; Liu *et al.*, 1995). The membrane-anchored proteoglycan, betaglycan or endoglin, also known as TGF-β type III receptor (TβRIII), has a large extracellular domain, a single transmembrane domain and a short cytoplasmic region lacking apparent signalling function (Gomes *et al.*, 2005; Massague, 1998; Lopez-Casillas *et al.*, 1991; Cheifetz *et al.*, 1988).

The steps leading to receptor activation are tightly controlled by two classes of molecules with opposing function. One class acts as ligand binding traps, binding to TGF-β and stopping access to membrane receptors, as seen for example with the LAP, which is the pro-region of the TGF-β precursor. The other class includes membrane anchored proteins that act as co-receptors, promoting ligand binding to the signalling receptors. TβRIII mediates TGF-β binding to TβRII, which is particularly important for TGF-β2, but so far there is no evidence of it being able to transduce the signal (Javelaud & Mauviel, 2004; Shi & Massague, 2003; Brown *et al.*, 1999; Massague, 1998).

Once TGF-β binds to TβRII, it forms a heteromeric complex with TβRI, with subsequent phosphorylation and activation of TβRI (Govinden & Bhoola, 2003; Attisano & Wrana, 2000; Padgett, 1999a; Massague, 1998; Heldin *et al.*, 1997; Wrana *et al.*, 1994). The activated TβRI interacts with an adaptor protein, Smad anchor for receptor activation (SARA) (Duenker, 2005; Shi & Massague, 2003; Tsukazaki *et al.*, 1998), which transfers signals to intracellular mediators known as Smads (ten Dijke & Hill, 2004; Govinden & Bhoola, 2003; Attisano & Wrana, 2000; Derynck *et al.*, 1998; Massague, 1998; Heldin *et al.*, 1997).

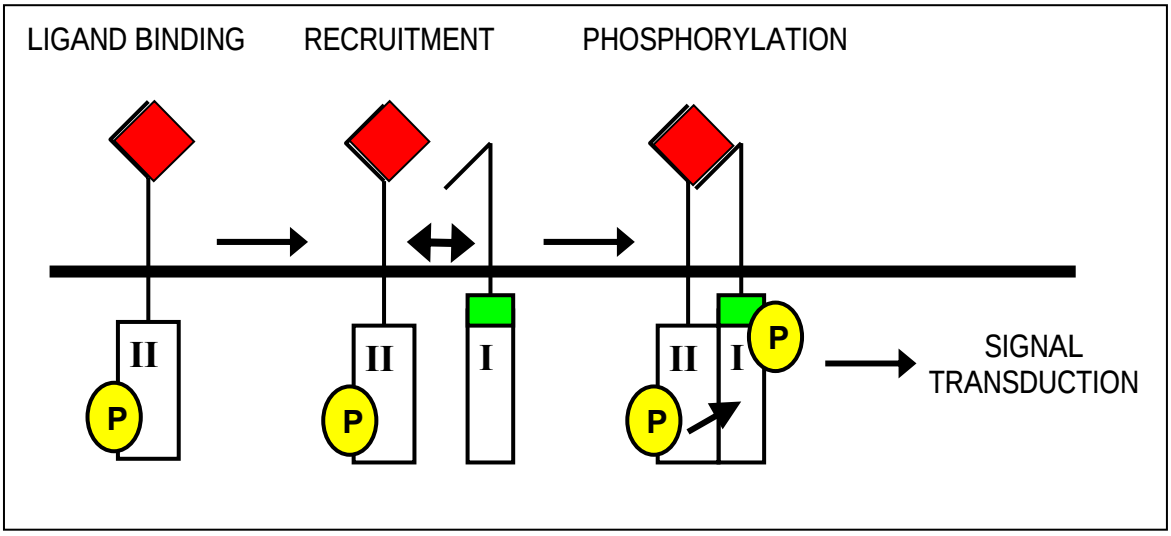

FIGURE 1.14 Simplified diagram of TGF-β ligand (red square) binding to TβRII, recruiting TβRI with subsequent phosphorylation resulting in signal transduction.

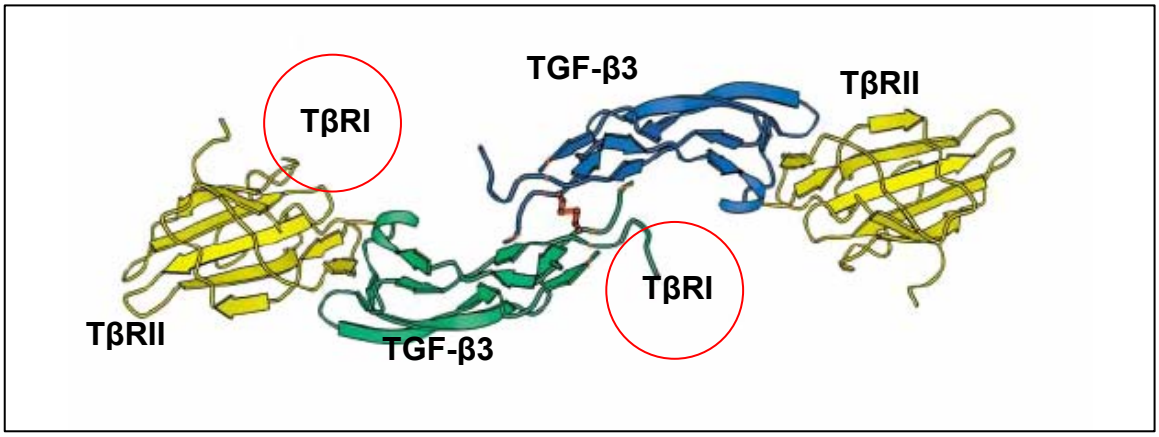

FIGURE 1.15 Structure of the extracellular ligand binding domain of TβRII bound to TGF-β3 (Hart *et al.*, 2002). The predicted TβRI binding sites are shown by red circles. Disulfide bond is marked by a red line. (Adapted from figure 4C, Shi and Massague, 2003).

Although each Smad has a specific role, all have conserved amino (N-terminal) and carboxyl terminal Mad-homology (MH) domains known as MH1 and MH2 respectively (Javelaud & Mauviel, 2004; Govinden & Bhoola, 2003). There are eight Smad proteins constituting three functional classes: receptor regulated Smads (R-Smad), Co-mediator Smads (Co-Smad) and inhibitory Smads (I-Smad) (Bottner *et al.*, 2000).

R-Smads (Smad 1,2,3,5 and 8) are directly phosphorylated and activated by the TβRI kinases and undergo homotrimerisation and formation of heteromeric complexes with Co-Smad, Smad 4 (Bottner *et al.*, 2000; Heldin *et al.*, 1997; Chen *et al.*, 1996; Lagna *et al.*, 1996; Zhang *et al.*, 1996). The activated Smad complexes are translocated into the nucleus and together with other nuclear cofactors, activate specific target genes via interactions with DNA and DNA-binding proteins (Govinden & Bhoola, 2003; Zhang *et al.*, 1998). Smad 4 only translocates to the nucleus when complexed with R-Smads, whereas ligand-activated Smad 2 and Smad 3 may translocate into the nucleus in a Smad 4 independent fashion. In the absence of Smad 4, neither Smad 2 nor Smad 3 is capable of transcriptional activity, suggesting that the principal function of Smad 4 is to regulate transcription rather than to transmit signals from the cytoplasm to the nucleus (Javelaud & Mauviel, 2004; Massague & Chen, 2000).

I-Smads, Smad 6 and Smad 7, negatively regulate TGF-β signalling by competing with R-Smads for receptor or Co-Smad interaction, and by targeting the receptors for degradation (Duenker, 2005; ten Dijke & Hill, 2004; Shi & Massague, 2003; Bottner *et al.*, 2000; Hill, 1999).

Aside from the Smads that are highly specific substrates for the TGF-β receptor kinases, other signalling pathways may also be activated by TGF-β in a context and cell type specific manner. These include the mitogen activated protein kinase (MAPK) cascades (p38, ERK, JNK), phosphatidyl-inositol-3-kinase, and PP2A/p70s6K, though the molecular details of these couplings are obscure (Javelaud & Mauviel, 2004; de Caestecker *et al.*, 2000; Mulder, 2000).

1.2.3 TRANSFORMING GROWTH FACTOR-β FUNCTION

The biological activity of TGF-β is multifunctional and TGF-β is involved in cell-cycle control, regulation of early development, differentiation, ECM formation, hematopoiesis, angiogenesis, chemotaxis, and immune functions (Bottner *et al.*, 2000; Cox, 1995).

TGF-βs are contextually acting molecules that can either stimulate or repress cell proliferation depending on cell type, differentiation status, cellular environment, and the presence or absence of other growth factors, cytokines and ECM components (Duenker, 2005; Unsicker & Krieglstein, 2000; Combs *et al.*, 2000; Gold, 1999; Ashley *et al.*, 1998; Roberts *et al.*, 1990a; Roberts *et al.*, 1990b), are neurotrophic (Duenker, 2005; Krieglstein *et al.*, 1998a; Krieglstein *et al.*, 1998b; Krieglstein *et al.*, 1998c) or induce cell death (Duenker, 2005; Krieglstein *et al.*, 2000; Hata *et al.*, 1998; de Luca *et al.*, 1996). They are important mediators of normal developmental and repair processes in the embryo, neonate and adult, with roles in tissue morphogenesis and differentiation, regulating cell proliferation, differentiation and expression of ECM proteins that may induce fibrosis and angiogenesis (Cox, 1995; Kingsley, 1994; Roberts *et al.*, 1990a; Roberts & Sporn, 1993; Sporn & Roberts, 1992; Pasquale *et al.*, 1993; Lutty *et al.*, 1991; Mustoe *et al.*, 1987; Ignotz & Massague, 1986; Laiho *et al.*, 1986; Roberts *et al.*, 1986; Sporn *et al.*, 1983).

TGF-β can enhance or antagonise the action of other growth factors on cells. For example, TGF-β can stimulate proliferation of osteoblasts, chondroblasts and mesothelial cells but inhibit proliferation of hepatocytes, haematopoietic stem cells, lymphocytes, endothelial cells and epithelial cells (Pfeffer *et al.*, 1994; Hunter *et al.*, 1993; Roberts *et al.*, 1990a; Roberts *et al.*, 1990b; Leschey *et al.*, 1990; Silberstein & Daniel, 1987; Jetten *et al.*, 1986). TGF-β1 enhances mitogenic effects of acidic fibroblast growth factor (aFGF, now known as FGF-1) and basic fibroblast growth factor (bFGF, now known as FGF-2) on osteoblasts (Pfeffer *et al.*, 1994; Hunter *et al.*, 1993; Flaumenhaft *et al.*, 1992; Globus *et al.*, 1988) but inhibits mitogenic effects of FGF-1 and FGF-2 on endothelial cells (Hunter *et al.*, 1993; Baird & Durkin, 1986).

Function of TGF-β in Brain and Nervous System

TGF-β expression starts early in the development of the nervous system and even though TGF-β1, TGF-β2 and TGF-β3 are often co-expressed, they have distinct spatiotemporal patterns. Each of the isoforms act as coordinated mediators of mesenchymal epithelial interactions, via their effects on the synthesis and composition of the ECM (Duenker, 2005).

The reported distribution and roles of TGF-βs in the developing and adult CNS are summarised in Table 1.1.

TABLE 1.1 TGF-β actions in the nervous system

GROWTH FACTOR	FUNCTION
TGF-β1	Neuroprotection against glutamate toxicity (Prehn *et al.*, 1993; Prehn & Krieglstein, 1994; Bruno *et al.*, 1998; Buisson *et al.*, 1998; Docagne *et al.*, 2002)
	Survival of neurons (Krieglstein & Unsicker, 1994; Prehn & Krieglstein, 1994; Krieglstein *et al.*, 1998a; Krieglstein *et al.*, 1998b; Krieglstein *et al.*, 1998c; Schober *et al.*, 1999; Zhu *et al.*, 2000b; Roussa *et al.*, 2004; Roussa & Krieglstein, 2004; Gomes *et al.*, 2005)
	Neuronal differentiation (Ishihara *et al.*, 1994; Abe *et al.*, 1996; Gomes *et al.*, 2005)
	Control of neuronal death and microgliosis (de Luca *et al.*, 1996; Brionne *et al.*, 2003)
	Control of astrocytic cytoskeleton, morphology and motility (Labourdette *et al.*, 1990; Toru-Delbauffe *et al.*, 1990; Morganti-Kossmann *et al.*, 1992; Baghdassarian *et al.*, 1993; Gagelin *et al.*, 1995; Laping *et al.*, 1994; Bottner *et al.*, 2000)
	Astrocyte differentiation (Rich *et al.*, 1999; Perillan *et al.*, 2002; de Sampaio e Spohr *et al.*, 2002; Sousa Vde *et al.*, 2004; Gomes *et al.*, 2005)

	Inhibition of astrocyte proliferation (Johns *et al.*, 1992; Lindholm *et al.*, 1992; Morganti-Kossmann *et al.*, 1992; Baghdassarian *et al.*, 1993; Hunter *et al.*, 1993; Vergeli *et al.*, 1995; Rich *et al.*, 1999)
	Extracellular matrix production (Liesi, 1985; Sanes, 1989; Wujek *et al.*, 1990; Baghdassarian *et al.*, 1993; Wyss-Coray *et al.*, 1995; Buisson *et al.*, 1998; Docagne *et al.*, 1999; Docagne *et al.*, 2002; Brionne *et al.*, 2003)
	Wound healing and immunosuppression (Pratt & McPherson, 1997)
	Cell migration in the cerebral cortex (Siegenthaler & Miller, 2004)
	Influence MHC expression (Schluesener, 1990; Johns *et al.*, 1992; Bottner *et al.*, 2000)
	Apoptosis in microglia (Xiao *et al.*, 1997; Bottner *et al.*, 2000)
	Inhibition of microglia proliferation (Bottner *et al.*, 2000)
	Inhibition of oligondendroglia migration (Fok-Seang *et al.*, 1998)
	Organisation of a glial scar (da Cunha *et al.*, 1993; Pratt & McPherson, 1997; Flanders *et al.*, 1998; Moon & Fawcett, 2001)
	Induction of blood brain barrier characteristics in endothelial cells (Garcia *et al.*, 2004)
TGF-β2	Neuroprotection against glutamate toxicity (Bruno *et al.*, 1998)
	Neuronal differentiation (Flanders *et al.*, 1991; Ishihara *et al.*, 1994; Unsicker *et al.*, 1996; Miller, 2003)
	Inhibition of mitogen-induced neuronal proliferation (Constam *et al.*, 1994)

	Neuronal migration (Flanders *et al.*, 1991; Miller, 2003)
	Survival of neurons (Poulsen *et al.*, 1994; Krieglstein & Unsicker, 1994; Krieglstein *et al.*, 1998a; Krieglstein *et al.*, 1998b; Krieglstein *et al.*, 1998c; Schober *et al.*, 1999; Farkas *et al.*, 2003; Roussa *et al.*, 2004; Roussa & Krieglstein, 2004)
	Apoptosis of cerebellar neurons (de Luca *et al.*, 1996)
	Inhibition of mitogen-induced astrocyte proliferation (Hunter *et al.*, 1993)
	Induction of microglia proliferation (Flanders *et al.*, 1991; Dobbertin *et al.*, 1997; Miller, 2003)
	Influence MHC expression (Schluesener, 1990; Johns *et al.*, 1992; Bottner *et al.*, 2000)
TGF-β3	Neuroprotection against glutamate toxicity (Prehn *et al.*, 1993; Prehn & Krieglstein, 1994)
	Neuronal differentiation (Flanders *et al.*, 1991; Unsicker *et al.*, 1996)
	Neuronal migration (Flanders *et al.*, 1991)
	Survival of neurons (Krieglstein & Unsicker, 1994; Poulsen *et al.*, 1994; Krieglstein *et al.*, 1998a; Krieglstein *et al.*, 1998b; Krieglstein *et al.*, 1998c; Schober *et al.*, 1999; Farkas *et al.*, 2003; Roussa *et al.*, 2004; Roussa & Krieglstein, 2004)
	Apoptosis of cerebellar neurons (de Luca *et al.*, 1996)
	Induction of midbrain dopaminergic phenotype (Farkas *et al.*, 2003)
	Inhibition of mitogen-induced astrocyte proliferation (Hunter *et al.*, 1993)

TGF-β and its Role in the Eye

All three TGF-β isoforms and type I and II receptors are present in developing and adult human eyes (Zhao & Overbeek, 2001a). TGF-βs are present in the cytoplasm of cells in the retina-RPE-choroid complex, including photoreceptors, ganglion cells, Müller cells, RPE and vascular cells (choroidal and retinal) as well as in the cornea, lens, tears, aqueous and vitreous humour (Duenker, 2005; Hu *et al.*, 1998; Majima, 1997; Kokawa *et al.*, 1996; Anderson *et al.*, 1995; Pfeffer *et al.*, 1994; Tripathi *et al.*, 1994b; Tanihara *et al.*, 1993; Helbig *et al.*, 1991; Knisely *et al.*, 1991; Jampel *et al.*, 1990). The primary ligand in the postnatal retina is TGF-β2, mainly expressed by inner retinal neurons. TGF-β receptors have been found in cornea, ciliary body, iris, lens, retinal cells, RPE and brain (Duenker, 2005; Gomes *et al.*, 2005; Dunker & Krieglstein, 2003; Miller, 2003; MacConell *et al.*, 2002; Yamanaka *et al.*, 2002; Bottner *et al.*, 2000; Galter *et al.*, 1999; Obata *et al.*, 1999; Bottner *et al.*, 1996).

TGF-β And Eye Growth

TGF-β isoforms play an important role in normal eye development and growth, and during pathology (Table 1.2).

For example, TGF-β1 and TGF-β3 deficient mice have no ocular abnormalities but TGF-β2 deficient mice display several ocular defects including a thinned cornea with loss of corneal endothelium, a shallow anterior chamber, an immature retina and persistent vitreous vessels (Saika, 2005; Proetzel *et al.*, 1995; Shull & Doetschman, 1994; Kaartinen *et al.*, 1995; Sanford *et al.*, 1997). Overexpression of TGF-β1 in TGF-β2 null mice rescues the abnormalities in ocular development caused by the deletion of TGF-β2 (Saika, 2005; Zhao & Overbeek, 2001a).

Transgenic mice expressing a self-activating form of TGF-β1 exhibit anterior subcapsular cataracts by 3 weeks postnatal, with corneal opacities and defects in the iris and ciliary body and retinal vascular deficiency, with subsequent retinal degeneration (Zhao & Overbeek, 2001a; Srinivasan *et al.*, 1998). Retinal thickness is reduced in this model, due to an absence of blood vessels in some areas of the retina (Zhao & Overbeek, 2001a). Corneal

stromal growth is stimulated, reversing the corneal phenotype found in TGF-β2-null embryos (Zhao & Overbeek, 2001a).

As mentioned above, TGF-β2 deficient mice revealed ocular malformations, including hyperplastic retinas and decreased corneal stromal thickness, suggesting that these defects did not overlap with other TGF-β knockout mice defects (Sanford *et al.*, 1997). TGF-β3 knockout mice do not reveal an eye phenotype, only defects in palate fusion and lung development (Duenker, 2005; Kaartinen *et al.*, 1997; Proetzel *et al.*, 1995). However when TGF-β2 and TGF-β3 knockout mice were studied, the neural retina was consistently detached from the underlying RPE, with a thickened inner retina and a vascularised accumulation of cells in the posterior chamber of the eye (Dunker & Krieglstein, 2003). The retinal detachment being probably due to the fact that TGF-βs are regulators of mesenchymal-epithelial interactions and ECM assembly (Duenker, 2005; Roberts & Sporn, 1992; Heine *et al.*, 1987). Increased retinal thickness may be due to decreased programmed cell death, rather than an increase in proliferation, mediated by TGF-β signalling (Dunker & Krieglstein, 2003).

TGF-β3 exhibits unique antiscarring properties in knockout animals in which embryonic wound healing is not scarless, as opposed to embryos expressing TGF-β3 (Javelaud & Mauviel, 2004; O'Kane & Ferguson, 1997). Manipulation of the ratios of TGF-β, especially by raising the levels of TGF-β3 relative to TGF-β1 and TGF-β2 reduces scarring and fibrosis (O'Kane & Ferguson, 1997; Giri *et al.*, 1993).

The loss of Smad-3 does not produce ocular abnormalities, indicating that multiple signalling pathways are involved in ocular tissue morphogenesis (Saika, 2005).

Even in the postnatal eye the control of ocular growth is important in order to ensure high visual acuity with the correct relationship between axial eye length and the optical power of the eye. In the chicken embryo it was found that TGF-β1 and FGF-2 act in a push-pull fashion to control the release of matrix degrading proteases from capillary endothelial cells to regulate scleral thickness (Anderson *et al.*, 1995; Rohrer & Stell, 1994; Hageman *et al.*, 1991; Edwards *et al.*, 1987; Presta *et al.*, 1986; Ignotz & Massague, 1986).

TABLE 1.2 Effects of TGF-β in the Eye

GROWTH FACTOR	FUNCTION
TGF-β overall	Inhibition of progenitor proliferation in the retina (Close *et al.*, 2005)
	Induction of apoptosis in the retina (Duenker, 2005; Duenker *et al.*, 2005; Siegel & Massague, 2003; Schuster *et al.*, 2003; Schuster *et al.*, 2002; Valderrama-Carvajal *et al.*, 2002; Dunker *et al.*, 2001; Buenemann *et al.*, 2001; Larisch *et al.*, 2000; Frade & Barde, 1999)
	Enhancement of corneal epithelium migration and matrix deposition in wound repair (Kim *et al.*, 2004; Saika, 2004; Nishimura *et al.*, 1998; Mita *et al.*, 1998; Honma *et al.*, 1997; Wilson *et al.*, 1994; Mishima *et al.*, 1992)
	Inhibition of corneal epithelium proliferation (Nishida *et al.*, 1995)
	Promotion of lens fibre differentiation (Saika, 2005; Beebe *et al.*, 2004; Saika *et al.*, 2000; Pasquale *et al.*, 1993; Pelton *et al.*, 1991)
	Induction of cataract formation (Wormstone *et al.*, 2002; de Iongh *et al.*, 2001; Gordon-Thomson *et al.*, 1998)
	Inhibition of endothelial cell proliferation in vitreous (Zhao & Overbeek, 2001a; Spranger *et al.*, 1999; Lutty *et al.*, 1993; Connor *et al.*, 1989; Lutty *et al.*, 1985; Lutty *et al.*, 1983; Patz *et al.*, 1978; Jacobson *et al.*, 1984)
TGF-β1	TGF-β1 in the chick retina in vitro was found to inhibit DNA synthesis and induce an increase in the number of ECM molecules (Carri, 2003; Calvaruso *et al.*, 1997)
	Possible regulation of metabolism or healthy maintenance of photoreceptor or interphotoreceptor matrix (IPM) production in rod outer segments of adult eyes

	(Anderson *et al.*, 1995; Pfeffer *et al.*, 1994; Lutty *et al.*, 1991; Lutty *et al.*, 1993; Sporn *et al.*, 1987; Polans *et al.*, 1986)
	Stimulation of conjunctival scarring (Cordeiro *et al.*, 1999)
	Upregulation of ECM production in monkey eyes with experimentally induced glaucoma to aid remodelling of the lamina cribrosa of the optic nerve head (Fukuchi *et al.*, 2001)
	Upregulation of matrix degrading proteases to regulate scleral thickness in eye growth (Anderson *et al.*, 1995; Rohrer & Stell, 1994; Hageman *et al.*, 1991; Edwards *et al.*, 1987; Presta *et al.*, 1986; Ignotz & Massague, 1986)
TGF-β2	Inhibition of Müller cell proliferation (Close *et al.*, 2005; Ikeda & Puro, 1995)
	Possible regulation of metabolism or healthy maintenance of photoreceptor or IPM production in rod outer segments of adult eyes (Anderson *et al.*, 1995; Pfeffer *et al.*, 1994; Lutty *et al.*, 1991; Lutty *et al.*, 1993; Sporn *et al.*, 1987; Polans *et al.*, 1986)
	Stimulation of conjunctival scarring (Cordeiro *et al.*, 1999; Connor *et al.*, 1989)
	Transdifferentiation of conjunctival epithelium to corneal epithelium in wound repair (Pasquale *et al.*, 1993)
	Prevent apoptosis in the region of the optic nerve head assisting development (Duenker, 2005; Pena *et al.*, 1999)
	Related to intraocular pressure with increased TGF-β2 levels in aqueous humour in eyes with glaucoma (Lutjen-Drecoll, 2005; Gottanka *et al.*, 2004; Picht *et al.*, 2001; Tripathi *et al.*, 1994b; Cousins *et al.*, 1991; Jampel *et al.*, 1990)
	Upregulation of ECM production in eyes with glaucoma to aid remodelling of the lamina cribrosa of the optic nerve head

	(Fukuchi *et al.*, 2001; Pena *et al.*, 1999)
	Inhibition of endothelial cell proliferation by RPE (Anderson *et al.*, 1995; Pfeffer *et al.*, 1994)
TGF-β3	Possible regulation of metabolism or healthy maintenance of photoreceptor or IPM production in rod inner segments of adult eyes (Anderson *et al.*, 1995; Pfeffer *et al.*, 1994; Lutty *et al.*, 1991; Lutty *et al.*, 1993; Sporn *et al.*, 1987; Polans *et al.*, 1986)
	Stimulation of conjunctival scarring (Cordeiro *et al.*, 1999)
	Reduction in scarring and fibrosis by raising the levels of TGF-β3 relative to TGF-β1 and TGF-β2 (O'Kane & Ferguson, 1997; Giri *et al.*, 1993)
	Prevent apoptosis in the region of the optic nerve head during development (Duenker, 2005)

Effect of TGF-β on Neurons and Müller Cells

Retinal progenitor proliferation is regulated by extrinsic and intrinsic factors, it peaks around the day of birth and declines until approximately the end of the first postnatal week (Close *et al.*, 2005; Young, 1985). After this time there seems to be no renewed proliferation of either progenitors or Müller glia in the mammalian retina except under abnormal conditions (Close *et al.*, 2005; Fariss *et al.*, 2000; Sueishi *et al.*, 1996; Nork *et al.*, 1987). TGF-β has been implicated in the inhibition of proliferation in the nervous system as the postnatal decline in cerebellar precursor proliferation is paralleled by an increase in neuronal TGF-β2 expression, and TGF-β2 inhibits precursor proliferation in culture (Close *et al.*, 2005; Constam *et al.*, 1994).

Retinal neurons appear to provide both mitogenic and cytostatic factors. TGF-β signalling has an antiproliferative effect on cells of the postnatal rat retina, and inhibiting this endogenous signal with a TGF-β receptor blocker maintains proliferation of the progenitors past the developmental period in which the retina would normally become mitotically quiescent. Hence TGF-β

is an important inhibitor of progenitor proliferation in the postnatal retina (Close *et al.*, 2005). Mitogenic and growth inhibitory signals from one source

might finely tune the numbers and ratios of cells as they are born or as neurons die, resulting in properly functioning circuits (Close *et al.*, 2005; Alexiades & Cepko, 1996).

Müller cells express type I and II TGF-β receptors and TGF-β1 and TGF-β3 is localised to the cytoplasm in Müller cells which are uniquely positioned to deliver factors to retinal neurons as they span the entire retina (Anderson *et al.*, 1995). TGF-β receptors I and II are located in nestin positive progenitors early in development (P4) and Glast positive Müller glia later in development (P10) (Close *et al.*, 2005). They secrete TGF-β after stimulation with mitogens and scavenge debris in diabetic retinas (Close *et al.*, 2005; Ikeda *et al.*, 1998; Lutty *et al.*, 1991; Assoian *et al.*, 1987; Bloodworth & Molitor, 1965). Normally mammalian Müller glia do not proliferate after retinal development is complete. Even in disease states, such as diabetic retinopathy and retinitis pigmentosa few Müller glia enter mitosis (Close *et al.*, 2005; Fariss *et al.*, 2000; Sueishi *et al.*, 1996; Robison *et al.*, 1990; Nork *et al.*, 1987). A retina derived TGF-β signal may be responsible for the developmental decline in retinal proliferation without affecting cell death and Müller glial quiescence (Close *et al.*, 2005; Ikeda & Puro, 1995).
Inhibition of TGF-β signalling potentiates epidermal growth factor (EGF) stimulated Müller glial proliferation in vivo, enhancing the ability of Müller glia to re-enter the cell cycle in response to EGF so that TGF-β negatively regulates the proliferation of retinal progenitors and Müller glia in the developing retina (Close *et al.*, 2005; Milenkovic *et al.*, 2003; Ikeda & Puro, 1995; Scherer & Schnitzer, 1994; Roque *et al.*, 1992; Mascarelli *et al.*, 1991). The antagonistic interaction between the EGF and TGF-β pathways intracellularly may allow EGF to play a mitogenic role in the presence of anti-mitogenic TGF-β signals in the postnatal retina (Close *et al.*, 2005; ten Dijke *et al.*, 2000). The response to EGF and TGF-β signals received by a given cell are determined by the expression pattern of factors such as the Fox proteins, which are transcription factors that regulate Smad mediated transcription. Foxo-1 is more abundant centrally compared to the periphery, where it might facilitate TGF-β signalling in the central retina (Close *et al.*,

2005; Seoane *et al.*, 2004). The response to mitotic inhibitors such as TGF-β as well as the availability of mitogens shifts from conditions favouring proliferation to conditions that maintain quiescence at the termination of neurogenesis (Close *et al.*, 2005).

Role of TGF-β on Photoreceptors

The immunohistochemical localisation of TGF-β1 and TGF-β2 to photoreceptors in human donor eyes was the first suggestion of a retinal site of TGF-β although its function is speculative (Anderson *et al.*, 1995; Pfeffer *et al.*, 1994; Lutty *et al.*, 1991; Lutty *et al.*, 1993). Extracellular TGF-β1 was observed in cytoplasmic membrane of photoreceptor inner and outer segments whilst intracellular TGF-β2 was found in outer segments almost exclusively in rods as opposed to cone photoreceptors (Lutty *et al.*, 1993; Polans *et al.*, 1986). TGF-β1 and TGF-β2 are distributed more or less uniformly throughout the rod outer segment cytoplasm – maybe to regulate photoreceptor metabolism or to help in maintenance of healthy outer segments (Anderson *et al.*, 1995; Lutty *et al.*, 1991). In monkey retina, TGF-β1 and less intensely, TGF-β2 antibodies reacted with photoreceptor outer segments particularly rod outer segments with no difference between central and peripheral retina. TGF-β2 immunolabelling viewed with electron micrographs showed it to be intracellular, in outer segments, and not in the interphotoreceptor matrix (IPM-extracellular compartment between the photoreceptor outer segments and the RPE) (Pfeffer *et al.*, 1994). TGF-β3 is absent in photoreceptor outer segments but is compartmentalised in inner segments, within mitochondria concentrated in the rod and cone ellipsoids-possibly to regulate mitochondrial function. Moderate levels of TGF-β3 antibody labelling could be detected in the RPE cytoplasm within the mitochondrial rich zone of the photoreceptor inner segments (ellipsoid) and in the cytoplasm of the various cell types that form the retinal vasculature (Anderson *et al.*, 1995).

TGF-β function may affect secretion of extracellular protein constituents (eg IPM) associated with and synthesised by photoreceptors that do not accumulate in outer segments, but are secreted from the inner segment portion of the cell where protein synthesis occurs and where the cellular machinery for processing and release is located (Pfeffer *et al.*, 1994; Bok,

1985; Hollyfield *et al.*, 1985; Feeney, 1973). TGF-β is known to stimulate production of basement membrane components like collagen and fibronectin in several cells, so it could stimulate production of IPM components (Lutty *et al.*, 1991; Sporn *et al.*, 1987).

TGF-β in the Lens

Much of our understanding of the effects of TGF-β has come from studies done in the lens (McAvoy *et al.*, 2000). Heterogenous expression of all TGF-β isoforms is found in developing and adult human and animal crystalline lens (Saika, 2005; Saika *et al.*, 2000; Pasquale *et al.*, 1993; Pelton *et al.*, 1991).

Lens fibre differentiation is controlled by FGF, BMP and TGF-β (Saika, 2005; Tanaka *et al.*, 2004; Beebe *et al.*, 2004; McAvoy *et al.*, 2000). However, studies have shown that TGF-β can disrupt normal lens architecture and induce changes in lens cells that are similar to those described in human subcapsular cataracts (de Iongh *et al.*, 2005; Lovicu *et al.*, 2002; Hales *et al.*, 1995; Hales *et al.*, 1999; Schulz *et al.*, 1996). TGF-β induces the formation of spindle shaped cells containing α-smooth muscle actin, capsule wrinkling, apoptotic cell death and accumulation of ECM proteins such as laminin and fibronectin (de Iongh *et al.*, 2001). All isoforms can induce cataractous changes but TGF-β2 and TGF-β3 are around ten times more potent than TGF-β1 (de Iongh *et al.*, 2001; Wormstone *et al.*, 2002; Gordon-Thomson *et al.*, 1998).

TGF-β in the Vitreous

TGF-β is also found in the posterior chamber of the eye where all its isoforms were localised to hyalocytes (amoeboid and ovoid) in cortical vitreous (Lutty *et al.*, 1993). Hyalocytes were the only cells in the posterior segment of the eye that were immunoreactive for TGF-β1, TGF-β2 and TGF-β3 (Lutty *et al.*, 1993; Balazs, 1984). Most TGF-β activity in the vitreous is from TGF-β2, 84-100% whilst 10-21% is due to TGF-β1 (Dieudonne *et al.*, 2004; Connor *et al.*, 1989).

In this case, the main role for TGF-β appears to be anti-angiogenic. Production of a vitreous inhibitor of endothelial cells by hyalocytes has been

demonstrated (Jacobson *et al.*, 1984). It is thought that TGF-β in the vitreous inhibits endothelial cell proliferation in vitro, and inhibits neovascularisation in vivo in the chick chorioallantoic membrane assay and in the rabbit corneal assay to maintain the avascularity of this gel (Zhao & Overbeek, 2001a; Spranger *et al.*, 1999; Lutty *et al.*, 1993; Lutty *et al.*, 1985; Lutty *et al.*, 1983; Patz *et al.*, 1978).

TGF-β in the Choroid and RPE

TGF-β1 and TGF-β2 are found in the capillary endothelium, and within connective tissue of large choroidal arterial walls and in choroidal stroma respectively (Anderson *et al.*, 1995; Pfeffer *et al.*, 1994; Lutty *et al.*, 1993; Kane *et al.*, 1991). TGF-β3 immunoreactivity was seen in intravascular leukocytes and in a few choroidal interstitial cells, possibly histiocytes (Lutty *et al.*, 1993).

RPE cells have been shown to express TGF-β and its receptors and respond to many growth factors from the TGF-β superfamily (Mitsuhiro *et al.*, 2003; Guerin *et al.*, 2001; Anderson *et al.*, 1995; Pfeffer *et al.*, 1994; Hiscott *et al.*, 1985). Resemblance between secretory granules and anti-TGF-β2 positive granules identified in monkey RPE cells supports the view that the RPE synthesises and secretes TGF-β2 into the choroid or apically into the interphotoreceptor space (Anderson *et al.*, 1995). The antiangiogenic effects of TGF-β are again noted as photocoagulated RPE cells containing TGF-β2 inhibit proliferation of bovine aortic endothelial cells and bovine retinal endothelial cells (Yoshimura *et al.*, 1995).

Effects of TGF-β on Astrocytes and Endothelial Cells

A number of studies in astrocytes, identify these cells as a source of TGF-β1, TGF-β2, and TGF-β3 with all TGF-β receptors expressed (Anderson *et al.*, 1995; Constam *et al.*, 1992; Morganti-Kossmann *et al.*, 1992).

Retinal astrocytes emerge from precursor cells that express Pax 2 and the platelet derived growth factor receptor α (PDGFRα) in the optic nerve head and migrate just ahead of the developing vascular network to form a template for the developing retinal vasculature (West *et al.*, 2005; Fruttiger, 2002; Sandercoe *et al.*, 1999; Zhang & Stone, 1997; Fruttiger *et al.*, 1996; Jiang *et*

al., 1995; Huxlin *et al.*, 1992; Ling *et al.*, 1989; Watanabe & Raff, 1988; Stone & Dreher, 1987). Astrocytes invade the retina from around 14WG in humans, and begin to express low levels of GFAP, which increases during development and into maturity (Gariano, 2003).

Little is known about the guidance mechanisms that determine the pattern of the vascular template. Only species with vascularised retinas are known to have retinal astrocytes (Gariano *et al.*, 1996; Schnitzer, 1987), and disturbances to the astrocytic network strongly affect vascular patterning (Fruttiger *et al.*, 1996). Once astrocytes migrate beyond the retinal vasculature where it is hypoxic, they differentiate, altering their shape and increasing their branching, known as stellation, to attach to blood vessels, where they end their migration (Zhang *et al.*, 1999).

Hypoxia induces retinal astrocytes to express VEGF which causes astrocytes to undergo stellation and promotes endothelial cell proliferation and migration (Zhang *et al.*, 1999; Provis *et al.*, 1997; Pierce *et al.*, 1996; Stone *et al.*, 1995; Laterra *et al.*, 1990). The endothelial cells at the leading edge of vascularisation possess filopodia that follow the accompanying astrocytic template and appear directly influenced by VEGF (Gerhardt *et al.*, 2003). As the hypoxic front moves to the new edge of retinal vessels, migrating astrocytes repeat this process until the entire retina is covered by astrocytes (Zhang *et al.*, 1999).

Astrocytes may therefore direct endothelial cell growth and guidance during retinal developmental angiogenesis by secretion of VEGF and also the expression of adhesion molecules such as R-cadherin (Dorrell *et al.*, 2002). In the mouse retina, superficial and deep vascular layers were shown to use filopodial extensions and R-cadherin cell adhesion molecules as guidance cues (Dorrell *et al.*, 2002). Co-staining for GFAP (astrocytes) and collagen IV (endothelial cells) showed a strong correlation between the pattern of retinal vessels and retinal astrocytes. Endothelial cells were never observed in regions without underlying astrocytes in the superficial vascular plexus. During the initial formation of the deeper vascular plexus no GFAP+ cells were observed. However, in the later stages, GFAP+ cells resembling Müller cells were seen between the inner nuclear and outer plexiform layers where

the deep vascular plexus had formed. In association with astrocytes, filopodial processes were noted extending from endothelial cells at the developing vascular front and at the tips of migrating endothelial cells as vessels branched to form the interconnections with the deep vasculature. Antibodies to R-cadherin found in astrocytes and in filopodial extensions of endothelial cells resulted in incomplete retinal vascularisation with an unaffected astrocytic template (Dorrell *et al.*, 2002).

Astrocyte proliferation and migration across the retina is also thought to be due to platelet derived growth factor (PDGFa) produced by retinal neurons (Fruttiger *et al.*, 1996; Mudhar *et al.*, 1993). However, it is not clear whether hypoxia induces PDGFa upregulation (Zhang *et al.*, 1999). When transgenic mice contained astrocytes which produced PDGFa themselves there was an initial hyperproliferation of astrocytes and blood vessels, but cell proliferation still stopped within a week after birth as seen in normal mice, suggesting that other factors limit retinal astrocyte proliferation even when PDGFa is in excess, raising the possibility of TGF-β being one such factor (West *et al.*, 2005).

When the astrocyte number is greatly increased by overexpression of PDGFa, there is a proportional overgrowth of retinal vessels (Fruttiger *et al.*, 1996). Furthermore, when rats are subjected to a cyclic hyperoxic environment, there is a depletion of superficial retinal vessels followed by neovascularisation with death of astrocytes and defects in the *glia limitans* of retinal vessels resulting in microaneurysms (Zhang & Stone, 1997). In a hypoxic environment, retinal vessels hypertrophy beyond the astrocytic template, astrocytes degenerate and breaches in the *glia limitans* of large veins occur with subsequent bleeding into the vitreous (Zhang & Stone, 1997). Astrocytes clearly play an important role in constraining newly formed retinal vessels to the retina and maintaining vascular structural integrity (Zhang & Stone, 1997).

Factors that stimulate astrocyte proliferation in vitro are: PDGF, EGF, FGF-2 and IL-1 which is consistent with findings that PDGF, EGF and interleukin 1 (IL1) are found in developing CNS (Hunter *et al.*, 1993; Yeh *et al.*, 1991; Huff & Schreier, 1989; Giulian *et al.*, 1988; Kniss & Burry, 1988; Richardson *et al.*,

1988; Walicke & Baird, 1988; Giulian & Lachman, 1985; Fallon *et al.*, 1984; Leutz & Schachner, 1981).

Mitogenic (induces mitosis) response of astrocytes to PDGF, EGF, FGF-2 and IL1 is inhibited by each of the isoforms TGF-β1, TGF-β2 and TGF-β3 without TGF-β itself directly affecting the rate of astrocyte proliferation (Close *et al.*, 2005; Sousa Vde *et al.*, 2004; Bachoo *et al.*, 2002; Doetsch *et al.*, 2002; Rabchevsky *et al.*, 1998; Hunter *et al.*, 1993; Huff & Schreier, 1990; Leutz & Schachner, 1981). A small reduction in the rate of proliferation in astrocytes with TGF-β alone may be due to inhibiting the small amounts of PDGF and EGF that astrocytes produce in culture so that TGF-β may modulate response of astrocytes to growth factors and thereby control the rate of astrocyte proliferation in vivo (Hunter *et al.*, 1993; Richardson *et al.*, 1988). For example, in cultured astrocytes, exogenous TGF-β1 inhibits proliferation and modulates the expression of cytoskeletal and ECM proteins such as fibronectin and laminin (Anderson *et al.*, 1995; Laping *et al.*, 1994; Baghdassarian *et al.*, 1993; Hunter *et al.*, 1993; Gallo & Bertolotto, 1990).

TGF-β mostly inhibits growth of astrocytes (Bottner *et al.*, 2000; Flanders *et al.*, 1998; Hunter *et al.*, 1993; Koontz & Hendrickson, 1993). The anti-mitogenic effect of TGF-β is particularly noted with the presence of FGF-2, where FGF-2 would otherwise be a mitogen for astroglial cells (Bottner *et al.*, 2000); Flanders et al., 1993). Region specific responses of astrocytes to TGF-β1 have been reported where astroglial cell proliferation of brainstem but not forebrain is stimulated by TGF-β1 (Bottner *et al.*, 2000; Johns *et al.*, 1992). TGF-β1 best suppressed proliferation induced by PDGF, and TGF-β3 best suppressed FGF induced proliferation (Gomes *et al.*, 2005; Hunter *et al.*, 1993).

Early studies suggested that TGF-β was not associated with retinal vasculature in human eyes (Lutty *et al.*, 1991), however intracellular TGF-β1 and TGF-β2 were subsequently found in smooth muscle cells (SMC-associated with arteries, arterioles and large veins), in pericytes (abluminal on capillaries and small venules) and also in adventitia of large arteries (Lutty *et al.*, 1993). Extracellular TGF-β1 was observed in pericytes, SMC, EC and their basement membrane (Lutty *et al.*, 1993).

Vascular endothelial cell proliferation is regulated by TGF-β and interestingly TGF-β can be either antiangiogenic or angiogenic (Zhao & Overbeek, 2001a; Pepper, 1997). Although TGF-β induces growth inhibition and apoptosis of cultured EC (Siegel & Massague, 2003; Hyman *et al.*, 2002; Goumans *et al.*, 2002; Hogg *et al.*, 1999; Choi & Ballermann, 1995; Pepper *et al.*, 1993; RayChaudhury & D'Amore, 1991) and an injection of TGF-β elicits an angiogenic response in vivo (Siegel & Massague, 2003; Yang & Moses, 1990; Roberts *et al.*, 1986) TGF-β is vital for vasculogenesis and angiogenesis during development (Siegel & Massague, 2003; Larsson *et al.*, 2001; Oshima *et al.*, 1996; Dickson *et al.*, 1995).

In vitro studies have shown that TGF-β can inhibit proliferation of vascular endothelial cells and smooth muscle cells induced by FGF-1 and FGF-2 in both small and large vessels (Zhao & Overbeek, 2001a; Beck & D'Amore, 1997; Pepper, 1997; Pasquale *et al.*, 1993; Passaniti *et al.*, 1992; Lutty *et al.*, 1991; Sato *et al.*, 1990; Bensaid *et al.*, 1989; Orlidge & D'Amore, 1987; Baird & Durkin, 1986; Eichler *et al.*, 2004).

TGF-β1 also inhibits chemotaxis of EC, tube formation and vascular tumour growth without inflammatory reactions (Zhao & Overbeek, 2001a; Dong *et al.*, 1996; Pepper *et al.*, 1990; Pepper *et al.*, 1991; Pepper *et al.*, 1993; Mignatti *et al.*, 1989; Muller *et al.*, 1987).

However, in inflammation, TGF-β has been shown to be angiogenic when administered subcutaneously to mice or rats, (Zhao & Overbeek, 2001a; Frank *et al.*, 1994; Rubbia-Brandt *et al.*, 1991; Sprugel *et al.*, 1987; Roberts *et al.*, 1986) when applied to the chick chorioallantoic membrane, (Zhao & Overbeek, 2001a; Yang & Moses, 1990) the rabbit cornea (Zhao & Overbeek, 2001a; Phillips *et al.*, 1992; Phillips *et al.*, 1993) or in the disc angiogenesis system (Zhao & Overbeek, 2001a; Fajardo *et al.*, 1996). TGF-β1 has been shown to promote the organisation of single EC embedded in three dimensional collagen gels into tube-like structures (Pepper *et al.*, 1993; Merwin *et al.*, 1990; Madri *et al.*, 1988) playing an important function in vascular remodelling (Govinden & Bhoola, 2003; Pepper, 1997; Risau, 1997). All three isoforms have an effect on angiogenesis (Cox, 1995; Merwin *et al.*, 1991a; Merwin *et al.*, 1991b). TGF-β3 is more potent than TGF-β1 and TGF-

β2 in chicken chorioallantoic membrane assay in stimulating neovascularisation and in vascular rearrangements in vivo to help restore damaged vessels and increase blood flow in injured areas (Cox, 1995). This suggests that angiogenesis may be stimulated by VEGF and other angiogenic factors released by the chemoattractant effect on inflammatory cells and therefore a secondary effect (Govinden & Bhoola, 2003; Zhao & Overbeek, 2001a; Pasquale *et al.*, 1993; Roberts & Sporn, 1989; Wahl *et al.*, 1987).

TGF-β1 has a dose-dependent effect on angiogenesis, where low concentrations of TGF-β enhance, whereas high concentrations reduce, the invasiveness of cultured EC following treatment with angiogenic factors such as VEGF and FGF-2 (Govinden & Bhoola, 2003; Gajdusek *et al.*, 1993; Pepper *et al.*, 1993). The nature of the angiogenic response to TGF-β also depends on the presence of other cytokines in the endothelial microenvironment (Pepper *et al.*, 1993). Overall, the response of cells to growth factors can be considered to be on the presence and concentration of other cytokines in surrounding environment, interactions between cells, cytokines and the ECM, and the organisation of the cells (Pepper, 1997).

Recent studies may explain the contradictory effects of TGF-β on EC. EC express two TGF-β type I receptors activin receptor-like kinase 1 (ALK-1) and ALK-5 (TβRI). ALK-1 signalling via Smad-1 increases proliferation and migration of endothelial cells, whereas ALK-5 signalling via Smad-2 and Smad-3 inhibits these actions. These two effects may occur at different TGF-β concentrations, providing a possible basis for the opposing responses depending on the amount of TGF-β (Siegel & Massague, 2003; Goumans *et al.*, 2002; Oh *et al.*, 2000).

Astrocytes, as described above, express VEGF and TGF-β that blocks endothelial cell growth and induces their apoptosis in vitro (Eichler *et al.*, 2004; Eichler *et al.*, 2001; Eichler *et al.*, 2000; Behzadian *et al.*, 1998; Behzadian *et al.*, 1995; Ikeda *et al.*, 1998; Pierce *et al.*, 1995; Stone *et al.*, 1995). Although hypoxia is probably a cause of pathologic angiogenesis, it is not clear whether endothelial cells respond to the low oxygen directly or they react to signals via an autocrine/paracrine method. Pathological

angiogenesis secondary to conditions of ischemia and hypoxia is accompanied by expression of factors including TGF-β and VEGF (Behzadian *et al.*, 1998; Damert *et al.*, 1997; Dvorak *et al.*, 1995; Ijichi *et al.*, 1995; Khaliq *et al.*, 1995; Nomura *et al.*, 1995; Pierce *et al.*, 1995; Shima *et al.*, 1995; Stone *et al.*, 1995; D'Amore, 1994; Breier *et al.*, 1992; Shweiki *et al.*, 1992; Leung *et al.*, 1989).

Müller cell conditioned medium (MCM) from normoxic and hypoxic cultures, can stimulate or inhibit bovine retinal capillary endothelial cell proliferation respectively (Behzadian *et al.*, 1998). Hypoxia activates the TGF-β released by Müller cells, and VEGF expression is enhanced by exogenous TGF-β and by hypoxia, supporting a primary role for glial cell-derived TGF-β in hypoxia induced angiogenesis (Behzadian *et al.*, 1998).

At low MCM concentrations the VEGF effect predominates over the TGF-β effect resulting in increased cell number but at high MCM concentrations the effect is reversed, as perhaps a threshold is reached at which the VEGF effect does not increase further and the TGF-β inhibiting activity begins. In the *in vitro* model, TGF-β at low concentrations is angiogenic (0.2-0.5ng/ml) but angiostatic at high concentrations (5-10ng/ml) (Behzadian *et al.*, 1998; Pepper *et al.*, 1993). This is also supported by the observation that overexpression of TGF-β in transgenic mice does not induce angiogenesis (Zhao & Overbeek, 2001a; Zhou *et al.*, 1996; Lee *et al.*, 1995; Sanderson *et al.*, 1995; Wyss-Coray *et al.*, 1995; Jhappan *et al.*, 1993; Nabel *et al.*, 1993; Pierce *et al.*, 1993).

Similarly, cultured Müller cells in a hypoxic environment release not only the proangiogenic cytokine VEGF but the antiangiogenic factors TGF-β2, PEDF and TSP-1 (Eichler *et al.*, 2004). The proliferation of bovine retinal endothelial cells (BREC) was stimulated by elevated concentrations of VEGF alone but not if the Müller cell derived antiangiogenic factors; TGF-β2, PEDF or TSP-1 were present. The PEDF levels in the Müller cell cultures were lower than those necessary to inhibit endothelial cell migration but sufficient to inhibit the growth of retinal endothelial cells (Eichler *et al.*, 2004). Müller cells are thought to help control the onset of endothelial activation and

neovascularisation largely by releasing anti-angiogenic cytokines (Eichler *et al.*, 2004).

Since vascular cells express both type I and II receptors (Zhao & Overbeek, 2001a; Obata *et al.*, 1999; Srinivasan *et al.*, 1998) TGF-β probably modulates retinal vascular development by directly acting upon vascular endothelial cells and/or pericytes promoting differentiation and physical interactions between them which leads to maturation of blood vessels (Antonelli-Orlidge *et al.*, 1989). A subset of pericytes producing TGF-β is exclusively associated with stable vessels as exogenous TGF-β1 protects retinal capillaries against oxygen-induced loss through the induction of VEGFR-1 which provides protection against vessel degeneration (Shih *et al.*, 2003). Overexpression of TGF-β1 in endothelial cells causes hyperplasia (Shih *et al.*, 2003; Schulick *et al.*, 1998) and gene studies have shown that in embryos lacking TGF-β1 or TβRII receptor, contacts between vascular endothelial cells do not form or are disrupted in the yolk sac (Zhao & Overbeek, 2001a; Oshima *et al.*, 1996; Dickson *et al.*, 1995). Capillary like tubes are absent so that TGF-β1 deficiency markedly affects the establishment and maintenance of vessel wall integrity.

Angiogenesis plays a major role in many blinding ocular diseases including retinopathy of prematurity (ROP), diabetic retinopathy (DR) and in “wet” (exudative) age-related macular degeneration (Zhao & Overbeek, 2001a; Campochiaro, 2000; Maslim *et al.*, 1997). Proteins that counterbalance the effects of VEGF and modulate ocular angiogenesis, such as TGF-β have implications for treatment of ocular diseases caused by abnormal angiogenesis.

In normal development, TGF-β may inhibit astrocyte proliferation within the central retina, retarding blood vessel growth and maintaining an avascular fovea.

1.3 THESIS PROPOSAL

Despite considerable evidence showing that the developing primate fovea ‘needs’ a vascular supply, and expresses growth factors and conditions conducive for endothelial cells and accompanying astrocytes to grow into this

region, at no time during development is the incipient or developing fovea vascularised. In fact, as blood vessels approach the incipient primate fovea, proliferation of endothelial cells and astrocytes decreases in this region and along the horizontal meridian, with the FAZ defined *prior to* formation of the foveal depression. Furthermore, the incipient fovea with its impending metabolic demands is supplied predominantly by diffusion from the underlying choriocapillaris.

Taken together, these observations suggest that a factor(s) with anti-proliferative, anti-migratory and/or anti-angiogenic properties may be expressed in the incipient foveal region, prior to physical marking of the FAZ by astrocytes and endothelial cells (before 23 to 25WG in humans, and before ~fd100 in monkey). One candidate growth factor that may display these properties given appropriate conditions and cell types is Transforming Growth Factor- β (TGF-β).

This thesis aimed to investigate the relationship between the metabolic demands of the primate retina, particularly the fovea, and its vascular supply during development. Further, the possible role of TGF-β in regulating the patterning of blood vessel growth during development, particularly in the incipient fovea, is investigated. Specifically the thesis addressed the following questions:

1. Does differentiation of the developing human retina, with onset of synaptic activity and associated increased metabolic demand, affect development of the human choriocapillaris? (Chapter 3)

2. Does the incipient (avascular) human fovea express higher levels of TGF-β mRNA than peripheral retina, and how does this compare with adult retina? (Chapter 4)

3. Is there a distinct spatial and temporal distribution of TGF-β and receptors (gene and protein) in the developing human and primate retina and does this reflect a relationship to the distinct pattern of blood vessel growth observed during development? (Chapter 5)

CHAPTER 2 – MATERIALS AND METHODS

2.1 SPECIMENS

Human foetal eyes (13-19WG) were obtained from terminations of pregnancy with informed maternal consent, following approval from the Human Ethics Committee, University of Sydney. The gestational age was determined by preoperative obstetric ultrasound and dimensions of eyes including corneal diameter, equator and central cornea-to-foveal distance were recorded to compare size with age. Specimens that were appropriate for size and age were selected for RNA extraction or either frozen or paraffin sectioning depending on the experiment.

Human adult eyes (10-40 years) were obtained from the NSW Lions Eye Bank with ethical approval from the Human Ethics Committee, University of Sydney. All these specimens had *post mortem* times less than 16 hours, and were used for RNA extraction.

Macaque *(Macaca fascicularis)* eyes (Fd64-P11y) were obtained from Bogor Agriculture University, Indonesia with approval from the Ethics Committee of The University of Washington, Seattle, USA. Foetuses were delivered by caesarean section and euthanased by administration of intravenous barbiturate. Eyes were enucleated, fixed in methyl Carnoy's and prepared for paraffin embedding.

2.2 FIXATION AND FROZEN SECTIONING

Following removal of the anterior segment and vitreous, eyecups were fixed for 2 hours in 2% paraformaldehyde in 0.1M phosphate buffered saline (PBS; pH 7.4), washed in PBS, and then placed in 30% sucrose in PBS at 4ºC for 3 hours for cryoprotection. Eyecups were embedded in TissueTek OCT Compound (Sakura Finetek, Torrance, CA, USA), snap frozen in liquid nitrogen-cooled isopentane (BDH, Sydney, NSW, Australia) and stored at -80ºC. Transverse frozen sections of 20µm thickness were cut on a Leitz 1720 Kryostat (Leitz, Stuttgart, Germany) and collected onto poly-L-lysine (Sigma-Aldrich, Sydney, NSW, Australia) and gelatin coated slides (BDH). Four sections were collected per slide, and only sections passing through the incipient fovea and the optic disc were used for analysis.

2.3 FIXATION AND PARAFFIN SECTIONING

The superior margin of the eye/s were marked using a fine suture. Methyl Carnoy's fixative was prepared immediately before use as follows: 6ml methanol (4˚C), 3ml chloroform (4˚C), 1ml glacial acetic acid (room temperature - RT). Approximately 20-50µl fixative was injected into the vitreous chamber, via the *pars plana*, to gently 'inflate' the globe. The eye was then immersed in fixative and left overnight at 4˚C, then placed in 100% methanol. A scalpel blade was used to remove the superior calotte in the horizontal plane, approximately at the level of the superior border of the iris (Figure 2.1), and the eye was then stored in 70% alcohol. For eyes that were fixed in 2% paraformaldehyde, both superior and inferior calottes were removed.

For sectioning, eyes were washed in several changes of 100% methanol and then processed for paraffin embedding (Leica ASP 200 Automated Tissue Processor). Specimens were embedded with the superior cut edge facing down and sectioned in the horizontal plane at 10µm (Finesse 325). Only sections through the optic disc and fovea were analysed.

2.4 RNA EXTRACTION

Whole retinas were used for RNA extraction, except for analysis of TGF-β using quantitative PCR (QPCR) (Chapter 4). For QPCR experiments, a 5 mm trephine of retina from the central retina including the incipient fovea, and 5 mm trephine from the nasal retina was used; RNA was extracted from each sample separately.

To extract RNA, retinas were carefully placed in a sterile 1.7ml eppendorf tube, and homogenised in 200µl of Trizol (Invitrogen) using a tissue pestle. A further 600µl of Trizol was added, followed by incubation at RT for 7 minutes. Then, 200µl of cold chloroform was added and tubes were shaken vigorously for no more than 20 seconds, and centrifuged at 13000 rpm at 4˚C for 15 minutes.

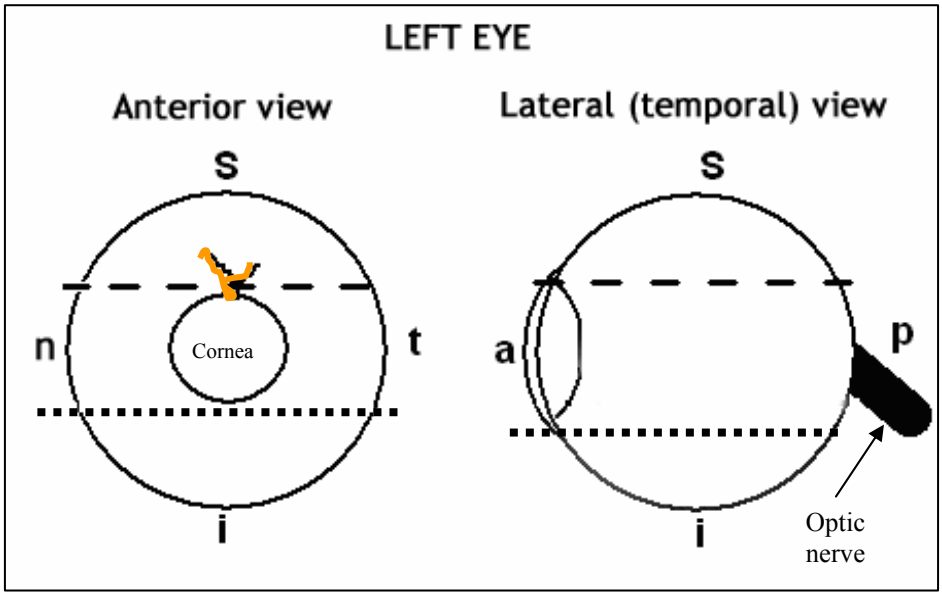

FIGURE 2.1 Diagram showing the position of the horizontal incision (dashed line-superior calotte, dotted line-inferior calotte). The location of the suture is shown in orange. s: superior; n: nasal; i: inferior; t: temporal; a: anterior; p: posterior.

The aqueous layer (containing about 600µl RNA) was removed to clean tubes, mixed gently with 400µl of cold isopropyl alcohol, and RNA precipitated by incubating at -20˚C for 20 minutes to increase the yield of extracted RNA. RNA was pelleted by centrifugation at 13000 rpm, 4˚C for 15 minutes, the supernatant discarded and the pellet washed in 1ml 75% ethanol, at 7500 rpm, 4˚C for 15 minutes, and air dried at RT for approximately 10 minutes. The RNA was dissolved in 25µl RNAse free water, incubated at 42˚C for 10 minutes and then stored at -80˚C. RNA quantity and purity was determined by spectrophotometer (Biorad SmartSpec^{TM}3000), and samples with an absorbance ratio of A260/A280 > 1.8 were used for analysis.

2.5 POLYMERASE CHAIN REACTION (PCR)

Target nucleotides for TGF-β1, TGF-β2 and TGF-β3 were identified from the National Centre for Biotechnology Information (NCBI) GenBank. PCR primers with sequences complementary to the known sequences flanking the target DNA were designed for TGF-β1, TGF-β2 and TGF-β3, and primers were synthesised by Sigma Genosys Australia. Forward and reverse primers used are shown in Tables 2.1 and 2.2.

For QPCR, the amplicon length (between the forward and reverse primers) was less than 150bp and the primers themselves were around 20 bases to optimise the efficiency of real time QPCR.

For riboprobe design, the amplicon length was longer, 200-400 bp for TGF-β1 (267 base pairs (bp)), TGF-β2 (225 bp) and TGF-β3 (367 bp) so as to improve visualisation of target mRNA.

Protein	Accession number	Forward primer Sequence 5' to 3'	Reverse primer Sequence 5' to 3'	Amplicon size (bp)
TGF-β1	X02812	GCAACAATTCCTGGCGATAC	CTAAGGCGAAAGCCCTCAA	136
TGF-β2	NM03238	CATCCCGCCCACTTTCTAC	AATCCGTTGTTCAGGCACTC	148
TGF-β3	X14149	CGAGTGGCTGTTGAGGAGAG	CATTGGGCTGAAAGGTGTG	80

TABLE 2.1 Primers used for QPCR

Protein	Accession number	Forward primer Sequence 5' to 3'	Reverse primer Sequence 5' to 3'	Amplicon size (bp)
TGF-β1	X02812	AACCCACAACGAAATCTATGAC	ACTCCGGTGACATCAAAAGATA	267
TGF-β2	NM03238	AAGCAGAGTTCAGAGTCTTTCG	AATCCCAGGTTCCTGTCTTTAT	225
TGF-β3	X14149	AGTCGGAATACTATGCCAAAGA	GTTGGACTCTCTTCTCAACAGC	367

TABLE 2.2 Primers used for reverse transcriptase PCR (RTPCR) and Riboprobe Design

RNA (1-5μg) was reverse transcribed to cDNA using the Superscript ^{TM} II Firststrand Synthesis System for Reverse Transcriptase PCR (Invitrogen, Ca, USA). The following RNA/Primer mixture was prepared: 1μg RNA, 1μl 10nM DNTP mix, 1μl Oligo (dT) (0.5μg/μl) with remaining volume up to 10μl provided by DEPC treated water.

Samples were incubated for 5 minutes at 65˚C and then placed on ice for 1 minute. The following reaction mixture was prepared: 2μl 10x RT-Buffer (PCR buffer), 4μl 25mM $MgCl_2$, 2μl 0.1M DTT and 1μl RNAse Out (RNAse inhibitor) and 9μl of reaction mixture was added to each tube, mixed gently and collected by centrifugation, then incubated at 42˚C for 2 minutes. Finally, 1μl of Superscript II RT was then added to each tube (except for the negative controls), mixed and incubated at 42˚C for a further 50 minutes.

The reaction was terminated by increasing the temperature to 70˚C for 15 minutes, followed by chilling on ice. The reactions were collected by brief centrifugation and 1μl of RNAse H was added all samples to remove any remaining RNA, with a further incubation of 20 minutes at 37˚C. cDNA was stored at –20˚C for a maximum of 2-3 months.

PCR was performed using Biotaq Red DNA polymerase kit (Bioline, stored at -20˚C) and the following reaction mixture: 2.5μl 10x NH_4 buffer, 1.25μl $MgCl_2$ 50mM solution, 2.5μl 100mM dNTP mix, 0.5μl BIOTAQ red enzyme, 14.75μl RNAse free water, 1μl ss cDNA template (see above), 1.25μl TGF-β Forward & 1.25μl TGF-β Reverse primer (10μM). The final program for RTPCR was as follows: denaturating at 94˚C for 3min, and amplified through 40 cycles with denaturing at 94˚C for 25s, annealing at 58˚C for 25s, followed by extension at 72˚C for 25s, with a final extension of 72˚C for 5min (PCRExpress, Hybaid Sciences). PCR products and DNA ladder were run at

100V on 1% agarose gels using TBE buffer and 0.2ng/ml ethidium bromide. Gels were viewed under UV light using a GelDoc system (UVitech) and images taken using WinFast Software.

Spectrophotometry (Biorad SmartSpec^{TM}3000) was used to measure the concentration of dsDNA as follows:

concentration dsDNA (µg/ml)	=	absorbance @ 260nm	x	dilution factor (mL)	x	dsDNA constant (50µg/ml)*

*absorbance of 1 at A260=50µg/ml

2.6 QUANTITATIVE PCR

The Superscript II Synthesis System was used with the Platinum SYBR Green qPCR Supermix UDG kit (Invitrogen, USA) to detect quantitative changes in RNA expression. SYBR Green is a fluorescent dye that binds directly to double stranded DNA (dsDNA); as the dsDNA accumulates, the dye generates a signal proportional to the concentration of DNA, that can be detected by a real-time PCR machine.

The following components per sample were prepared on ice as a master mix: 12.5µl Platinum SYBR Green qPCR SuperMix-UDG, 0.5µl TGF-β Forward primer (10mM), 0.5µl TGF-β Reverse primer (10mM) and 6.5µl of RNAse free water. Forward and reverse primers for housekeeping genes including for β-actin, GAPDH and 18sRNA were used to determine an endogenous standard. A total of 0.5µl of cDNA was used per reaction.

A two-step cycling program was carried out in the Rotorgene 3000 thermal cycler (Corbett Research, Australia) (Table 2.3). Rotorgene version 6.0 (Corbett Research, Australia) was used to interpret the intensity of the fluorescent signal and thus DNA synthesis in real time, by providing a platform to analyse comparative quantitation and melt curves through graphs and tables. The tables were then converted into Excel spreadsheets and analysed (see Chapter 4).

Number of cycles	Reaction temperature (C°)	Time per cycle
1	50	2 min
1	95	2 min
40	95	15 s
40	60	30 s

TABLE 2.3 Cycling program for QPCR

2.7 RIBOPROBE PREPARATION

As described in Section 2.4, RNA isolated from human foetal retinas was reverse transcribed to cDNA and amplified by PCR amplification using specific primers.

PCR products were purified by gel extraction and inserted into a pGemT Easy DNA vector (Promega), cloned in heat-shocked competent cells (JM109, Promega), purified, further grown up in *E. coli* cells and further purified using Miniprep (QIAprep Miniprep) and Midiprep (Jet Star) kits. DNA was used as a template for preparing digoxigenin (DIG)-labelled riboprobes for *in situ* hybridisation.

Following PCR amplification, DNA was run on 2% agarose gels, and extracted and purified from using QIAquick Gel Extraction Kit (Qiagen). The purity was checked on UV spectrophotometer (Biorad SmartSpec^{TM}3000, A260/A280=1.7-2.1) and stored at -20ºC until used.

The PCR product was ligated using a pGEM-T vector kit (Promega) with a vector: insert ratio of 1:1 (50ng:50ng). The product was cloned in JM109 competent cells using the pGEM-T vector system protocol. Briefly, cells were heat shocked for 30 seconds in a water bath at 42ºC without shaking, and returned to ice immediately for 2 minutes. Cells were plated and incubated overnight at 37ºC. A single white colony containing the insert was selected and grown overnight in LB/ampicillin (50mg/ml) at 37ºC in a shaking incubator. (NB: Blue colonies contain β-galactosidase activity coded by the Lac Z gene and rarely contain the insert). The QIAprep Spin Miniprep Kit Protocol was used to purify high-copy plasmid DNA, which was run on 1% agarose gels and measured by spectrophotometry.

Samples were subsequently sent for sequencing to Supamac (University of Sydney). Once sequencing was done and orientation of fragment sequence was confirmed as correct, the bulk plasmid was grown in *E. coli* cells. Purification was then performed using Jet Star Midi Prep columns. Briefly, cells were pelleted by centrifugation, resuspended and lysed before loading on equilibrated columns; plasmid DNA was eluted and precipitated, then washed and recentrifuged in ethanol. The DNA plasmid pellets were dried and redissolved in 50µl TE and quantified using the spectrophotometer (2µl DNA solution in 98µl TE)**.**

Plasmid DNA was linearised to produce the sense and anti-sense templates which constituted the riboprobes. To linearise plasmid DNA, reactions were set up as follows: 10µl plasmid (4000µg/ml), 10µl of 10x restriction buffer, 0.7µl BSA, 4µl restriction enzyme of choice (e.g. *Sal-1, Nco-1* (GE Healthcare) and 45.3µl RNA free water was combined for 3 hours at 37ºC. The presence of linearised plasmid DNA was confirmed on a 1% agarose gel, and plasmids stored at -20ºC.

Plasmid template DNA was purified using phenol:chloroform: isoanylalcohol (25:24:1) with centrifugation at 13000 rpm for 5 minutes at 4ºC. The aqueous layer was collected in clean eppendorf tube, and mixed with 3M Na-Acetate and 100% cold ethanol by inversion. The DNA was stored at -20ºC overnight, then spun at 13000 rpm for 15 minutes at 4ºC and the supernatant discarded. The DNA pellet was dislodged and washed in 70% cold ethanol, then centrifuged at 10000 rpm for 10 minutes at 4ºC. The supernatant was discarded and the DNA pellet was air dried before resuspending in 20-30µl of DEPC-treated water. The purified plasmid template DNA was assessed by spectrophotometer and run on a 1% agarose gel.

Riboprobes were prepared by adding 1µg of DNA template (e.g. TGF-β1 *nco*, TGF-β1 *sal*) to DEPC-treated water to a final volume of 13µl. On ice, 2µl 10x NTP labelling mixture, 2µl 10x Transcription buffer, 1µl RNAse inhibitor and 2µl RNA polymerase (SP6 or T7, Roche) were added, so that TGF-β1 *sal-I* T7, TGF-β2 *sal-I* T7 and TGF-β3 *nco-I* SP6 made “sense” strands and TGF-β1 *nco-I* SP6, TGF-β2 *nco-I* SP6 and TGF-β3 *sal-I* T7 made “antisense” strands. After gentle mixing, this mixture was incubated at 37ºC for 2 hours,

then 2µl of DNAse I was added to remove the DNA template, followed by a further incubation at 37ºC for 15 mins. The reaction was stopped by adding 2µl of 0.2M EDTA pH 8.0.

Probes were purified by adding 2.5µl 4M LiCl (to prevent DNA precipitation) and 60µl ice-cold 100% ethanol to the final reaction product**.** After mixing, probes were left at -20ºC overnight to precipitate RNA. Riboprobes were centrifuged at 13000 rpm for 15 mins at 4ºC, the supernatant removed and the pellet washed in 100µl of ice-cold 70% ethanol. After further centrifugation at 13000 rpm for 5 mins at 4ºC, the supernatant was again discarded and the pellet air dried. The pellet was finally resuspended in 50µl of DEPC-treated water. The riboprobes were run on a 1% agarose gel to confirm their presence.

A dot-blot dilution method on dry nylon positively-charged membrane (BIODYNE B 0.45µm – Pall, Gelman Sciences) was used to quantify the probes. Serial dilutions (1µl) of RNA standards or ribroprobes (unknown concentration) were blotted and subsequently fixed to the dry membrane with 1 min UV exposure. The membrane was subsequently washed in a Washing Buffer (0.1mM maleic acid, 0.15mM NaCl and 0.3% Tween 20) for 1 min and incubated in Blocking Buffer (Blocking Reagent (Roche) dissolved in maleic acid) for 30 mins. The membrane was then incubated in 1:5000 anti-DIG-AP (Fab fragments) antibody (Roche) for 30 mins, and washed twice in Washing Buffer for 15 mins. The membrane was then rinsed in Detection Buffer (0.1MTris-HCl, 0.1M NaCl, 10mM $MgCl_2$, pH 8.0) for 2 mins. Dots were visualised using NBT/BCIP colour substrate (Roche; 200µl in 10ml Detection Buffer) added in the dark. The colour reaction was stopped in RNase-free water when the most dilute control dot was just visible. The RNA concentration was estimated by comparison with dilutions of the RNA standards.

2.8 IN SITU HYBRIDISATION

Paraffin sections were dewaxed in xylene and hydrated through a graded series of alcohols. Following an initial rinse in PBS for 5 minutes, frozen or dewaxed paraffin sections were fixed in 10% Neutral Buffer Formalin (NBF)

for 20 mins, then washed twice in PBS for 5 mins. Sections were incubated in 20µg/ml Proteinease K for 7 mins at 37ºC, rinsed in PBS for 5 mins, then re-fixed in 10% NBF for 20 mins, followed by incubation in 0.1M triethanolamine (TEA, pH 8.0) supplemented with 630µl of acetic anhydride for 10 mins. Slides were then washed in PBS for 5 mins, then 0.9% NaCl for 5 mins, dehydrated through graded ethanols and air dried.

The pre-hybridisation solution without probe was pre-heated to 65 ºC before being applied to the sections under a coverslip. The hybridisation mixture with probe was heated at 55 ºC for at least 2 mins, then 100-150µl added; slides were then placed in a hybridisation chamber (containing 50ml of 50% formamide, 25ml of 20x SCC, 25ml of milliq water) and incubated at 55 ºC for 90 mins. Optimal temperatures were determined on several preliminary experiments.

Sections were washed in posthybridisation washes as follows; twice in 4x SSC (saline sodium citrate pH7.4) at 60 ºC for 30 min, twice in 2x SSC at 60 ºC for 45 min, once in 1.0x SSC at 60 ºC for 30 min, twice in 0.1x SSC at 60 ºC for 30 min and once in 0.1x SSC at RT for 5 min.

For DIG detection, slides were rinsed in Washing Buffer and blocked in Blocking Buffer for 30 min, then incubated for 1 hour in anti-DIG-AP antibody diluted 1:2000 in Blocking Buffer. Slides were washed twice in Washing Buffer for 15min, then rinsed in detection buffer (0.1M Tris HCl, 0.1M NaCl, 10mM $MgCl_2$ pH8.0) for 5 min. Sections were incubated in colour substrate (10µl HNPP solution (Roche), 10µl solution Fast Red (Roche, 2.5mg /0.0025g powder dissolved in 100µl RNAfree water), 980µl detection buffer) for 1 hour at 37°C to produce a red fluorescence. The reaction was stopped in water for 10 min. Sections were rinsed twice in PBS for 5 min, then coverslipped or prepared for immunohistochemistry (see Section 2.9). For immunohistochemistry, sections were blocked in 10% normal goat serum for 30 min, incubated with appropriate primary antibody overnight at 4˚C, followed by secondary antibody for 30 min. After a final rinse in PBS, sections were coverslipped with Universal mounting medium (Open Biosystems).

2.9 IMMUNOHISTOCHEMISTRY

Paraffin sections were dewaxed in xylene and hydrated through graded alcohols. Following an initial rinse in PBS for 5 minutes, frozen or dewaxed paraffin sections were placed in 0.01M citrate buffer (pH 6.0) with 0.4% saponin at 80ºC for 5 minutes to enhance antigen detection. After cooling to room temperature and further rinsing in PBS for 10 minutes, slides were incubated in 10% normal serum (species in which the secondary antibody/ies was raised) in PBS for 60 minutes, to reduce non-specific immunolabelling. Sections were incubated in either one or two primary antibodies (Table 2.4) at 4ºC overnight. After rinsing in PBS for 10 minutes, sections were incubated for 60 minutes at RT in secondary antibody fluorochrome/s conjugates (Table 2.5, 1:1000; Molecular Probes) in a light proof slide box. After rinsing in PBS for 10 minutes, sections were coverslipped with glycerol/PBS/DABCO (Triethylenediamine; Sigma) and sealed with nail varnish or Universal mounting medium. Negative controls, omitting the primary antibody, and using non-specific isotype control antibody or immunoglobulins were included in each experiment.

Primary antibody Species	Dilution	Manufacturer	Labelling site
CD34 Monoclonal mouse anti-human	1:100	Zymed, Invitrogen	Vascular endothelial cells
Ki-67 Polyclonal rabbit anti-human	1:50	Zymed, Invitrogen	Proliferating cells (except G0 phase)
Synaptophysin Polyclonal rabbit anti-human	1:200	DAKO	Synaptic vesicles in neurons
Vimentin Monoclonal mouse anti-human	1:100	DAKO	Intermediate filaments of Müller cells and immature astrocytes
GFAP (glial fibrillary acidic protein) Polyclonal rabbit anti-cow	1:1000	DAKO	Intermediate filaments
Calbindin Polyclonal rabbit anti-human	1:50	Prof J Stone, Australian National University	Amacrine and horizontal cells
S-opsin (Short-wavelength opsin) Polyclonal rabbit anti-human	1:10000	Prof J Saari, University of Washington	Short wavelength cones
RG-opsin(Long-Medium wavelength) Polyclonal rabbit anti-human	1:1000	Prof J Saari, University of Washington	Medium-long wavelength cones
Rhodopsin Monoclonal mouse anti-human	1:500	Prof J Stone, Australian National University	Rods
TGF-β1 Polyclonal rabbit anti-human	1:200	Santa Cruz Biotechnology, Inc	TGF-β1 protein
TGF-β2 Polyclonal rabbit anti-human	1:200	Santa Cruz Biotechnology, Inc	TGF-β2 protein
TGF-β3 Polyclonal rabbit anti-human	1:200	Santa Cruz Biotechnology, Inc	TGF-β3 protein
TβRI (TGF-β receptor type I) Polyclonal rabbit anti-human	1:50	Santa Cruz Biotechnology, Inc	TGF-β receptor type I
TβRII (TGF-β receptor type II) Polyclonal rabbit anti-human	1:50	Santa Cruz Biotechnology, Inc	TGF-β receptor type II
IgG_1 isotype control Mouse	1:100	DAKO	Negative control
Immunoglobulins Rabbit	1:100	DAKO	Negative control

TABLE 2.4 Primary antibodies - Species, dilution, manufacturer and labelling site.

Secondary antibody Species	Dilution	Manufacturer
Alexa 594 Goat anti-rabbit	1:1000	Molecular Probes
Alexa 488 Goat anti-mouse	1:1000	Molecular Probes

TABLE 2.5 Secondary antibodies - species, dilution and manufacturer

2.10 CONFOCAL MICROSCOPY, IMAGING AND DATA ANALYSIS

Image analysis aims to provide quantitative data from images including number of immunoreactive structures or intensity of immunolabelling. In Chapter 3, a Leica laser scanning confocal microscope using Leica TCSNT software version 1.6.587 (Leica Microsystems, Germany) was used to capture images as z-series. These were combined to measure the number of Ki-67 immunolabelled mitotic endothelial cells and the area of the CD34 immunolabelled choriocapillaris. Adobe Photoshop version 5.0.2 was used in preparing the images for measurement and NIH software (version 1.62 http://rsb.info.nih.gov/nih-image/) macros were used to quantify relevant parameters (area and proliferation). Measurements were recorded and analysed in Excel.

In Chapter 5, the intensity of mRNA expression was quantified by preparing montages of confocal images captured with LSM 5 Pascal (Carl Zeiss) software in Adobe Photoshop version 7.0. The montages were then re-imported into the LSM 5 Pascal software, and measurement tools were used to measure the intensity across each montage. Results were compiled in an Excel database and presented graphically.

CHAPTER 3 – ENDOTHELIAL CELL PROLIFERATION IN CHORIOCAPILLARIS

The study described in this chapter has been published in the following paper:

Allende A, Madigan MC and Provis JM (2006) *Endothelial Cell Proliferation in the Choriocapillaris During Human Retinal Differentiation.* Br J Ophthalmol. 90:1046-1051.

3.1 INTRODUCTION

The choroid develops early, with primitive endothelium-lined elements present in the mesenchyme surrounding the anterior optic cup as early as 29 days' gestation, and its development into a loosely stratified aggregation of vessels being largely complete by 24 weeks' gestation (WG) (Heimann, 1972; Ozanics *et al.*, 1978). The *choriocapillaris* is the innermost capillary layer of the choroid. It comprises a close, thin-walled, highly permeable network of endothelial cells (EC) with little or no basement membrane material, and supplies the neural retina by diffusion across the retinal pigmented epithelium (RPE) and Bruch's membrane. Little is known about mechanisms that regulate choroidal growth as only recently groups have began to look at mechanisms of development in the choroid (Steinle *et al.*, 2005; Saint-Geniez *et al.*, 2006; Hasegawa *et al.*, 2007).

In contrast, development of the retinal vasculature is better understood and the mechanisms regulating its growth and development are well documented. The retinal vessels form later than those in the choroid, the first vessels forming at the optic disc at approximately 14WG, the final stage of development being formation of the perifoveal capillary plexus just after birth (Michaelson, 1948; Nilhausen, 1958; Mann, 1964; Ashton, 1970; Provis *et al.*, 1997; Provis, 2001). Initially the retinal vessels grow in a lobular arrangement, each lobule defining the territories of one of the quadrantic arteries of the mature retina (Michaelson, 1954; Patz, 1966; Provis *et al.*, 1997; Sandercoe *et al.*, 1999). Nasal to the optic disc the superior and inferior lobes merge along the equator at ~20WG. Temporally, the superior and inferior lobes of vasculature skirt around the foveal region to meet along the equator, peripheral to the foveal region, at ~25WG (Gariano *et al.*, 1994; Provis *et al.*, 2000; Provis, 2001). The long trajectory of temporal vessels,

combined with a slow growth rate (Engerman, 1976), results in the central retina remaining avascular for a much longer period than other parts of the retina. The central fovea itself is not normally vascularized at any stage of development (Gariano *et al.*, 1994; Provis *et al.*, 2000).

It has been argued that development of the retinal circulation is determined by the ability/inability of the choroid to deliver nutrients to the retina (Chase, 1982; Stone, 2006). Indeed, it is widely accepted that formation of the retinal vasculature is induced by a transient hypoxia associated with increased metabolic activity in maturing retinal neurons and photoreceptors, resulting in the proliferation and migration of retinal endothelial cells, mediated by growth factors including HIF1-α and VEGF (Stone *et al.*, 1995; Stone, 1997; Ozaki *et al.*, 1999; Semenza, 2000; Morita *et al.*, 2003). Because the retina matures from centre (fovea) to periphery, the differentiation patterns of the neural retina and its retinal vasculature are not well matched. In humans, all of the retinal layers are evident and there is a full complement of cells at the incipient fovea by 11WG (Provis & van Driel, 1985; Linberg & Fisher, 1990), but the perifoveal capillary bed does not begin to form until 25WG and is not complete until after birth. This delay in central retinal vascularization means that the metabolic demands of rapidly maturing central neurons are supplied by diffusion from the choroid, along with some diffusion from the hyaloid vessels via the vitreal body, until relatively late in development (Michaelson, 1954; Bernstein & Hollenberg, 1965).

In this study, it was hypothesized that during the period when the central retina is largely avascular, metabolic activity in central retinal neurons might be supported by increased capacity in the choriocapillaris, reflected by increased proliferation of choriocapillaris EC. Consistent with the accepted mechanism of retinal vascularization (Michaelson, 1948; Stone *et al.*, 1995), it was predicted that maturation of neurons at the incipient fovea and adjacent retina might drive EC proliferation in the adjacent choriocapillaris during the early phases of retinal vascular development. The results, however, indicate that proliferation of choroidal EC is not regulated by maturation of retinal neurons.

3.2 MATERIALS AND METHODS

Please refer to Chapter 2 for a more detailed explanation of methods.

SPECIMENS

Five human foetal eyes aged 14, 15, 17, 17.5 and 18.5WG were obtained from terminations of pregnancy with informed maternal consent, following approval from the Human Ethics Committee, University of Sydney. Gestational age was determined by preoperative obstetric ultrasound and *post mortem* ocular morphometry. Following removal of the anterior segment and vitreous, eyecups were fixed for 2 hours in 2% paraformaldehyde/0.1M phosphate buffered saline (PBS; pH7.4), washed in PBS, and then placed in 30% sucrose/PBS at 4ºC for 3 hours for cryoprotection. Eyecups were embedded in TissueTek OCT (Sakura Finetek, Torrance, CA, USA), snap frozen in liquid nitrogen-cooled isopentane (BDH, Sydney, Australia) and stored at -80ºC. Transverse frozen sections (20µm) were cut on a Leitz-1720-cryostat and collected onto poly-L-lysine (Sigma-Aldrich, Sydney, Australia) and gelatin coated slides (BDH). Only sections passing through the incipient fovea and the optic disc were used for analysis.

IMMUNOHISTOCHEMISTRY

After rinsing in PBS, sections were placed in 0.01M citrate buffer (pH 6.0) with 0.4% saponin at 80ºC for 5 minutes to enhance antigen detection. They were cooled to room temperature, rinsed, then blocked in 10% normal goat serum (NGS) in PBS for 60 minutes. Sections were incubated in polyclonal rabbit anti-human Ki-67 antibody (1:50) to label proliferating cells, and monoclonal mouse anti-human CD34 antibody (1:100) to label the vascular endothelium (Sandercoe *et al.*, 1999), at 4ºC overnight. After rinsing in PBS, sections were incubated for 60 minutes in goat anti-rabbit Alexa-488 (1:1000; Molecular Probes) to detect bound anti-Ki-67 and goat anti-mouse Alexa-594 (1:1000; Molecular Probes) to detect bound anti-CD34. Sections were then rinsed in PBS, mounted in glycerol/DABCO (Triethylenediamine; Sigma) and coverslipped. A negative control, omitting the primary antibody, was included in each experiment.

CONFOCAL MICROSCOPY

For each specimen, three sections from three different slides were analysed. Fifteen areas/section were sampled (135 sample areas/specimen) and subsequently grouped into five chorioretinal regions – incipient fovea (foveal, F), peripheral (nasal, N; temporal, T) and transitional/intermediate regions (nasofoveal, NF; temporofoveal, TF) - using morphological criteria (Figure 3.1A). The incipient fovea was identified by (1) the absence of proliferating cells, (2) the presence of cone photoreceptors only (no rods), and (3) the presence of all characteristic layers of the neural retina (Provis *et al.*, 1985). The peripheral regions (T and N) were identified as having only a differentiated ganglion cell layer (GCL), the deeper retina having no layers and comprising a maximum density of Ki-67 immunoreactive (IR) cells (Walcott & Provis, 2003). The intermediate regions (TF and NF), like the peripheral ones, had a fully differentiated GCL and partially differentiated outer retina containing relatively few (<15) Ki-67-IR cells.

Sections were imaged using a Leica upright scanning laser confocal microscope (Leica TCSNT software, version 1.6.587). An argon-krypton laser with dual filters for maximum excitation (488nm and 594nm) was used to visualise anti-Ki-67-IR (Alexa-488) proliferating cells and anti-CD34-IR (Alexa-594) vascular endothelium respectively. Each sample area (250µmx250µm) was viewed using a 40x oil immersion objective. Ten optical z-sections at 1µm intervals were collected from each sample location (total of 1350 images/specimen). Photomultiplier gain, offset, aperture and laser power settings were standardised and maintained for all measurements for comparisons between specimens.

IMAGE ANALYSIS

Counting Proliferating cells

Immunolabelled confocal images were opened in Adobe Photoshop 5.0.2 (Figure 3.1B) with z-sections of each field comprising different layers of each image. Proliferating cells were counted in each layer and identified as cells with a green-labelled (Ki-67-IR) nucleus within the red-stained (CD34-IR)

FIGURE 3.1

A: Diagrammatic representation of sample areas analysed; inset showing central region (fovea shaded in blue). **B:** Adobe Photoshop image (250μm x 250μm; 512 pixels x 512 pixels) of a chorioretinal sample showing Ki-67-IR proliferating cells (green) and the CD34-IR choriocapillaris endothelium (red). **C:** Single red channel, after blue and green channels are filled with black. The choriocapillaris is selected as shown by the white outline. **D:** Cropped image of the selected choriocapillaris. **E:** The inverted cropped image is imported into NIH Image in greyscale. **F:** Thresholding of the image into binary form, where red pixels above background are changed into black pixels. Measurement macros were then used to calculate the vascular area of the choriocapillaris.

ONZ, outer neuroblastic zone; CC, choriocapillaris; RPE, retinal pigmented epithelium; BV, blood vessel

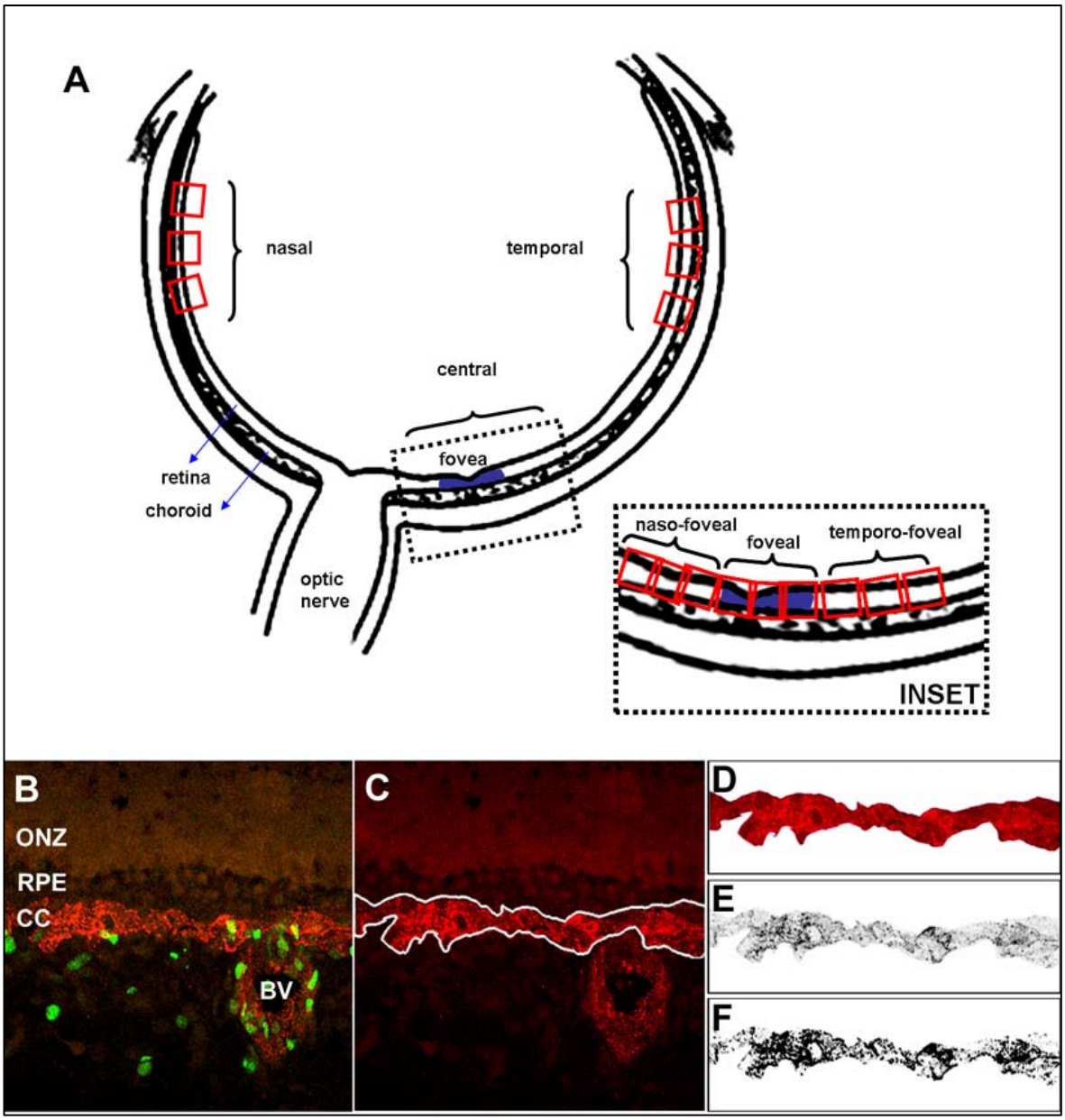
A
nasal
temporal
central
fovea
retina
choroid
optic
nerve
naso-foveal
foveal
temporo-foveal
INSET
B
ONZ
RPE
CC
BV
C
D
E
F

blood vessel wall, present in at least three adjacent layers. Each double-labelled cell was counted only once.

Estimating Choriocapillaris Area

Layers were flattened and the green and blue channels filled with black to allow visualisation of the single red channel (Figure 3.1C). The length of choriocapillaris was a constant of 250μm (Figure 3.1D). The choriocapillaris was identified as the part of the choroid lying immediately adjacent to Bruch's Membrane and containing no large vessels. The identified region of choriocapillaris was copied, pasted into a new Photoshop document, colour-inverted, saved in TIFF format and imported into NIH Image software (version 1.62 http://rsb.info.nih.gov/nih-image/) with the units set to pixels (Figure 3.1E). Three estimates of area, which varied by no more than 4%, were taken from each flattened image and the average area recorded in pixels, and converted to microns (μm^2).

The amount of red in the background of each image was determined by sampling at least three vessel-free areas. After thresholding, each image was converted into binary form, (Figure 3.1F) and measurement macros used to calculate the vascular area using the "Compute Percent Black and White" command. All sections were processed in this way. Counts of proliferating cells versus CD34-IR choriocapillaris area were recorded in Microsoft Excel according to gestational age and chorioretinal region. The rate of cell proliferation in the choriocapillaris was calculated: (number of proliferating cells in a sample region)/(area of the choriocapillaris).

STATISTICAL ANALYSIS

After normalizing the data we used ANOVA to compare the fovea with other locations (NF, N, TF and T) at each age for (a) mean choriocapillaris area and (b) mean rates of choriocapillaris proliferation. To elucidate trends in choriocapillaris development we grouped the data based on degree of retinal differentiation. Prior to 16WG only a very small area of central retina is differentiated; after this age the differentiated region grows rapidly in size, beyond the incipient macular region. We use '<16WG' and '>16WG' to indicate these groups, respectively. Grouped data was tested for significance

using the Kruskal-Wallis and the Conover Inman *post hoc* tests (StatsDirect, $p<0.05$).

3.3 RESULTS

IMMUNOLABELLING

The antibody to CD34 (red) consistently labelled cells in the choroid and choriocapillaris (Figure 3.2A and B). Few retinal blood vessels were identified at 14 and 15WG. In the 17 to 18.5WG specimens, endothelial cell labelling was evident at the nerve fibre layer/GCL interface, temporal to the optic disc. No labelling was present in control sections when primary antibody was omitted.

Ki-67-IR (green), indicative of proliferating cells, was seen consistently throughout the choroid within the vascular endothelium and stroma (Figures 3.2A and B, Figure 3.3) and in the nuclei of neuroblasts in undifferentiated retina of all specimens (Figure 3.2B, Figure 3.3). In the choriocapillaris, the proliferating cells were most commonly seen on the sclerad aspect of vessel walls, away from the RPE.

Proliferating cells were also seen in the optic nerve, in presumed endothelial cells in inner retina of some specimens, but rarely in the RPE. No labelling was present in control sections with the primary antibody omitted.

Choriocapillaris Area

The choriocapillaris endothelium appeared as CD34-IR, small-calibre profiles oriented parallel to the RPE (Figure 3.1). Vessels outside the choriocapillaris could be identified travelling obliquely over several sections, were generally larger in diameter, but not readily identifiable as belonging to either Sattler's or Haller's layer (Figure 1.4).

Choriocapillaris area by location and age is illustrated in Figure 3.4. Measurements from the transitional areas (NF and TF) are omitted from Figure 3.4A for clarity. When choriocapillaris area at the foveal location is compared with nasal and temporal locations the differences are statistically significant ($p<0.001$, ANOVA), except for the foveal *vs* nasal samples at

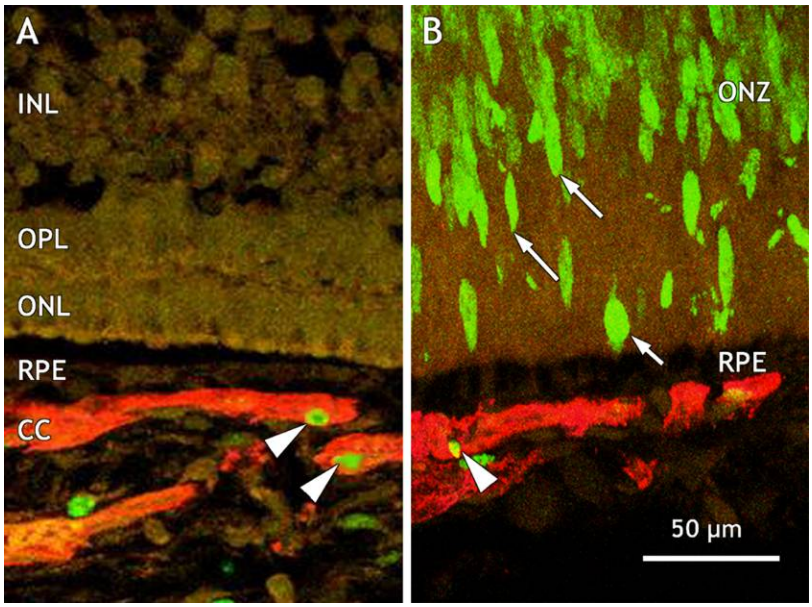

FIGURE 3.2 Cell proliferation in 18.5WG human chorioretinal locations.

A: In the incipient fovea ('Foveal' location), no Ki-67-IR proliferating cells (green, arrowheads) are present in the retina but are seen in the CD34-IR choriocapillaris (red).

B: Numerous Ki-67-IR proliferating cells (green, arrows) are seen in the outer neuroblastic zone in a peripheral sample. In the choriocapillaris, proliferating cell nuclei are generally seen in vessel walls away from the retina (arrowhead).

CC, choriocapillaris; INL, inner nuclear layer; ONL, outer nuclear layer; ONZ, outer neuroblastic zone; OPL, outer plexiform layer; RPE, retinal pigmented epithelium.

FIGURE 3.3 Comparison of cell proliferation between young (14-15WG) and old (17-18.5WG) human chorioretinal locations. Ki-67-IR proliferating cells (green) are seen in the outer neuroblastic zone (arrows) of the retina and in choroidal endothelial cells (arrowheads). No proliferation is observed in the foveal region of the retina.

CC, choriocapillaris; INL, inner nuclear layer; ONL, outer nuclear layer; ONZ, outer neuroblastic zone; OPL, outer plexiform layer; RPE, retinal pigmented epithelium.

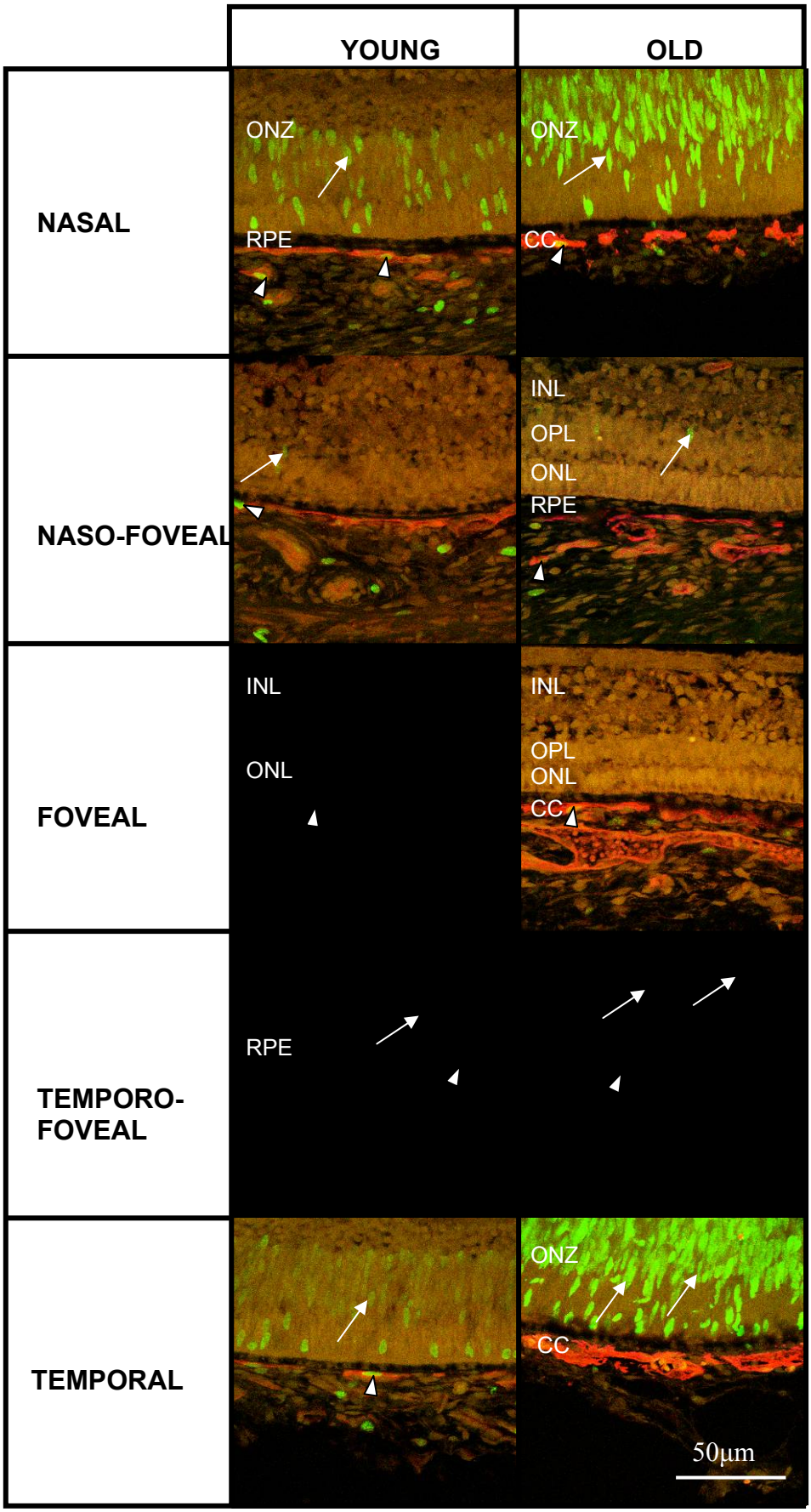
YOUNG
OLD
NASAL
NASO-FOVEAL
FOVEAL
TEMPORO-FOVEAL
TEMPORAL
ONZ
RPE
CC
INL
OPL
ONL
50µm

FIGURE 3.4 Analysis of choriocapillaris endothelial area, by location and by age.

A: Graphs showing the area of CD34 immunolabelling in the choriocapillaris (±standard error), shown at three of the five locations analyzed – nasal, temporal and foveal - for clarity. The graphs show that (a) there is a steady increase in choriocapillaris area over the age range studied and (b) the area of choriocapillaris at the incipient fovea is greater than in the peripheral locations at all the ages analyzed.

Foveal choriocapillaris area is significantly different from the other locations by ANOVA ($p<0.001$) at each age except one sample at 17.5WG (F *vs* N).

B: Data from all five locations in which measurements from the two youngest retinas (14 and 15WG) are grouped and compared with data from the three older retinas (17-18.5WG) (±standard error). The data shows that in the transitional locations (NF and TF) choriocapillaris area is greater than in the periphery, but not as high as in the fovea, in both age-groups. Thus, the data indicates a progressive decrease in choriocapillaris area from central to peripheral locations. * denotes significant differences, $p<0.05$ (Kruskal-Wallis test and Conover Inman *post hoc* test).

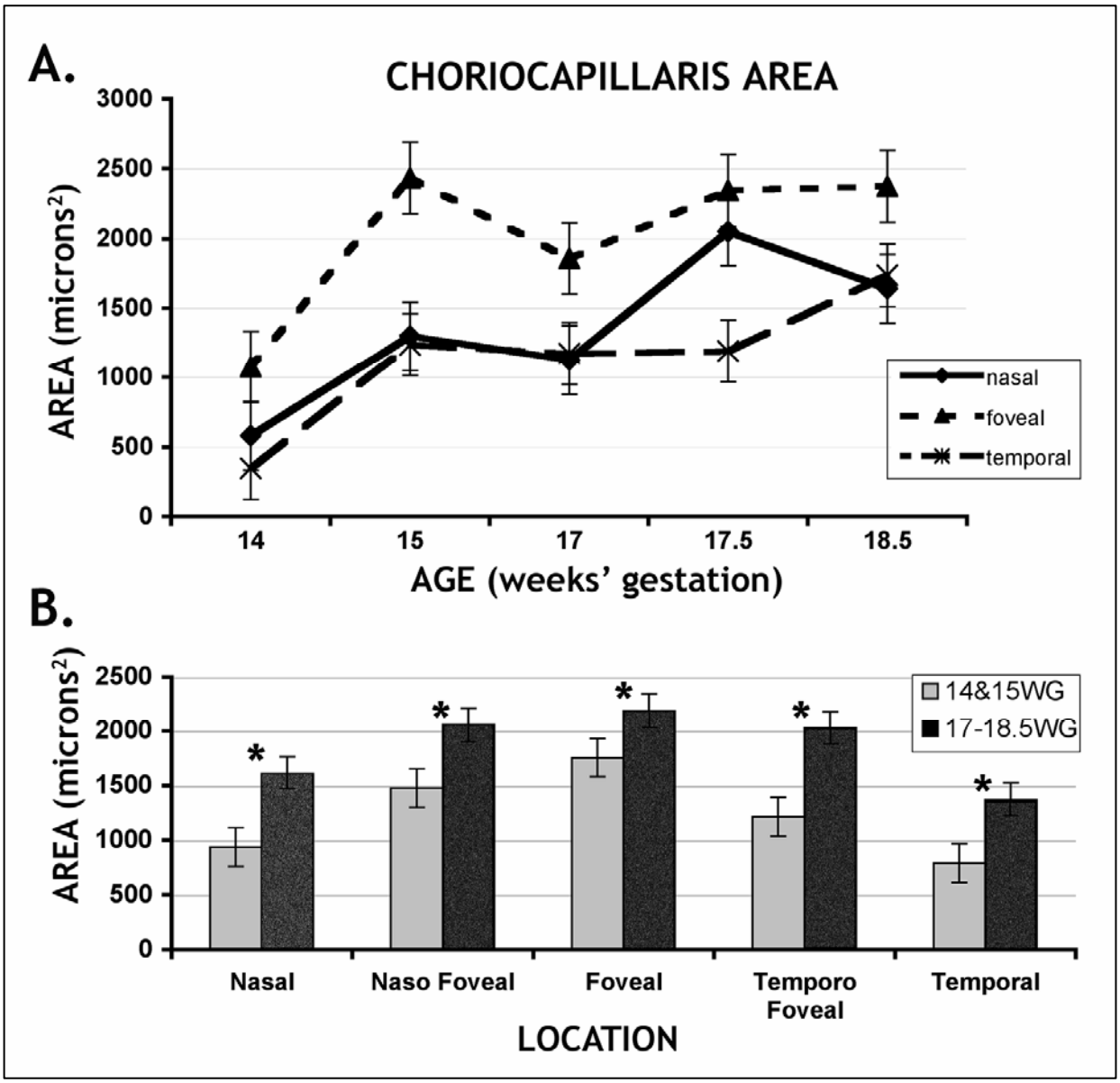
A.
CHORIOCAPILLARIS AREA
AREA (microns²)
3000
2500
2000
1500
1000
500
0
14
15
17
17.5
18.5
AGE (weeks' gestation)
nasal
foveal
temporal
B.
AREA (microns²)
2500
2000
1500
1000
500
0
14&15WG
17-18.5WG
Nasal
Naso Foveal
Foveal
Temporo Foveal
Temporal
LOCATION

17.5WG (Figure 3.4A). The grouped data also indicate a significant increase in choriocapillaris area with age at all locations ($p<0.05$, Kruskal-Wallis test and Conover Inman *post hoc* test) (Figure 3.4B).

EC Proliferation

In general, fewer proliferating cells were observed in the choriocapillaris underlying the foveal region compared with other locations (Figure 3.5). In the <16WG group peak numbers of proliferating cells were observed at NF and TF locations (2.33 cells/field ±0.33SE; 1.67 ±0.21SE) but in the >16WG group peak numbers were in the peripheral chorioretinal locations (N, 1.67 ±0.24SE; T, 2.22 ±0.15SE). This suggests a proliferation gradient in the choroid, but did not reach statistical significance, probably due to the relatively small sample size.

The rate of cell proliferation was calculated as the number of proliferating cells/unit of choriocapillaris EC area. The highest mean rate of choriocapillaris EC proliferation occurred at 14WG, and declined as a function of age (Figure 3.6A). Analysis by age and location indicated that the lowest rates of proliferation were in central locations compared with peripheral (N and T) locations at all ages (Figure 3.6B), reaching statistical significance in samples at 14WG (F vs N; F vs T), 17.5WG (F vs T) and 18.5WG (F vs N; F vs T) (ANOVA, $p<0.001$).

3.4 DISCUSSION

These data support three new findings. First, the area of the choriocapillaris endothelium is greater in the foveal region at all ages studied, and declines toward the periphery. Choriocapillaris area also increases, at all locations analyzed, as development progresses (Figure 3.4). Second, the rate of choriocapillaris EC proliferation declines dramatically over the period studied (14–18.5WG, Figure 3.6A). Third, when the rate of EC proliferation is calculated (number of proliferating cells/unit area of choriocapillaris), the lowest rates of EC proliferation are at the incipient fovea for all ages (Figure 3.6B).

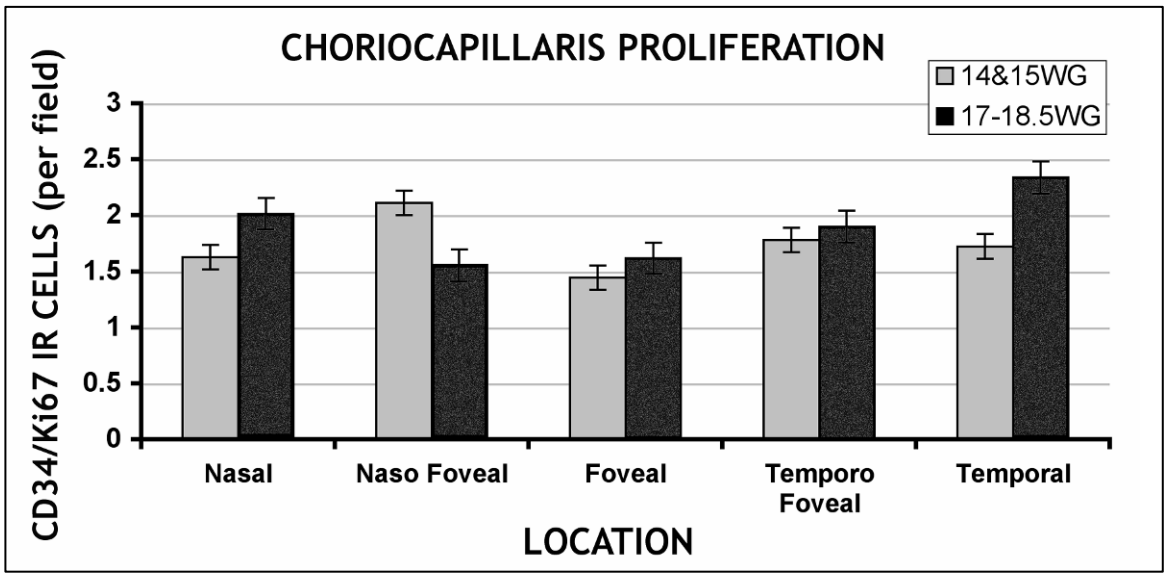

FIGURE 3.5 Numbers of Ki-67-IR cells in choriocapillaris endothelium in two groups (14 and 15WG, compared with 17, 17.5 and 18.5WG) at five chorioretinal locations. In the younger specimens, the peak numbers of proliferating cells are in the transitional regions (naso-foveal and temporo-foveal), subjacent to areas nearing retinal differentiation. In the older group the peak numbers of proliferating cells are in the more peripheral nasal and temporal regions. Error bars show standard error.

FIGURE 3.6 Rates of choriocapillaris EC proliferation (±standard error) per unit area of choriocapillaris.

A: The mean rate of EC proliferation in the choriocapillaris (all locations) is shown for each age. The data indicate a reduction in the proliferation rate, with increasing age.

B: Graphs showing the rate of EC proliferation at three locations at each age. Naso- and temporo-foveal locations are omitted for clarity. The data suggest that (a) there is a decline in the rate of proliferation with age at the foveal and peripheral locations, and (b) rates of proliferation at the fovea are less than in the periphery at all ages studied. Proliferation rates at the foveal locations are significantly different from the other locations at 14WG (F *vs* N; F *vs* T), 17.5WG (F *vs* T) and 18.5WG (F *vs* N; F *vs* T) by ANOVA ($p<0.001$).

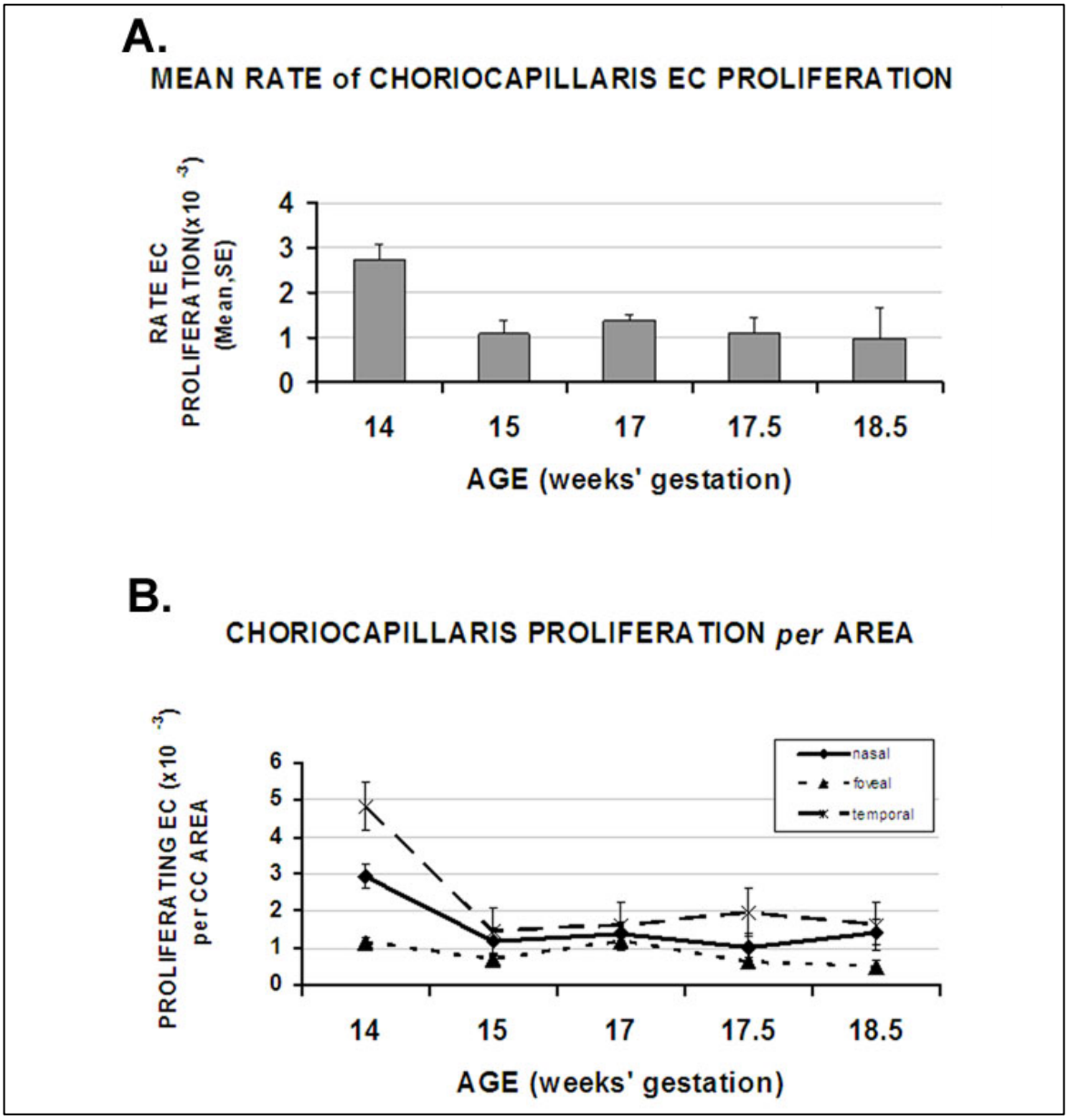
A.
MEAN RATE of CHORIOCAPILLARIS EC PROLIFERATION
RATE EC PROLIFERATION(x10 -3) (Mean,SE)
4
3
2
1
0
14
15
17
17.5
18.5
AGE (weeks' gestation)
B.
CHORIOCAPILLARIS PROLIFERATION per AREA
PROLIFERATING EC (x10 -3) per CC AREA
6
5
4
3
2
1
0
nasal
foveal
temporal
14
15
17
17.5
18.5
AGE (weeks' gestation)

The increase in choriocapillaris endothelium area in the foveal region at all ages studied is consistent with other observations of specialization of the choriocapillaris underlying the foveal region of the adult retina.

This specialization may allow for a higher rate of oxygen and nutrient delivery to central photoreceptors/unit time, compared with other parts of the retina (Fryczkowski & Sherman, 1988; Provis *et al.*, 1998). While the data suggests that choriocapillaris area increases as development progresses neither the full timecourse of this expansion, nor at what stage choriocapillaris area stabilizes, is established. Analysis of proliferating EC by location suggests that there may be a wave of proliferation passing towards the periphery over the timecourse of the present study (NF/TF <16WG *cf* N/T >16WG). Although not statistically significant, this is an unexpected finding worthy of further investigation. One possible explanation for the larger areas of choriocapillaris at foveal locations earlier in development is that at <14WG peak EC proliferation occurs centrally, establishing a substantial choriocapillaris that is added to by subsequent EC proliferation. However suitable specimens are not available to validate this suggestion at this stage.

Most significantly, this study indicates that EC proliferation in the choriocapillaris *does not* appear to be promoted by increased metabolic activity in central retinal neurons. Such a mechanism is widely thought to regulate development of the retinal vasculature (Stone, 1997). If retinal maturation regulated choriocapillaris EC proliferation, peak EC proliferation would be expected at foveal locations, and to increase with increasing age – at least until there is a significant retinal vasculature in temporal retina. However, reduced EC proliferation is found at foveal locations for all ages studied. Furthermore, the rate of EC proliferation at foveal locations is stable between 14 and 18.5WG ($0.6 – 1.2 \times 10^{-3}$ proliferating cells/μm^2 choriocapillaris), when the central retina is undergoing rapid maturation (Xiao & Hendrickson, 2000; Georges *et al.*, 2006), suggesting no dynamic relationship between the differentiating retina and choroid during this period.

Earlier studies in this laboratory suggest that a factor/s expressed in central retina inhibit the growth of retinal vessels in the foveal region (Provis *et al.*,

2000; Sandercoe *et al.*, 2003) and may reduce rates of EC proliferation in central retina (Stone, 2006). Such factors may also act on the adjacent choriocapillaris, resulting in the reduced rates of EC proliferation in the 'foveal' chorioretinal location described here. While such an effect cannot be discounted, other evidence regarding EC growth, origins and phenotypes need to be considered.

In very early human ocular development (<10WG) both VEGF and the KDR receptor are reported to be expressed at relatively high levels in the choroid, while at stages comparable with those investigated here, very little VEGF or KDR is detected (Gogat *et al.*, 2004). Consistent with this, little VEGF mRNA expression is seen in the choroid of human and monkey eyes at equivalent ages of ≥14WG (Provis *et al.*, 1997; Sandercoe *et al.*, 2003), although VEGF mRNA is detected in the RPE (Provis *et al.*, 1997). Although conditional inactivation of VEGF expression in the RPE results in absence of the choriocapillaris and microphthalmia in mice (Marneros *et al.*, 2005), *in vitro* studies show that VEGF has only mild effects on choroidal EC proliferation compared with strong effects for FGF-2 (Zubilewicz *et al.*, 2001; Geisen *et al.*, 2006). Furthermore, choroidal EC, in contrast to retinal EC, display increased proliferation and migration when stimulated with nerve growth factor (NGF) (Steinle & Granger, 2003).

Other evidence indicates divergent lineages of EC with different response characteristics. Lineage negative haematopoietic, bone-marrow derived stem cells give rise to endothelial precursor cells that can integrate into peripheral vasculature (Asahara *et al.*, 1997; Kalka *et al.*, 2000a; Kalka *et al.*, 2000b; Isner *et al.*, 2001; Csaky *et al.*, 2004) and, when injected intravitreally, selectively seek out astrocytes and are incorporated into retinal vessels (Otani *et al.*, 2002; Otani *et al.*, 2004). Bone marrow stromal cells (BMSC) - non-haematopoietic pluripotent cells – can give rise to a variety of mesenchymal phenotypes, including EC (Prockop, 1997; Reyes *et al.*, 2002). BMSC-derived EC are more responsive to FGF-2 than VEGF, proliferating at double the rate (Annabi *et al.*, 2004). Studies with DNA microarrays have shown that EC from different blood vessels such as arteries and veins, as well as large and small vessels, and EC from different tissues have distinct

gene expression profiles (Ho *et al.*, 2003). A very recent study using DNA microarrays and quantitative PCR has shown that there are marked differences in the gene expression profile (up to 263 fold) between EC from the retina and the choroid in up to 9% of genes supporting the notion of retinal and choroidal vascular endothelium each having a unique molecular phenotype (Smith *et al.*, 2007).

Given the time lag of at least 10 weeks between initial formation of the choroid and vascularization of the retina, and that formation of a retinal vasculature is not a constant feature of vertebrate eye development, the possibility that choriocapillaris EC and retinal EC derive from different lineages appears strong. This may explain some of the differences in response characteristics of retinal and choroidal EC, including the lack of response of choriocapillaris EC to the metabolic demands of the differentiating retina described here.

CHAPTER 4 – TRANSFORMING GROWTH FACTOR-β mRNA IN CENTRAL AND PERIPHERAL HUMAN RETINA

4.1 INTRODUCTION

Previous studies in this laboratory suggested that a factor(s) expressed in the central retina could define the region of the incipient fovea, subsequently inhibiting the growth/migration of retinal vessels and astrocytes into the foveal region (Provis *et al.*, 2000; Sandercoe *et al.*, 2003) and reducing rates of endothelial cell proliferation in central retina (Stone, 2006).

In Chapter 3, I have described reduced rates of endothelial cell proliferation in the choriocapillaris between 14WG and 18.5WG in choroid sampled at the 'foveal' chorioretinal location. Thus, increased metabolic demands of central retina resulting from dark current and neuronal maturation appear not to promote proliferation of endothelial cells in the choriocapillaris supplying the central region. As discussed in Chapter 3, this may reflect different endothelial lineages and thus responses to growth factors. It may also be possible that anti-angiogenic/proliferative growth factors within the retina in the incipient foveal region also influence choriocapillaris endothelium.

Further evidence for inhibitory factor(s) in central retina include presence of blind-ended capillaries directed towards, but not entering, the foveal region (Provis, 2001); reduced cell proliferation in retinal vessels on the horizontal meridian (Provis *et al.*, 1998); and, exclusion of astrocytes and endothelial cells from the fovea during development (Provis *et al.*, 2000; Provis, 2001). Not only are astrocytes excluded from the incipient fovea but they retreat once the perifoveal plexus has been formed (Provis *et al.*, 2000).

It is important to note that such a factor(s) would be required to be expressed within the incipient fovea *prior to* any physical marking of the FAZ by the developing vasculature and astrocytes (before 23-25WG, or fd100). TGF-β is such a candidate molecule (Chapter 1.2).

In this chapter, the expression of TGF-β mRNA is examined in developing and adult human retina. Reverse transcription polymerase chain reaction (RTPCR) and quantitative PCR (QPCR) are used to detect and quantify mRNA of TGF-β isoforms in the central and peripheral retina. According to the proposed hypothesis (Chapter 1.3), TGF-β mRNA is expected to be preferentially expressed at the incipient fovea, prior to definition of the FAZ.

4.2 MATERIALS AND METHODS

SPECIMENS

Seven human foetal eyes aged 16, 16, 17.5, 18, 18, 18.5 and 19WG were obtained from terminations of pregnancy with informed maternal consent, following approval from the Human Ethics Committee, University of Sydney. Gestational age was determined by preoperative obstetric ultrasound and *post mortem* ocular morphometry. Two human eyes from a 10 year old juvenile and a 20 year old man were obtained with ethical approval from the NSW Lions Eye Bank. Following removal of the anterior segment and vitreous, retinas were carefully removed from the choroid and placed into a separate sterile 1.5ml eppendorf tube.

RNA EXTRACTION

In some cases RNA was extracted from whole retinas (one 16WG and one 18WG eye) for RTPCR; for other retinas, a 5mm trephine was used to excise samples from central retina (including the incipient fovea) and nasal retina, to compare transcript levels for each of the TGF-β isoforms.

RNA was extracted using Trizol (Invitrogen) according to manufacturer's instructions. Briefly, tissue was homogenised in Trizol and incubated at room temperature for 7 minutes. Chloroform was added, the tube shaken vigorously, centrifuged, and the aqueous layer collected into a clean eppendorf tube. RNA was precipitated using isopropyl alcohol, and incubated at -20˚C for 20 minutes, then centrifuged. The pellet was washed in 75% ethanol, centrifuged and allowed to air dry for approximately 10 minutes. The RNA was then dissolved in 25µl RNAse free water, incubated at 42˚C for 10 minutes and stored at -80˚C for later use. Purity was determined by spectrophotometery (Biorad SmartSpec^{TM}3000). Only samples with an absorbance ratio A260/A280 greater than 1.8 were utilised in these experiments (see Chapter 2.4).

REVERSE TRANSCRIPTION PCR (RTPCR)

Target nucleotides for TGF-β1, TGF-β2 and TGF-β3 were identified from the National Centre for Biotechnology Information (NCBI) GenBank. PCR

primers with sequences complementary to the known sequences flanking the target DNA were designed for TGF-β1, TGF-β2 and TGF-β3, and primers were synthesised by Sigma Genosys Australia. Forward and reverse primers used are shown in Table 4.1.

TABLE 4.1 Primers used for QPCR

Protein	Accession number	Forward primer Sequence 5' to 3'	Reverse primer Sequence 5' to 3'	Amplicon size (bp)
TGF-β1	X02812	GCAACAATTCCTGGCGATAC	CTAAGGCGAAAGCCCTCAA	136
TGF-β2	NM03238	CATCCCGCCCACTTTCTAC	AATCCGTTGTTCAGGCACTC	148
TGF-β3	X14149	CGAGTGGCTGTTGAGGAGAG	CATTGGGCTGAAAGGTGTG	80

RNA (1-5μg) was reverse transcribed to cDNA using the Superscript ™ II Firststrand Synthesis System for Reverse Transcriptase PCR (Invitrogen, Ca, USA). PCR was performed using Biotaq Red DNA polymerase kit (Bioline) using the cycle shown in Table 4.2. Presence and concentration of DNA was assessed on a 1% agarose gel and by spectrophotometry (Biorad SmartSpec™3000) (Chapter 2.5). Isoform identities were confirmed by sequencing.

TABLE 4.2 Cycling program for RTPCR

Number of cycles	Reaction temperature (C°)	Time
1	94	3 min
40	94	25s
40	58	25s
40	72	25s
1	72	5 min

QUANTITATIVE PCR

The Superscript II Synthesis System was used with the Platinum SYBR Green qPCR Supermix UDG kit (Invitrogen, USA) to detect quantitative changes in RNA expression by means of a fluorescent signal. Forward and reverse primers for housekeeping genes including β-actin, GAPDH and 18sRNA were used to determine an endogenous standard. Triplicates of each sample with a total of 0.5μl of cDNA per reaction were used. A two-step cycling program was carried out in the Rotorgene 3000 thermal cycler (Corbett Research, Australia) (Table 4.3) to interpret the intensity of the fluorescent signal and thus DNA synthesis in real time. Melt curve analysis

was done to verify specificity of the reaction after cycling finished (Chapter 2.6).

TABLE 4.3 Cycling program for QPCR

Number of cycles	Reaction temperature (C˚)	Time per cycle
1	50	2 min
1	95	2 min
40	95	15 s
40	60	30 s

PFAFFL ANALYSIS

Relative quantification of target genes in comparison to reference house keeping genes is done using a mathematical model (See Appendix A). In this mathematical model it is necessary to determine the "crossing points" (CP) or replicate "takeoff points" for each transcript. CP is defined as the point at which the fluorescence rises appreciably above the background fluorescence (Pfaffl, 2001). The "takeoff point", is calculated from the second derivative of the raw data and is the point determined where the reaction is increasing most rapidly. This is the "peak" of the exponential reaction and occurs shortly after the "takeoff" of the reaction. The "takeoff" point is estimated as 80% below the peak level (Rotorgene version 6.0, Corbett Research).

Relative quantification of target and reference genes was done by using the Pfaffl mathematical equation which despite different cDNA input concentrations to mimic different RT efficiencies, all target transcripts as well as reference transcripts are affected in parallel (Pfaffl, 2001) (see Appendix A). Results were tabulated and graphed on an Excel spreadsheet.

4.3 RESULTS

REVERSE TRANSCRIPTION PCR (RTPCR)

In the 17.5WG foetal retina, all TGF-β isoforms were present, although the TGF-β3 band appeared weaker than the other two isoforms (Figure 4.1A). When expression was compared in central *versus* nasal samples from an 18.5WG foetal eye, no difference was seen in the appearance of the bands

between sample locations (Figure 4.1B); TGF-β2 was clearly the most abundant isoform present (Figure 4.1B). Comparison of results obtained from a 19WG and a 10yo retina showed more intense bands in the foetal compared to juvenile retina for all three isoforms (Figure 4.1C).

QUANTITATIVE PCR

House Keeping Genes

After comparing GAPDH, β-actin and 18sRNA house keeping genes, the least variability in “average amplification” and “replication take off” between adult and foetal eyes as well as between central and peripheral retina was found for GAPDH (variability of 0.4 compared with 0.7 for β-actin and >1 for 18sRNA). Therefore, GAPDH was used as the endogenous standard in all analyses.

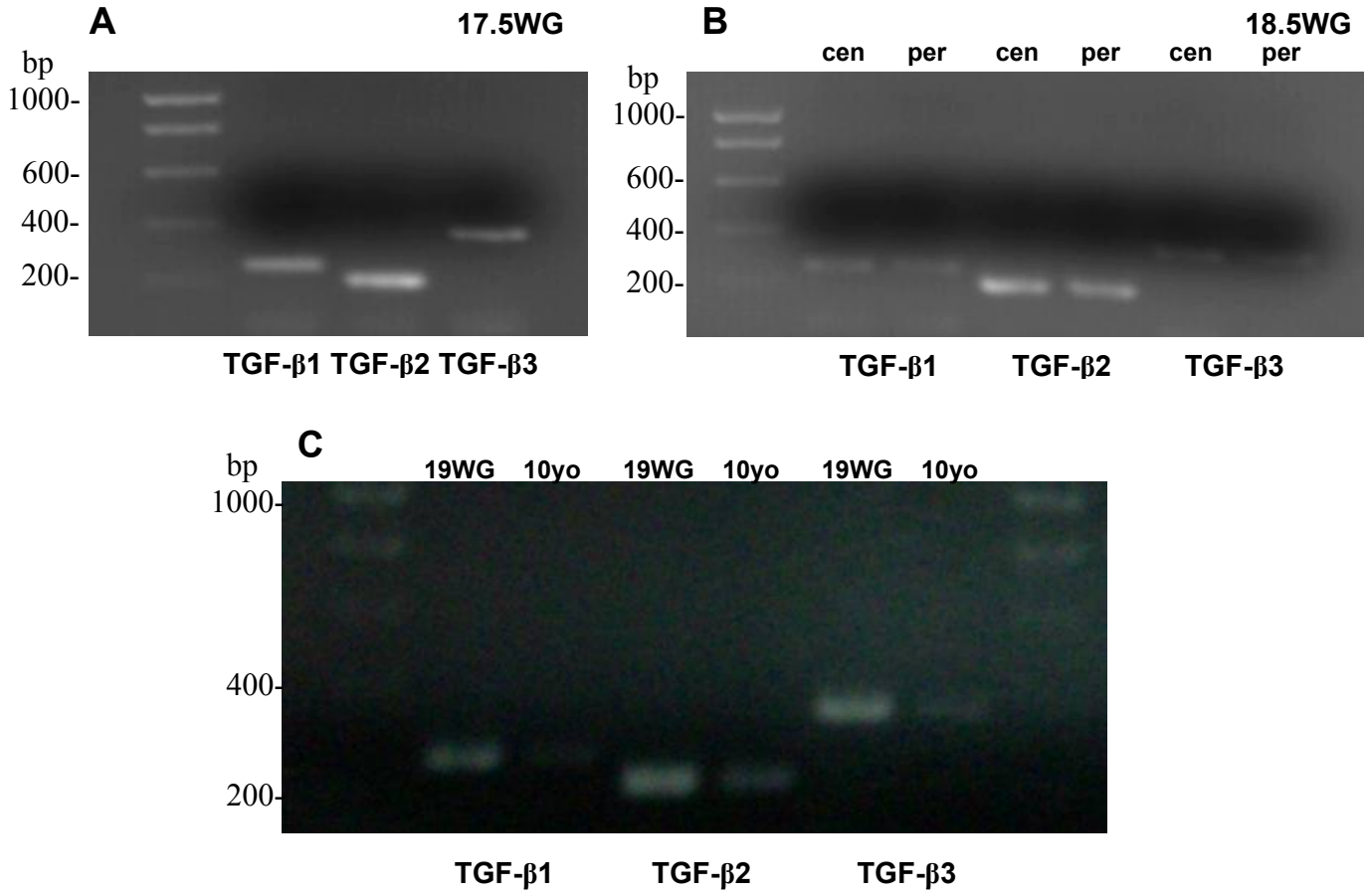

FIGURE 4.1

A: All TGF-β isoforms were present at 17.5WG, with amplicon sizes of 267bp- TGF-β1; 225bp- TGF-β2; 367bp - TGF-β3.

B: Peripheral (per) *versus* central (cen) expression for all three TGF-β isoforms in an 18.5WG eye shows more intense bands for TGF-β2 but little difference between peripheral and central expression.

C: Less TGF-β expression of all isoforms was noted in a 10 year old eye when compared to 19WG foetal eye.

TGF-β1 isoform

The take off point for TGF-β1 occurred late in the course of the quantitative PCR amplification cycles, suggesting very low amounts of mRNA in the retina source tissue. Using the Pfaffl equation, the highest amounts of TGF-β1 were found in the central retina at 18WG and in the peripheral retina for the 20yo retina (Figure 4.2). The lowest amounts were seen in the 16-18WG peripheral retina. When central and nasal retinas were compared at each age, TGF-β1 expression was highest in the central retina at 16WG, 18WG, but in the peripheral retina in the 20yo samples (Figure 4.2). Amplification specificity was confirmed when PCR products were subjected to a melting curve analysis and showed a single predominant product.

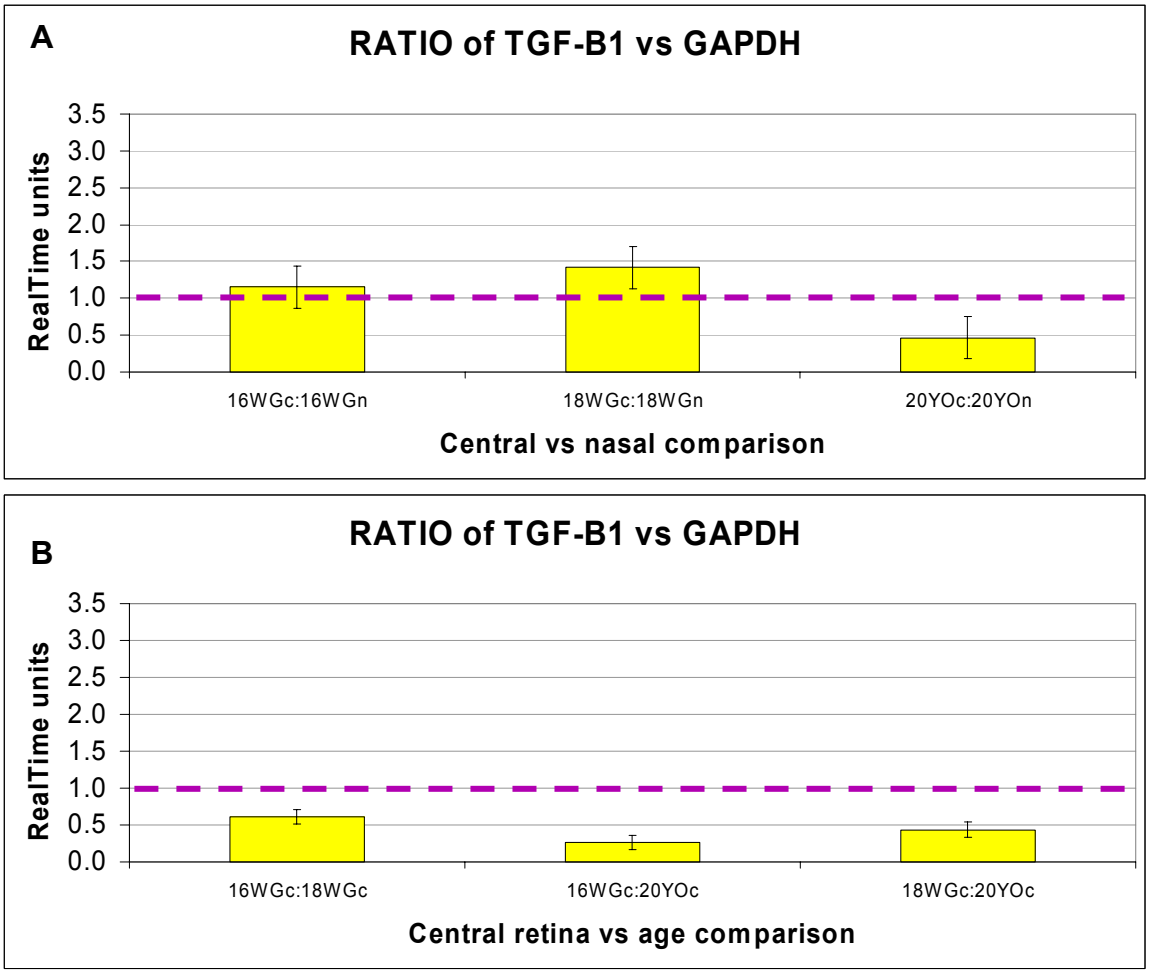

FIGURE 4.2 Ratio of TGF-β-1 gene expression relative to GAPDH. Error bars are standard error measurements (SEM). Ratios >1 indicate higher TGF-β1 gene expression in the central sample, whilst ratios <1 show lower gene expression in the central sample.

A. Central versus nasal expression of TGF-β1 at three ages. Ratios are calculated using replication take off values for TGF-β1 and GAPDH in the Pfaffl equation. The graphs show values for 16WG, 18WG and 20yo central (c) and nasal (n) retina indicating that higher levels for TGF-β1 expression are found in the central foetal retina when compared to the periphery. In the adult retina TGF-β1 expression is higher in the nasal retina when compared to the central retina.

B. TGF-β1 expression in central retina at different ages. The findings indicate that the adult central retina has the highest levels of TGF-β1 expression, followed by the 18WG central retina.

TGF-β2 isoform

The replication take off points for TGF-β2 were the earliest in the amplification cycles for all samples, suggesting a relative abundance of TGF-β2 isoform in the retina. Using the Pfaffl equation, the highest amounts of TGF-β2 were found in the central retina at all ages when compared to the corresponding nasal retina (Figure 4.3A). When central retina was compared between ages, little difference was observed between the 16WG-18WG and the 20yo retina, however that slight difference showed TGF-β2 expression was highest at 16WG and lowest in the 20yo retina (Figure 4.3B). When nasal retina was compared between ages, TGF-β2 expression was found to be highest in the 20yo retina and lowest in the 18WG retina.

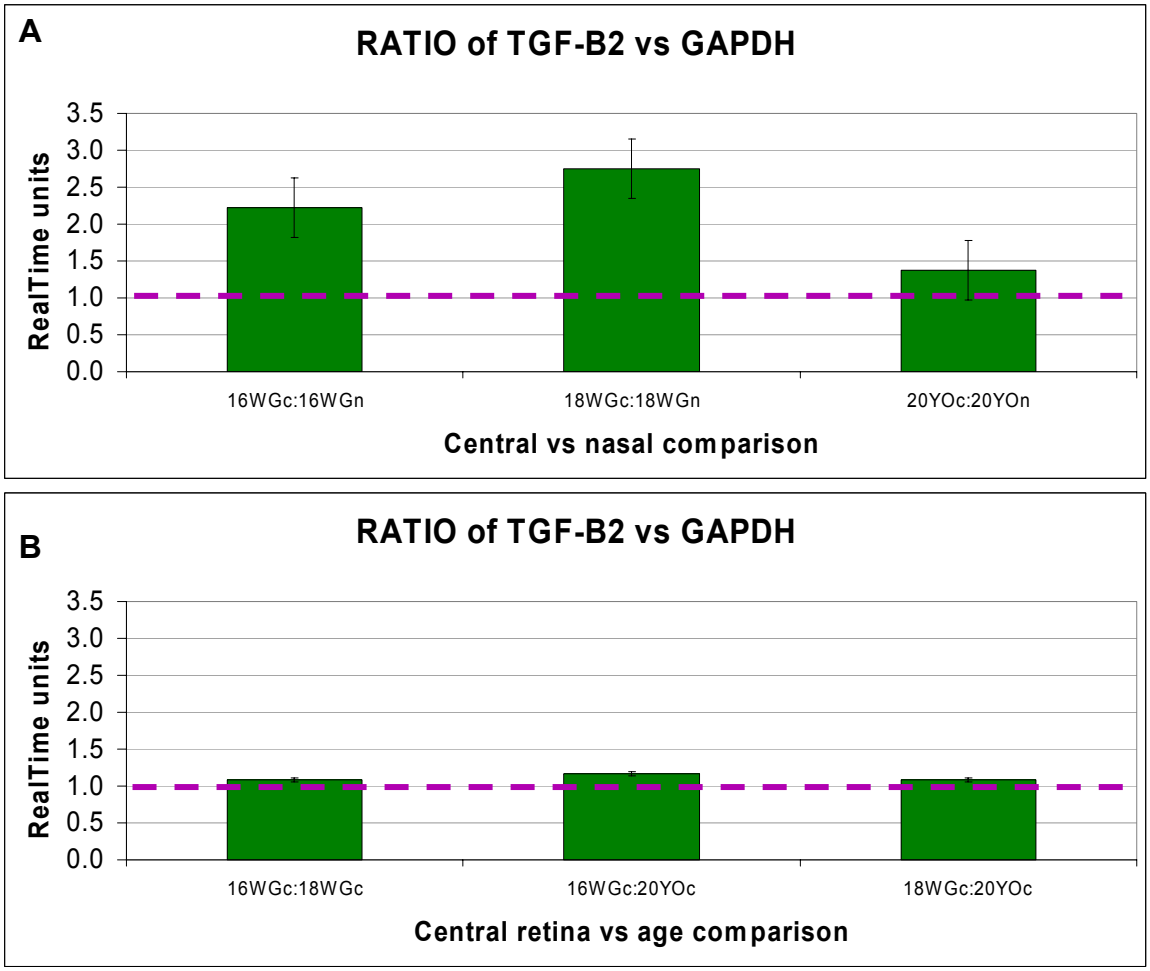

FIGURE 4.3 Ratio of TGF-β-2 gene expression relative to GAPDH. Error bars are SEM.

A. Central versus nasal TGF-β2 expression comparison. A ratio>1 indicates higher levels of TGF-β2 expression in the central retina compared with peripheral retina at all ages.

B. Central retina TGF-β2 expression versus age comparison indicates that levels of TGF-β2 in central retina do not change significantly between 16-18WG and adulthood. The mildly increased levels of TGF-β2 are seen in the central retina at 16WG and the lowest levels at adulthood.

TGF-β3 isoform

An almost identical pattern to TGF-β2 expression is seen for TGF-β3 in the foetal retinas. TGF-β3 is predominantly expressed in the central retina compared with nasal retina in the youngest retinas (Figure 4.4A) and does not change over time (16-18WG compared to 20yo) (Figure 4.4B). When both central and nasal retinas are compared between ages, although the difference is small, TGF-β3 expression is highest centrally at 16WG and lowest in the 20yo nasal retina. Amplification specificity was confirmed when PCR products were subjected to a melting curve analysis and showed a single predominant product.

These quantitative analyses indicate that in foetal retinas higher levels of all TGF-β isoforms are expressed in the central retina when compared to the peripheral retina (Figure 4.5). TGF-β2 and TGF-β3 are most highly expressed in the youngest retina at 16WG with only low levels of TGF-β1 detected at all ages. In the adult, TGF-β2 is preferentially expressed in the central retina. Also TGF-β1 levels expressed in the adult nasal retina exceed those observed in the developing retina. Overall the quantitative analyses indicate that higher levels of all TGF-β isoforms are found in the developing retina compared to adult human retina. TGF-β2 is the most abundant of the isoforms, followed by TGF-β3, and TGF-β1.

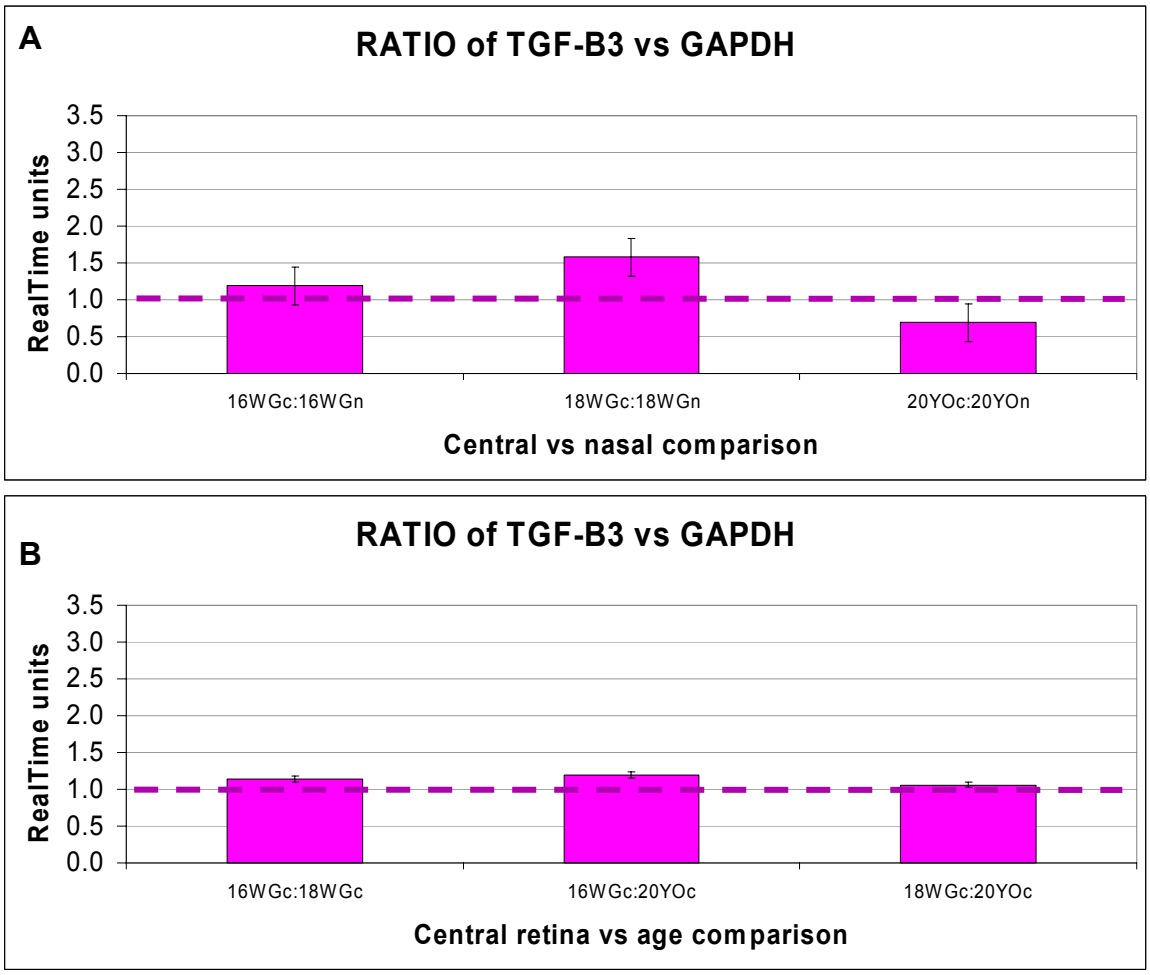

FIGURE 4.4 Ratio of TGF-β-3 gene expression relative to GAPDH. Error bars are SEM.

A. Central versus nasal TGF-β3 expression comparison, indicating central retina TGF-β3 expression is greater than in the peripheral retina in foetal retinas, but not in adult retina.

B. Central retina TGF-β3 expression versus age comparison showing TGF-β3 expression in central retina is mildly increased when the developing central retina is compared to the adult retina, with higher TGF-β3 levels seen in 16WG-18WG and lowest levels in the 20yo retina.

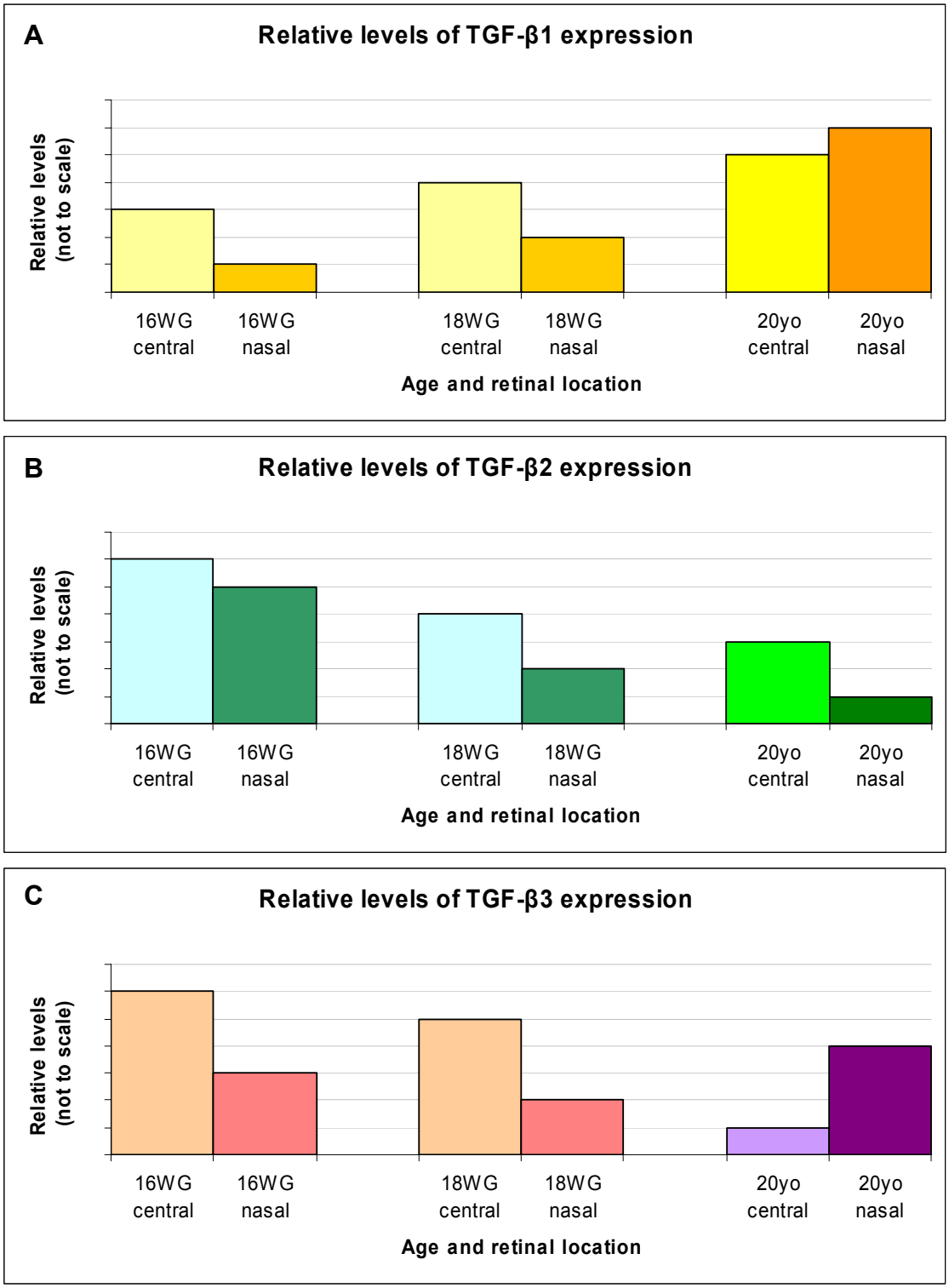

FIGURE 4.5 Relative levels of expression of **A.** TGF-β1, **B.** TGF-β2 and **C.** TGF-β3 in central compared with nasal retina at 16WG, 18WG and at 20 years. All TGF-β isoforms are present at higher levels in central compared with nasal retina in the samples from foetal retinas. TGF-β1 and TGF-β3 were more abundant in nasal retina in the 20yo sample.

4.4 DISCUSSION

RTPCR followed by QPCR is the most powerful method for analysing mRNA expression from small samples. For quantitative purposes traditional methods rely on endpoint analyses which are not very accurate due to variations in amplification efficiency in the later stages of the PCR reaction (Simpson *et al.*, 2000). The use of fluorescent hybridisation probes has enabled real-time monitoring of the amplification reaction (Simpson *et al.*, 2000). The high affinity double-stranded (ds) DNA binding dye SYBR green has negligible fluorescence in the absence of dsDNA, but high fluorescence upon binding to dsDNA. It can be used with any primer pair provided no non-specific PCR products are amplified (Lee *et al.*, 1993; Wittwer *et al.*, 1997; Morrison *et al.*, 1998; Simpson *et al.*, 2000). Monitoring each PCR reaction by means of fibre optic fluoroimetry results in a curve of fluorescence which can be used to quantify the product of interest.

In this study RTPCR confirmed the presence of all three TGF-β isoforms in the human retina and suggested that TGF-β2 is the predominant isoform in developing and adult human retina. QPCR confirmed those findings, also indicating that TGF-β2 is the predominant isoform expressed in the retina (Figure 4.3A compared to Figure 4.2A, 4.4A). The developing and adult human retina showed lower levels of TGF-β3, with very little evidence of TGF-β1 detectable. These results are consistent with previous investigations of TGF-β isoforms in the normal primate vitreous and ocular tissues (Pfeffer *et al.*, 1994; Connor *et al.*, 1989). In the Pfeffer study, high levels of TGF-β2 expression were reported in the vitreous humour, neural retina and RPE-choroid using enzyme linked immunosorbent assay (ELISA) (Pfeffer *et al.*, 1994). Growth factors in the vitreous are generally agreed to originate from the retina, and it has been reported that most TGF-β activity in the vitreous is from TGF-β2 (84-100%), and only 10-21% from TGF-β1 (Connor *et al.*, 1989). No quantitative information is available on TGF-β3 expression from those studies for comparison.

The significance of the TGF-β1/ TGF-β2 isoforms in retinal development is emphasized in TGF-β2 deficient mice, which show ocular malformations

including hyperplastic retinas (Sanford *et al.*, 1997). Overexpression of TGF-β1 in TGF-β2 null mice rescues the abnormalities in ocular development caused by the deletion of TGF-β2 (Saika, 2005).

The present data also indicate higher levels of expression of TGF-β during retinal development compared to adult retina, with higher levels in developing central retina compared to peripheral retina. In this chapter, the expression of TGF-β in the developing central retina adds support to the idea that the antiproliferative effects of this factor may be responsible for helping to define the FAZ by suppressing astrocyte and endothelial cell proliferation and/or migration during retinal development (see also Chapter 1).

While the present data indicate differences in the levels of expression of TGF-β isoforms in central versus peripheral retina; and in developing versus adult retina, they provide no details concerning the precise distributions of mRNA and protein. Such information is critical in understanding the processes involved in the spatial and temporal development of the human retina, particularly the fovea. Further investigations of the distribution of the TGF-β isoforms and receptors in developing human and primate retinal retina, using *in situ* hybridization and immunohistochemistry, are the subject of Chapter 5.

CHAPTER 5 – TRANSFORMING GROWTH FACTOR-β DISTRIBUTION IN CENTRAL AND PERIPHERAL RETINA

5.1 INTRODUCTION

Evidence for expression of an antiproliferative factor in central retina includes the presence of blind-ended capillaries directed towards the incipient fovea but not entering it (Provis, 2001); reduced cell proliferation in macaque fovea along the horizontal meridian (Stone, 2006) and exclusion of astrocytes and endothelial cells from the fovea during development (Provis *et al.*, 2000). When the ganglion cell vascular plexus - comprising new endothelial cells and astrocytes - forms at the foveal edge at fd105 in the macaque, both cell types appear to be blocked from entering this region even though there are no structural boundaries. Furthermore both astrocytes and ganglion cells in the vicinity express the endothelial proliferation factor, VEGF (Provis *et al.*, 2000; Provis, 2001). Astrocytes are not only excluded from the incipient fovea, but retreat once the perifoveal plexus has formed (Provis *et al.*, 2000; Distler *et al.*, 1993; Distler & Kirby, 1996; Distler *et al.*, 2000).

In Chapter 4, I reported on the quantitative analysis of TGF-β expression in developing and adult human retina, using reverse transcription polymerase chain reaction (RTPCR) and real time quantitative PCR (QPCR). According to the proposed hypothesis (Chapter 1.3), TGF-β was expected to be preferentially expressed at the incipient fovea. Indeed, for all the foetal retinas examined, there was relatively higher expression of all TGF-β isoforms in the central compared with peripheral retina, although level of expression varied for the different isoforms. The lower levels of TGF-β1 found using QPCR suggests potential difficulties in accurately quantifying this isoform in the retina when using relatively less sensitive techniques such as *in situ* hybridisation (Nuovo, 1996).

In order to clarify the RTPCR and QPCR results described in chapter 4, I further investigated the expression and distribution of mRNA and protein for the different TGF-β isoforms, in sections of human and macaque retina, during development and in the postnatal period. The development of the visual pathways and retinas in humans and macaques is similar as they share not only a common developmental timetable but the same retinal cell types and connections (Dreher & Robinson, 1988; Kolb *et al.*, 1992). As such, a comprehensive developmental profile for TGF-β1, TGF-β2 and TGF-

β3 mRNA and protein expression and distribution as well as localisation of TβRI and TβRII proteins was possible for both human and macaque retinas.

5.2 MATERIALS AND METHODS

SPECIMENS

Fourteen human foetal eyes between 11 and 19 WG were obtained from terminations of pregnancy with informed maternal consent, following approval from the Human Ethics Committee, University of Sydney (Chapter 2.1). Gestational age was determined by preoperative obstetric ultrasound and *post mortem* ocular morphometry. Fifteen macaque (*Macaca fascicularis*) eyes aged foetal day (fd) 64, fd73, fd85, fd95, fd105, fd115, fd130, fd155, fd169, postnatal day 6 (p6d), postnatal week 12 (p12wk), postnatal month 4 (p4mo), postnatal month 6 (p6mo), postnatal 2.5 years (p2.5y) and postnatal 11 years (p11y) were obtained from Bogor Agriculture University, Indonesia following approval from the Ethics Committee of the University of Washington, Seattle, USA. Sections from macaque retina were processed in paraffin, human sections frozen, as described in Chapter 2. Only sections through the optic disc and fovea were analysed quantitatively.

IMMUNOHISTOCHEMISTRY

Details of Immunohistochemistry methods are described in detail in Chapter 2.9. Briefly, sections were incubated at 4ºC overnight in polyclonal rabbit anti-human TGF-β1, TGF-β2, TGF-β3, TβRI or TβRII antibodies (1:200) and either antibodies to TAU (ganglion cells, 1:200), vimentin (Müller cell intermediate filaments, 1:100), GFAP (astrocytes , 1:1000), calbindin (amacrine and horizontal cells, 1:50), S-opsin (short wavelength opsin in cones, 1:10000), RG-opsin (medium-long wavelength opsin in cones, 1:1000) or rhodopsin (rods, 1:500) (see also Table 2.4). After rinsing in PBS, sections were incubated for 60 minutes in goat anti-rabbit Alexa-488 (1:1000; Molecular Probes) to visualise bound anti-TGF-β or TβR and/or goat anti-mouse Alexa-594 (1:1000; Molecular Probes) to visualise the remaining antibodies. For some antibodies raised in the same species as the TGF-β and TβR antibodies, adjacent retinal sections of tissue were immunolabelled with a single antibody.

RNA EXTRACTION

As described in Chapter 2.4, retinas were carefully removed from the choroid and the Trizol-extracted RNA was dissolved in 25µl RNAse free water, incubated at 42˚C for 10 minutes and then stored at -80˚C until used. Purity was determined by using spectrophotometer (Biorad SmartSpec^{TM}3000) where samples having absorbance ratio A260/A280 greater than 1.8 were used for analysis.

POLYMERASE CHAIN REACTION (PCR)

PCR primers with base sequences complementary to the known sequences flanking the target DNA were designed for TGF-β1, TGF-β2 and TGF-β3 (Table 5.1, Chapter 2.5). The three forward and three reverse primers were synthesised by Sigma Genosys Australia. For probe design, the amplicon length was longer compared with QPCR products, that is, 200-400 base pairs (bp), so that more labelling molecules would bind to the probe improving visualisation of target mRNA.

TABLE 5.1 Primer sequences used for riboprobe construction.

Protein	Accession number	Forward primer Sequence 5' to 3'	Reverse primer Sequence 5' to 3'	Amplicon size (bp)
TGF-β1	X02812	AACCCACAACGAAATCTATGAC	ACTCCGGTGACATCAAAAGATA	267
TGF-β2	NM03238	AAGCAGAGTTCAGAGTCTTTCG	AATCCCAGGTTCCTGTCTTTAT	225
TGF-β3	X14149	AGTCGGAATACTATGCCAAAGA	GTTGGACTCTCTTCTCAACAGC	367

Using Superscript ^{TM}II Firststrand Synthesis System for Reverse Transcriptase-PCR (Invitrogen, Ca, USA) cDNA was produced and stored at –20˚C for a maximum of 2-3 months.

A standard PCR was performed using Platinum Taq (Invitrogen), and a Hybaid PCR Express thermocycler, where amplification of dsDNA occurred. A 1% agarose gel and spectrophotometry (Biorad SmartSpec^{TM}3000) were used to assess dsDNA size and concentration respectively.

RIBOPROBE PREPARATION

RNA isolated from foetal retinas was reverse transcribed to cDNA and amplified by PCR amplification using specific primers (see Chapter 2.5). PCR products were purified by gel extraction and inserted into pGemT Easy DNA vector (Promega), cloned in heat shocked competent cells (JM109, Promega), further grown up in *E. coli* cells and purified using Miniprep (QIAprep Miniprep) and Midiprep (Jet Star) kits. DNA was used as a template for preparing digoxigenin (DIG)-labelled riboprobes for *in situ* hybridisation (see Chapter 2.7).

IN SITU HYBRIDISATION

Frozen and dewaxed paraffin sections were incubated in the hybridisation mix, which was combined with 1µl DIG RNA transcript (Sense or Antisense) and finally incubated with anti-DIG AP (Fab fragments) antibody (see Chapter 2.8). After the reaction was stopped, selected slides were subsequently immunolabelled (see Chapter 2.9).

CONFOCAL MICROSCOPY

A retinal montage of a section from a 16WG eye was used to assess the validity of analysing retinal regions as representative of TGF-β distribution across the whole retina. Six retinal regions; the incipient/established fovea (foveal, F), peripheral (nasal, N; temporal, T) and transitional regions (nasal parafoveal, PFN; temporal parafoveal, PFT; nasal to optic disc, ND) were selected using morphological criteria (discussed in Chapter 3).

Sections were imaged using a Carl Zeiss upright scanning laser confocal microscope (Carl Zeiss LSM5 Pascal software). An argon-krypton laser with dual filters for maximum excitation (488nm and 594nm) was used to visualise green Alexa-488 labelled cells/structures and/or red anti-TGFβ or anti-TβR (Alexa-594/Fast Red) labelled structures respectively. Photomultiplier gain, offset, aperture and laser power settings were standardised and maintained for all measurements for comparisons between specimens.

All confocal image sample areas (230µmx230µm) were acquired using a 40x water immersion objective and processed in one of two ways. A 16WG

human retinal montage was compiled from 77 samples images adjacent to each other (Figure 5.1, Appendix B). All remaining human and macaque specimens of varying ages were compiled into a representative minimontage by combining a sample area from each of the six retinal regions described above (Figure 5.2, Appendix B).

IMAGE ANALYSIS - Quantifying distribution of TGF-β

Confocal images were opened in Adobe Photoshop 7.0 and organised into either (1) a 77 image montage for the whole 16 WG retina specimen or (2) several six image montages, with each image corresponding to a particular retinal location for all other remaining specimens (Figure 5.1 and 5.2, Appendix B). All montages were saved in TIFF format and then reimported into LSM5 Pascal software (Carl Zeiss). Protein or mRNA expression distribution intensity was recorded using the Pascal measurement tool. Optical density recordings were made at 1μm intervals across the ganglion cell layer (GCL), outer neuroblastic zone (ONZ) and superior, middle and inferior aspects of the photoreceptor (PR) layer and were tabulated (Figure 5.3). Optical density recordings from undifferentiated peripheral photoreceptor regions were not recorded. Finally, the optical density values were compiled and graphed using an Excel spreadsheet.

VALIDATION OF SAMPLING

As described above and in Appendix B, representative regions across the retinas, (T, PFT, F, PFN, ND and N) were assembled as minimontages. To validate that the distribution of optical density values obtained from sampling of the six retinal regions was representative of optical density values obtained when measurements were made across a whole retinal section, the data corresponding to the optical densities across the GCL and the ONZ were compared. Median optical density values (MD) and standard deviations (SD) were not significantly different in the minimontage samples compared with the whole eye section. Comparison of graphs showing the optical densities across the photoreceptor layer in both the whole eye and minimontage also showed little variation between corresponding retinal regions. Further details of this analysis are given in Appendix B.

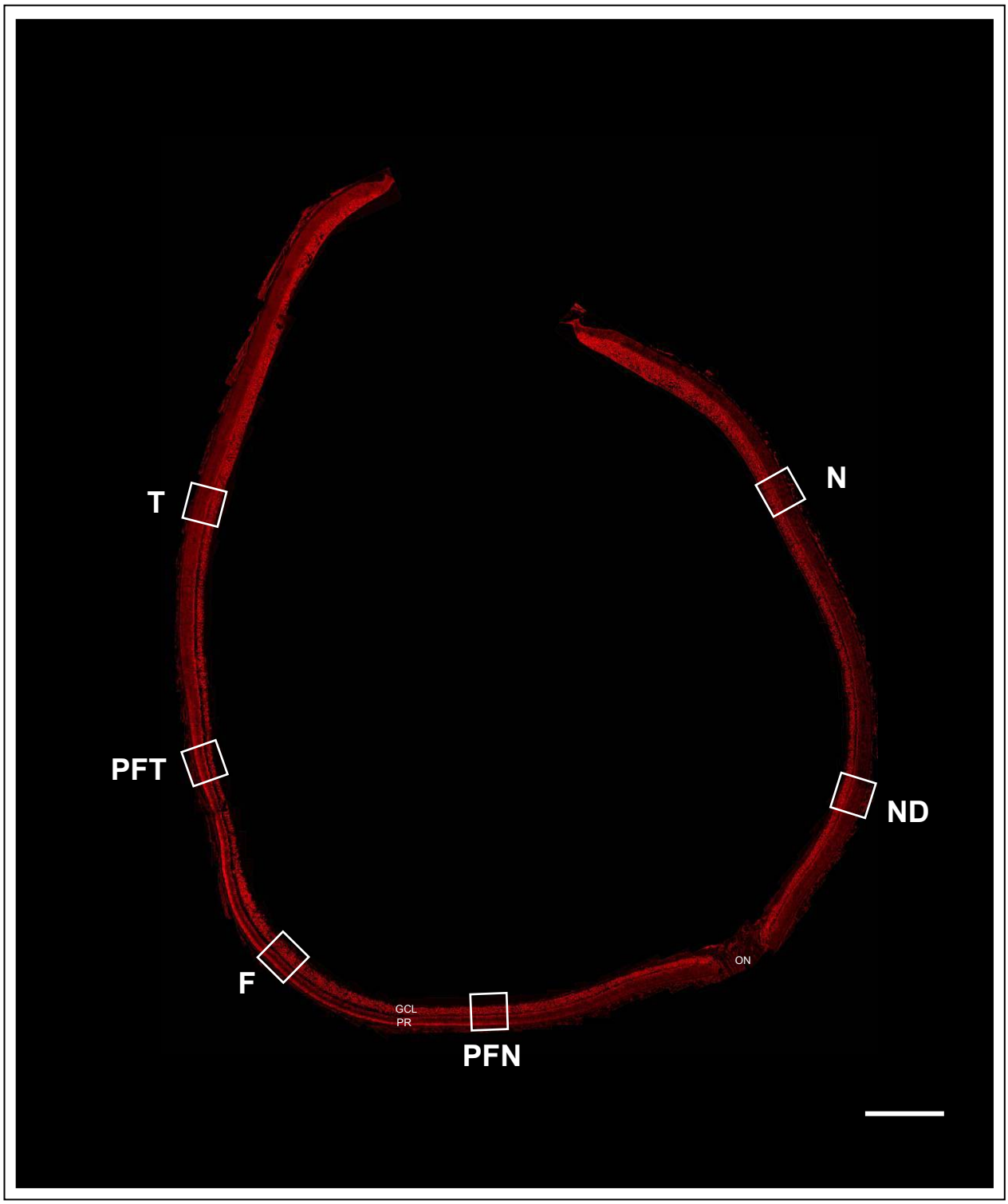

FIGURE 5.1 Montage of 16WG human retina demonstrating TGF-β2 mRNA expression in ganglion cell layer (GCL) and photoreceptor (PR) layer. The representative sample areas used for the minimontages are also shown (white boxes) - T: temporal, PFT: temporal parafoveal, F: foveal, PFN: nasal parafoveal, ND: nasal to disc and N: nasal. Optic nerve (ON) is also shown. Bar= 500μm.

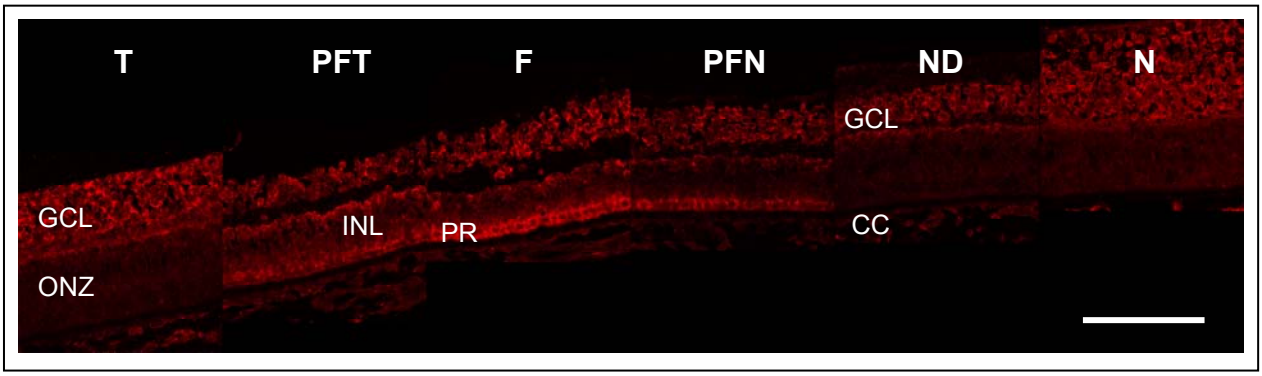

FIGURE 5.2 Representative example of six retinal regions in a minimontage, showing TGF-β2 mRNA expression in a 16WG retina. (GCL: ganglion cell layer; INL: inner nuclear layer; ONZ: outer neuroblastic zone; PR: photoreceptor layer; CC: choriocapillaris). Bar = 100μm.

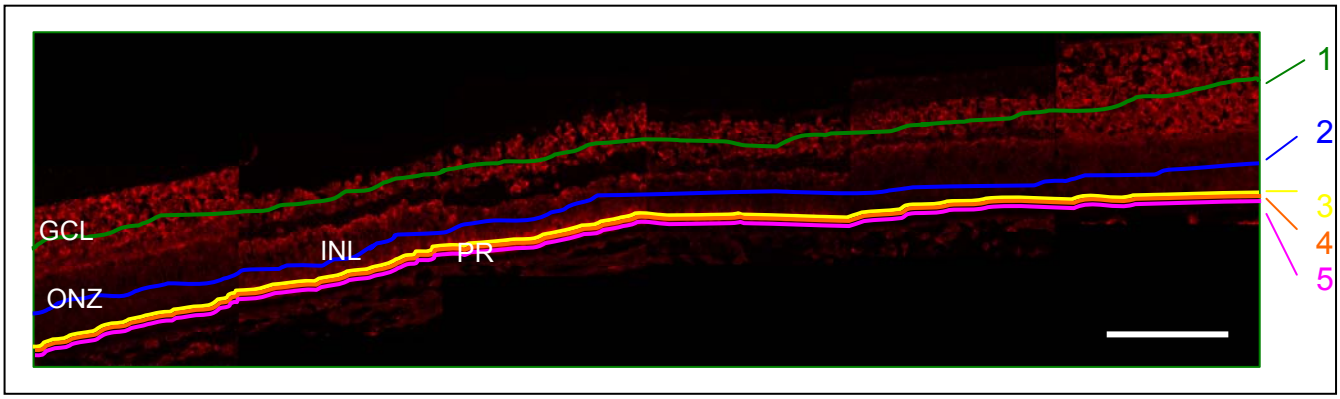

FIGURE 5.3 Representative example of the 5 tracks (coloured lines) within the retina along which optical density measurements were made at 1μm intervals. GCL (Measurement 1: green); ONZ/INL (2: blue); PR top (3: yellow); PR middle (4: orange); PR bottom (5: pink). In the younger specimens where photoreceptors have not differentiated in the peripheral retina optical density measurements were not recorded. Bar = 100μm.

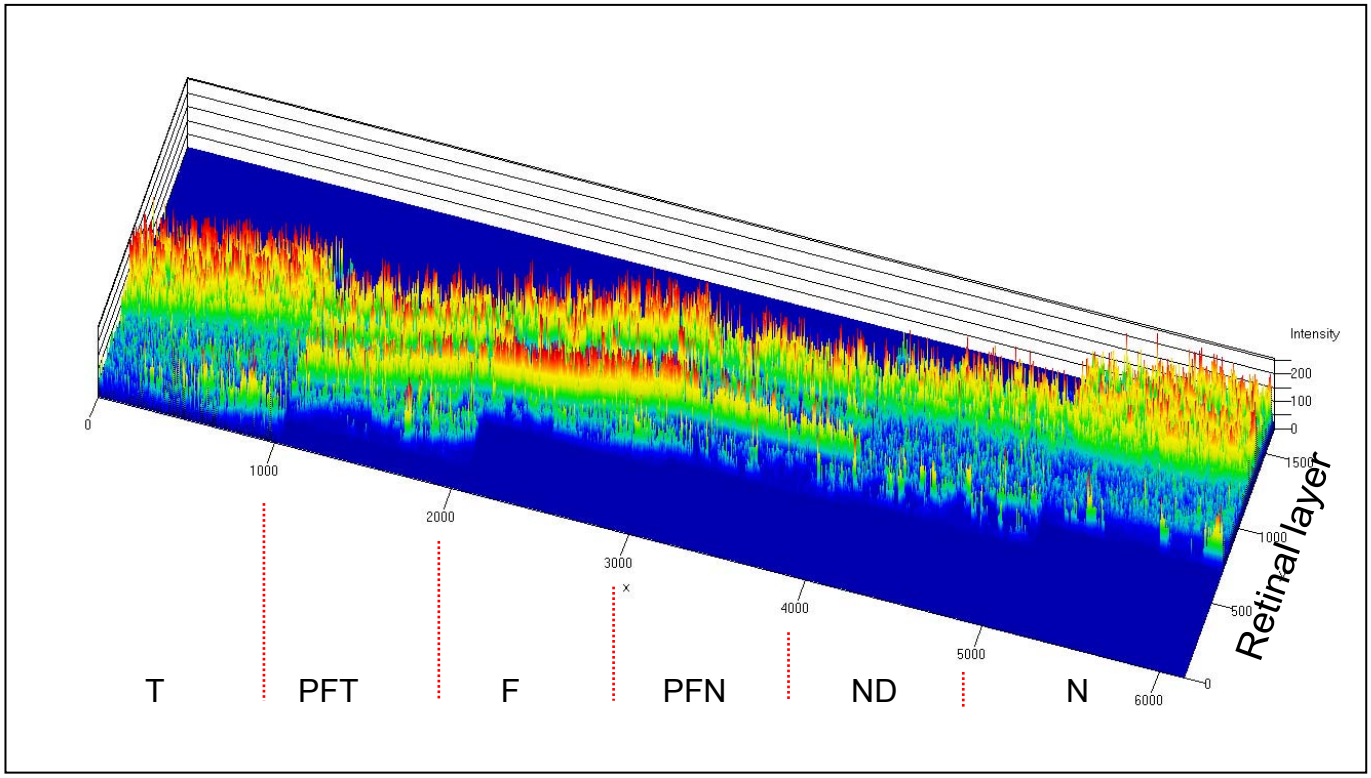

FIGURE 5.4 3D colour diagram of optical density in a minimontage of a 16WG human retina. Optical density is proportional to colour. The highest optical density for TGF-β2 protein is shown as red peaks in the GCL (top row) and in the photoreceptor layer (bottom row), particularly in the foveal region.

5.3 RESULTS

A rabbit IgG negative control also showing specificity was included in each set of experiments (Figure 5.5)

TGF-β1 PROTEIN

Location

Cytoplasmic TGF-β1 protein is seen in the photoreceptors and ganglion cells of developing retina (Figures 5.6, 5.7). At 13WG minimal immunolabelling is seen in the photoreceptors. Older retinas have more prominent immunolabelling that initially involves the outer segments (Figure 5.6 PFT and PFN) and progresses to include entire photoreceptors by 16-17WG (Figure 5.6 F). Higher intensity immunolabelling is also seen in the central photoreceptors compared to the periphery from 14WG onwards. The variable labelling in the ganglion cell layer shows no central to peripheral variation and is seen for all ages studied. Vessels in the choriocapillaris are inconsistently immunolabelled. Positive labelling in the macaque is seen only in the postnatal retina, in both photoreceptors and ganglion cells (Figure 5.8).

Distribution

Optical densitometry analysis of immunolabelled sections was used to observe the relative levels of TGF-β1 protein in the photoreceptor, ganglion cell and ONZ layers. A centro-peripheral gradient of optical densities is seen in the photoreceptor layer with peak relative levels of TGF-β1 protein in the central retina including the parafoveal regions for all ages examined (Figure 5.9). In the macaque, levels of TGF-β1 protein are low in foetal retinas (Figure 5.10A, 5.10B, 5.10C), although a centroperipheral gradient of TGF-β1 immunoreactivity is evident in the postnatal specimens (Figure 5.10D).

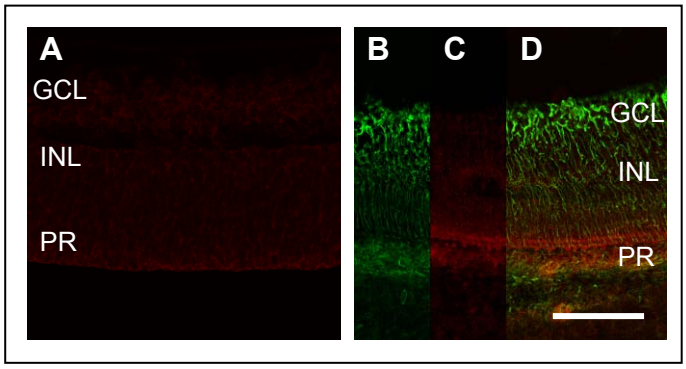

FIGURE 5.5 A Sample of rabbit IgG negative control for TGF-β in 14WG retina **B-D** Positive labelling with TGF-β (red) and vimentin (green) with **B** showing vimentin only, **C** showing TGF-β only and **D** showing both TGF-β and vimentin labelling. (GCL: ganglion cell layer; INL: inner nuclear layer; PR: photoreceptor layer). Bar = 100μm.

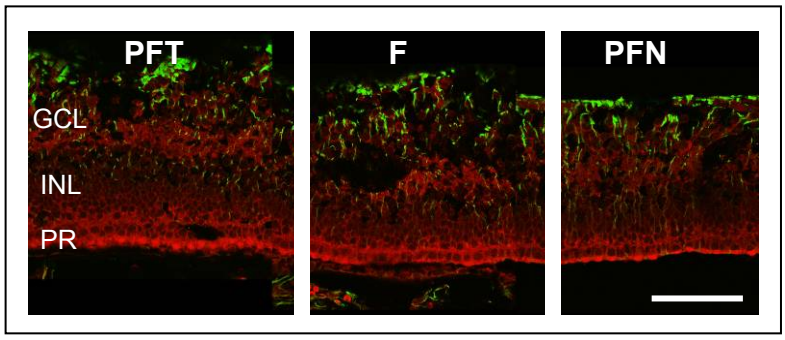

FIGURE 5.6 Distribution of TGF-β1 protein (red) and vimentin (green) across central 17WG retina. Weak immunolabelling is seen in the GCL, with moderate labelling in the photoreceptor (PR) layer in the foveal (F) and parafoveal regions (PFT- parafoveal temporal, PFN- parafoveal nasal). (INL; inner nuclear layer). Bar = 100μm.

FIGURE 5.7 Distribution of TGF-β1 protein (red) and vimentin (green) in (A) incipient fovea and fovea, (B) parafoveal and (C) peripheral (nasal) regions of a 15 and 19WG human retina. (GCL: ganglion cell layer; INL: inner nuclear layer; ONZ: outer neuroblastic zone; PR: photoreceptor layer). Bar = 50μm.

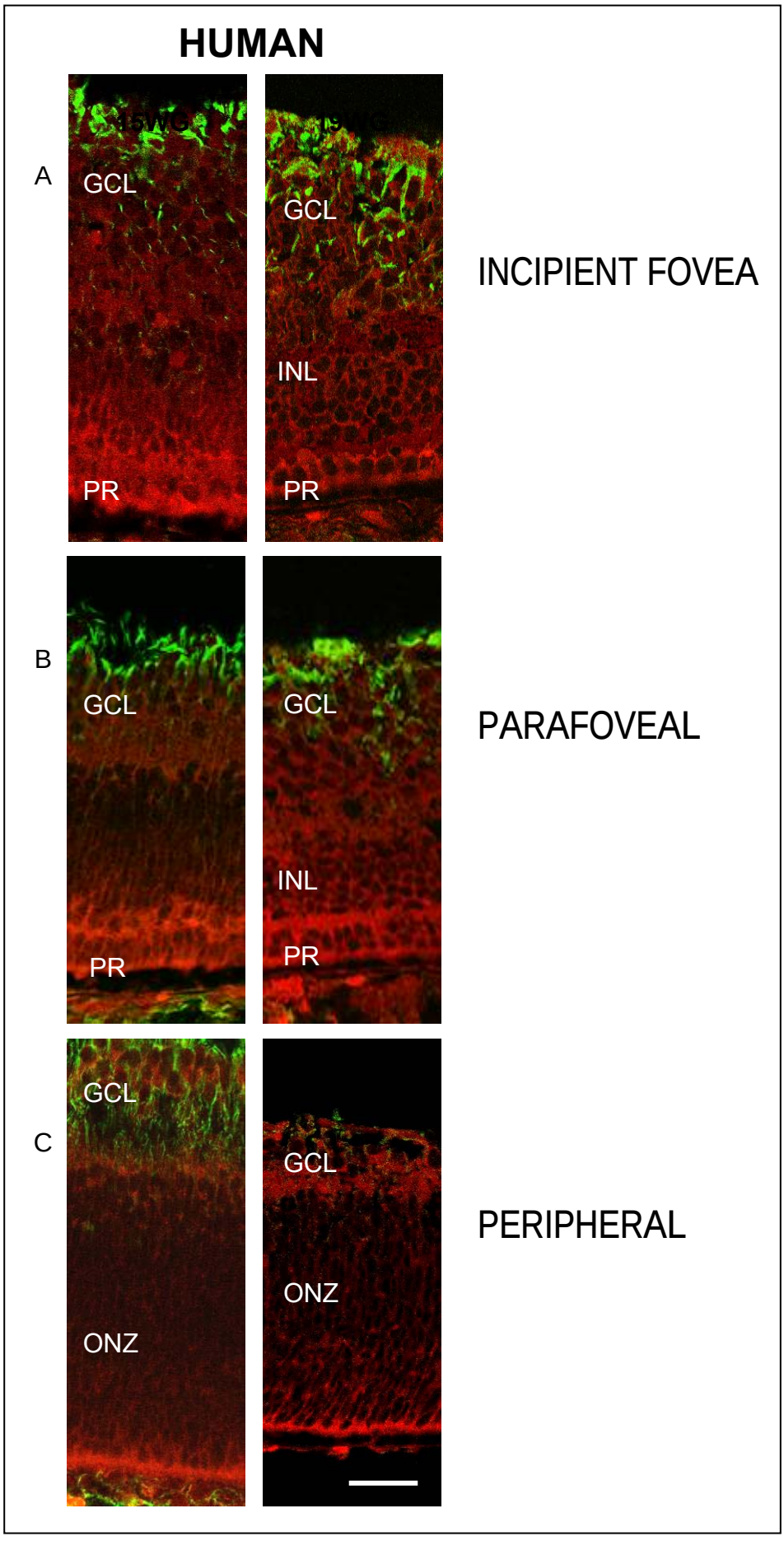
HUMAN
A
15WG
GCL
PR
GCL
INL
PR
INCIPIENT FOVEA
B
GCL
PR
GCL
INL
PR
PARAFOVEAL
C
GCL
ONZ
GCL
ONZ
PERIPHERAL

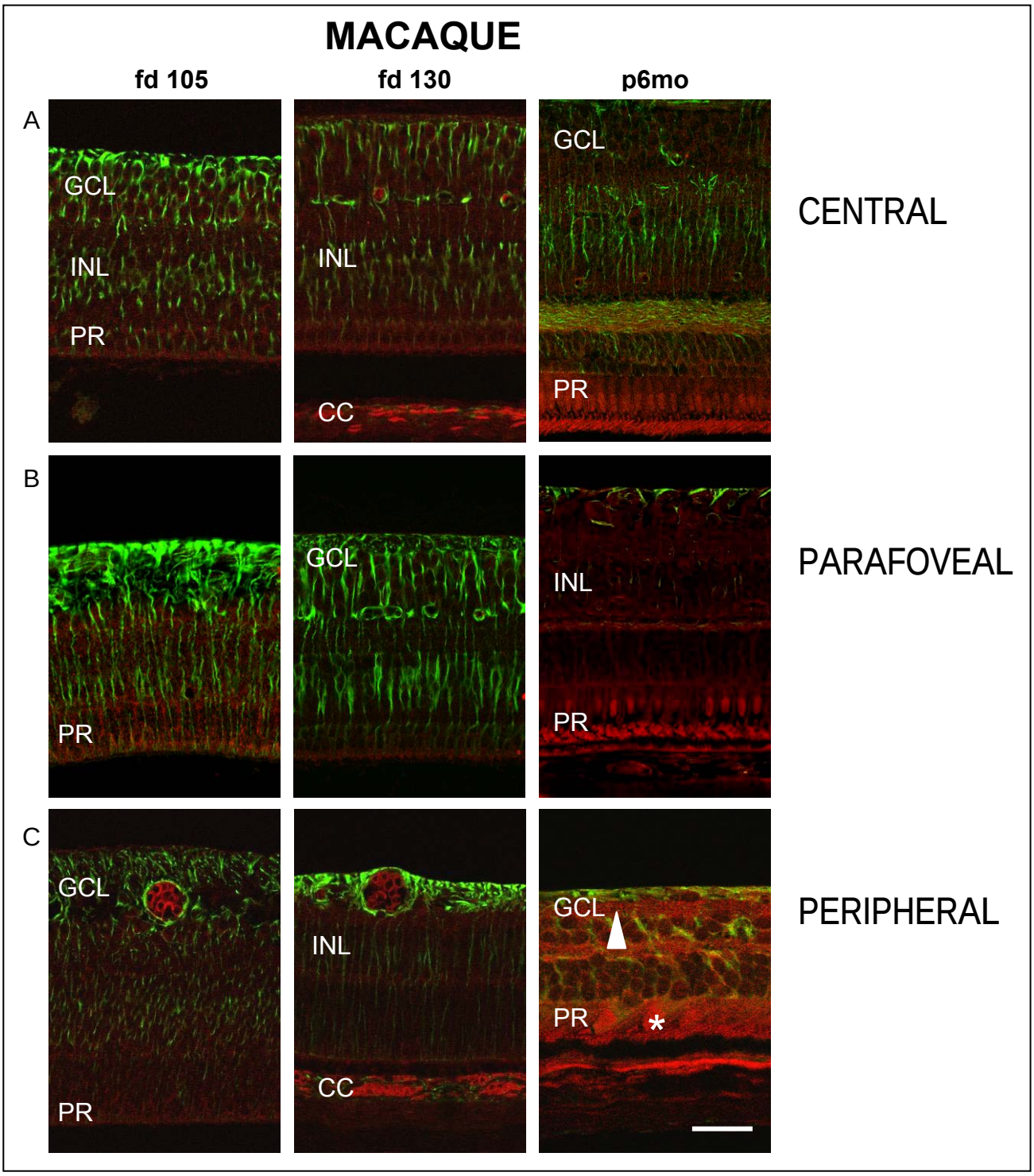

FIGURE 5.8 Distribution of TGF-β1 protein (red) and vimentin (green) in (A) central retina, (B) parafoveal and (C) peripheral (nasal) macaque retina at fd105(~25WG), fd130(~31WG) and post natal 6 months (p6mo). Inconsistent immunostaining of ganglion cells (arrowhead) and mild to moderate staining of photoreceptors (asterisk) is observed as well as in the choriocapillaris. (GCL: ganglion cell layer; INL: inner nuclear layer; ONZ: outer neuroblastic zone; CC: choriocapillaris). Bar = 50μm.

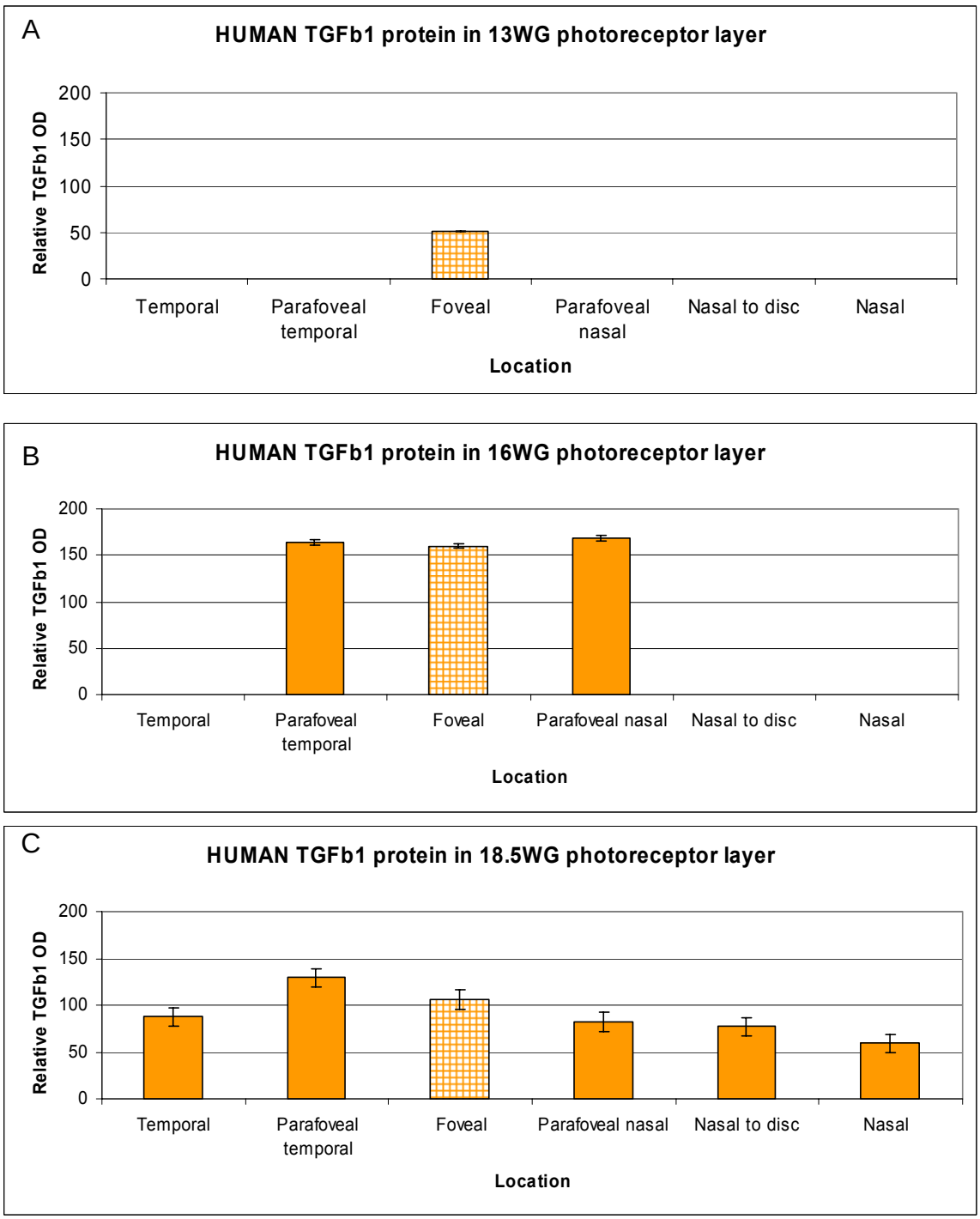

FIGURE 5.9 Relative levels of TGF-β1 protein determined by optical densitometry (OD) in temporal, parafoveal temporal, foveal, parafoveal nasal, nasal to disc and nasal regions of human retina at (A) 13WG - prior to FAZ formation, (B) 16WG and (C) 18.5WG - during FAZ formation. Photoreceptors have not differentiated in the peripheral retina of the younger specimens and therefore no measurements have been graphed for these regions. Error bars = SEM.

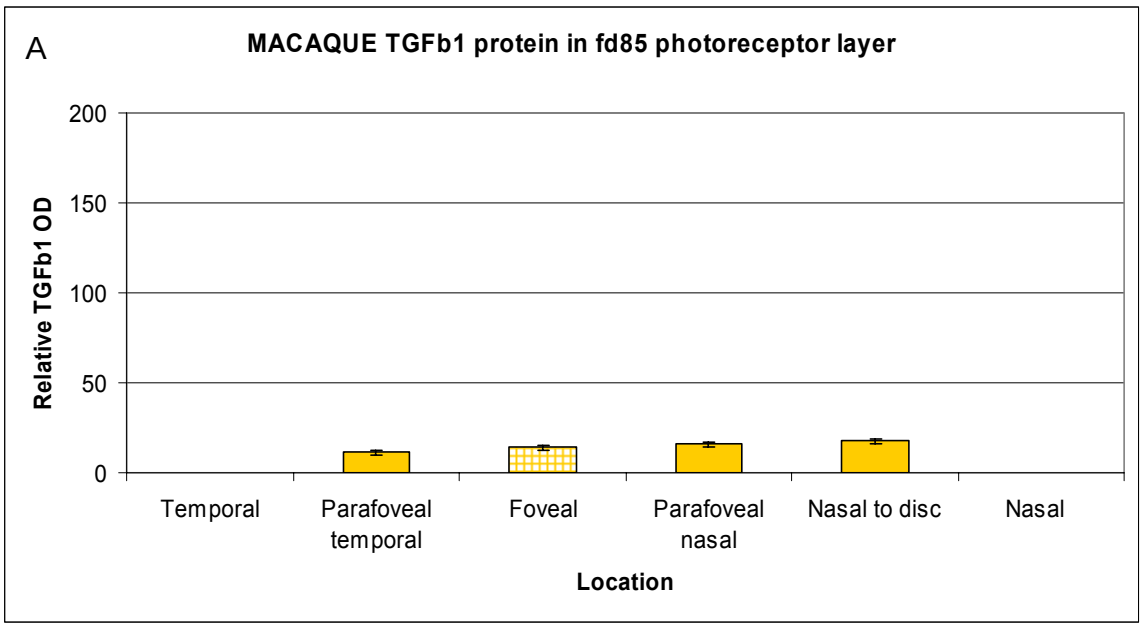
A
MACAQUE TGFb1 protein in fd85 photoreceptor layer
Relative TGFb1 OD
200
150
100
50
0
Temporal
Parafoveal temporal
Foveal
Parafoveal nasal
Nasal to disc
Nasal
Location

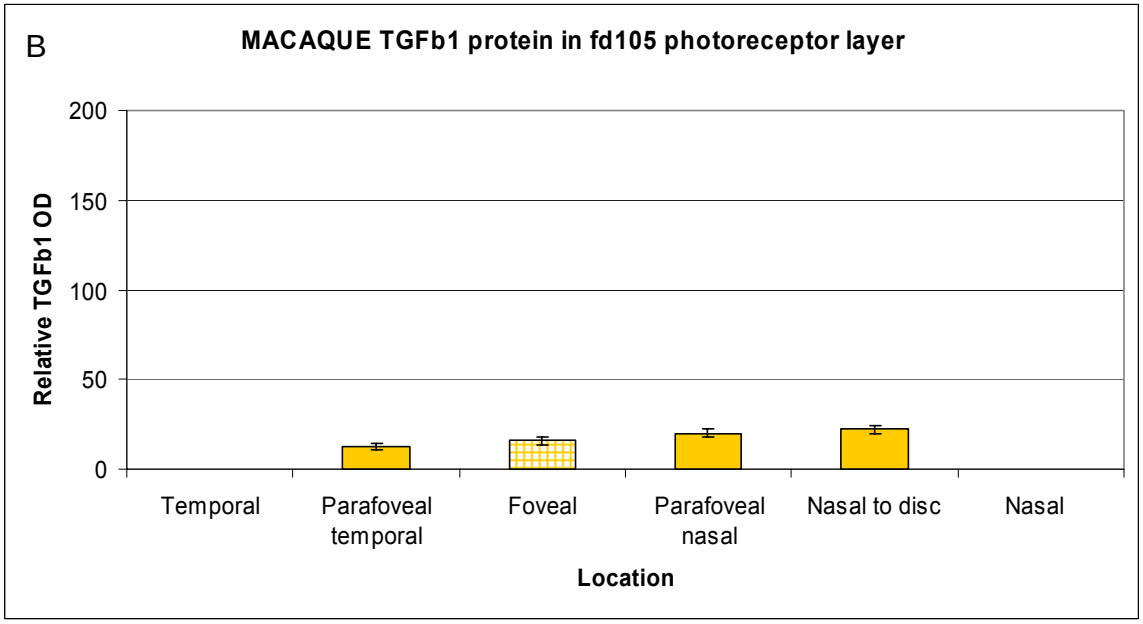
B
MACAQUE TGFb1 protein in fd105 photoreceptor layer
Relative TGFb1 OD
200
150
100
50
0
Temporal
Parafoveal temporal
Foveal
Parafoveal nasal
Nasal to disc
Nasal
Location

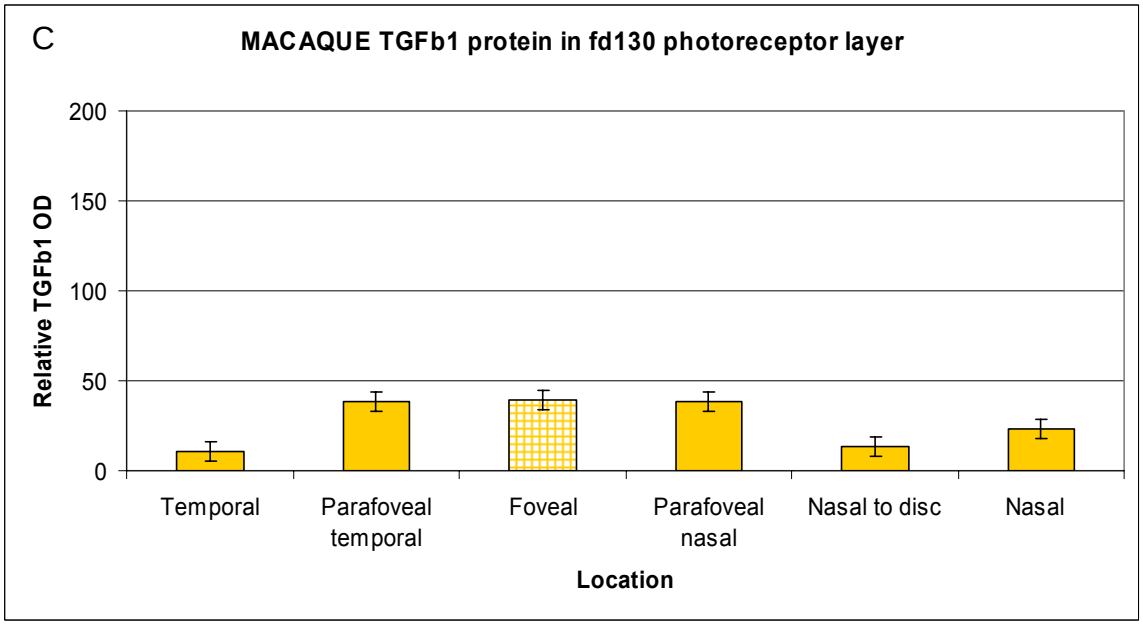
C
MACAQUE TGFb1 protein in fd130 photoreceptor layer
Relative TGFb1 OD
200
150
100
50
0
Temporal
Parafoveal temporal
Foveal
Parafoveal nasal
Nasal to disc
Nasal
Location

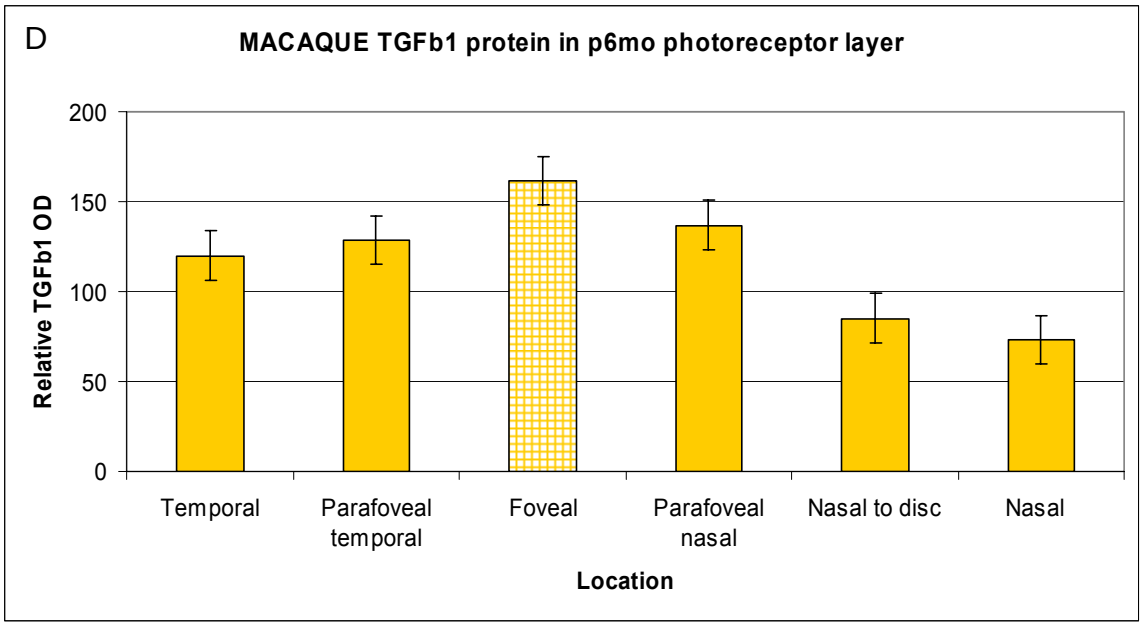

FIGURE 5.10 Relative levels of TGF-β1 protein in macaque retina photoreceptors at five locations (temporal, parafoveal temporal, foveal, parafoveal nasal, nasal to disc and nasal) at four different ages (between fd85-p6mo). High levels of TGF-β1 protein are seen in the macaque photoreceptors postnatally, particularly in the foveal region.

TGF-β1 mRNA

TGF-β1 mRNA expression could not be detected in these experiments, despite multiple attempts at constructing riboprobes for *in situ* hybridisation. The sequence for the riboprobes in each of these attempts was verified to be correct by sequencing, so that problems interfering with probe effectiveness occurred after this step. The restriction enzymes Apa I and Pst I were subsequently treated with T4 DNA polymerase, which catalyses the synthesis of DNA in the 5' > 3' direction causing the 3' overhang removal to form blunt ends. As this did not work, alternative restriction enzymes were used (Nco I and Sal I), that were known not to leave the 3' overhangs which could cause loops to form in the DNA and prevent probe binding to mRNA in tissue. Despite these modifications in the methods, the *in situ* hybridisation could not be successfully performed, most probably due an inability to detect the very small amounts of TGF-β1 mRNA in the retina, consistent with results reported in Chapter 4.

TGF-β2 PROTEIN

Location

Cytoplasmic TGF-β2 protein is detected in photoreceptors and ganglion cells of human and macaque retinas (Figures 5.11, 5.12). At 13WG-14WG, low levels of immunolabelling are seen in the photoreceptors. However from 15WG there is prominent immunolabelling involving the entire photoreceptor. Moderate to strong labelling is seen in the central photoreceptors compared to somewhat lower levels in the periphery of both species (Figures 5.11, 5.12). TGF-β2 expression was variable in the ganglion cell layer (GCL) of human retinas, but more consistent in macaque retinas, with weak to moderate staining of ganglion cells and no obvious central to peripheral variation. Occasionally individual cells in other retinal layers (not GCL or photoreceptor layer) were also immunoreactive for TGF-β2. As described above (Chapter 5); using a panel of antibodies for various retinal cell types, these cells may be identified as astrocytes or horizontal cells. Vessels in the choriocapillaris are also sometimes immunolabelled for TGF-β2 (Figure 5.12).

FIGURE 5.11 Distribution of TGF-β2 (red) and vimentin (green) immunolabelling in (A) incipient fovea and fovea, (B) parafovea and (C) peripheral (nasal) regions of a 15WG and 19WG human retina. TGF-β2 is seen clearly in photoreceptors (asterisks) and in some ganglion cells (arrowheads). (GCL: ganglion cell layer; INL: inner nuclear layer; ONZ: outer neuroblastic zone; PR: photoreceptor layer). Bar = 50μm.

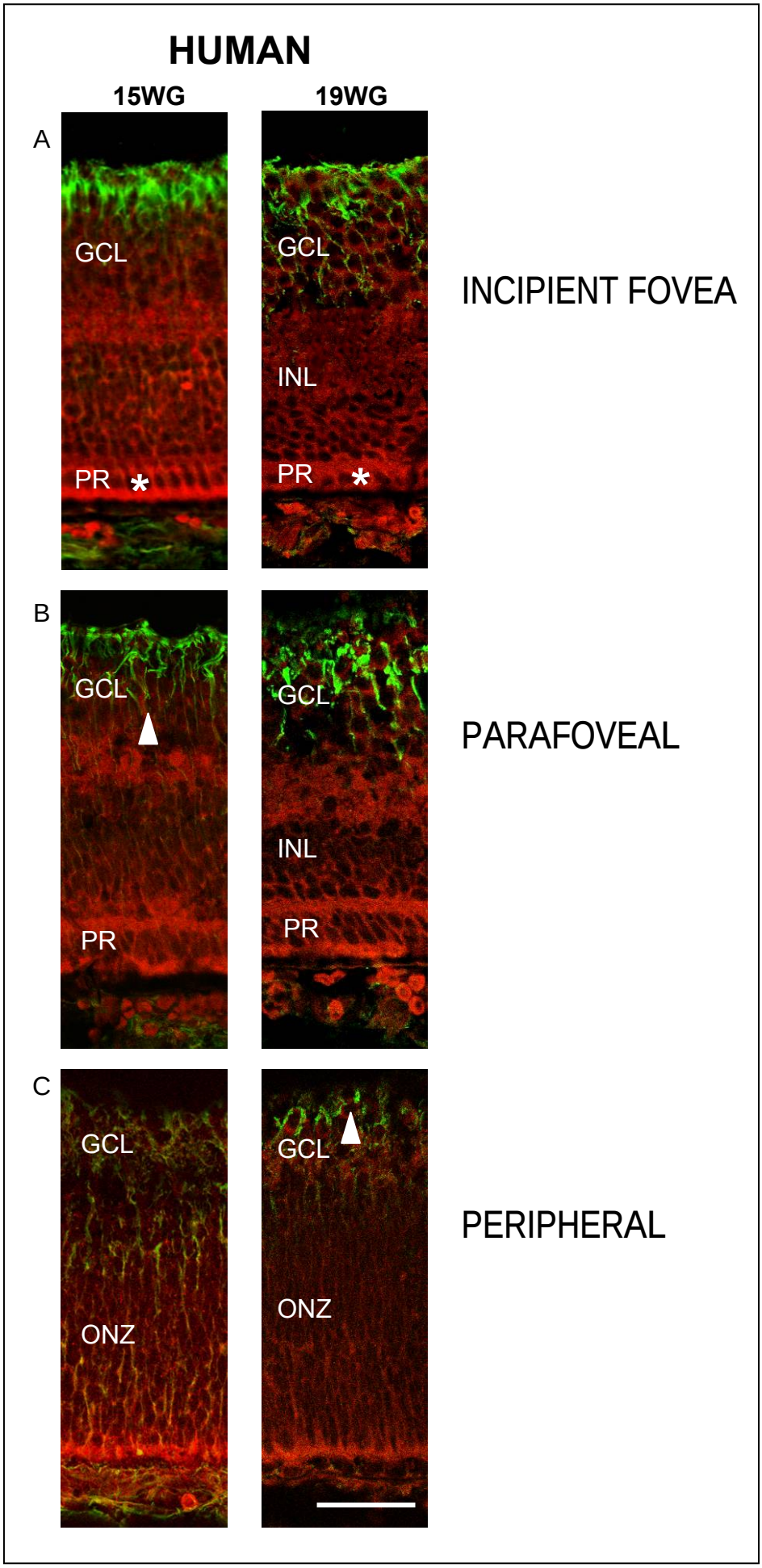
HUMAN
15WG
19WG
A
GCL
PR
GCL
INL
PR
INCIPIENT FOVEA
B
GCL
PR
GCL
INL
PR
PARAFOVEAL
C
GCL
ONZ
GCL
ONZ
PERIPHERAL

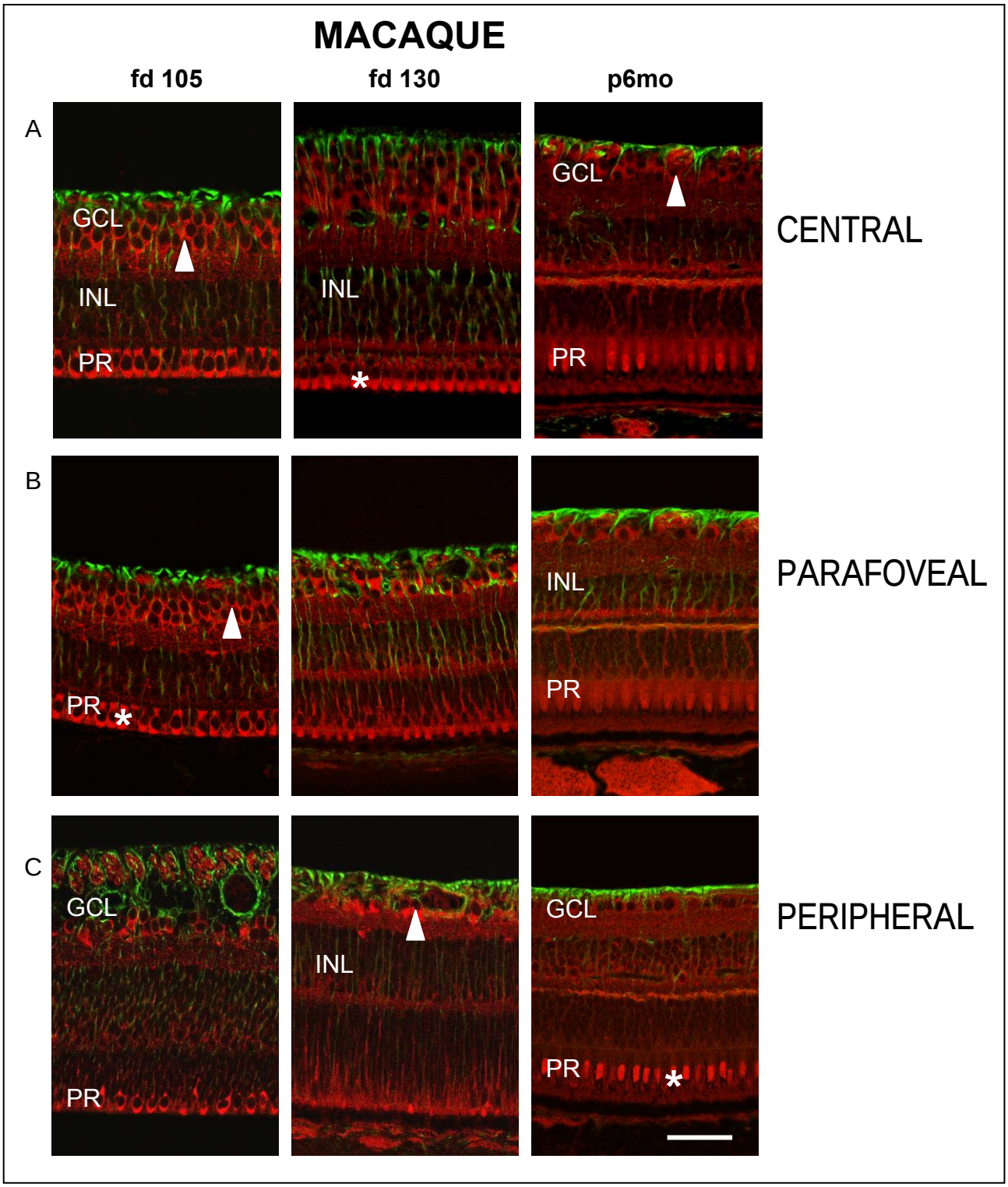

FIGURE 5.12 Distribution of TGF-β2 (red) and vimentin (green) immunolabelling in (A) central, (B) parafoveal and (C) peripheral (nasal) macaque retina at fd105 (~25WG), fd130 (~31WG) and p6mo. Weak to moderate labelling of ganglion cells (arrowheads) and moderate to strong labelling of photoreceptors (asterisks) is observed. (GCL: ganglion cell layer; INL: inner nuclear layer; PR: photoreceptor layer; CC: choriocapillaris). Bar = 50μm.

Distribution

Optical densitometry analyses of immunolabelled sections were used to determine the relative levels of TGF-β2 protein in the photoreceptor layer (Appendix B). A centro-peripheral gradient of TGF-β2 protein was detected, with peak levels of TGF-β2 protein in the central retina for all ages examined, but most prominent in the 15WG-17.5WG period (Figure 5.13). TGF-β2 protein is observed in the foveal region well before formation of the FAZ at 14WG (Figure 5.13A).

In the macaque retina, peak levels of TGF-β2 protein are also detected centrally in photoreceptors at fd105 (~25WG). In general, TGF-β2 levels decrease with increasing age, the lowest relative levels of TGF-β2 being measured in the p6mo specimen (Figure 5.14).

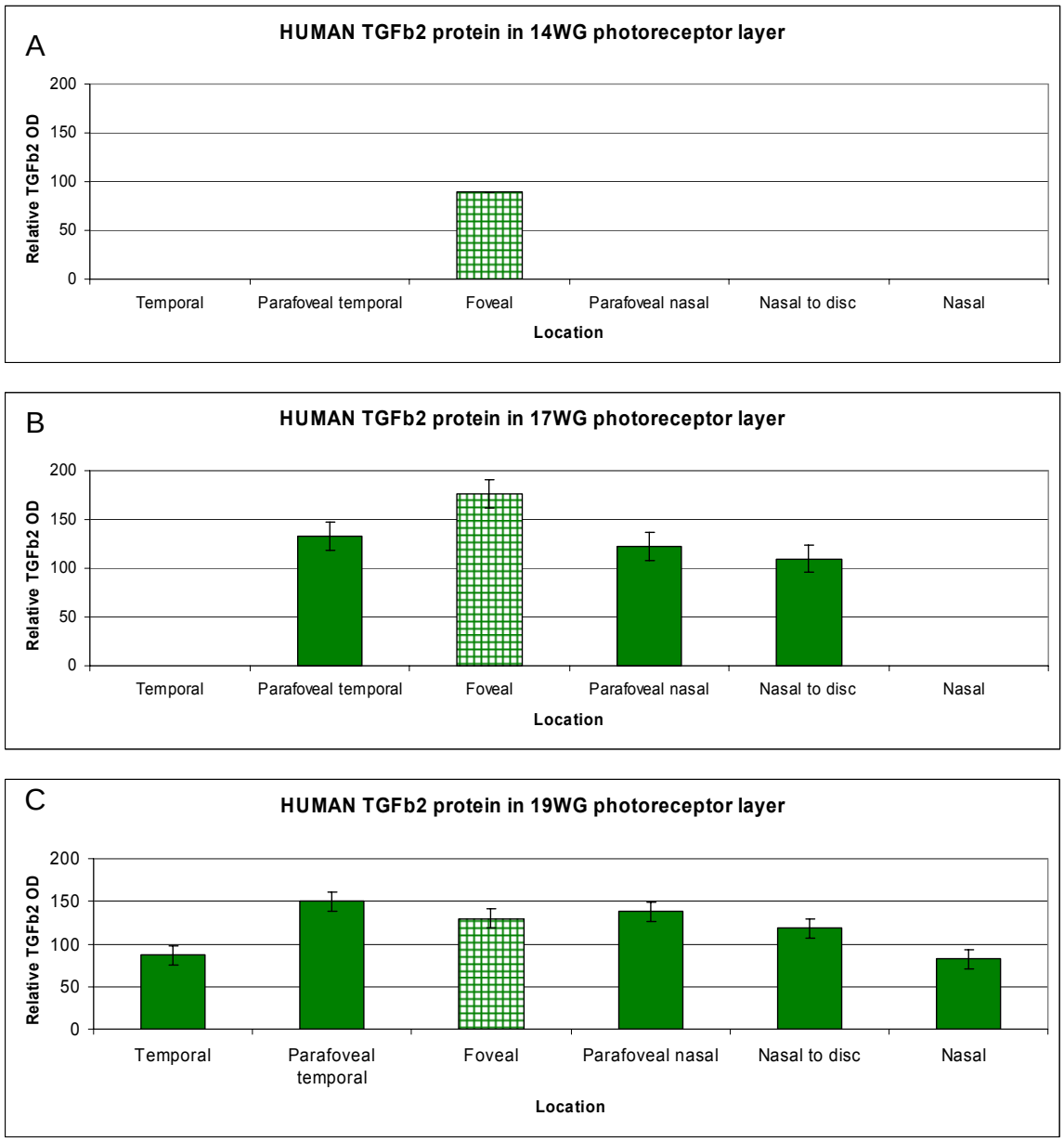

FIGURE 5.13 Relative TGF-β2 protein levels as indicated by optical densitometry (OD), in differentiated regions of temporal, parafoveal temporal, foveal, parafoveal nasal, nasal to disc and nasal locations of human retinas aged (A) 14WG - prior FAZ formation, (B) 17WG, and (C) 19WG - during FAZ formation. Higher levels of TGF-β2 protein are seen in foveal and parafoveal regions compared with more peripheral locations. Photoreceptors have not differentiated in the peripheral retina of the youngest specimens and therefore OD measurements are not included. Error bars = SEM.

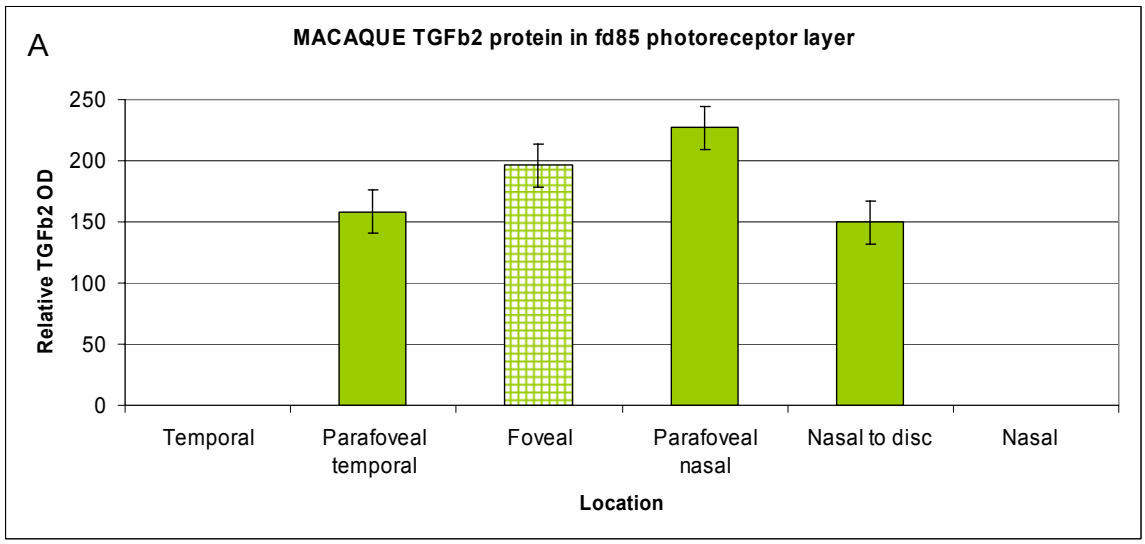
A
MACAQUE TGFb2 protein in fd85 photoreceptor layer
Relative TGFb2 OD
250
200
150
100
50
0
Temporal
Parafoveal temporal
Foveal
Parafoveal nasal
Nasal to disc
Nasal
Location

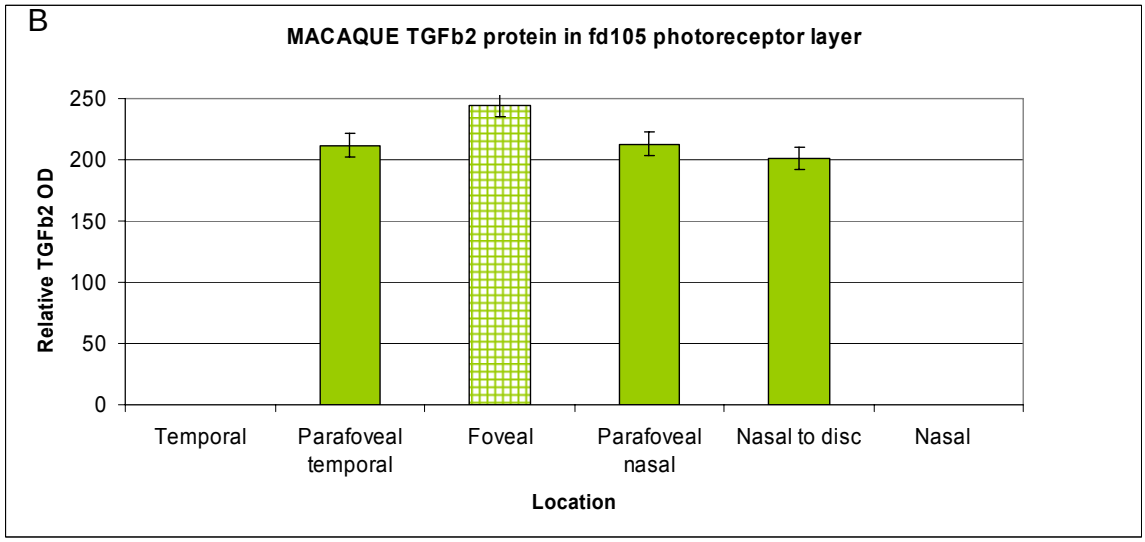
B
MACAQUE TGFb2 protein in fd105 photoreceptor layer
Relative TGFb2 OD
250
200
150
100
50
0
Temporal
Parafoveal temporal
Foveal
Parafoveal nasal
Nasal to disc
Nasal
Location

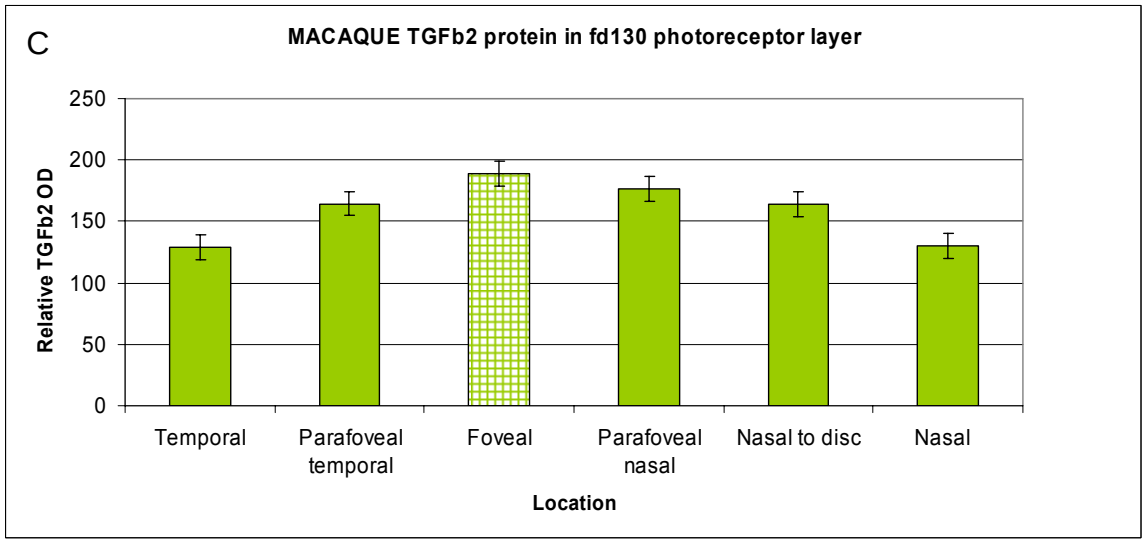
C
MACAQUE TGFb2 protein in fd130 photoreceptor layer
Relative TGFb2 OD
250
200
150
100
50
0
Temporal
Parafoveal temporal
Foveal
Parafoveal nasal
Nasal to disc
Nasal
Location

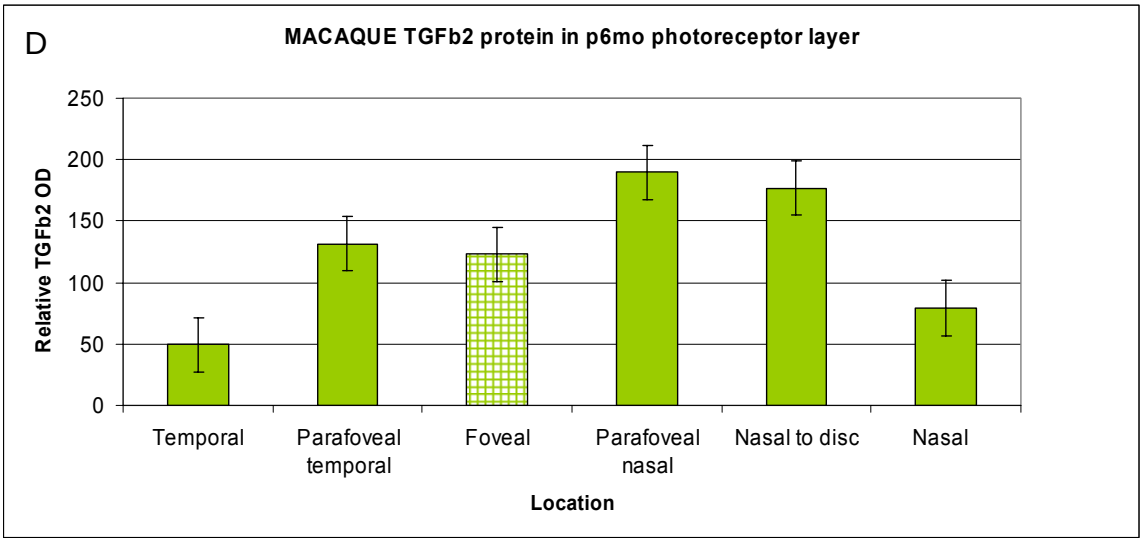

FIGURE 5.14 Relative TGF-β2 protein levels as indicated by optical densitometry in differentiated macaque retina at temporal, parafoveal temporal, foveal, parafoveal nasal, nasal to disc and nasal locations of macaque retinae aged (A) fd85, (B) fd105, (C) fd130 (C) and (D) p6mo. Note that during prenatal development the relative levels of TGF-β2 protein are generally highest in the fovea (between fd105 (~25WG) and fd130 (~31WG), then decrease with age. At p6mo (after formation of the FAZ), the level of TGF-β2 in the fovea is lower than in corresponding parafoveal locations, and when compared to younger ages. Photoreceptors have not differentiated in the peripheral retina of the two younger specimens, and therefore measurements from the peripheral locations are not included. Error bars = SEM.

TGF-β2 mRNA

Location

TGF-β2 mRNA is expressed in the GCL and photoreceptor layer of human and macaque retinas (Figures 5.15, 5.16, 5.17, 5.18).

Distribution

Optical densitometry analyses of TGF-β2 mRNA expression in sections were used to measure the relative levels of TGF-β2 in the photoreceptor layer (Appendix B). A centro-peripheral gradient of TGF-β2 mRNA is seen, with peak levels in the central retina for all ages examined (Figures 5.19, 5.20).

In the developing macaque retina, relative levels of TGF-β2 mRNA are highest in central retina before and during the formation of the FAZ. These decrease with increasing age, with the lowest relative levels of TGF-β2 being measured at p6mo (Figure 5.20). These data are consistent with the optical density measurements of protein expression.

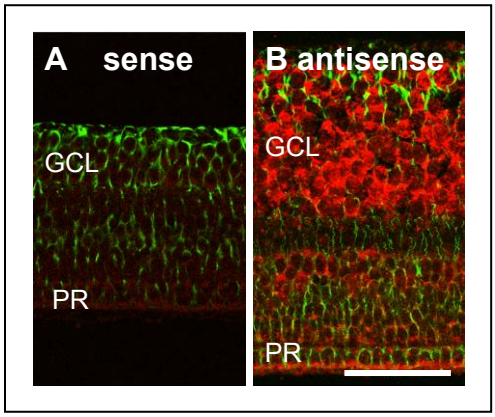

FIGURE 5.15 Sample sense (A) and antisense (B) TGF-β2 riboprobe in central human retina at 14WG. Sections are also immunolabelled for vimentin (green). Similar results were obtained with macaque retinas (not shown), (GCL: ganglion cell layer; PR: photoreceptor layer). Bar = 100μm.

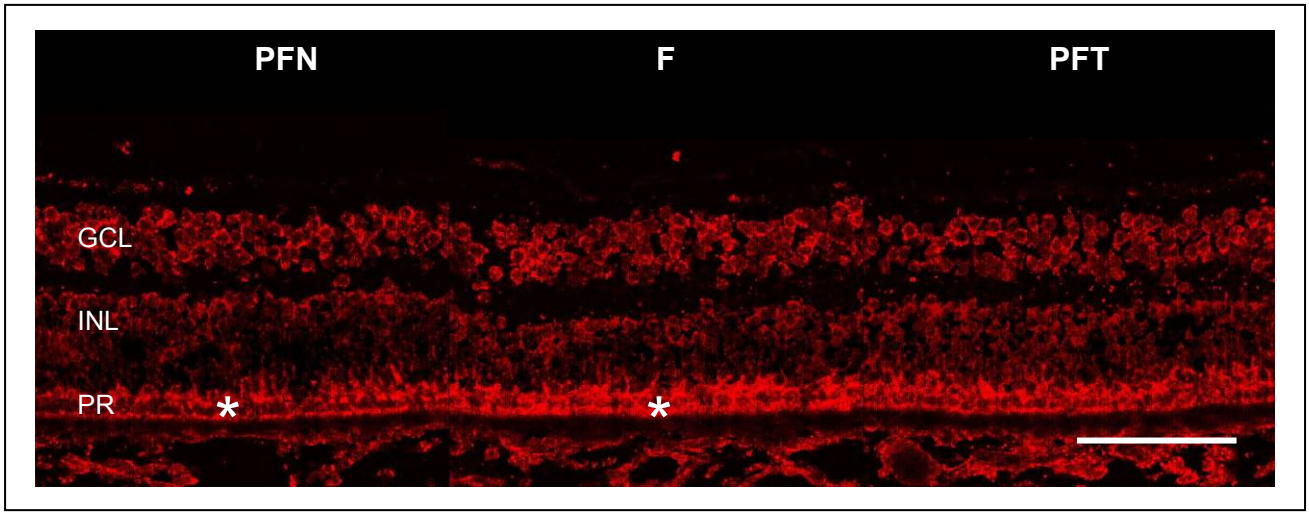

FIGURE 5.16 In situ hybridisation to detect TGF-β2 mRNA (red) expression in central 16WG human retina. Weak to moderate expression is seen in the GCL. A centro-peripheral gradient of expression (between asterisks) can be detected in the photoreceptor layer (PR), with increased TGF-β2 mRNA expression in the foveal (F) and parafoveal regions (PFN, PFT). (INL: inner nuclear layer). Bar = 100μm.

FIGURE 5.17 In situ hybridisation; showing TGF-β2 mRNA expression (red) in (A) incipient fovea and fovea, (B) parafovea and (C) peripheral (nasal) regions of a 14WG and 19WG human retina. Sections for 19WG are also immunolabelled for vimentin (green). Expression is strong in the GCL in both locations at all ages, but is upregulated in the outer retina as the photoreceptors (asterisks) differentiate (A compared with C) (GCL: ganglion cell layer; INL: inner nuclear layer; ONZ: outer neuroblastic zone; PR: photoreceptor layer). Bar = 50μm.

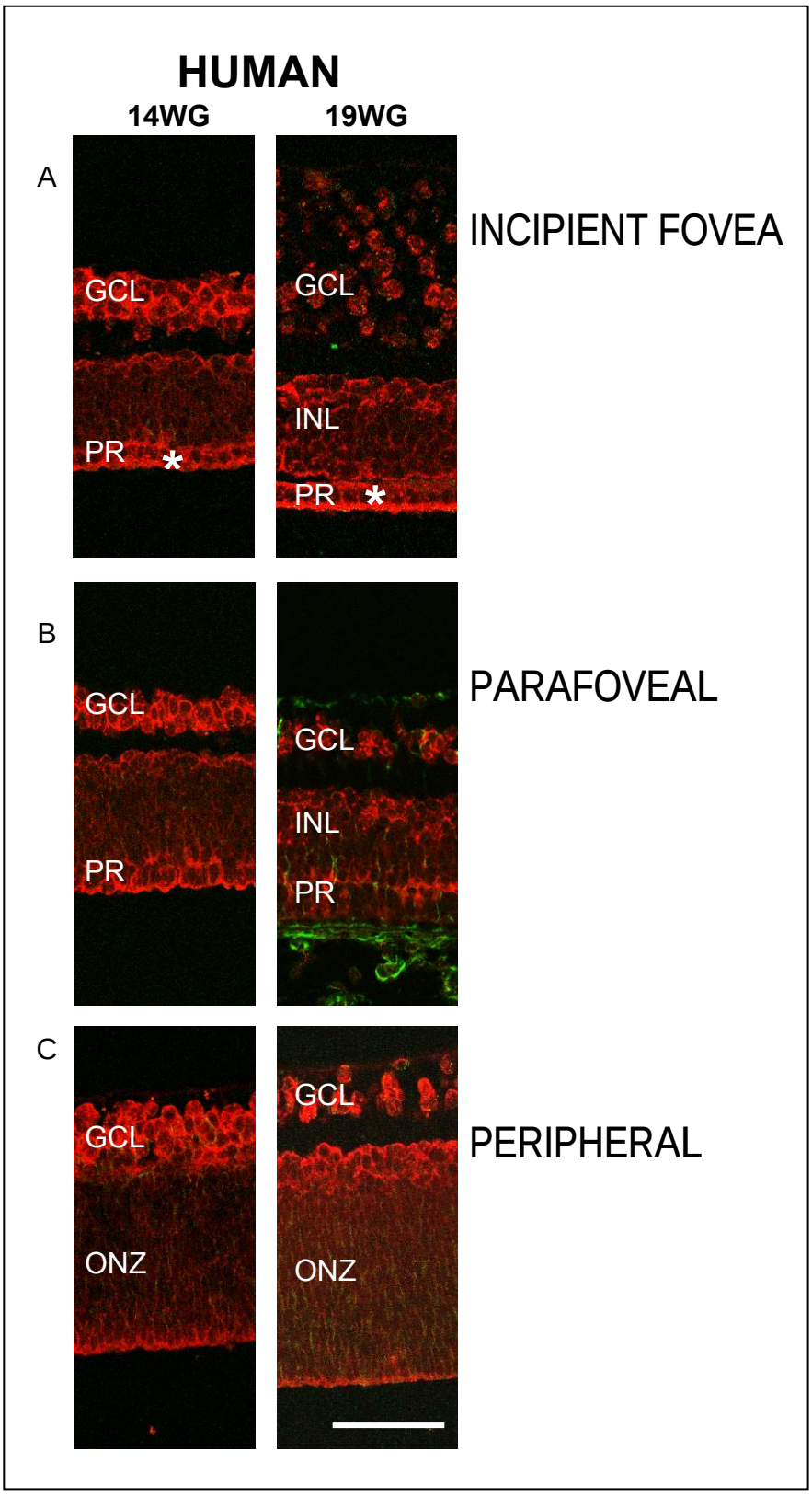
HUMAN
14WG
19WG
A
GCL
PR
GCL
INL
PR
INCIPIENT FOVEA
B
GCL
PR
GCL
INL
PR
PARAFOVEAL
C
GCL
ONZ
GCL
ONZ
PERIPHERAL

FIGURE 5.18 Distribution of TGF-β2 mRNA (red) and vimentin (green) in (A) central, (B) parafoveal and (C) peripheral (nasal) regions of fd64, fd105, p12wk and p11y macaque retinas. TGF-β2 mRNA is most strongly expressed in ganglion cells (arrowheads) and photoreceptors (asterisks) with intermediate levels of expression detected in the INL. The images also show a decline in levels of mRNA expression from the postnatal period to adulthood. (GCL: ganglion cell layer; INL: inner nuclear layer; ONZ: outer neuroblastic zone; PR: photoreceptor layer). Bar = 50μm.

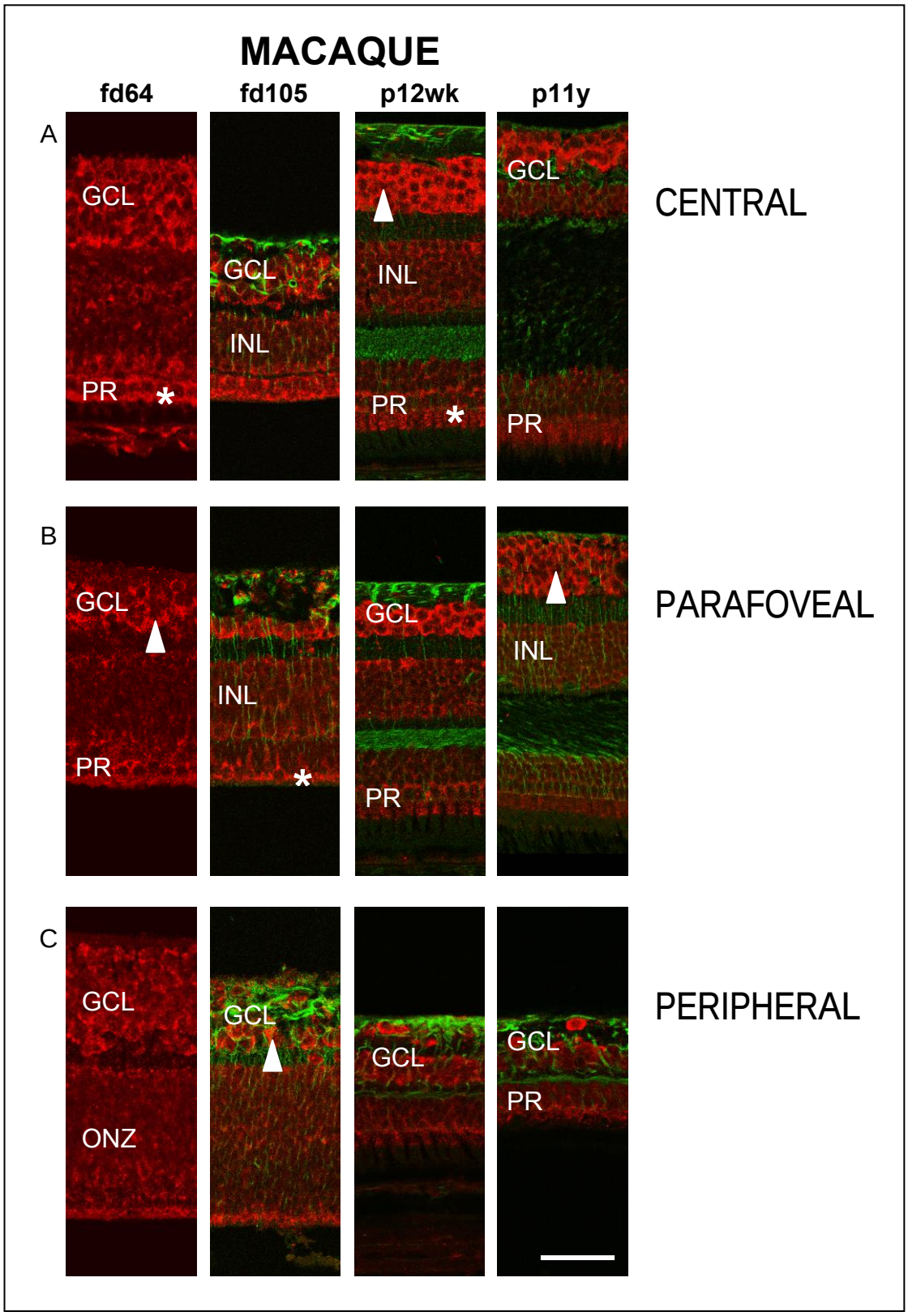
MACAQUE
fd64
fd105
p12wk
p11y
A
GCL
PR
GCL
INL
INL
PR
GCL
PR
CENTRAL
B
GCL
PR
INL
GCL
PR
INL
PARAFOVEAL
C
GCL
ONZ
GCL
GCL
GCL
PR
PERIPHERAL

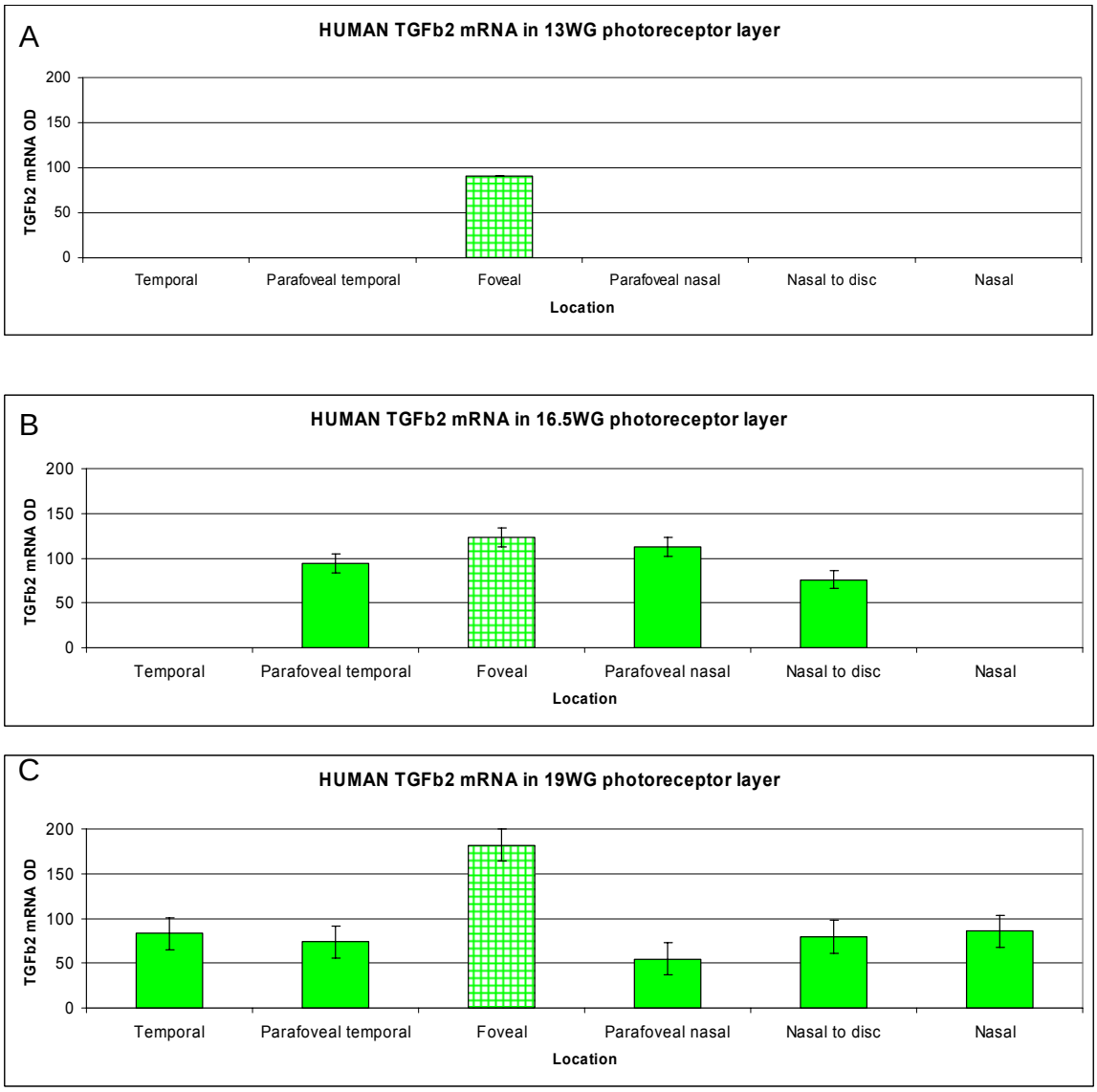

FIGURE 5.19 Relative levels of TGF-β2 mRNA expression as indicated by optical densitometry (OD) in differentiated regions of the photoreceptor layer at temporal, parafoveal temporal, foveal, parafoveal nasal, nasal to disc and nasal locations in human retinas aged (A) 13WG - prior FAZ formation, (B) 16.5WG, and (C) 19WG - during FAZ formation. Peak relative amounts of TGF-β2 mRNA are seen in the foveal region up to 19WG. Photoreceptors have not differentiated in the peripheral retina of the youngest specimen and therefore no measurements have been graphed for these regions. Error bars = SEM.

FIGURE 5.20 Relative levels of photoreceptor TGF-β2 mRNA expression assessed by optical densitometry in differentiated regions of temporal, parafoveal temporal, foveal, parafoveal nasal, nasal to disc and nasal locations in macaque retinas at (A) fd64 - prior to FAZ formation, (B) fd155 - during formation of the FAZ, (C) p6d and (D) p11y (both after formation of the FAZ). Relative levels of TGF-β2 mRNA are highest in the foveal region in the prenatal samples; however in postnatal and adult retinas, TGF-β2 mRNA is uniformly expressed across the entire retina. Note photoreceptors have not differentiated in the peripheral retina of the youngest specimen and measurements are not included. Error bars = SEM.

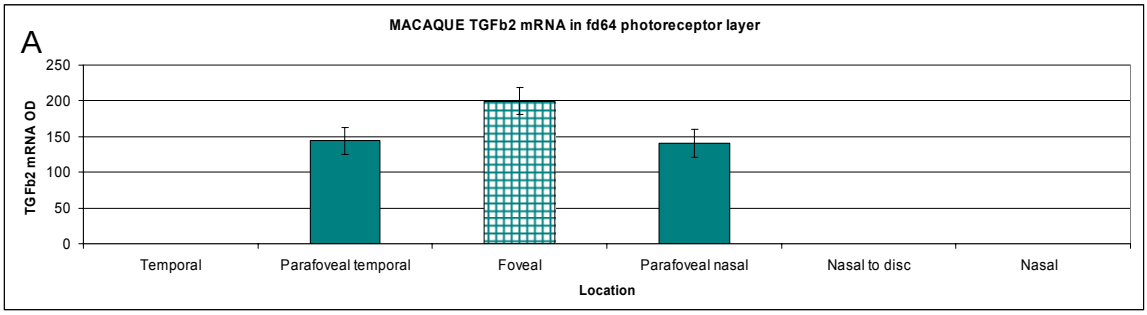
A
MACAQUE TGFb2 mRNA in fd64 photoreceptor layer
TGFb2 mRNA OD
250
200
150
100
50
0
Temporal
Parafoveal temporal
Foveal
Parafoveal nasal
Nasal to disc
Nasal
Location

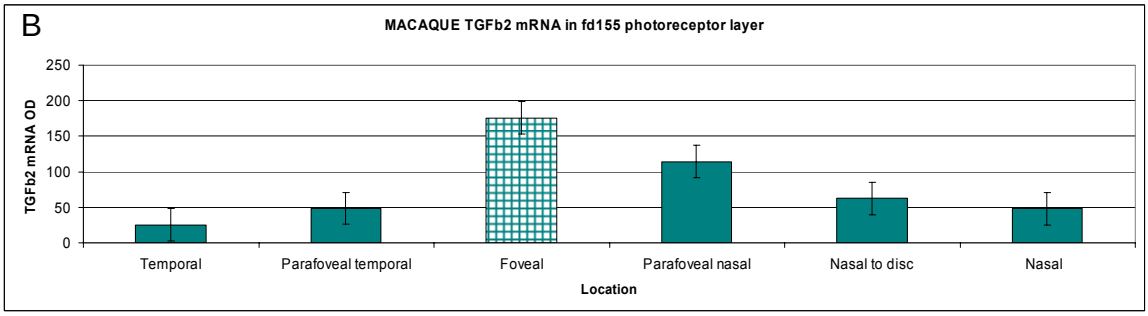
B
MACAQUE TGFb2 mRNA in fd155 photoreceptor layer
TGFb2 mRNA OD
250
200
150
100
50
0
Temporal
Parafoveal temporal
Foveal
Parafoveal nasal
Nasal to disc
Nasal
Location

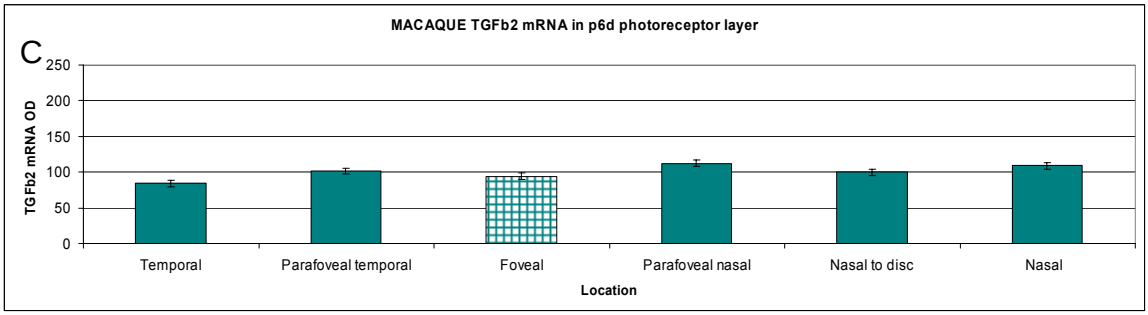
C
MACAQUE TGFb2 mRNA in p6d photoreceptor layer
TGFb2 mRNA OD
250
200
150
100
50
0
Temporal
Parafoveal temporal
Foveal
Parafoveal nasal
Nasal to disc
Nasal
Location

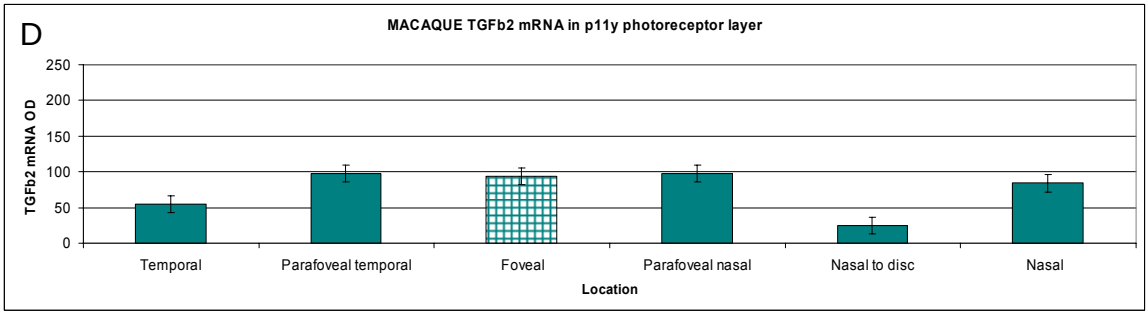
D
MACAQUE TGFb2 mRNA in p11y photoreceptor layer
TGFb2 mRNA OD
250
200
150
100
50
0
Temporal
Parafoveal temporal
Foveal
Parafoveal nasal
Nasal to disc
Nasal
Location

TGF-β3 protein

Location

Cytoplasmic TGF-β3 protein is expressed in ganglion cells and photoreceptors (Figures 5.21, 5.22, 5.23). This is seen in photoreceptors from 14WG and is evident up to 19WG (Figures 5.21, 5.22). TGF-β3 protein is weak and variable in the ganglion cells similar to TGF-β2 (see previous TGF-β2 section).

In the macaque retina, photoreceptor outer segments expressed TGF-β3 protein from fd105 (~25WG), and this is still seen at p6mo (Figure 5.23).

Distribution

Optical densitometry analyses of immunolabelled sections were used to determine the relative levels of TGF-β3 protein in different regions of the photoreceptor layer (Appendix B). A centro-peripheral gradient of TGF-β3 protein is seen, with peak levels of TGF-β3 protein in the central retina for all ages examined, with the steepest gradient detected in the 17WG-18WG retina (Figure 5.24).

In the developing macaque retina, peak relative levels of TGF-β3 protein are found centrally between fd105 (~25WG) and fd130 (~31WG), with the lowest relative levels of TGF-β3 found at p6mo (Figure 5.25).

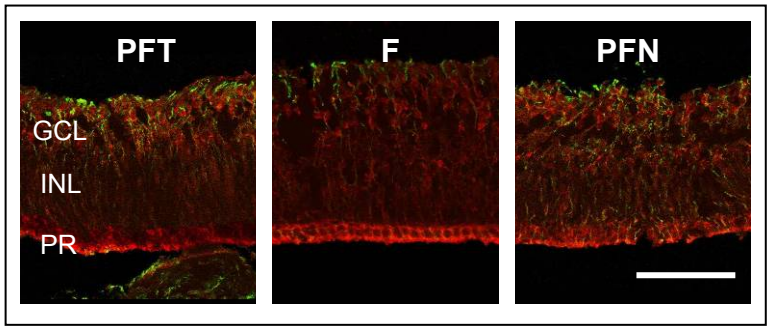

FIGURE 5.21 Double immunolabelling shows distribution of TGF-β3 protein (red) and vimentin (green) across central retina. Staining in the GCL is weak, compared with labelling in the photoreceptor layer where there is a centro-peripheral gradient evident at 17.5WG. (PFT- temporal parafovea; PFN-nasal parafovea). (INL: inner nuclear layer). Bar = 100μm.

FIGURE 5.22 Distribution of TGF-β3 (red) and vimentin (green) immunolabelling in (A) incipient fovea and fovea, (B) parafovea and (C) peripheral (nasal) region of a 15WG and 19WG human retina. (GCL: ganglion cell layer; INL: inner nuclear layer; ONZ: outer neuroblastic zone; PR: photoreceptor layer) Bar = 50μm.

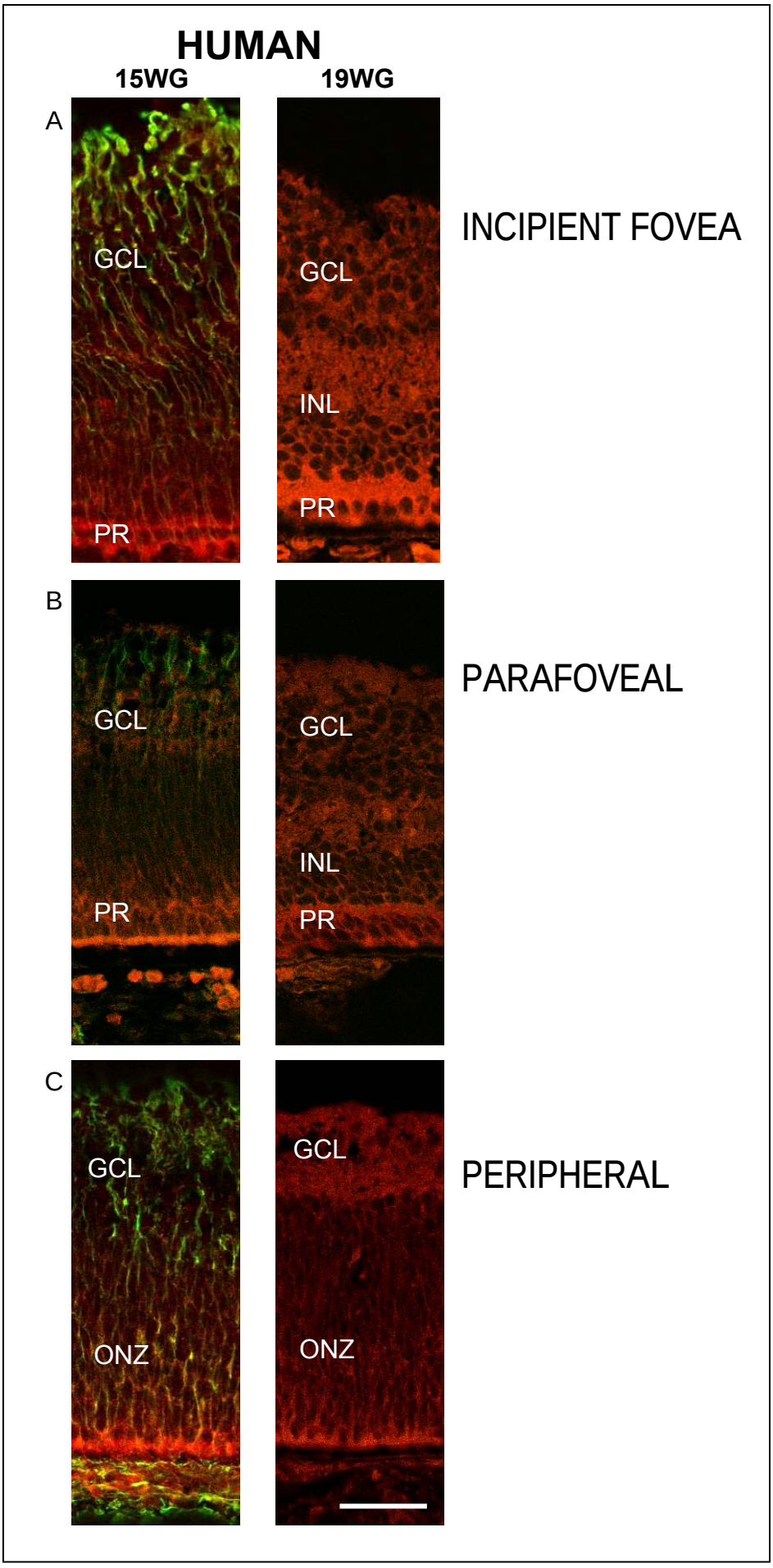
HUMAN
15WG
19WG
A
GCL
PR
GCL
INL
PR
INCIPIENT FOVEA
B
GCL
PR
GCL
INL
PR
PARAFOVEAL
C
GCL
ONZ
GCL
ONZ
PERIPHERAL

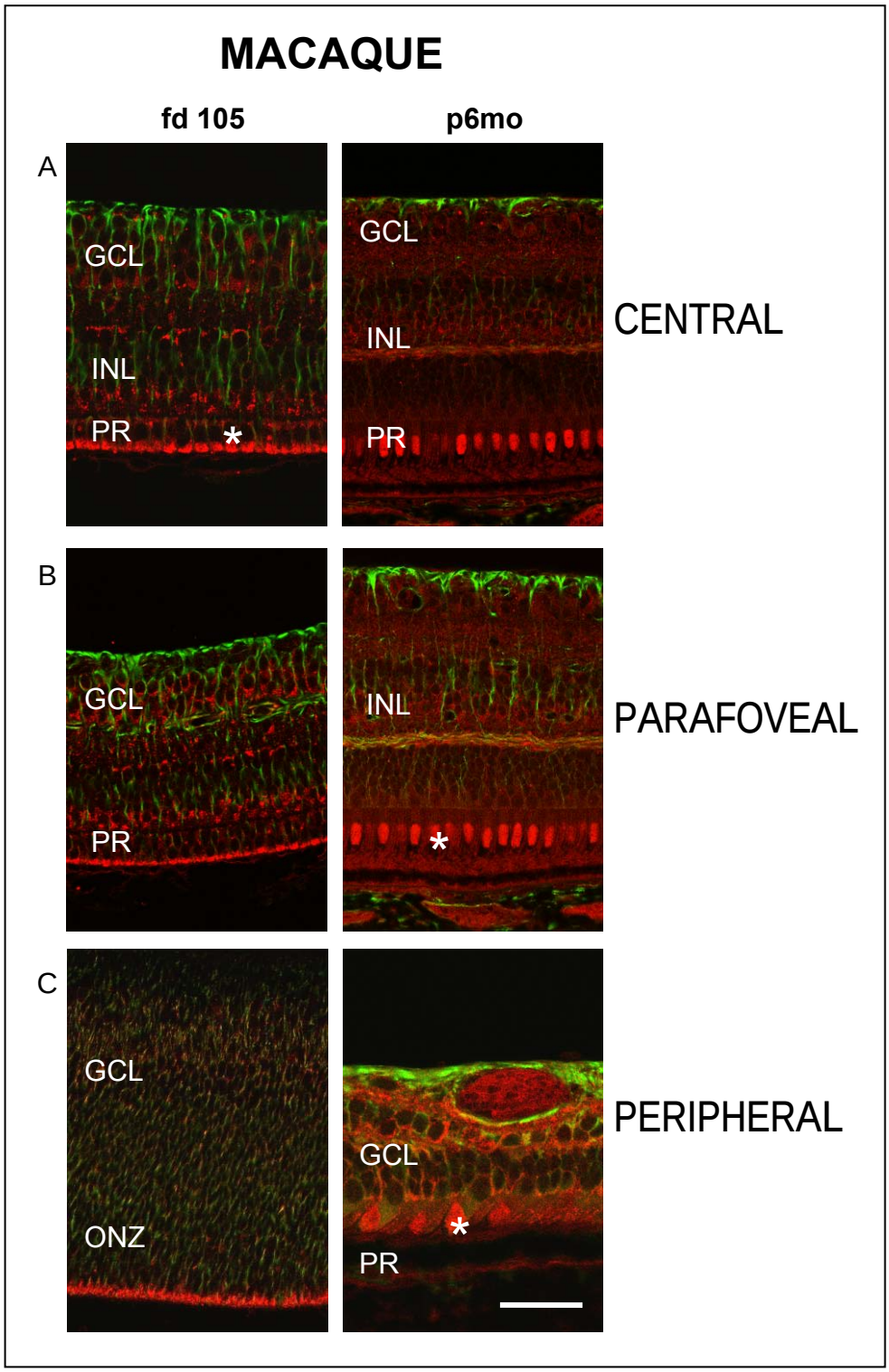

FIGURE 5.23 Immunoreactivity for TGF-β3 (red) and vimentin (green) in (A) central, (B) parafovea and (C) peripheral (nasal) macaque retina at fd105 (~25WG) and p6mo. Note TGF-β3 expression in photoreceptors (asterisks). (GCL: ganglion cell layer; INL: inner nuclear layer; ONZ: outer neuroblastic zone; PR: photoreceptor layer). Bar = 50μm.

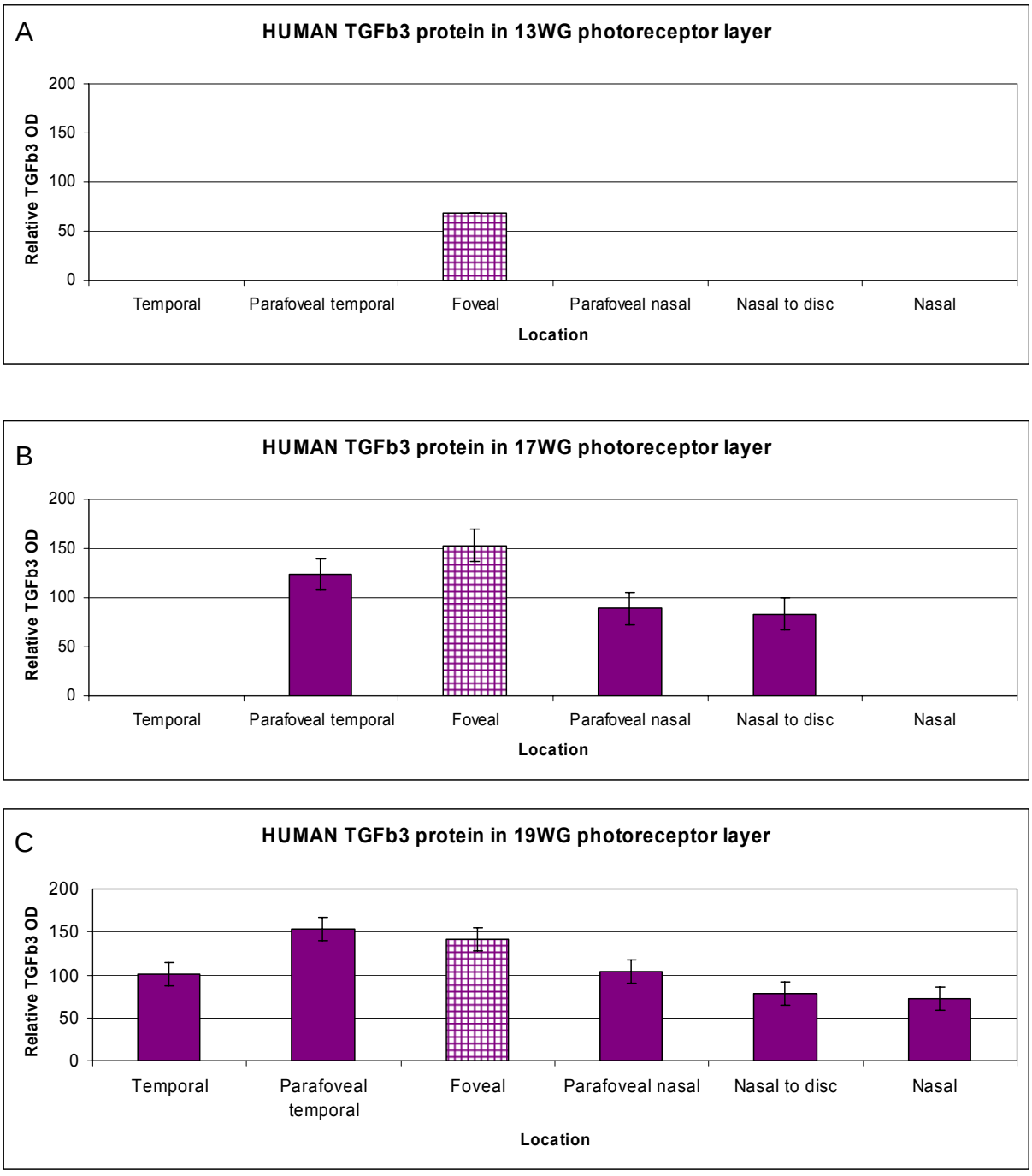

FIGURE 5.24 Relative levels of TGF-β3 protein determined by optical densitometry (OD) at different sample locations in human retinas at (A) 13WG - prior to FAZ formation, (B) 17WG and (C) 19WG - during FAZ formation. The peak protein levels are in central retina for all ages. Measurements were not taken from undifferentiated regions of the photoreceptor layer. Error bars = SEM.

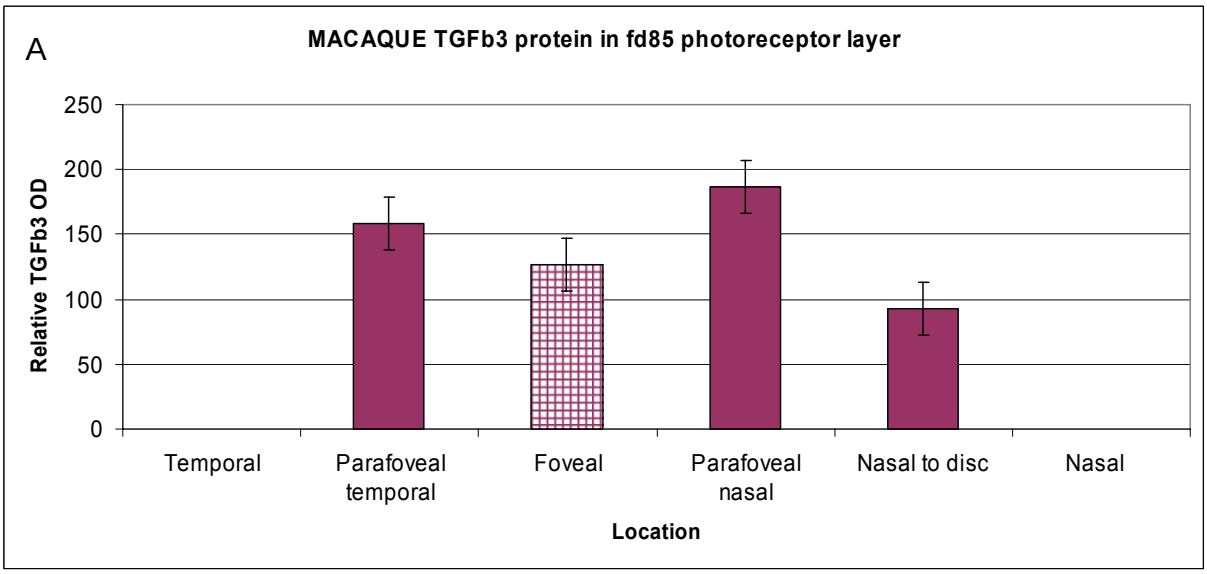
A
MACAQUE TGFb3 protein in fd85 photoreceptor layer
Relative TGFb3 OD
250
200
150
100
50
0
Temporal
Parafoveal temporal
Foveal
Parafoveal nasal
Nasal to disc
Nasal
Location

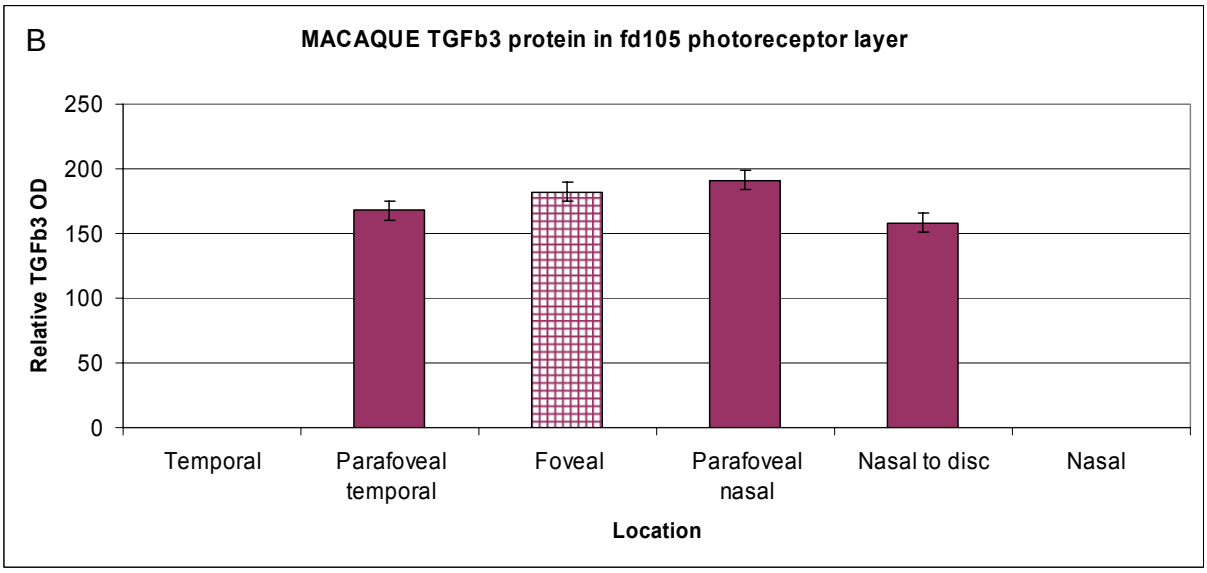
B
MACAQUE TGFb3 protein in fd105 photoreceptor layer
Relative TGFb3 OD
250
200
150
100
50
0
Temporal
Parafoveal temporal
Foveal
Parafoveal nasal
Nasal to disc
Nasal
Location

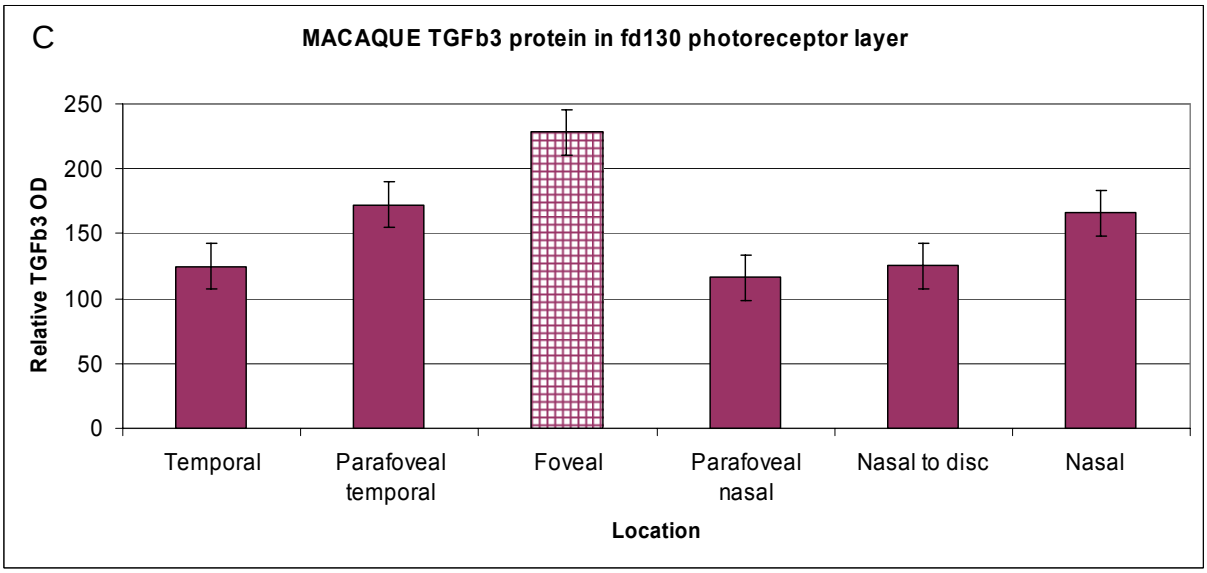
C
MACAQUE TGFb3 protein in fd130 photoreceptor layer
Relative TGFb3 OD
250
200
150
100
50
0
Temporal
Parafoveal temporal
Foveal
Parafoveal nasal
Nasal to disc
Nasal
Location

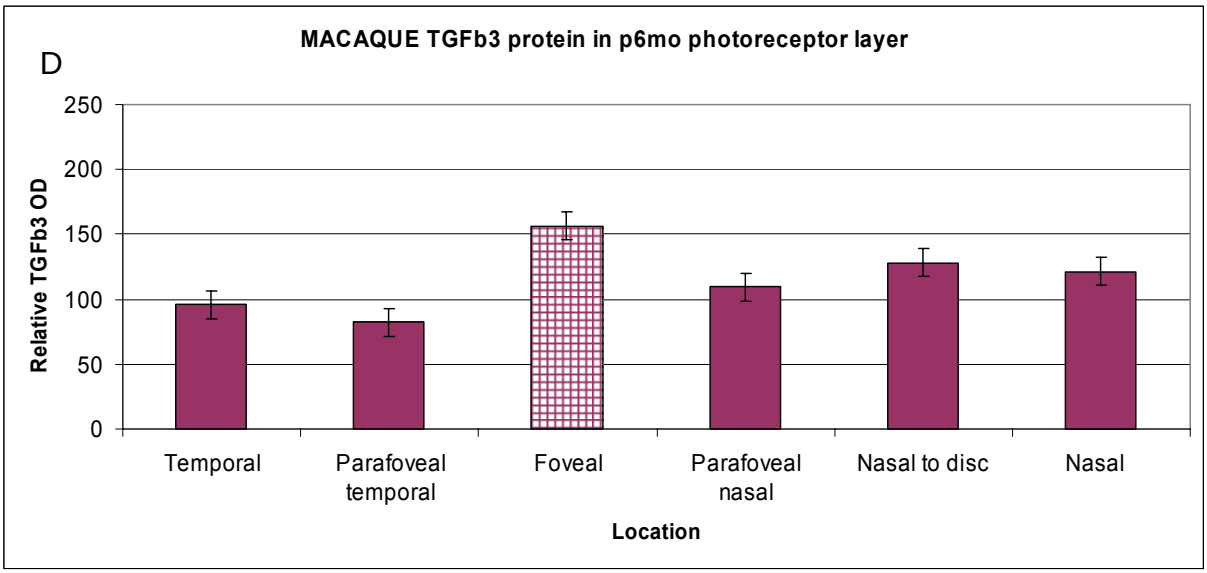

FIGURE 5.25 Relative levels of TGF-β3 protein determined by optical densitometry at different locations in macaque retinas aged (A) fd85, (B) fd105, (C) fd130 (C) and (D) p6mo. TGF- β3 protein levels increased were lower in the fovea compared with parafovea in early development (A), but during formation of the FAZ a relative increase in the level of TGF-β3 protein in the fovea was detected (B,C). Postnatally TGF-β3 levels remain high in the foveal region (D). No measurements were taken from undifferentiated parts of the photoreceptor layer. Error bars = SEM.

TGF-β3 mRNA

Location

TGF-β3 mRNA was detected in both the GCL and photoreceptor layer of human and macaque retinas (Figures 5.26, 5.27, 5.28).

Distribution

Optical densitometry analyses indicate high levels of TGF-β3 mRNA expression in the central compared with surrounding retina at 19WG (Figure 5.29) when the FAZ is forming; at earlier stages TGF-β3 mRNA distribution in photoreceptors is relatively uniform.

In the macaque retina, elevated levels of TGF-β3 mRNA are evident in the central photoreceptors at fd105 (Figure 5.30B), when the FAZ is forming, but not in the postnatal period (Figure 5.30C, D).

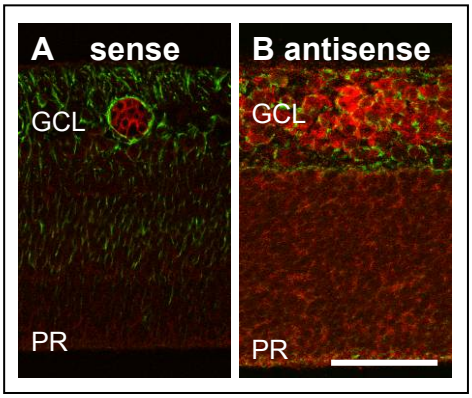

FIGURE 5.26 Sample sense (A) and antisense (B) TGF-β3 riboprobe in peripheral 14WG human retina. Sections are also immunolabelled for vimentin (green). Similar results were obtained with macaque retinas (not shown), (GCL: ganglion cell layer; PR: photoreceptor layer). Bar = 50μm.

FIGURE 5.27 Distribution of TGF-β3 mRNA (red) in (A) incipient fovea and fovea, (B) parafovea and (C) peripheral (nasal) regions of a 14WG and 17WG human retina. Low levels of mRNA expression are detected in the ganglion cells (arrowheads) compared with photoreceptors (asterisks). Sections for 14WG are also immunolabelled for vimentin (green). (GCL: ganglion cell layer; INL: inner nuclear layer; ONZ: outer neuroblastic zone; PR: photoreceptor layer). Bar = 50μm.

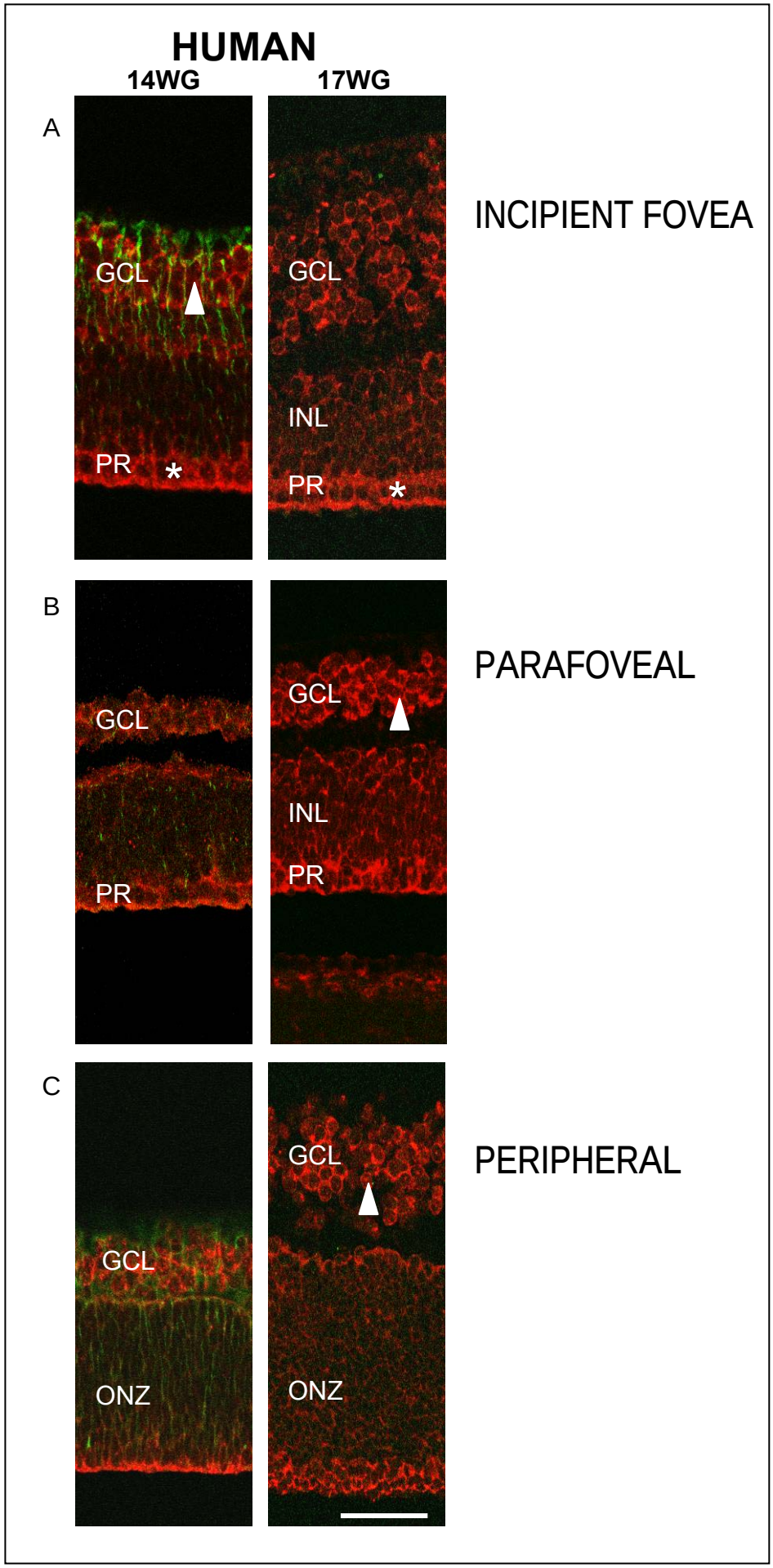
HUMAN
14WG
17WG
A
GCL
PR
*
GCL
INL
PR
*
INCIPIENT FOVEA
B
GCL
PR
GCL
INL
PR
PARAFOVEAL
C
GCL
ONZ
GCL
ONZ
PERIPHERAL

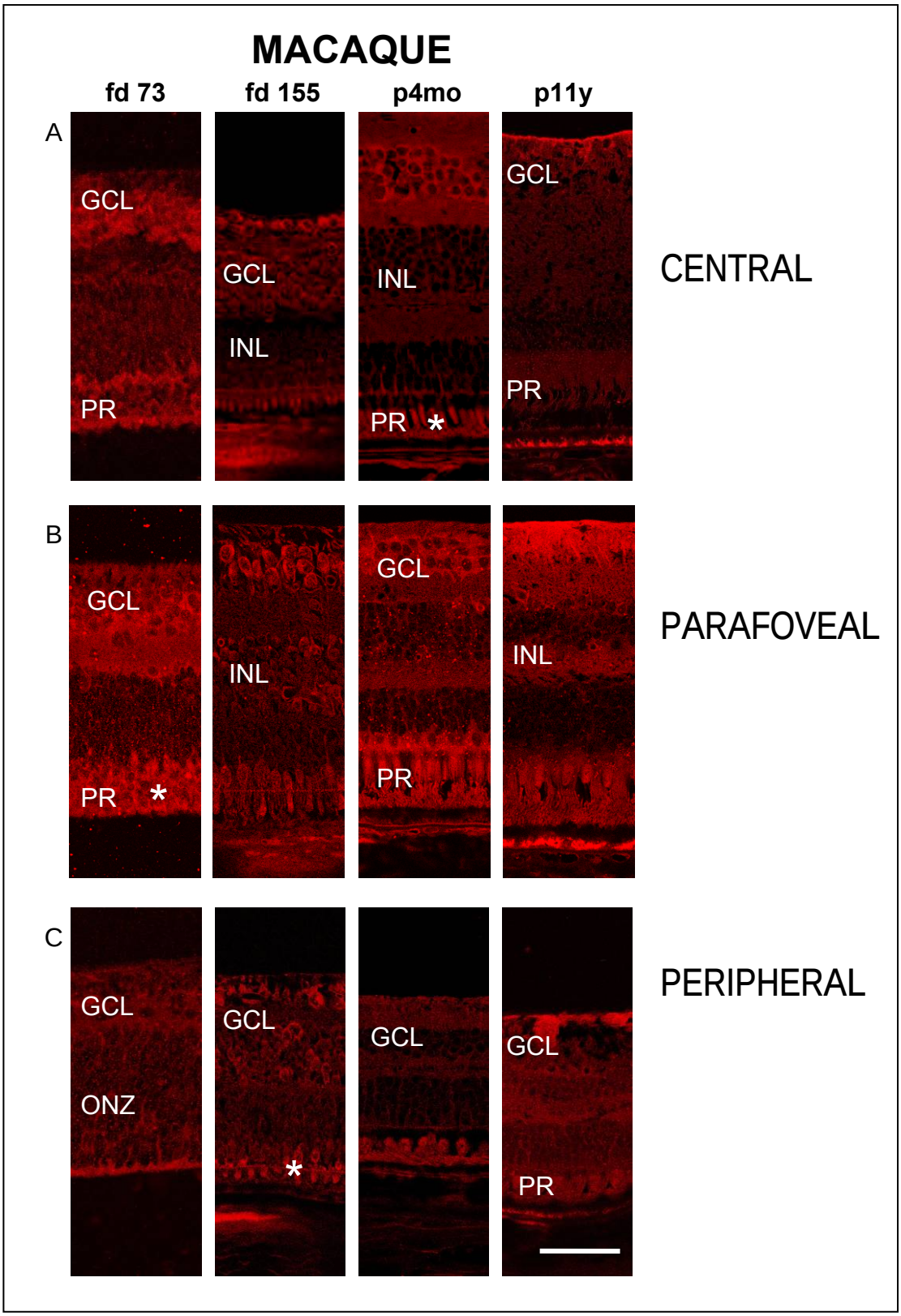

FIGURE 5.28 Distribution of TGF-β3 mRNA (red) in (A) central retina, (B) parafovea and (C) peripheral (nasal) regions of fd73, fd155, p4mo and p11y macaque retina. Photoreceptors (asterisks) show mRNA expression in the foetal and early postnatal period but not in adult retina. (GCL: ganglion cell layer; INL: inner nuclear layer; ONZ: outer neuroblastic zone; PR: photoreceptor layer). Bar = 50μm.

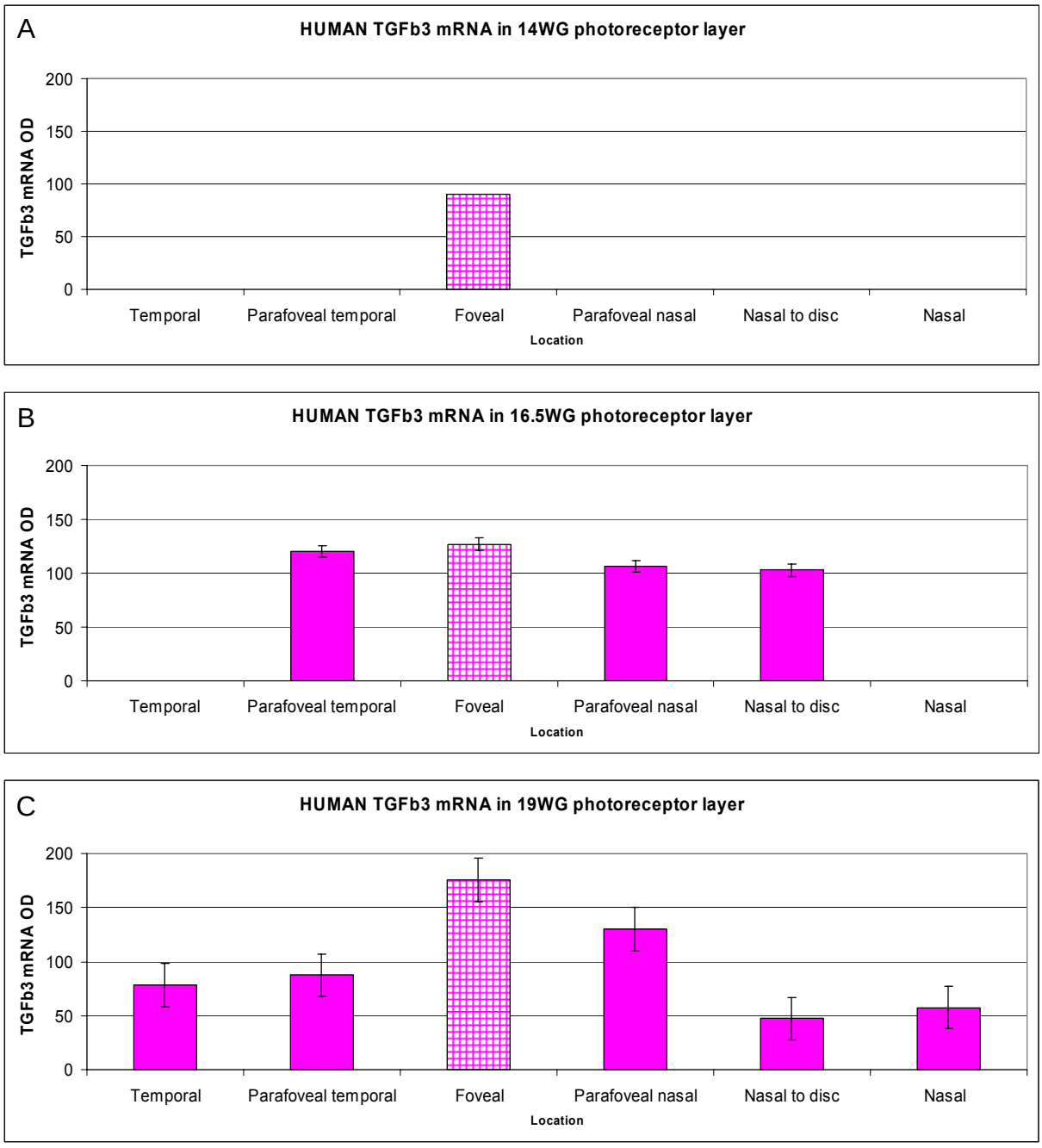

FIGURE 5.29 Relative levels of TGF-β3 mRNA expression determined by optical densitometry (OD) at different sample locations in human retinas aged (A) 14WG - prior to FAZ formation, (B) 16.5WG and (C) 19WG - during FAZ formation. Peak TGF-β3 mRNA expression is found in the foveal region of the photoreceptor layer, particularly at 19WG. Photoreceptors have not differentiated in the peripheral retina of the youngest specimens and therefore OD measurements are not included. Error bars = SEM.

FIGURE 5.30 Relative levels of photoreceptor TGF-β3 mRNA expression in different regions of the photoreceptor layer of macaque retina at (A) fd73 - prior FAZ formation, (B) fd105 - during FAZ formation, (C) p12wk and (D) p11y - both ages after formation of the FAZ). There is evidence of elevated levels of TGF-β3 mRNA in central photoreceptors at fd105, during formation of the FAZ, but not earlier (fd73) or later stages (p12wk) of development or in the adult. Photoreceptors have not differentiated in the peripheral retina of the youngest specimens and therefore OD measurements are not included. Error bars = SEM.

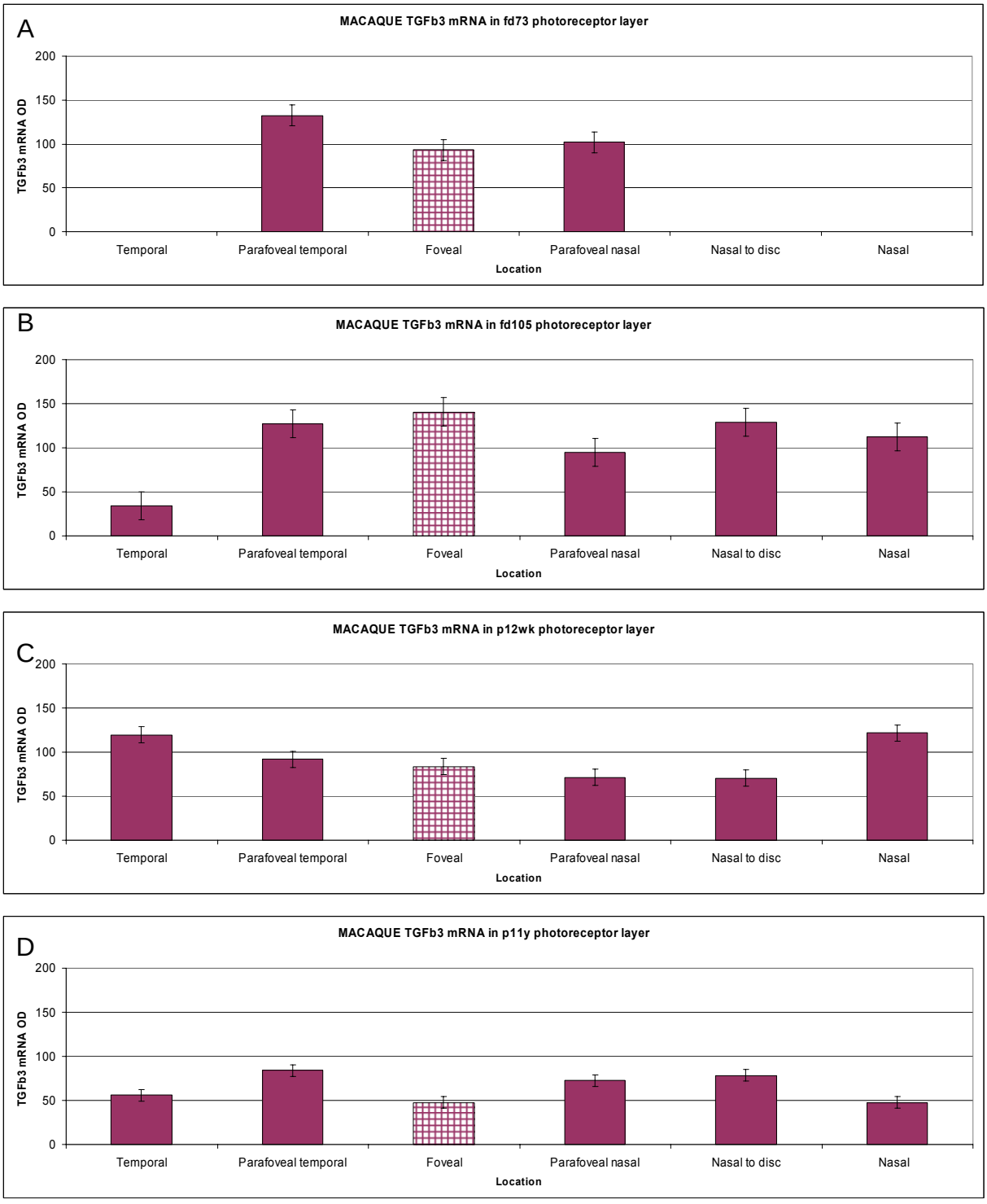
A
MACAQUE TGFb3 mRNA in fd73 photoreceptor layer
TGFb3 mRNA OD
200
150
100
50
0
Temporal
Parafoveal temporal
Foveal
Parafoveal nasal
Nasal to disc
Nasal
Location
B
MACAQUE TGFb3 mRNA in fd105 photoreceptor layer
TGFb3 mRNA OD
200
150
100
50
0
Temporal
Parafoveal temporal
Foveal
Parafoveal nasal
Nasal to disc
Nasal
Location
C
MACAQUE TGFb3 mRNA in p12wk photoreceptor layer
TGFb3 mRNA OD
200
150
100
50
0
Temporal
Parafoveal temporal
Foveal
Parafoveal nasal
Nasal to disc
Nasal
Location
D
MACAQUE TGFb3 mRNA in p11y photoreceptor layer
TGFb3 mRNA OD
200
150
100
50
0
Temporal
Parafoveal temporal
Foveal
Parafoveal nasal
Nasal to disc
Nasal
Location

TGF-βI receptor

Location

TGF-βI receptor (TβRI) protein was detected by immunohistochemistry in ganglion cells and their axons from 11WG (human) and fd64 (macaque), in the astrocytes or Müller cells from 16WG and fd105 respectively and in photoreceptors from 16WG and fd85 respectively.

In the human retina, the TβRI antibody immunolabelled differentiated ganglion cells and photoreceptors in both the foveal and parafoveal regions (Figure 5.31). Occasional immunoreactive cells in the parafoveal GCL were also seen and most likely were either astrocytes or inner processes of Müller cells.

In the macaque retina, the TβRI protein was present in ganglion cells and axons, across the entire retina and in the outer segments of the photoreceptors although not uniformly. Outer segment labelling was seen in the fovea at fd85 and fd105, in the parafovea at fd130 and in the nasal retina at fd130, p6mo and p2.5y. TβRI immunolabelling was present in macroglia that were later determined to be astrocytes in the parafoveal region at all ages examined (Figures 5.32, 5.33).

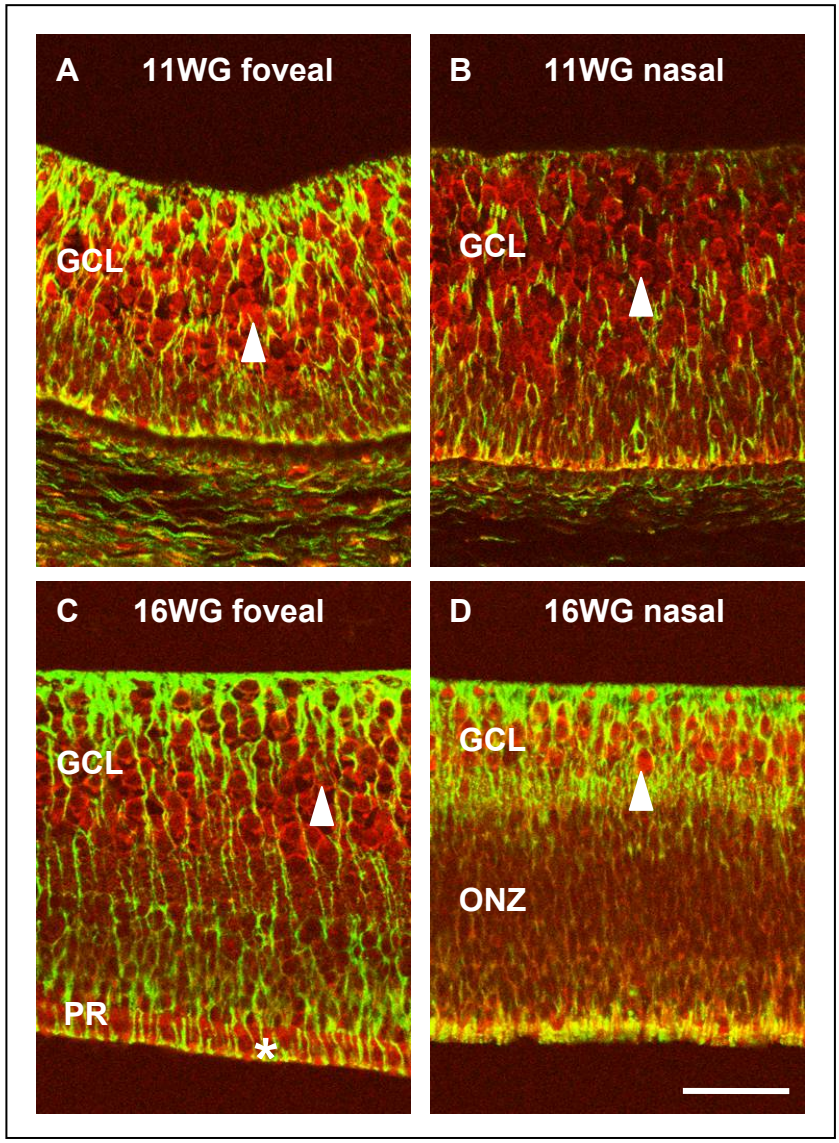

FIGURE 5.31 TβRI (red) and vimentin (green) immunolabelling in the foveal and nasal region of (A, B) 11WG and (C,D) 16WG human retinas. Immunolabelling is detected in ganglion cells (arrowheads) and photoreceptors (asterisks). (GCL: ganglion cell layer; ONZ: outer neuroblastic zone, PR: photoreceptor layer). Bar= 100μm.

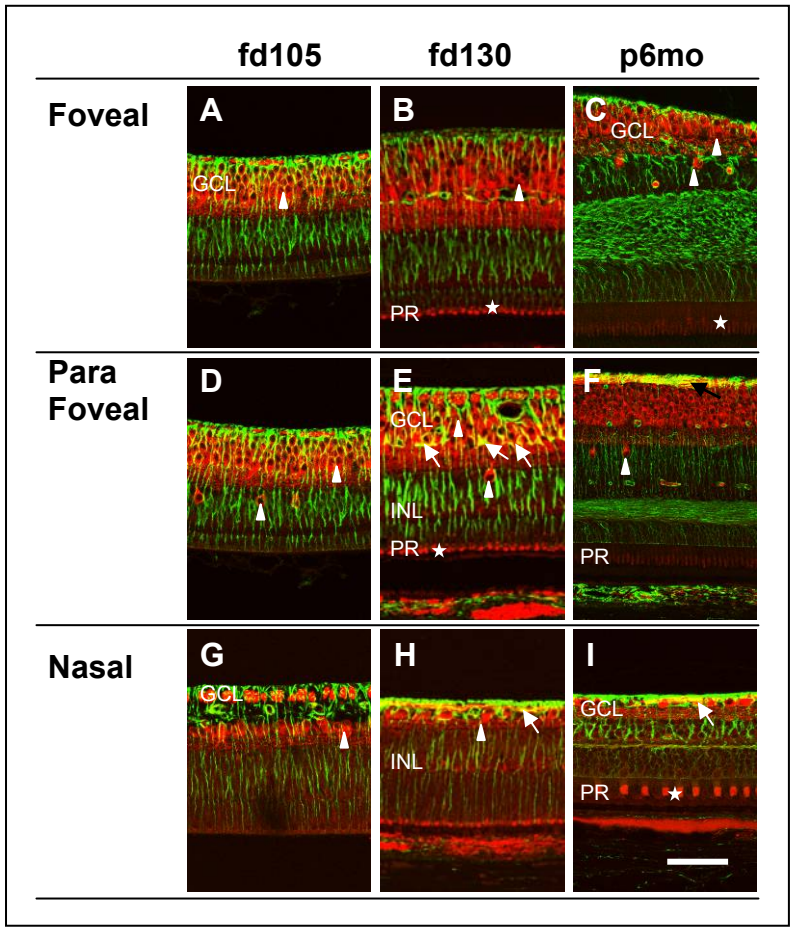

FIGURE 5.32 TβRI (red) and vimentin (green) immunoreactivity in macaque retinas at fd105, fd130 and p6mo. TβRI immunolabelling is detected in photoreceptors (asterisks, B, E, I), ganglion cells (white arrowheads, A-I) as well as in astrocytes (white arrows, E ,H, I). (Black arrow = ganglion cell axons (F)). (GCL: ganglion cell layer, INL: inner nuclear layer, PR: photoreceptor layer). Bar= 100µm.

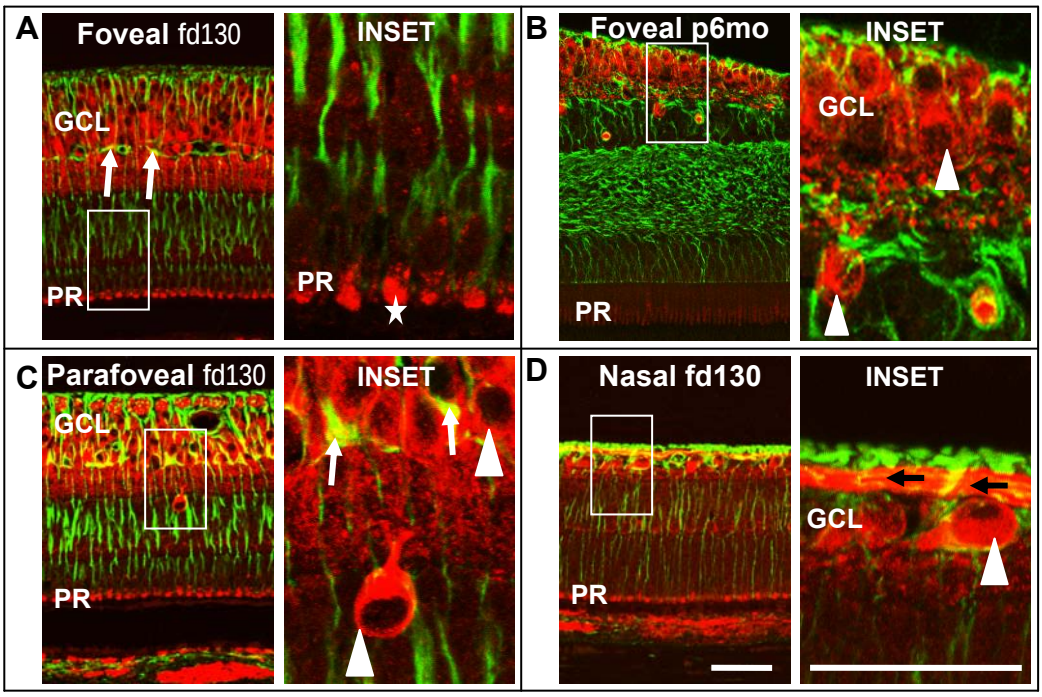

FIGURE 5.33 TβRI (red) and vimentin (green) immunoreactivity in the foveal region of fd130 (A) and p6mo (B), and in the parafoveal (C) and nasal region (D) of fd130 macaque retina. Insets (4xzoom) show intense TβRI immunolabelling in the photoreceptors (asterisks, A), ganglion cells (white arrowheads, B, C, D), ganglion cell axons (black arrows, D) as well as in astrocytes (white arrows, C). (GCL: ganglion cell layer, INL: inner nuclear layer, PR: photoreceptor layer). Bar= 100µm.

TGF-βII receptor

Location

TGF-βII receptor (TβRII) protein was detected in the ganglion cells from 11WG, and in the photoreceptors from 16WG in human retina (Figure 5.34).

In the macaque, TβRII immunolabelled ganglion cells were seen in the foveal region from fd85 and in the parafoveal and nasal region from fd130 (Figure 5.35). TβRII labelled photoreceptors were also found in the foveal region from fd85 and parafoveal and nasal regions from fd130 (Figures 5.36, 5.37). In addition, entire photoreceptors in the fovea appeared to express TβRII during the fd85-p2.5y period which was later localised to the outer segments throughout the retina from p6mo to p2.5y (Figures 5.36, 5.37).

TβRI is expressed in ganglion cells earlier than TβRII in the macaque retina (fd64 *versus* fd130). Although TβRI was seen in astrocytes, TβRII did not colocalise with vimentin (a marker of immature astrocytes). Both TβRI and TβRII immunolabelled photoreceptor outer segments, however, postnatally, TβRI was confined to the peripheral retina whilst TβRII was found across all retinal regions.

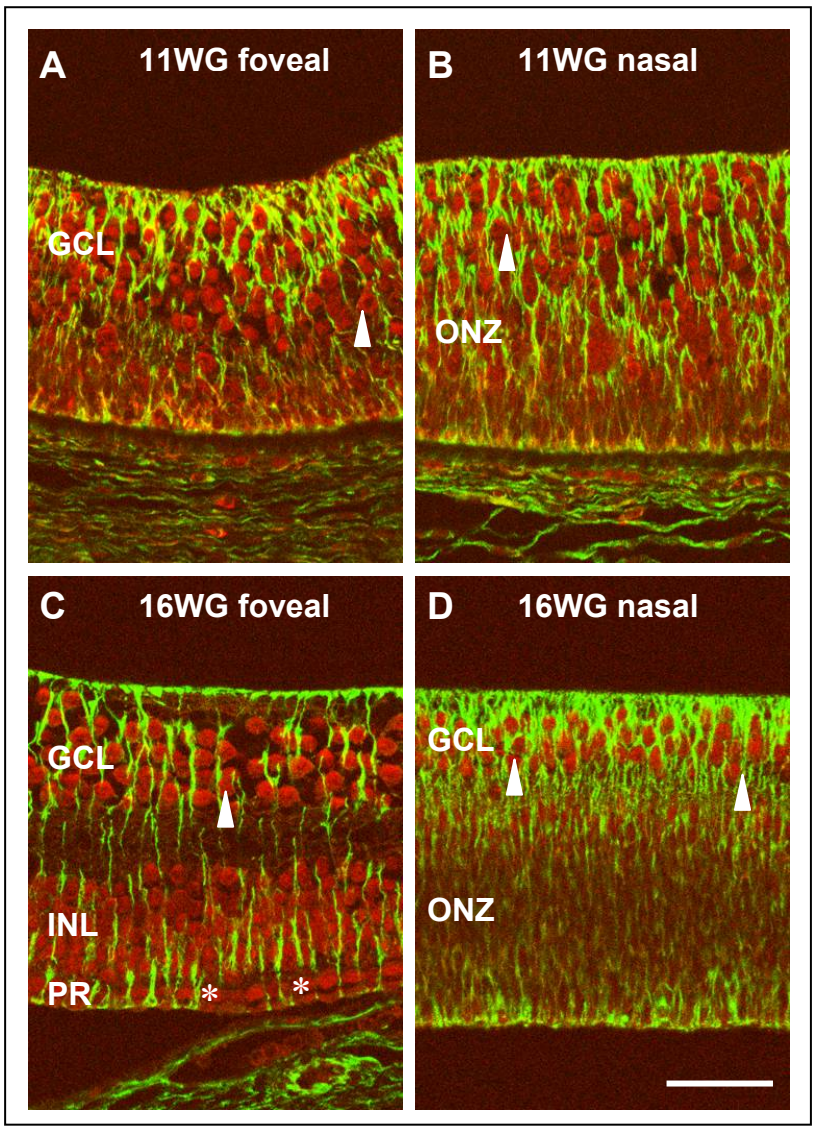

FIGURE 5.34 TβRII (red) and vimentin (green) immunoreactivity in the foveal and nasal regions of (A,B) 11WG and (C,D) 16WG human retina. Photoreceptors are not differentiated in the 11WG retina or in the 16WG peripheral retina. TβRII immunoreactivity is detected in the ganglion cells (A-D (white arrowheads)) and differentiated photoreceptors (C (asterisks)). (GCL: ganglion cell layer, INL: inner nuclear layer, ONZ: outer neuroblastic zone, PR: photoreceptor layer). Bar= 100μm.

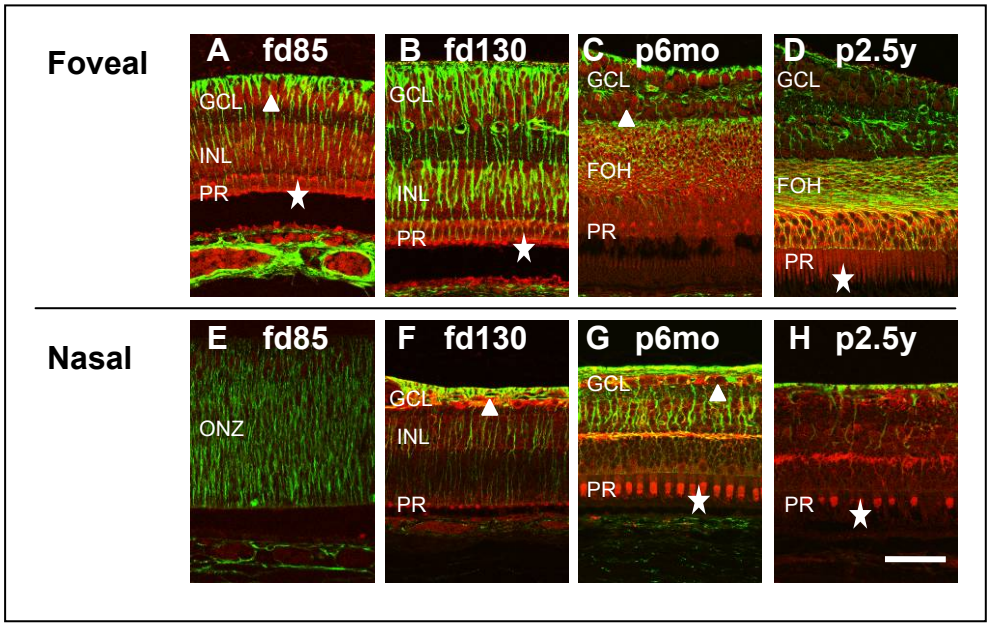

FIGURE 5.35 TβRII (red) and vimentin (green) immunoreactivity in four macaque retinas of different ages. Strong TβRII expression is detected in differentiated photoreceptors (A-D, G, H). Ganglion cells are also mildly immunoreactive (A, C, F, G). There is no TβRII immunoreactivity in undifferentiated retina. Immunoreactivity is also detected in the fibres of Henle (FOH, photoreceptor axons) in postnatal retina (C,D). (ganglion cells (white arrowheads) and differentiated photoreceptors (asterisks). (GCL: ganglion cell layer, INL: inner nuclear layer, ONZ: outer neuroblastic zone, PR: photoreceptor layer). Bar= 100μm.

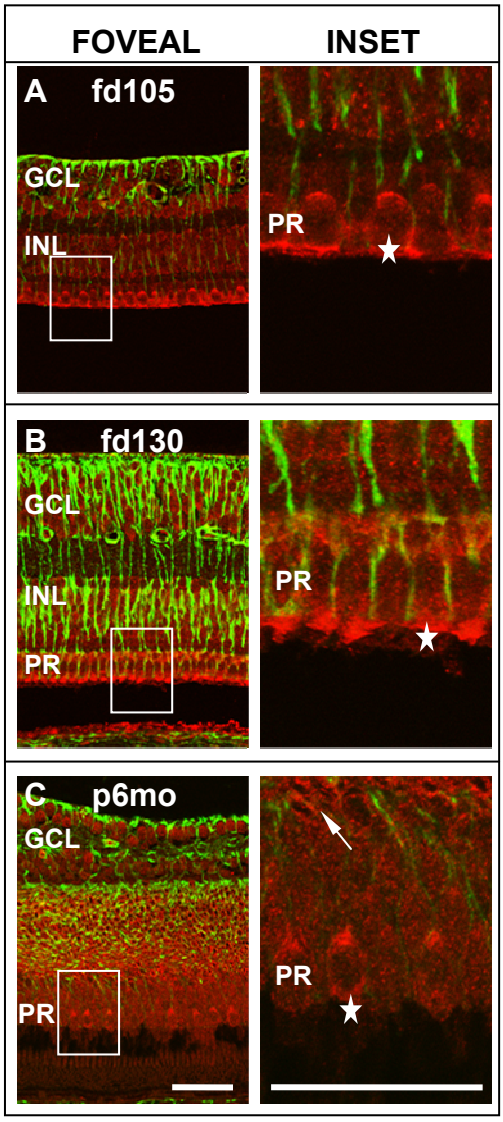

FIGURE 5.36 TβRII protein (red) and vimentin (green) immunoreactivity in sections of macaque retina from fd105 to p6mo. Insets show labelled photoreceptors (asterisks) including immunoreactivity in axon of photoreceptor (white arrow in C). TβRII immunolabelling involves the entire photoreceptor in the foveal region, pre and postnatally. (GCL: ganglion cell layer, INL: inner nuclear layer, PR: photoreceptor layer). Bar= 100μm.

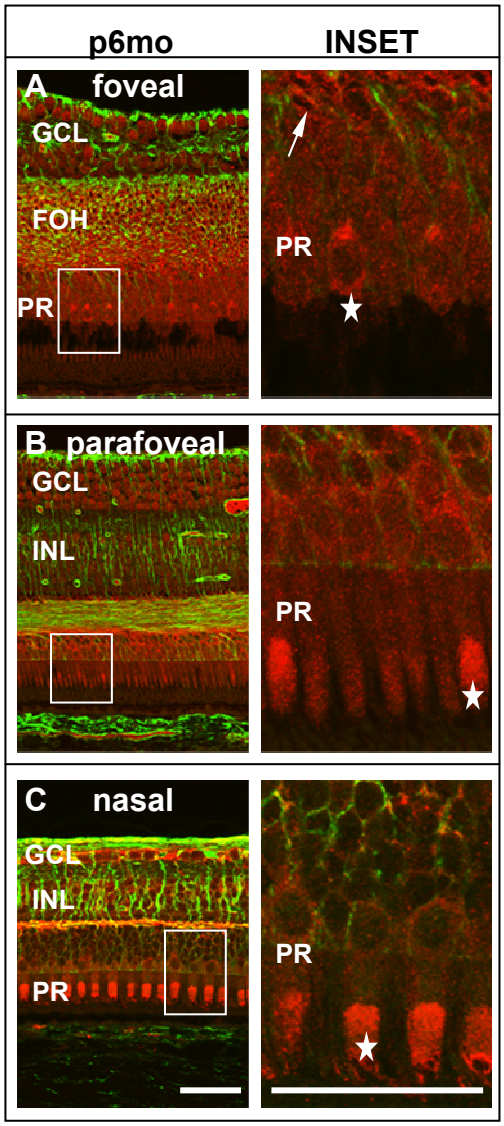

FIGURE 5.37 TβRII (red) and vimentin (green) immunoreactivity in a p6mo macaque retina. Insets show labelled photoreceptors (asterisks) including immunoreactive fibres of Henle (FOH, A). TβRII immunolabelling is initially seen in the entire photoreceptor in the fovea but later, in the postnatal retina, localises to the outer segments in the peripheral retina. (GCL: ganglion cell layer, INL: inner nuclear layer, PR: photoreceptor layer). Bar= 100μm.

TABLE 5.2 Summary of TGF-β protein and mRNA distribution

Marker	Type	GCL	PR	Astrocytes	Centroperipheral gradient (prenatal)
TGF-β1	protein	+/-	+	-	+
	mRNA	NA	NA	NA	NA
TGF-β2	protein	+/-	++	-	+
	mRNA	+	++	-	+
TGF-β3	protein	+/-	++	-	+
	mRNA	+	++	-	+
TβRI	protein	+	+	++	-
TβRII	protein	+	+	-	-

GCL: ganglion cell layer, PR: photoreceptor layer, NA: not applicable

5.4 DISCUSSION

All TGF-β protein and mRNA isoforms and receptors were detected in human and macaque retinas (Table 5.2), TGF-β2 and TGF-β3 mRNA and protein were detected at low to moderate levels in the GCL and moderate to high levels in the photoreceptor layers of both species. Immunoreactivity for TGF-β1 was low in both species, being somewhat higher in the PR layer compared to the GCL. TGF-β1 was not detectable by *in situ* hybridisation, consistent with PCR studies in Chapter 4. The receptors, TβRI and TβRII were detected in the GCL and PR layer during development, but in addition there was strong TβRI immunoreactivity in astrocytes.

There was some suggestion of a centro-peripheral gradient of TGF-β1 expression in the postnatal monkey retina, but not during vascularization of the macular region. However, there was strong evidence of a gradient of distribution of both TGF-β2 and TGF-β3 protein in both species; this is consistent with distinct gradients of TGF-β3 mRNA expression, and less distinct gradients of TGF-β2 mRNA expression observed in both species. In all cases, the peak density of labelling was seen in the central retina (‘foveal’), and the gradient was strongly evident during the period of vascularization of the macular region prior and during formation of the FAZ. Furthermore, the localisation of TβRI in astrocytes is consistent with the

hypothesis that, gradients of TGF-β expression affect astrocyte proliferation and /or migration around the macular region.

Astrocytes expressing TβRI were associated with the development of, the retinal blood vessels in the GCP (ganglion cell layer plexus). These stellate astrocytes with long processes migrate into central retina deep in the GCL but are excluded from the incipient fovea (reviewed in Provis, 2000). Due to the relative hypoxia in the retina just ahead of the advancing front of blood vessels when they grow towards the central retina, astrocytes leading the actively growing vascular network, express VEGF inducing proliferation of EC that follow them (Provis *et al.*, 2000). Immature astrocytes are immunoreactive for both vimentin and GFAP as are Müller cells (Provis *et al.*, 2000). In this study, astrocytes can be readily distinguished from Müller cells, with processes running horizontally and radially and, confined to the deep GCL, whilst the Müller cells extend vertically throughout all retinal layers (Provis *et al.*, 2000).

An interesting finding in this study was seeing a TGF-β gradient in the outer retina, while the blood vessels are located in the inner retina. TGF-β has been shown previously to be present in photoreceptors (Lutty *et al.*, 1991; Lutty *et al.*, 1993; Pasquale *et al.*, 1993; Pfeffer *et al.*, 1994; Anderson *et al.*, 1995), astrocytes (Constam *et al.*, 1992; Baghdassarian *et al.*, 1993; Anderson *et al.*, 1995) and ganglion cells (Anderson *et al.*, 1995; Close *et al.*, 2005). However, a developmental study for TGF-β has not been carried out.

It is possible that TGF-β2 and TGF-β3 protein and mRNA gradients arising in the photoreceptors, together with diffusion of oxygen and nutrients from the choriocapillaris may affect retinal vascular patterning via effects on astrocytes expressing TβRI. It is unclear why TβRI was identified in astrocytes without the associated TβRII.

TGF-β has been shown to upregulate GFAP expression in astrocytes, although this may indicate different responses (Reilly *et al.*, 1998). When exogenous TGF-β is added to cultured astrocytes their proliferation ceases and when TGF-β stimulates neurotrophic factors such as nerve growth factor (NGF) produced by astrocytes neuronal survival is promoted (Lindholm *et al.*, 1992; Baghdassarian *et al.*, 1993; Hunter *et al.*, 1993; Anderson *et al.*, 1995)

so that their dual role may vary possibly depending on other growth factors or conditions present but would be understandable considering the metabolic stress inner retinal foveal neurons are in, in the hypoxic central retina.

It is also possible that regression of astrocytes from around the edge of the FAZ, as astrocytes never enter the fovea is partly due to the anti-angiogenic or anti-migratory effects of TGF-β, creating a 'no-go' area for the astrocytes and hence inhibiting the growth of blood vessels; there would be no template for vessels to follow into the incipient fovea (Stone, 2006).

TGF-β can inhibit endothelial cell proliferation induced by acidic or basic fibroblast growth factors (FGF-1, FGF-2) and chemotaxis of endothelial cells (Baird & Durkin, 1986; Muller *et al.*, 1987; Bensaid *et al.*, 1989; Lutty *et al.*, 1991; Pasquale *et al.*, 1993). Interestingly, a gradient of TGF-β expression in the GCL rather than in the PR layer was expected due to the proximity of astrocytes to the ganglion cells but none was found. This suggests that TGF-β may either act at a distance or that it has other roles in the retina including a neuroprotective function (refer to Chapter 1.2.3).

Although many *in vitro* experiments study cells in isolation or in interaction with one other cell type in a defined cellular environment, the mechanisms controlling retinal development and blood vessel growth are extremely complicated. Several types of cells are involved endothelial cells, microglia and pericytes, and there may be dose-dependent effects of growth factors, consistent with the observed gradients of expression seen in the present studies. Combinations of numerous cytokines and changing cellular microenvironments are also important. The moderate TGF-β protein levels and expression of low mRNA levels for TGF-β2 and TGF-β3 isoforms in the GCL (Table 5.2) suggests that regulation of expression of these isoforms is translational rather than transcriptional.

The postnatal period in this study was assessed in macaque retina. Immunoreactivity for TGF-β1 protein was only seen postnatally in both the GCL and photoreceptors. TGF-β2 and TGF-β3 protein and mRNA profiles were similar. After high optical density levels of TGF-β2 and TGF-β3 protein and mRNA are observed in fd105 (~25WG), levels fall with age with the

lowest optical density recordings recorded postnatally (p6d-p11y) well after formation of the FAZ.

In conclusion, these studies establish a comprehensive developmental profile for TGF-β1, TGF-β2 and TGF-β3 mRNA and protein expression and distribution, and localisation of TβRI and TβRII proteins for both human and macaque retinas. Taken together, these observations support the proposal that inhibitory growth factors, such as TGF-β contribute to defining the FAZ early in development, well before 23-25 WG in humans and before fd100 in macaques.

CHAPTER 6 – CONCLUSION

In this thesis I have investigated the relationship between development of the fovea and its choroidal blood supply, as well as the distribution of TGF-β isoforms which might have a role in regulating the patterning and growth of blood vessels in central primate retina.

In primates there is a mismatch in the differentiation pattern of the neural retina and the formation of the retinal vasculature. The foveal region differentiates early (~11WG), but the surrounding region is not vascularised until much later in gestation (~24-6 WG) raising questions concerning how the immature central/foveal retina derives adequate oxygen and nutritional support. In Chapter 3 it was hypothesised that delayed vascularization of central retina might be compensated for by higher rates of endothelial cell proliferation in the central choriocapillaris. To the contrary, however, I observed *reduced* rates of EC proliferation in the 'foveal' chorioretinal locations at all ages studied between 14 and 18.5WG. These data indicate therefore, that EC proliferation in the choriocapillaris is *not* promoted by more advanced retinal differentiation, and oxygen uptake, as reported in animal models of retinal vascular development (Stone *et al.*, 1995; Stone, 1997; Ozaki *et al.*, 1999; Semenza, 2000; Morita *et al.*, 2003).

Rather, the findings reported in Chapter 3 suggest that mechanisms regulating proliferation and growth of the choroidal vasculature are independent of differentiation in the neural retina. These findings are consistent with reports that 9% of genes expressed by EC vary by more than 250 fold when choroidal and retinal EC are compared using DNA microarrays and QPCR (Smith *et al.*, 2007).

The RTPCR and QPCR studies in Chapter 4, demonstrated that all three TGF-β isoforms are expressed in the developing and adult primate retina, with TGF-β2 being the predominant isoform. Higher levels of TGF-β are present in developing compared with adult retina, and in central compared with peripheral retina. The early expression of TGF-β in the developing central retina, and the observed centro-peripheral gradient support the hypothesis that the antiproliferative and anti-angiogenic effects of this factor may help define the FAZ by suppressing astrocyte and endothelial cell proliferation and migration into this region during retinal development.

In situ hybridisation and immunohistochemistry studies presented in Chapter 5 further define the distributions of TGF-β mRNA and protein in the developing primate retina. Previous studies have shown that TGF-β is present in photoreceptors (Lutty *et al.*, 1991; Lutty *et al.*, 1993; Pasquale *et al.*, 1993; Pfeffer *et al.*, 1994; Anderson *et al.*, 1995), astrocytes (Constam *et al.*, 1992; Baghdassarian *et al.*, 1993; Anderson *et al.*, 1995) and ganglion cells (Anderson *et al.*, 1995; Close *et al.*, 2005) and a close interrelationship in the expression patterns of the different isoforms has been established. However, this is the first study of the expression of TGF-β and TGF-β receptors during development of the primate retina. The present study shows that all three isoforms are expressed in the photoreceptors in the incipient fovea, well before formation of the FAZ, although there are differences in the timings of expression. While TGF-β1 protein is present in relatively high levels postnatally, the other two isoforms are expressed at higher levels before and during FAZ formation, diminishing in the postnatal period. It is possible that TGF-β1 exerts an antiproliferative, or stabilizing, effect on the retinal vasculature in the postnatal period.

TβRI protein was detected by immunohistochemistry in astrocytes from 16WG (human) and fd105 (macaque). The high levels of TGF-β2 and TGF-β3 in central retina during early development, and the presence of TβRI on astrocytes in the retina is consistent with the hypothesis that TGF-β signalling may regulate vascular growth in central retina during development, by inhibiting astrocyte migration and proliferation and thereby, formation of the astrocyte template. A difficulty with the hypothesis, however, is that the highest levels of TGF- β protein are detected in the outer retina, while vessel formation takes place in the inner retina. Further studies are required to address this question. To this effect, recent experiments carried out in the laboratory show that TGF-β2 does inhibit primate retinal endothelial cell proliferation *in vitro*, but has little direct effect on migration. In contrast, those same experiments indicate that FGF-2 directly inhibits endothelial cell migration, *in vitro* (Phillip Romo, Honours 2006-7). The findings indicate that combinations of growth factors, and other molecules including those which regulate vessel guidance, are likely needed to regulate vascular development in central retina. Further research into genetic factors and the corresponding

cellular microenvironment that regulates TGF-β (and growth factor) signalling will ultimately lead to better understanding of the development of the fovea and its vascular supply.

APPENDIX

APPENDIX A

Relative quantification of target and reference genes was done by using the Pfaffl mathematical equation which despite different cDNA input concentrations to mimic different RT efficiencies, all target transcripts as well as reference transcripts are affected in parallel (Pfaffl, 2001).

In this mathematical model it is necessary to determine the “crossing points” (CP) or replicate “takeoff points” for each transcript. CP is defined as the point at which the fluorescence rises appreciably above the background fluorescence (Pfaffl, 2001). The “takeoff point”, is calculated from the second derivative of the raw data and is the point determined where the reaction is increasing most rapidly. This is the “peak” of the exponential reaction and occurs shortly after the “takeoff” of the reaction (Figure B.1). The “takeoff” point is estimated as 80% below the peak level (Rotorgene version 6.0, Corbett Research).

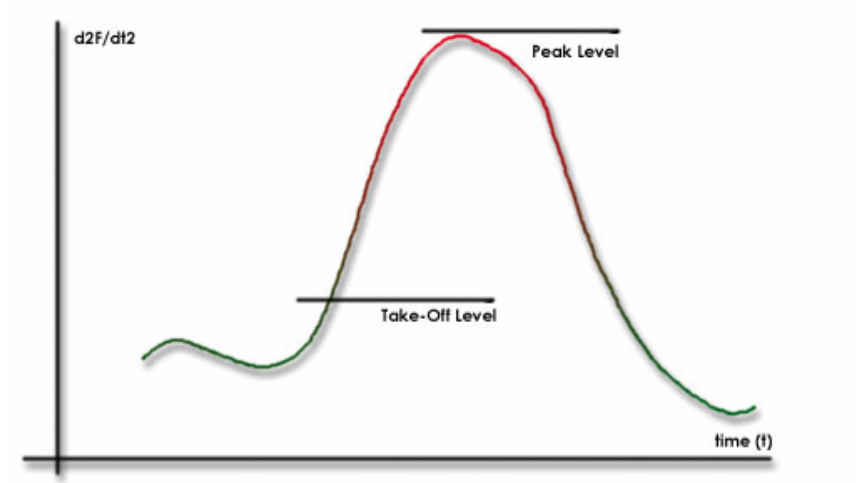

FIGURE A1 Graph shows the peak and the take off level of the reaction across time (Rotorgene version 6.0, Corbett Research).

The “efficiency” or “average amplification” of the particular sample is calculated by Rotorgene software (Rotorgene version 6.0, Corbett Research) which also provides confidence intervals for the data. The average increase in the four readings made following the “takeoff” is calculated and is defined as the sample's “amplification”. Outlier “amplifications” are removed to account for noise in background fluorescence and the non-outlier

“amplifications” are averaged to become a run "average amplification". A 100% efficient reaction would result in an amplification value of two for every sample, i.e. doubling of an amplicon takes place in every cycle. In terms of the raw data, the signal should increase by a doubling amount in the exponential phase. The more variation there is between the estimated amplification values of each sample, then the larger the confidence interval will be. The confidence interval, for large N, gives a 68.3% probability that the true amplification of the samples lies within one standard deviation. By doubling the ± interval, one achieves a 95.4% confidence interval for large N (i.e. within two standard deviations).

The mathematical model has been devised to determine the relative quantification of a target gene in comparison to a reference gene (Pfaffl, 2001). The relative expression ratio of a target gene is calculated based on efficiency and crossing points’ deviation of an unknown sample versus a control, and expressed in comparison to a reference gene using the following equation:

$$\text{Ratio} = \frac{(E_{\text{target}})^{\Delta CP_{\text{target (control-unknown)}}}}{(E_{\text{reference}})^{\Delta CP_{\text{reference (control-unknown)}}}}$$

where E= Efficiency = average amplification

ΔCP = change in crossing points = the point where the fluorescence rises sharply above the background fluorescence threshold = replication take off

Target = gene of interest TGF-β

Reference = reference gene = housekeeping gene GAPDH

Control = normal sample= Age sample number 1 of central/nasal retina or central retinal sample of a particular age

Treated = experimental sample = Age sample number 2 of central/nasal retina (same site as for age sample number 1) or nasal retinal sample of the same age as control

So for the equation;

$$\text{Ratio} = \frac{(\text{Average Amplification}_{\text{TGF-}\beta})^{\Delta\text{Replication take off for TGF-}\beta\text{ (Age\#1-Age\#2)}}}{(\text{Average Amplification}_{\text{GAPDH}})^{\Delta\text{Replication take off for GAPDH (Age\#1-Age\#2)}}}$$

and ratio=1 then there is no change in relative expression of target gene and reference gene. If ratio is greater than one then there is a positive fold change eg. If ratio = 1.5 then there is a 50% increase in expression when control or age sample number 1 is compared to sample number 2. Conversely if ratio = 0.5 then there is a 50% decrease when control or age sample number 1 is compared to sample number 2. When ratios are calculated the presence of negative numbers is irrelevant as absolute values are noted.

APPENDIX B

To assess the validity of using optical density values of mRNA and protein expression in samples from retinal regions *versus* optical density values across whole retinal sections, the following analysis was undertaken.

A section from a 16WG retina was selected for optical density analysis. Following *in situ* hybridisation with the TGF-β2 probe and labelling with Fast Red/HNPP, the fluorescence (TGF-β2 mRNA expression) was optically recorded by combining the 77 images acquired across the whole section into a montage (Figure 5.1, Chapter 5). Using the LSM5 Pascal software (Carl Zeiss) measurement tool, 13246 measurements at 1μm intervals were taken each time a line was traced across the superior, middle and inferior aspects of the photoreceptor layer from the temporal end, through the fovea, to the nasal end. Similarly, a line was traced across the GCL three times (values were subsequently averaged) and once across the outer neuroblastic zone (ONZ) in the same direction recording the optical density measurements at 1μm intervals for comparison. The ONZ layer optical density values provided the amount of 'background' staining present.

For the photoreceptors, the 13246 optical density values taken at the three different levels in the photoreceptor layer were averaged, and then grouped into six retinal locations as shown in Table B1. The values were also grouped using the same criteria but with 200 tail-values excluded at each retinal location for comparison (Table B1).

Additionally, six representative samples of the retinal regions were also assembled as a minimontage, to represent the distribution of TGF-β across the retina.
The graphs corresponding to the optical densities across the GCL and the ONZ for a section of the whole eye and the minimontage showed little variation between retinal regions (Figure B1 and B2).

Location	Range of optical density values averaged for each retinal location	Range of optical density values averaged for each retinal location (excluding 200 tail-end values)
T	1 to 2900	201-2700
PFT	2901 to 4000	3101-3800
F	4001 to 5760	4201-5560
PFN	5761 to 6860	5961-6660
ND	8400 to 9940	8600-9740
N	9941 to 13246	10141-13046

TABLE B1 Range of optical density values averaged for each region across the retina (T – temporal, PFT – parafoveal on temporal side, F - foveal, PFN – parafoveal on nasal side, ND – nasal to disc and N - nasal). Optical density values between 6860 and 8400 were excluded, as this area corresponded to the optic nerve and the area temporal to the optic nerve which does not belong to the PFN region.

This is also evident when the median values (MD) (Table B2) and standard deviations (SD) (Table B3) are calculated for each set of values. The largest variation in SD is seen across the photoreceptor (PR) layer between the minimontage and the whole eye possibly due to the differences in the average of labelling. Positive labelling seen across the sampled image for a retinal region in the multiple sampled images in the whole eye section for a particular retinal region, both weakly and strongly labelled areas are included in the sample and averaged. The highest optical density values for TGF-β2 mRNA are noted in the photoreceptor layer on the temporal side of the fovea, consistent with the earlier differentiation of the temporal retina (Figures B1C, B1D, B1E).

		Median Whole eye	Median Whole eye excluding tail values	Median Minimontage	Median comparison % between whole eye & minimontage	Median comparison % between whole eye excluding tail values & minimontage
T	GCL avg	145	147	144	-0.70%	-2.09%
	ONZ	55	56	53	-3.77%	-5.66%
	PR sup	81	80	80	-1.25%	0.00%
	PR mid	80	79	78	-2.56%	-1.28%
	PR inf	81	80	78	-3.85%	-2.56%
PFT	GCL avg	143	140	132	-7.94%	-5.67%
	ONZ	53	51	50	-6.00%	-2.00%
	PR sup	98	97	96	-2.08%	-1.04%
	PR mid	87	84	83	-4.82%	-1.20%
	PR inf	94	94	100	6.00%	6.00%
F	GCL avg	143	146	139	-3.00%	-5.16%
	ONZ	37	37	40	7.50%	7.50%
	PR sup	145	150	156	7.05%	3.85%
	PR mid	131	136	145	9.66%	6.21%
	PR inf	136	142	144	5.56%	1.39%
PFN	GCL avg	141	144	135	-4.95%	-6.68%
	ONZ	35	34	35	0.00%	2.86%
	PR sup	104	99	109	4.59%	9.17%
	PR mid	104	99	98	-6.67%	-1.54%
	PR inf	100	98	103	2.91%	4.85%
ND	GCL avg	124	125	126	1.46%	0.40%
	ONZ	38	38	37	-2.70%	-2.70%
	PR sup	95	88	85	-11.76%	-3.53%
	PR mid	87	87	82	-6.10%	-6.10%
	PR inf	86	84	81	-6.17%	-3.70%
N	GCL avg	129	129	141	8.62%	8.85%
	ONZ	42	43	41	-2.44%	-4.88%
	PR sup	86	86	89	3.37%	3.37%
	PR mid	88	89	88	0.00%	-1.14%
	PR inf	85	85	86	1.16%	1.16%

TABLE B2 Median values calculated from optical density measurements for each retinal layer for all six regions (T, PFT, F, PFN, ND, N) within the minimontage, the whole eye, and the whole eye excluding 200 optical density tail measurements (at each end of each region). The GCL average for optical density in the T region varies 0% compared to the ND region which varies up to 12% when the median is compared between the whole eye and the minimontage. [Calculation for comparison between minimontage and whole eye = (Median minimontage-Median whole eye)/Median minimontage x100. Calculation for comparison between minimontage and whole eye excluding tail values= (Median minimontage-Median whole eye without tail values)/Median minimontage x100.]

		SD Whole eye	SD Whole eye excluding tail values	SD Minimontage	SD comparison between whole eye & minimontage	SD comparison between whole eye excluding tail values & minimontage
	GCL avg	38.80	39.49	39.03	0.59%	-1.17%
	ONZ	23.18	23.63	21.62	-7.20%	-9.29%
T	PR sup	16.50	16.36	21.16	22.03%	22.66%
	PR mid	16.97	16.72	18.90	10.21%	11.52%
	PR inf	17.74	16.67	19.48	8.90%	14.44%
	GCL avg	42.25	45.13	40.05	-5.49%	-12.70%
	ONZ	18.50	18.38	28.17	34.32%	34.74%
PFT	PR sup	15.56	16.23	43.33	64.09%	62.54%
	PR mid	16.00	15.20	45.84	65.10%	66.83%
	PR inf	15.85	15.24	47.37	66.55%	67.82%
	GCL avg	31.26	31.95	40.00	21.85%	20.14%
	ONZ	14.78	13.71	29.63	50.12%	53.74%
F	PR sup	34.40	35.69	48.78	29.47%	26.84%
	PR mid	34.78	36.60	52.67	33.96%	30.51%
	PR inf	34.83	34.79	59.95	41.90%	41.96%
	GCL avg	28.13	27.09	33.98	17.23%	20.29%
	ONZ	14.85	15.31	22.23	33.21%	31.14%
PFN	PR sup	23.44	19.40	56.25	58.33%	65.51%
	PR mid	23.17	20.29	49.93	53.59%	59.36%
	PR inf	21.10	20.47	45.55	53.67%	55.06%
	GCL avg	32.18	33.23	27.59	-16.65%	-20.43%
	ONZ	16.35	16.32	18.36	10.95%	11.15%
ND	PR sup	17.95	16.94	25.42	29.39%	33.37%
	PR mid	19.03	16.95	23.13	17.73%	26.75%
	PR inf	17.97	17.13	26.29	31.66%	34.83%
	GCL avg	34.31	32.82	29.02	-18.23%	-13.08%
	ONZ	20.25	20.62	19.73	-2.60%	-4.49%
N	PR sup	16.79	16.08	21.03	20.16%	23.56%
	PR mid	18.77	18.07	21.06	10.84%	14.16%
	PR inf	18.38	18.29	20.72	11.32%	11.76%

TABLE B3 Standard deviations calculated from optical density measurements for each retinal layer for all six regions (T, PFT, F, PFN, ND, N) within the minimontage, the whole eye, and the whole eye excluding 200 optical density tail measurements (at each end of each region). The GCL average for optical density in the T region varies 1% compared to the PR bottom in the PFT region which varies up to 67%.

[Calculation for comparison between minimontage and whole eye = (SD minimontage – SD whole eye)/SD minimontage X100.

Calculation for comparison between minimontage and whole eye excluding tail values = (SD minimontage – SD whole eye without tail values)/SD minimontage X100.]

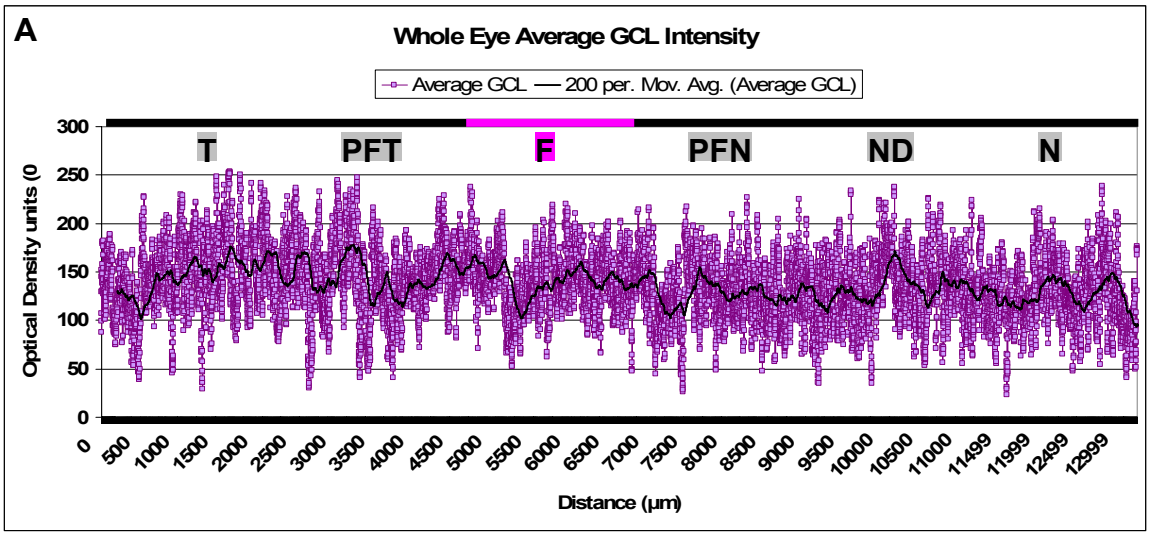
A
Whole Eye Average GCL Intensity
Average GCL
200 per. Mov. Avg. (Average GCL)
T
PFT
F
PFN
ND
N
Optical Density units (0
Distance (µm)

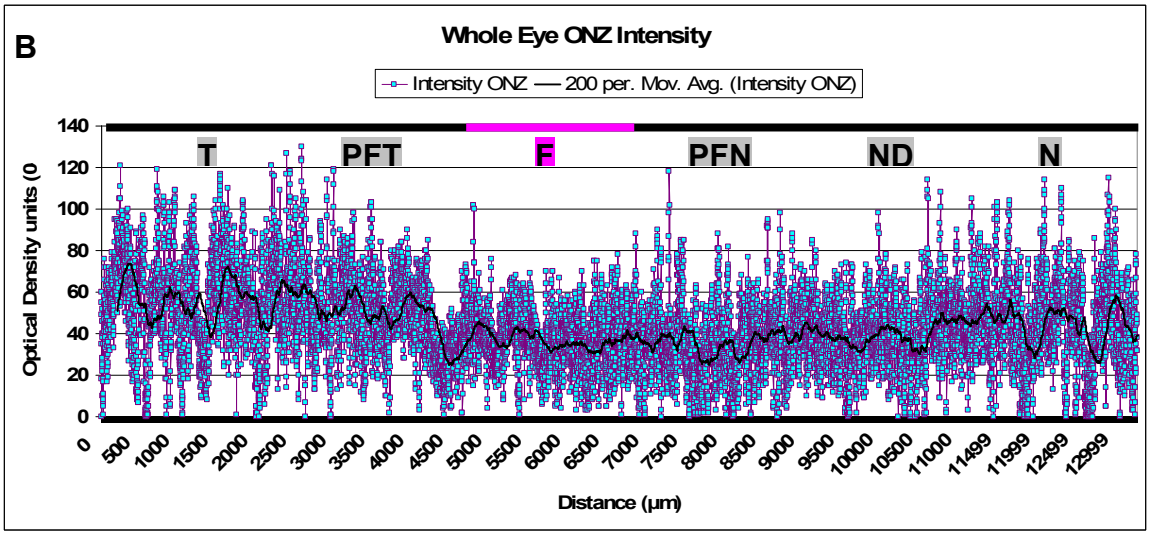
B
Whole Eye ONZ Intensity
Intensity ONZ
200 per. Mov. Avg. (Intensity ONZ)
T
PFT
F
PFN
ND
N
Optical Density units (0
Distance (µm)

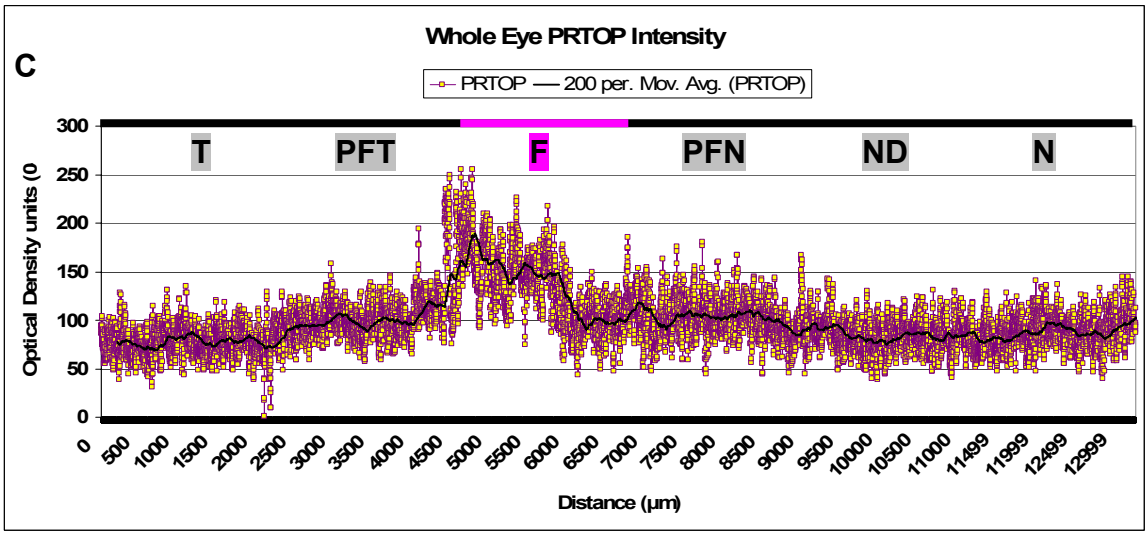
C
Whole Eye PRTOP Intensity
PRTOP
200 per. Mov. Avg. (PRTOP)
T
PFT
F
PFN
ND
N
Optical Density units (0
Distance (µm)

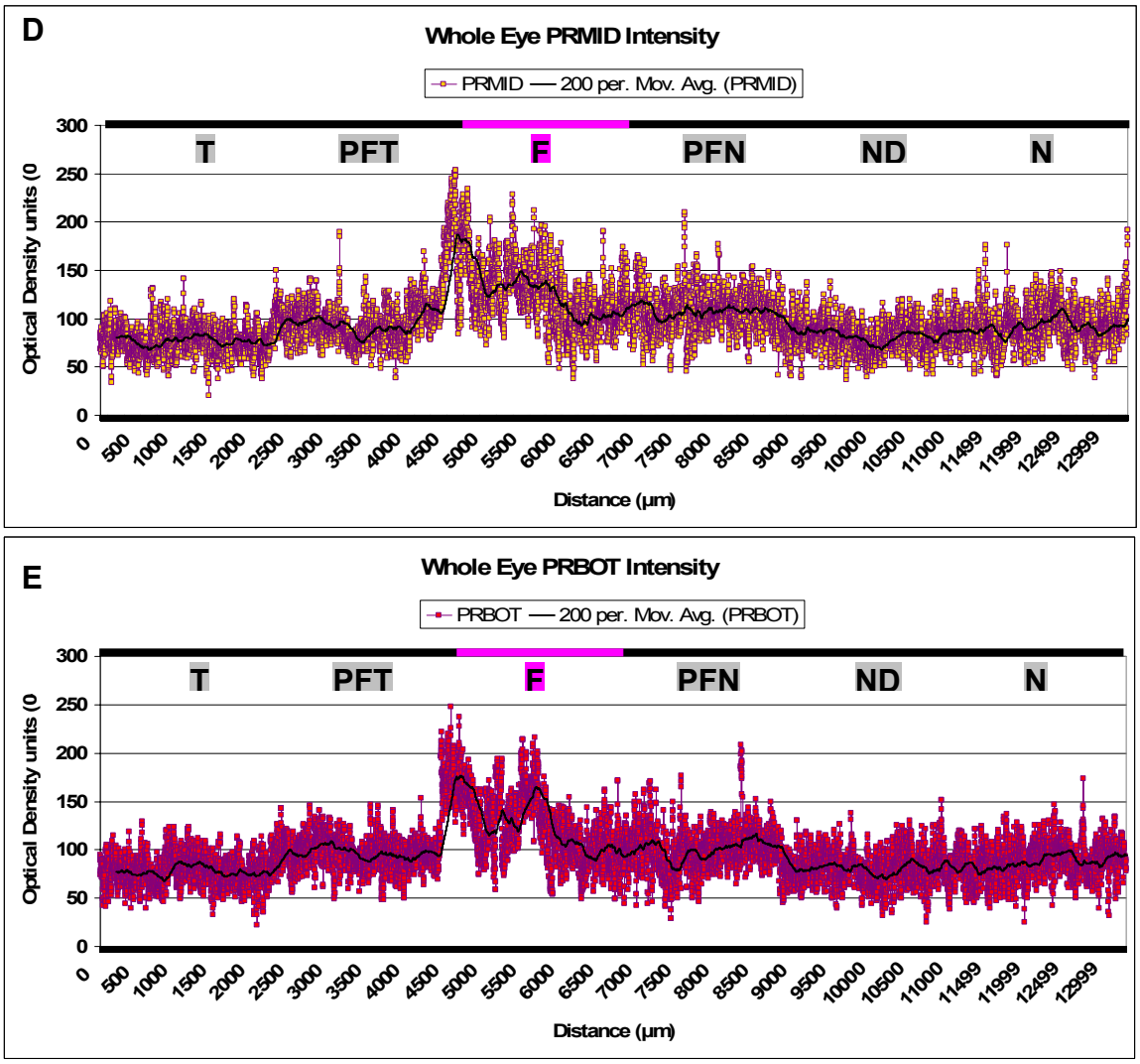

FIGURE B1 Graphs corresponding to the 13246 optical density values across the different layers of section of the whole eye from temporal, through the fovea, to the nasal side (T, PFT, F, PFN, ND, N). **A.** GCL average, **B.** ONZ, **C.** photoreceptor (PR) superior, **D.** PR middle and **E.** PR inferior. The black line graph corresponds to moving average of 200 values. The highest optical density of TGF-β2 in the photoreceptor layer is seen on the temporal side of the fovea, corresponding to earlier differentiation of the retina temporally.

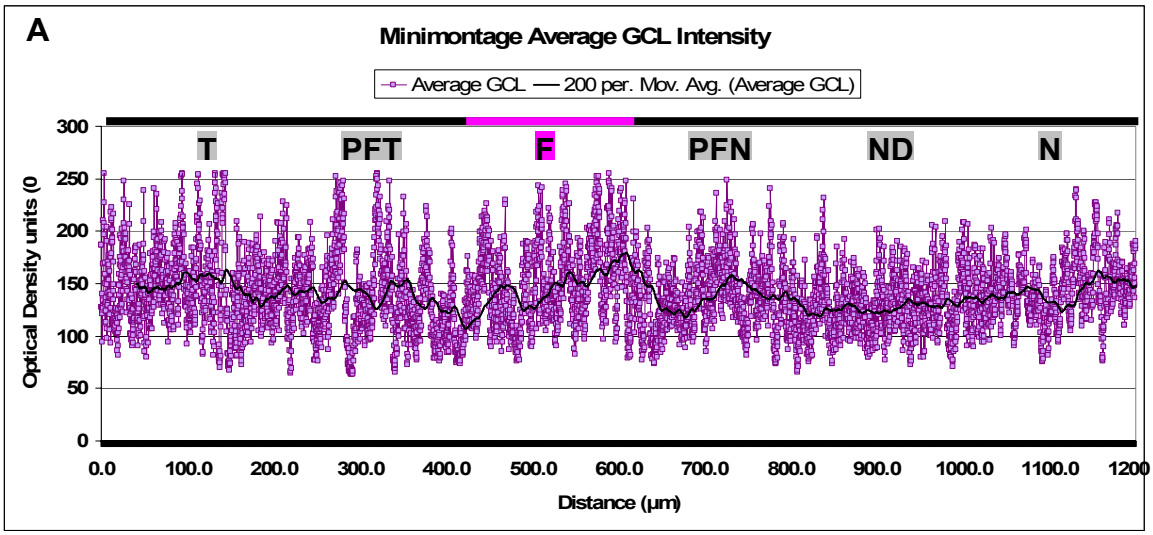
A
Minimontage Average GCL Intensity
Average GCL
200 per. Mov. Avg. (Average GCL)
T
PFT
F
PFN
ND
N
Optical Density units (0
300
250
200
150
100
50
0
0.0
100.0
200.0
300.0
400.0
500.0
600.0
700.0
800.0
900.0
1000.0
1100.0
1200
Distance (µm)

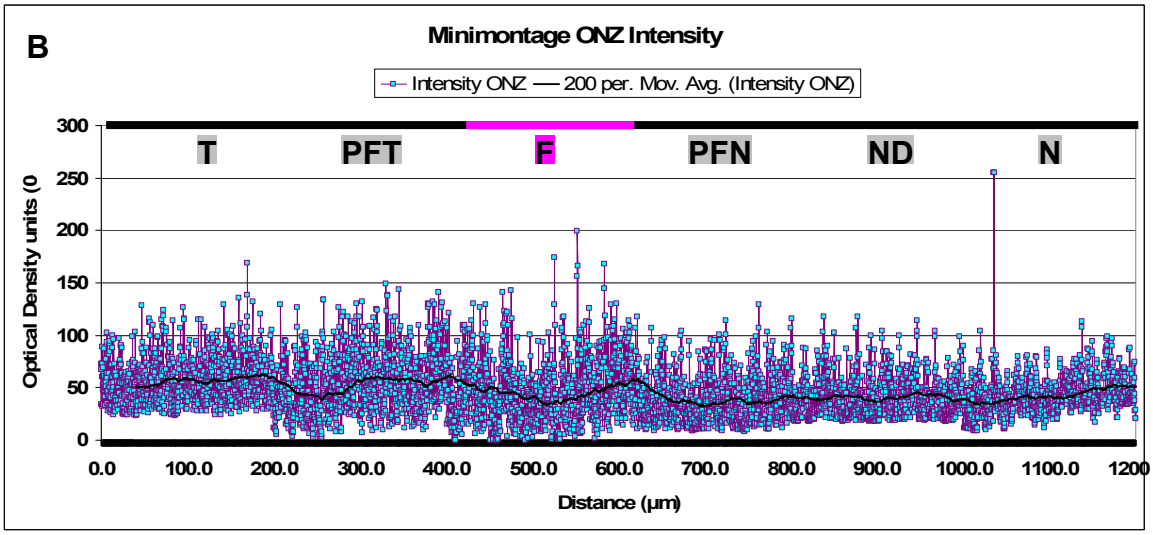
B
Minimontage ONZ Intensity
Intensity ONZ
200 per. Mov. Avg. (Intensity ONZ)
T
PFT
F
PFN
ND
N
Optical Density units (0
300
250
200
150
100
50
0
0.0
100.0
200.0
300.0
400.0
500.0
600.0
700.0
800.0
900.0
1000.0
1100.0
1200
Distance (µm)

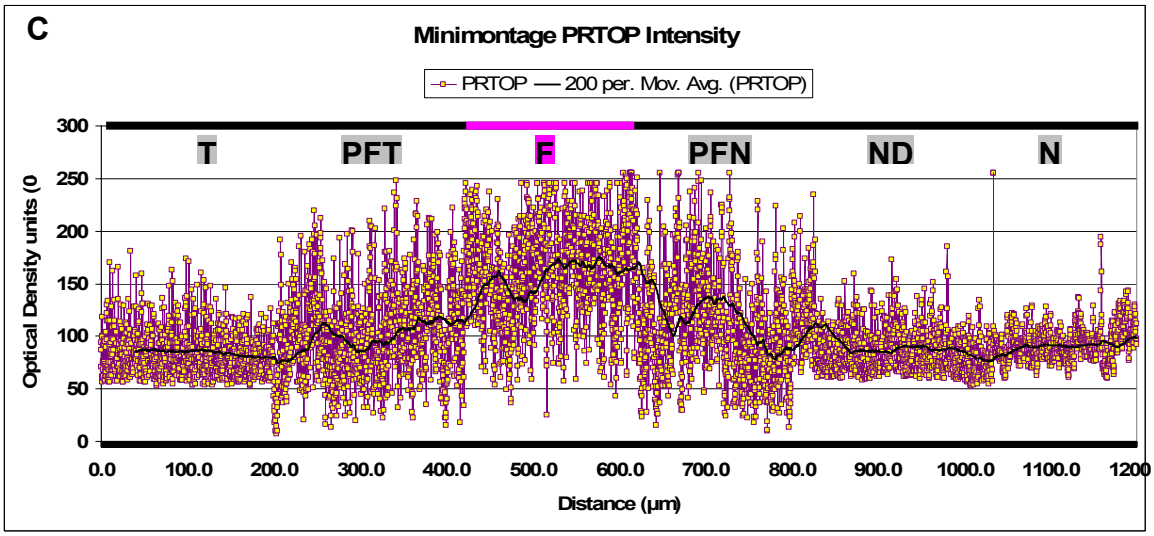
C
Minimontage PRTOP Intensity
PRTOP
200 per. Mov. Avg. (PRTOP)
T
PFT
F
PFN
ND
N
Optical Density units (0
300
250
200
150
100
50
0
0.0
100.0
200.0
300.0
400.0
500.0
600.0
700.0
800.0
900.0
1000.0
1100.0
1200
Distance (µm)

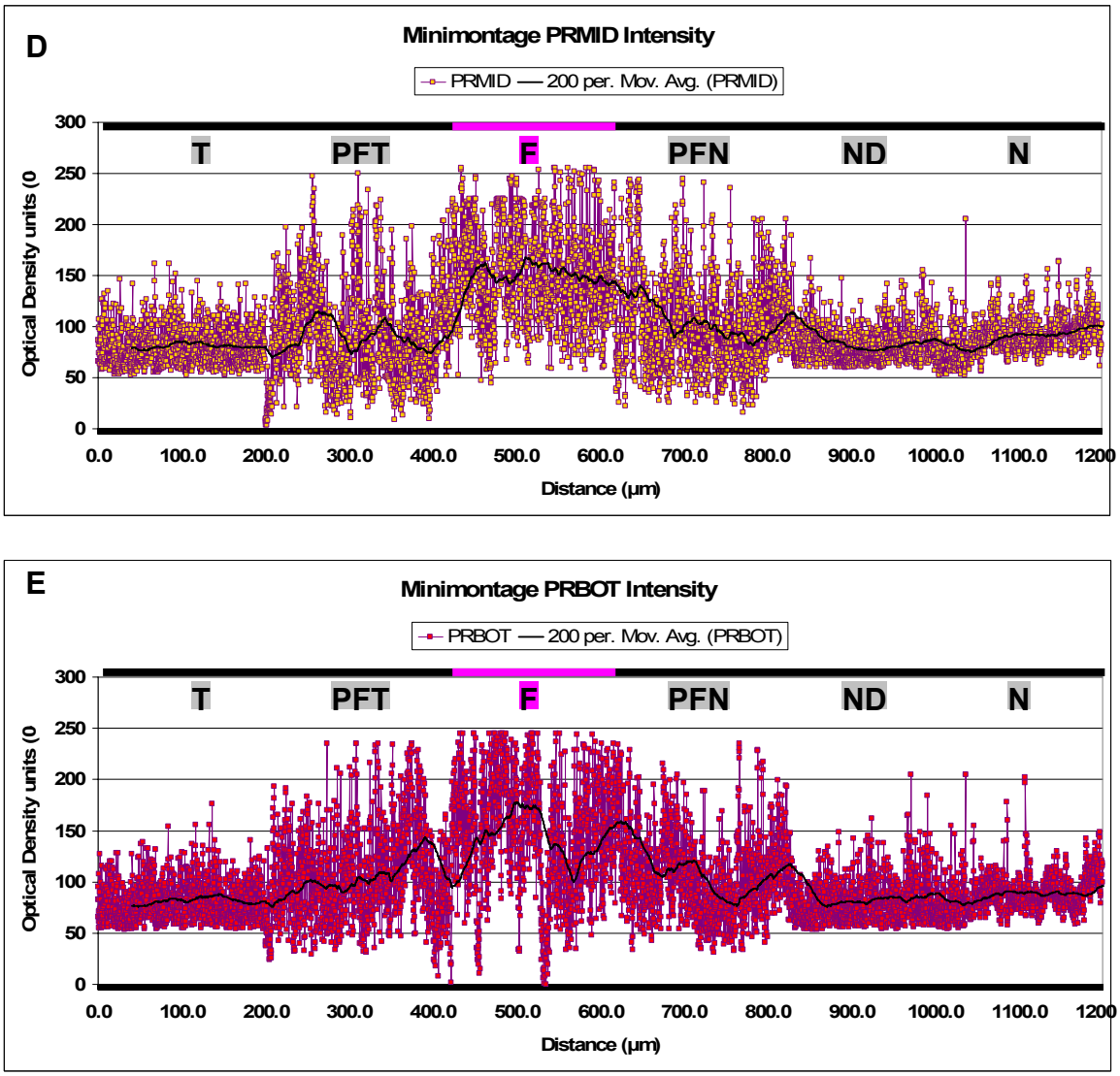

FIGURE B2 Graphs corresponding to optical density values across the different layers of the retina from the six sample regions (T, PFT, F, PFN, ND, N) in a minimontage, from top to bottom; **A.** GCL average, **B.** ONZ, **C.** PR superior, **D.** PR middle and **E.** PR inferior. Black line graph corresponds to moving average of 200 values.

REFERENCES

Abe K, Chu PJ, Ishihara A & Saito H. (1996) Transforming growth factor-beta 1 promotes re-elongation of injured axons of cultured rat hippocampal neurons. *Brain Res* **723**(1-2): 206-9.
Ahmed J, Braun RD, Dunn R, Jr. & Linsenmeier RA. (1993) Oxygen distribution in the macaque retina. *Invest Ophthalmol Vis Sci* **34**(3): 516-21.
Aiello LP, Northrup JM, Keyt BA, Takagi H & Iwamoto MA. (1995) Hypoxic regulation of vascular endothelial growth factor in retinal cells. *Arch Ophthalmol* **113**(12): 1538-44.
Alexiades MR & Cepko C. (1996) Quantitative analysis of proliferation and cell cycle length during development of the rat retina. *Dev Dyn* **205**(3): 293-307.
Anderson DH, Guerin CJ, Hageman GS, Pfeffer BA & Flanders KC. (1995) Distribution of transforming growth factor-beta isoforms in the mammalian retina. *J Neurosci Res* **42**(1): 63-79.
Annabi B, Naud E, Lee YT, Eliopoulos N & Galipeau J. (2004) Vascular progenitors derived from murine bone marrow stromal cells are regulated by fibroblast growth factor and are avidly recruited by vascularizing tumors. *J Cell Biochem* **91**(6): 1146-58.
Antonelli-Orlidge A, Saunders KB, Smith SR & D'Amore PA. (1989) An activated form of transforming growth factor beta is produced by cocultures of endothelial cells and pericytes. *Proc Natl Acad Sci U S A* **86**(12): 4544-8.
Asahara T, Murohara T, Sullivan A, Silver M, van der Zee R, Li T, Witzenbichler B, Schatteman G & Isner JM. (1997) Isolation of putative progenitor endothelial cells for angiogenesis. *Science* **275**(5302): 964-7.
Ashley DM, Sampson JH, Archer GE, Hale LP & Bigner DD. (1998) Local production of TGF beta1 inhibits cerebral edema, enhances TNF-alpha induced apoptosis and improves survival in a murine glioma model. *J Neuroimmunol* **86**(1): 46-52.
Ashton N. (1970) Retinal angiogenesis in the human embryo. *Br Med Bull* **26**(2): 103-6.
Assoian RK, Fleurdelys BE, Stevenson HC, Miller PJ, Madtes DK, Raines EW, Ross R & Sporn MB. (1987) Expression and secretion of type beta transforming growth factor by activated human macrophages. *Proc Natl Acad Sci U S A* **84**(17): 6020-4.
Attisano L & Wrana JL. (1996) Signal transduction by members of the transforming growth factor-beta superfamily. *Cytokine Growth Factor Rev* **7**(4): 327-39.
Attisano L & Wrana JL. (2000) Smads as transcriptional co-modulators. *Curr Opin Cell Biol* **12**(2): 235-43.
Bachoo RM, Maher EA, Ligon KL, Sharpless NE, Chan SS, You MJ, Tang Y, DeFrances J, Stover E, Weissleder R, Rowitch DH, Louis DN & DePinho RA. (2002) Epidermal growth factor receptor and Ink4a/Arf: convergent mechanisms governing terminal differentiation and transformation along the neural stem cell to astrocyte axis. *Cancer Cell* **1**(3): 269-77.
Baghdassarian D, Toru-Delbauffe D, Gavaret JM & Pierre M. (1993) Effects of transforming growth factor-beta 1 on the extracellular matrix and cytoskeleton of cultured astrocytes. *Glia* **7**(3): 193-202.
Baird A & Durkin T. (1986) Inhibition of endothelial cell proliferation by type beta-transforming growth factor: interactions with acidic and basic fibroblast growth factors. *Biochem Biophys Res Commun* **138**(1): 476-82.
Balazs EA, Denlinger, J.L. (1984) *The Vitreous in: The Eye.* New York: Academic Press.
Barcellos-Hoff MH. (1996) Latency and activation in the control of TGF-beta. *J Mammary Gland Biol Neoplasia* **1**(4): 353-63.
Beck L, Jr. & D'Amore PA. (1997) Vascular development: cellular and molecular regulation. *Faseb J* **11**(5): 365-73.

Beebe D, Garcia C, Wang X, Rajagopal R, Feldmeier M, Kim JY, Chytil A, Moses H, Ashery-Padan R & Rauchman M. (2004) Contributions by members of the TGFbeta superfamily to lens development. *Int J Dev Biol* **48**(8-9): 845-56.

Behzadian MA, Wang XL, Al-Shabrawey M & Caldwell RB. (1998) Effects of hypoxia on glial cell expression of angiogenesis-regulating factors VEGF and TGF-beta. *Glia* **24**(2): 216-25.

Behzadian MA, Wang XL, Jiang B & Caldwell RB. (1995) Angiostatic role of astrocytes: suppression of vascular endothelial cell growth by TGF-beta and other inhibitory factor(s). *Glia* **15**(4): 480-90.

Behzadian MA, Wang XL, Windsor LJ, Ghaly N & Caldwell RB. (2001) TGF-beta increases retinal endothelial cell permeability by increasing MMP-9: possible role of glial cells in endothelial barrier function. *Invest Ophthalmol Vis Sci* **42**(3): 853-9.

Bensaid M, Malecaze F, Bayard F & Tauber JP. (1989) Opposing effects of basic fibroblast growth factor and transforming growth factor-beta on the proliferation of cultured bovine retinal capillary endothelial (BREC) cells. *Exp Eye Res* **48**(6): 791-9.

Bernstein MH & Hollenberg MJ. (1965) Fine structure of the choriocappillaris and retinal capillaries. *Invest Ophthalmol* **4**(6): 1016-25.

Bloodworth JM, Jr. & Molitor DL. (1965) Ultrastructural aspects of human and canine diabetic retinopathy. *Invest Ophthalmol* **4**(6): 1037-48.

Bok D. (1985) Retinal photoreceptor-pigment epithelium interactions. Friedenwald lecture. *Invest Ophthalmol Vis Sci* **26**(12): 1659-94.

Bottner M, Krieglstein K & Unsicker K. (2000) The transforming growth factor-betas: structure, signaling, and roles in nervous system development and functions. *J Neurochem* **75**(6): 2227-40.

Bottner M, Unsicker K & Suter-Crazzolara C. (1996) Expression of TGF-beta type II receptor mRNA in the CNS. *Neuroreport* **7**(18): 2903-7.

Boycott BB & Wassle H. (1974) The morphological types of ganglion cells of the domestic cat's retina. *J Physiol* **240**(2): 397-419.

Boycott BB & Wassle H. (1991) Morphological Classification of Bipolar Cells of the Primate Retina. *Eur J Neurosci* **3**(11): 1069-88.

Braekevelt CR & Hollenberg MJ. (1970) Comparative electron microscopic study of development of hyaloid and retinal capillaries in albino rats. *Am J Ophthalmol* **69**(6): 1032-46.

Breier G, Albrecht U, Sterrer S & Risau W. (1992) Expression of vascular endothelial growth factor during embryonic angiogenesis and endothelial cell differentiation. *Development* **114**(2): 521-32.

Brionne TC, Tesseur I, Masliah E & Wyss-Coray T. (2003) Loss of TGF-beta 1 leads to increased neuronal cell death and microgliosis in mouse brain. *Neuron* **40**(6): 1133-45.

Bron AJ, Tripathi, R.C., Tripathi, B.J. (1997) *Wolff's Anatomy of the Eye and Orbit.* London: Chapman and Hall.

Brown CB, Boyer AS, Runyan RB & Barnett JV. (1999) Requirement of type III TGF-beta receptor for endocardial cell transformation in the heart. *Science* **283**(5410): 2080-2.

Bruno V, Battaglia G, Casabona G, Copani A, Caciagli F & Nicoletti F. (1998) Neuroprotection by glial metabotropic glutamate receptors is mediated by transforming growth factor-beta. *J Neurosci* **18**(23): 9594-600.

Buenemann CL, Willy C, Buchmann A, Schmiechen A & Schwarz M. (2001) Transforming growth factor-beta1-induced Smad signaling, cell-cycle arrest and apoptosis in hepatoma cells. *Carcinogenesis* **22**(3): 447-52.

Buisson A, Nicole O, Docagne F, Sartelet H, Mackenzie ET & Vivien D. (1998) Up-regulation of a serine protease inhibitor in astrocytes mediates the neuroprotective activity of transforming growth factor beta1. *Faseb J* **12**(15): 1683-91.

Bumsted K & Hendrickson A. (1999) Distribution and development of short-wavelength cones differ between Macaca monkey and human fovea. *J Comp Neurol* **403**(4): 502-16.

Bumsted K, Jasoni C, Szel A & Hendrickson A. (1997) Spatial and temporal expression of cone opsins during monkey retinal development. *J Comp Neurol* **378**(1): 117-34.

Buttery RG, Hinrichsen CF, Weller WL & Haight JR. (1991) How thick should a retina be? A comparative study of mammalian species with and without intraretinal vasculature. *Vision Res* **31**(2): 169-87.

Calvaruso G, Gerbino E, Lauricella M & Tesoriere G. (1997) The effects of TGF-beta1 on chick embryo retina development in vitro. *Int J Dev Neurosci* **15**(8): 973-81.

Campochiaro PA. (2000) Retinal and choroidal neovascularization. *J Cell Physiol* **184**(3): 301-10.

Carri NG. (2003) Multiple neurotrophic signalling: certain TGF molecules are involved in retinal development and maturation, but do they complement one another's actions? *Cell Biol Int* **27**(12): 1033-6.

Chan-Ling T, McLeod DS, Hughes S, Baxter L, Chu Y, Hasegawa T & Lutty GA. (2004) Astrocyte-endothelial cell relationships during human retinal vascular development. *Invest Ophthalmol Vis Sci* **45**(6): 2020-32.

Chan-Ling T & Stone J. (1991) Factors determining the migration of astrocytes into the developing retina: migration does not depend on intact axons or patent vessels. *J Comp Neurol* **303**(3): 375-86.

Chan-Ling TL, Halasz P & Stone J. (1990) Development of retinal vasculature in the cat: processes and mechanisms. *Curr Eye Res* **9**(5): 459-78.

Chase J. (1982) The evolution of retinal vascularization in mammals. A comparison of vascular and avascular retinae. *Ophthalmology* **89**(12): 1518-25.

Checchin D, Sennlaub F, Levavasseur E, Leduc M & Chemtob S. (2006) Potential role of microglia in retinal blood vessel formation. *Invest Ophthalmol Vis Sci* **47**(8): 3595-602.

Cheifetz S, Andres JL & Massague J. (1988) The transforming growth factor-beta receptor type III is a membrane proteoglycan. Domain structure of the receptor. *J Biol Chem* **263**(32): 16984-91.

Chen X, Rubock MJ & Whitman M. (1996) A transcriptional partner for MAD proteins in TGF-beta signalling. *Nature* **383**(6602): 691-6.

Choi ME & Ballermann BJ. (1995) Inhibition of capillary morphogenesis and associated apoptosis by dominant negative mutant transforming growth factor-beta receptors. *J Biol Chem* **270**(36): 21144-50.

Clark DA & Coker R. (1998) Transforming growth factor-beta (TGF-beta). *Int J Biochem Cell Biol* **30**(3): 293-8.

Close JL, Gumuscu B & Reh TA. (2005) Retinal neurons regulate proliferation of postnatal progenitors and Muller glia in the rat retina via TGF beta signaling. *Development* **132**(13): 3015-26.

Combs SE, Krieglstein K & Unsicker K. (2000) Reduction of endogenous TGF-beta increases proliferation of developing adrenal chromaffin cells in vivo. *J Neurosci Res* **59**(3): 379-83.

Connor TB, Jr., Roberts AB, Sporn MB, Danielpour D, Dart LL, Michels RG, de Bustros S, Enger C, Kato H, Lansing M & et al. (1989) Correlation of fibrosis and transforming growth factor-beta type 2 levels in the eye. *J Clin Invest* **83**(5): 1661-6.

Constam DB, Philipp J, Malipiero UV, ten Dijke P, Schachner M & Fontana A. (1992) Differential expression of transforming growth factor-beta 1, -beta 2, and -beta 3 by glioblastoma cells, astrocytes, and microglia. *J Immunol* **148**(5): 1404-10.

Constam DB, Schmid P, Aguzzi A, Schachner M & Fontana A. (1994) Transient production of TGF-beta 2 by postnatal cerebellar neurons and its effect on neuroblast proliferation. *Eur J Neurosci* **6**(5): 766-78.

Cordeiro MF, Reichel MB, Gay JA, D'Esposita F, Alexander RA & Khaw PT. (1999) Transforming growth factor-beta1, -beta2, and -beta3 in vivo: effects on normal and mitomycin C-modulated conjunctival scarring. *Invest Ophthalmol Vis Sci* **40**(9): 1975-82.

Cornish EE, Hendrickson AE & Provis JM. (2004a) Distribution of short-wavelength-sensitive cones in human fetal and postnatal retina: early development of spatial order and density profiles. *Vision Res* **44**(17): 2019-26.

Cornish EE, Madigan MC, Natoli R, Hales A, Hendrickson AE & Provis JM. (2005) Gradients of cone differentiation and FGF expression during development of the foveal depression in macaque retina. *Vis Neurosci* **22**(4): 447-59.

Cornish EE, Natoli RC, Hendrickson A & Provis JM. (2004b) Differential distribution of fibroblast growth factor receptors (FGFRs) on foveal cones: FGFR-4 is an early marker of cone photoreceptors. *Mol Vis* **10**: 1-14.

Cornish EE, Xiao M, Yang Z, Provis JM & Hendrickson AE. (2004c) The role of opsin expression and apoptosis in determination of cone types in human retina. *Exp Eye Res* **78**(6): 1143-54.

Cousins SW, McCabe MM, Danielpour D & Streilein JW. (1991) Identification of transforming growth factor-beta as an immunosuppressive factor in aqueous humor. *Invest Ophthalmol Vis Sci* **32**(8): 2201-11.

Cox DA. (1995) Transforming growth factor-beta 3. *Cell Biol Int* **19**(5): 357-71.

Crooks J & Kolb H. (1992) Localization of GABA, glycine, glutamate and tyrosine hydroxylase in the human retina. *J Comp Neurol* **315**(3): 287-302.

Crooks J, Okada M & Hendrickson AE. (1995) Quantitative analysis of synaptogenesis in the inner plexiform layer of macaque monkey fovea. *J Comp Neurol* **360**(2): 349-62.

Curcio CA, Sloan KR, Kalina RE, Hendrickson AE (1990) Human photoreceptor topography. *J Comp Neurol* **292**(4): 497-523.

Csaky KG, Baffi JZ, Byrnes GA, Wolfe JD, Hilmer SC, Flippin J & Cousins SW. (2004) Recruitment of marrow-derived endothelial cells to experimental choroidal neovascularization by local expression of vascular endothelial growth factor. *Exp Eye Res* **78**(6): 1107-16.

D'Amore PA. (1994) Mechanisms of retinal and choroidal neovascularization. *Invest Ophthalmol Vis Sci* **35**(12): 3974-9.

da Cunha A, Jefferson JA, Jackson RW & Vitkovic L. (1993) Glial cell-specific mechanisms of TGF-beta 1 induction by IL-1 in cerebral cortex. *J Neuroimmunol* **42**(1): 71-85.

Dacey DM. (1996) Circuitry for color coding in the primate retina. *Proc Natl Acad Sci U S A* **93**(2): 582-8.

Dacey DM, Lee BB, Stafford DK, Pokorny J & Smith VC. (1996) Horizontal cells of the primate retina: cone specificity without spectral opponency. *Science* **271**(5249): 656-9.

Damert A, Machein M, Breier G, Fujita MQ, Hanahan D, Risau W & Plate KH. (1997) Up-regulation of vascular endothelial growth factor expression in a rat glioma is conferred by two distinct hypoxia-driven mechanisms. *Cancer Res* **57**(17): 3860-4.

Das A & McGuire PG. (2003) Retinal and choroidal angiogenesis: pathophysiology and strategies for inhibition. *Prog Retin Eye Res* **22**(6): 721-48.

Dawson DW, Volpert OV, Gillis P, Crawford SE, Xu H, Benedict W & Bouck NP. (1999) Pigment epithelium-derived factor: a potent inhibitor of angiogenesis. *Science* **285**(5425): 245-8.

de Caestecker M. (2004) The transforming growth factor-beta superfamily of receptors. *Cytokine Growth Factor Rev* **15**(1): 1-11.

de Caestecker MP, Yahata T, Wang D, Parks WT, Huang S, Hill CS, Shioda T, Roberts AB & Lechleider RJ. (2000) The Smad4 activation domain (SAD) is a proline-rich, p300-dependent transcriptional activation domain. *J Biol Chem* **275**(3): 2115-22.

de Iongh RU, Lovicu FJ, Overbeek PA, Schneider MD, Joya J, Hardeman ED & McAvoy JW. (2001) Requirement for TGFbeta receptor signaling during terminal lens fiber differentiation. *Development* **128**(20): 3995-4010.
de Iongh RU, Wederell E, Lovicu FJ & McAvoy JW. (2005) Transforming growth factor-beta-induced epithelial-mesenchymal transition in the lens: a model for cataract formation. *Cells Tissues Organs* **179**(1-2): 43-55.
de Luca A, Weller M & Fontana A. (1996) TGF-beta-induced apoptosis of cerebellar granule neurons is prevented by depolarization. *J Neurosci* **16**(13): 4174-85.
de Sampaio e Spohr TC, Martinez R, da Silva EF, Neto VM & Gomes FC. (2002) Neuro-glia interaction effects on GFAP gene: a novel role for transforming growth factor-beta1. *Eur J Neurosci* **16**(11): 2059-69.
Dennler S, Goumans MJ & ten Dijke P. (2002) Transforming growth factor beta signal transduction. *J Leukoc Biol* **71**(5): 731-40.
Derynck R, Zhang Y & Feng XH. (1998) Smads: transcriptional activators of TGF-beta responses. *Cell* **95**(6): 737-40.
Diaz-Araya C & Provis JM. (1992) Evidence of photoreceptor migration during early foveal development: a quantitative analysis of human fetal retinae. *Vis Neurosci* **8**(6): 505-14.
Diaz-Araya CM, Provis JM, Penfold PL & Billson FA. (1995) Development of microglial topography in human retina. *J Comp Neurol* **363**(1): 53-68.
Diaz CM, Macnab LT, Williams SM, Sullivan RK & Pow DV. (2007) EAAT1 and D-serine expression are early features of human retinal development. *Exp Eye Res* **84**(5): 876-85.
Dickson MC, Martin JS, Cousins FM, Kulkarni AB, Karlsson S & Akhurst RJ. (1995) Defective haematopoiesis and vasculogenesis in transforming growth factor-beta 1 knock out mice. *Development* **121**(6): 1845-54.
Dieudonne SC, La Heij EC, Diederen R, Kessels AG, Liem AT, Kijlstra A & Hendrikse F. (2004) High TGF-beta2 levels during primary retinal detachment may protect against proliferative vitreoretinopathy. *Invest Ophthalmol Vis Sci* **45**(11): 4113-8.
Distler C & Kirby MA. (1996) Transience of astrocytes in the newborn macaque monkey retina. *Eur J Neurosci* **8**(4): 847-51.
Distler C, Kopatz K & Telkes I. (2000) Developmental changes in astrocyte density in the macaque perifoveal region. *Eur J Neurosci* **12**(4): 1331-41.
Distler C, Weigel H & Hoffmann KP. (1993) Glia cells of the monkey retina. I. Astrocytes. *J Comp Neurol* **333**(1): 134-47.
Dobbertin A, Schmid P, Gelman M, Glowinski J & Mallat M. (1997) Neurons promote macrophage proliferation by producing transforming growth factor-beta2. *J Neurosci* **17**(14): 5305-15.
Docagne F, Nicole O, Gabriel C, Fernandez-Monreal M, Lesne S, Ali C, Plawinski L, Carmeliet P, MacKenzie ET, Buisson A & Vivien D. (2002) Smad3-dependent induction of plasminogen activator inhibitor-1 in astrocytes mediates neuroprotective activity of transforming growth factor-beta 1 against NMDA-induced necrosis. *Mol Cell Neurosci* **21**(4): 634-44.
Docagne F, Nicole O, Marti HH, MacKenzie ET, Buisson A & Vivien D. (1999) Transforming growth factor-beta1 as a regulator of the serpins/t-PA axis in cerebral ischemia. *Faseb J* **13**(11): 1315-24.
Doetsch F, Petreanu L, Caille I, Garcia-Verdugo JM & Alvarez-Buylla A. (2002) EGF converts transit-amplifying neurogenic precursors in the adult brain into multipotent stem cells. *Neuron* **36**(6): 1021-34.
Dong G, Schulick AH, DeYoung MB & Dichek DA. (1996) Identification of a cis-acting sequence in the human plasminogen activator inhibitor type-1 gene that mediates transforming growth factor-beta1 responsiveness in endothelium in vivo. *J Biol Chem* **271**(47): 29969-77.
Dorn EM, Hendrickson L & Hendrickson AE. (1995) The appearance of rod opsin during monkey retinal development. *Invest Ophthalmol Vis Sci* **36**(13): 2634-51.

Dorrell MI, Aguilar E & Friedlander M. (2002) Retinal vascular development is mediated by endothelial filopodia, a preexisting astrocytic template and specific R-cadherin adhesion. *Invest Ophthalmol Vis Sci* **43**(11): 3500-10.

Dreher B & Robinson SR. (1988) Development of the retinofugal pathway in birds and mammals: evidence for a common 'timetable'. *Brain Behav Evol* **31**(6): 369-90.

Duenker N. (2005) Transforming growth factor-beta (TGF-beta) and programmed cell death in the vertebrate retina. *Int Rev Cytol* **245**: 17-43.

Duenker N, Valenciano AI, Franke A, Hernandez-Sanchez C, Dressel R, Behrendt M, De Pablo F, Krieglstein K & de la Rosa EJ. (2005) Balance of pro-apoptotic transforming growth factor-beta and anti-apoptotic insulin effects in the control of cell death in the postnatal mouse retina. *Eur J Neurosci* **22**(1): 28-38.

Duh EJ, Yang HS, Suzuma I, Miyagi M, Youngman E, Mori K, Katai M, Yan L, Suzuma K, West K, Davarya S, Tong P, Gehlbach P, Pearlman J, Crabb JW, Aiello LP, Campochiaro PA & Zack DJ. (2002) Pigment epithelium-derived factor suppresses ischemia-induced retinal neovascularization and VEGF-induced migration and growth. *Invest Ophthalmol Vis Sci* **43**(3): 821-9.

Duke-Elder S, Cook, C. (1963) *System of Ophthalmology.* London: Kimpton.

Dunker N & Krieglstein K. (2000) Targeted mutations of transforming growth factor-beta genes reveal important roles in mouse development and adult homeostasis. *Eur J Biochem* **267**(24): 6982-8.

Dunker N & Krieglstein K. (2003) Reduced programmed cell death in the retina and defects in lens and cornea of Tgfbeta2(-/-) Tgfbeta3(-/-) double-deficient mice. *Cell Tissue Res* **313**(1): 1-10.

Dunker N, Schuster N & Krieglstein K. (2001) TGF-beta modulates programmed cell death in the retina of the developing chick embryo. *Development* **128**(11): 1933-42.

Dvorak HF, Brown LF, Detmar M & Dvorak AM. (1995) Vascular permeability factor/vascular endothelial growth factor, microvascular hyperpermeability, and angiogenesis. *Am J Pathol* **146**(5): 1029-39.

Edwards DR, Murphy G, Reynolds JJ, Whitham SE, Docherty AJ, Angel P & Heath JK. (1987) Transforming growth factor beta modulates the expression of collagenase and metalloproteinase inhibitor. *Embo J* **6**(7): 1899-904.

Eichler W, Kuhrt H, Hoffmann S, Wiedemann P & Reichenbach A. (2000) VEGF release by retinal glia depends on both oxygen and glucose supply. *Neuroreport* **11**(16): 3533-7.

Eichler W, Yafai Y, Kuhrt H, Grater R, Hoffmann S, Wiedemann P & Reichenbach A. (2001) Hypoxia: modulation of endothelial cell proliferation by soluble factors released by retinal cells. *Neuroreport* **12**(18): 4103-8.

Eichler W, Yafai Y, Wiedemann P & Reichenbach A. (2004) Angiogenesis-related factors derived from retinal glial (Muller) cells in hypoxia. *Neuroreport* **15**(10): 1633-7.

Engerman RL. (1976) Development of the macular circulation. *Invest Ophthalmol* **15**(10): 835-40.

Esteve P & Bovolenta P. (2005) Secreted inducers in vertebrate eye development: more functions for old morphogens. *Current Opinion in Neurobiology* **16**: 1-7.

Etchevers HC, Vincent C, Le Douarin NM & Couly GF. (2001) The cephalic neural crest provides pericytes and smooth muscle cells to all blood vessels of the face and forebrain. *Development* **128**(7): 1059-68.

Fajardo LF, Prionas SD, Kwan HH, Kowalski J & Allison AC. (1996) Transforming growth factor beta1 induces angiogenesis in vivo with a threshold pattern. *Lab Invest* **74**(3): 600-8.

Fallon JH, Seroogy KB, Loughlin SE, Morrison RS, Bradshaw RA, Knaver DJ & Cunningham DD. (1984) Epidermal growth factor immunoreactive material in the central nervous system: location and development. *Science* **224**(4653): 1107-9.

Fariss RN, Li ZY & Milam AH. (2000) Abnormalities in rod photoreceptors, amacrine cells, and horizontal cells in human retinas with retinitis pigmentosa. *Am J Ophthalmol* **129**(2): 215-23.

Farkas LM, Dunker N, Roussa E, Unsicker K & Krieglstein K. (2003) Transforming growth factor-beta(s) are essential for the development of midbrain dopaminergic neurons in vitro and in vivo. *J Neurosci* **23**(12): 5178-86.

Feeney L. (1973) Synthesis of interphotoreceptor matrix. I. Autoradiography of 3H-fucose incorporation. *Invest Ophthalmol* **12**(10): 739-51.

Flanders KC, Ludecke G, Engels S, Cissel DS, Roberts AB, Kondaiah P, Lafyatis R, Sporn MB & Unsicker K. (1991) Localization and actions of transforming growth factor-beta s in the embryonic nervous system. *Development* **113**(1): 183-91.

Flanders KC, Ren RF & Lippa CF. (1998) Transforming growth factor-betas in neurodegenerative disease. *Prog Neurobiol* **54**(1): 71-85.

Flaumenhaft R, Abe M, Mignatti P & Rifkin DB. (1992) Basic fibroblast growth factor-induced activation of latent transforming growth factor beta in endothelial cells: regulation of plasminogen activator activity. *J Cell Biol* **118**(4): 901-9.

Fok-Seang J, DiProspero NA, Meiners S, Muir E & Fawcett JW. (1998) Cytokine-induced changes in the ability of astrocytes to support migration of oligodendrocyte precursors and axon growth. *Eur J Neurosci* **10**(7): 2400-15.

Fong GH, Rossant J, Gertsenstein M & Breitman ML. (1995) Role of the Flt-1 receptor tyrosine kinase in regulating the assembly of vascular endothelium. *Nature* **376**(6535): 66-70.

Frade JM & Barde YA. (1999) Genetic evidence for cell death mediated by nerve growth factor and the neurotrophin receptor p75 in the developing mouse retina and spinal cord. *Development* **126**(4): 683-90.

Francois J, Rabaey M & Lagasse A. (1963) Electron Microscopic Observations on Choroid, Pigment Epithelium and Pecten of the Developing Chick in Relation to Melanin Synthesis. *Ophthalmologica* **146**: 415-31.

Frank JM, Kaneko S, Joels C, Tobin GR, Banis JC, Jr. & Barker JH. (1994) Microcirculation research, angiogenesis, and microsurgery. *Microsurgery* **15**(6): 399-404.

Franzen P, Heldin CH & Miyazono K. (1995) The GS domain of the transforming growth factor-beta type I receptor is important in signal transduction. *Biochem Biophys Res Commun* **207**(2): 682-9.

Fruttiger M. (2002) Development of the mouse retinal vasculature: angiogenesis versus vasculogenesis. *Invest Ophthalmol Vis Sci* **43**(2): 522-7.

Fruttiger M, Calver AR, Kruger WH, Mudhar HS, Michalovich D, Takakura N, Nishikawa S & Richardson WD. (1996) PDGF mediates a neuron-astrocyte interaction in the developing retina. *Neuron* **17**(6): 1117-31.

Fryczkowski AW & Sherman MD. (1988) Scanning electron microscopy of human ocular vascular casts: the submacular choriocapillaris. *Acta Anat (Basel)* **132**(4): 265-9.

Fryczkowski AW, Sherman MD & Walker J. (1991) Observations on the lobular organization of the human choriocapillaris. *Int Ophthalmol* **15**(2): 109-20.

Fukuchi T, Ueda J, Hanyu T, Abe H & Sawaguchi S. (2001) Distribution and expression of transforming growth factor-beta and platelet-derived growth factor in the normal and glaucomatous monkey optic nerve heads. *Jpn J Ophthalmol* **45**(6): 592-9.

Gagelin C, Pierre M, Gavaret JM & Toru-Delbauffe D. (1995) Rapid TGF beta 1 effects on actin cytoskeleton of astrocytes: comparison with other factors and implications for cell motility. *Glia* **13**(4): 283-93.

Gajdusek CM, Luo Z & Mayberg MR. (1993) Basic fibroblast growth factor and transforming growth factor beta-1: synergistic mediators of angiogenesis in vitro. *J Cell Physiol* **157**(1): 133-44.

Gallo V & Bertolotto A. (1990) Extracellular matrix of cultured glial cells: selective expression of chondroitin 4-sulfate by type-2 astrocytes and their progenitors. *Exp Cell Res* **187**(2): 211-23.
Galter D, Bottner M & Unsicker K. (1999) Developmental regulation of the serotonergic transmitter phenotype in rostral and caudal raphe neurons by transforming growth factor-betas. *J Neurosci Res* **56**(5): 531-8.
Garcia CM, Darland DC, Massingham LJ & D'Amore PA. (2004) Endothelial cell-astrocyte interactions and TGF beta are required for induction of blood-neural barrier properties. *Brain Res Dev Brain Res* **152**(1): 25-38.
Gariano RF. (2003) Cellular mechanisms in retinal vascular development. *Prog Retin Eye Res* **22**(3): 295-306.
Gariano RF, Iruela-Arispe ML & Hendrickson AE. (1994) Vascular development in primate retina: comparison of laminar plexus formation in monkey and human. *Invest Ophthalmol Vis Sci* **35**(9): 3442-55.
Gariano RF, Sage EH, Kaplan HJ & Hendrickson AE. (1996) Development of astrocytes and their relation to blood vessels in fetal monkey retina. *Invest Ophthalmol Vis Sci* **37**(12): 2367-75.
Geisen P, McColm JR & Hartnett ME. (2006) Choroidal endothelial cells transmigrate across the retinal pigment epithelium but do not proliferate in response to soluble vascular endothelial growth factor. *Exp Eye Res* **82**(4): 608-19.
Georges P, Cornish EE, Provis JM & Madigan MC. (2006) Muller cell expression of glutamate cycle related proteins and anti-apoptotic proteins in early human retinal development. *Br J Ophthalmol* **90**(2): 223-8.
Georges P, Madigan MC & Provis JM. (1999) Apoptosis during development of the human retina: relationship to foveal development and retinal synaptogenesis. *J Comp Neurol* **413**(2): 198-208.
Gerhardt H, Golding M, Fruttiger M, Ruhrberg C, Lundkvist A, Abramsson A, Jeltsch M, Mitchell C, Alitalo K, Shima D & Betsholtz C. (2003) VEGF guides angiogenic sprouting utilizing endothelial tip cell filopodia. *J Cell Biol* **161**(6): 1163-77.
Girard MT, Matsubara M & Fini ME. (1991) Transforming growth factor-beta and interleukin-1 modulate metalloproteinase expression by corneal stromal cells. *Invest Ophthalmol Vis Sci* **32**(9): 2441-54.
Giri SN, Hyde DM & Hollinger MA. (1993) Effect of antibody to transforming growth factor beta on bleomycin induced accumulation of lung collagen in mice. *Thorax* **48**(10): 959-66.
Giulian D & Lachman LB. (1985) Interleukin-1 stimulation of astroglial proliferation after brain injury. *Science* **228**(4698): 497-9.
Giulian D, Young DG, Woodward J, Brown DC & Lachman LB. (1988) Interleukin-1 is an astroglial growth factor in the developing brain. *J Neurosci* **8**(2): 709-14.
Gleizes PE, Beavis RC, Mazzieri R, Shen B & Rifkin DB. (1996) Identification and characterization of an eight-cysteine repeat of the latent transforming growth factor-beta binding protein-1 that mediates bonding to the latent transforming growth factor-beta1. *J Biol Chem* **271**(47): 29891-6.
Globus RK, Patterson-Buckendahl P & Gospodarowicz D. (1988) Regulation of bovine bone cell proliferation by fibroblast growth factor and transforming growth factor beta. *Endocrinology* **123**(1): 98-105.
Gogat K, Le Gat L, Van Den Berghe L, Marchant D, Kobetz A, Gadin S, Gasser B, Quere I, Abitbol M & Menasche M. (2004) VEGF and KDR gene expression during human embryonic and fetal eye development. *Invest Ophthalmol Vis Sci* **45**(1): 7-14.
Gold LI. (1999) The role for transforming growth factor-beta (TGF-beta) in human cancer. *Crit Rev Oncog* **10**(4): 303-60.
Golz S, Muhleisen T, Schulte D, Mey J. (2008) Regulation of RALDH-1, RALDH-3 and CYP26A1 by transcription factors cVax/Vax2 and Tbx5 in the embryonic chick retina. *Int J Dev Neurosci* **26**(5): 435-45.

Gomes FC, Sousa Vde O & Romao L. (2005) Emerging roles for TGF-beta1 in nervous system development. *Int J Dev Neurosci* **23**(5): 413-24.
Gordon-Thomson C, de Iongh RU, Hales AM, Chamberlain CG & McAvoy JW. (1998) Differential cataractogenic potency of TGF-beta1, -beta2, and -beta3 and their expression in the postnatal rat eye. *Invest Ophthalmol Vis Sci* **39**(8): 1399-409.
Gottanka J, Chan D, Eichhorn M, Lutjen-Drecoll E & Ethier CR. (2004) Effects of TGF-beta2 in perfused human eyes. *Invest Ophthalmol Vis Sci* **45**(1): 153-8.
Goumans MJ, Valdimarsdottir G, Itoh S, Rosendahl A, Sideras P & ten Dijke P. (2002) Balancing the activation state of the endothelium via two distinct TGF-beta type I receptors. *Embo J* **21**(7): 1743-53.
Govinden R & Bhoola KD. (2003) Genealogy, expression, and cellular function of transforming growth factor-beta. *Pharmacol Ther* **98**(2): 257-65.
Grant MB, Khaw PT, Schultz GS, Adams JL & Shimizu RW. (1992) Effects of epidermal growth factor, fibroblast growth factor, and transforming growth factor-beta on corneal cell chemotaxis. *Invest Ophthalmol Vis Sci* **33**(12): 3292-301.
Gualandris A, Annes JP, Arese M, Noguera I, Jurukovski V & Rifkin DB. (2000) The latent transforming growth factor-beta-binding protein-1 promotes in vitro differentiation of embryonic stem cells into endothelium. *Mol Biol Cell* **11**(12): 4295-308.
Guerin CJ, Hu L, Scicli G & Scicli AG. (2001) Transforming growth factor beta in experimentally detached retina and periretinal membranes. *Exp Eye Res* **73**(6): 753-64.
Hageman GS, Kirchoff-Rempe MA, Lewis GP, Fisher SK & Anderson DH. (1991) Sequestration of basic fibroblast growth factor in the primate retinal interphotoreceptor matrix. *Proc Natl Acad Sci U S A* **88**(15): 6706-10.
Hales AM, Chamberlain CG, Dreher B & McAvoy JW. (1999) Intravitreal injection of TGFbeta induces cataract in rats. *Invest Ophthalmol Vis Sci* **40**(13): 3231-6.
Hales AM, Chamberlain CG & McAvoy JW. (1995) Cataract induction in lenses cultured with transforming growth factor-beta. *Invest Ophthalmol Vis Sci* **36**(8): 1709-13.
Harman AM & Ferguson J. (1994) Morphology and birth dates of horizontal cells in the retina of a marsupial. *J Comp Neurol* **340**(3): 392-404.
Harman AM, Snell LL & Beazley LD. (1989) Cell death in the inner and outer nuclear layers of the developing retina in the wallaby Setonix brachyurus (quokka). *J Comp Neurol* **289**(1): 1-10.
Hart PJ, Deep S, Taylor AB, Shu Z, Hinck CS & Hinck AP. (2002) Crystal structure of the human TbetaR2 ectodomain--TGF-beta3 complex. *Nat Struct Biol* **9**(3): 203-8.
Hasegawa T, McLeod DS, Bhutto IA, Prow T, Merges CA, Grebe R & Lutty GA. (2007) The embryonic human choriocapillaris develops by hemo-vasculogenesis. *Dev Dyn* **236**(8): 2089-100.
Hata A, Shi Y & Massague J. (1998) TGF-beta signaling and cancer: structural and functional consequences of mutations in Smads. *Mol Med Today* **4**(6): 257-62.
Hayashi K, Frangieh G, Wolf G & Kenyon KR. (1989) Expression of transforming growth factor-beta in wound healing of vitamin A-deficient rat corneas. *Invest Ophthalmol Vis Sci* **30**(2): 239-47.
Hayreh SS. (1974) Submacular choroidal vascular pattern. *Graefes Arch Clin Exp Ophthalmol* **192**: 165-79.
Heimann K. (1972) The development of the choroid in man. *Ophthalmic Research* **3**: 257-73.
Heine U, Munoz EF, Flanders KC, Ellingsworth LR, Lam HY, Thompson NL, Roberts AB & Sporn MB. (1987) Role of transforming growth factor-beta in the development of the mouse embryo. *J Cell Biol* **105**(6 Pt 2): 2861-76.

Helbig H, Kittredge KL, Coca-Prados M, Davis J, Palestine AG & Nussenblatt RB. (1991) Mammalian ciliary-body epithelial cells in culture produce transforming growth factor-beta. *Graefes Arch Clin Exp Ophthalmol* **229**(1): 84-7.

Heldin CH, Miyazono K & ten Dijke P. (1997) TGF-beta signalling from cell membrane to nucleus through SMAD proteins. *Nature* **390**(6659): 465-71.

Hendrickson AE. (1994) Primate foveal development: a microcosm of current questions in neurobiology. *Invest Ophthalmol Vis Sci* **35**(8): 3129-33.

Hendrickson AE. (1996) Synaptic development in macaque monkey retina and its implications for other developmental sequences. *Perspect Dev Neurobiol* **3**(3): 195-201.

Hendrickson AE & Yuodelis C. (1984) The morphological development of the human fovea. *Ophthalmology* **91**(6): 603-12.

Hill CS. (1999) The Smads. *Int J Biochem Cell Biol* **31**(11): 1249-54.

Hiscott PS, Grierson I & McLeod D. (1985) Natural history of fibrocellular epiretinal membranes: a quantitative, autoradiographic, and immunohistochemical study. *Br J Ophthalmol* **69**(11): 810-23.

Ho M, Yang E, Matcuk G, Deng D, Sampas N, Tsalenko A, Tabibiazar R, Zhang Y, Chen M, Talbi S, Ho YD, Wang J, Tsao P, Ben-Dor A, Yakhini Z, Bruhn L & Quertermous T. (2003) Identification of endothelial cell genes by combined database mining and microarray analysis. *Physiol Genomics* **13**: 249-62.

Hogan MJ, Alvarado, J.A., Weddell, J.E. (1971) *Histology of the Human Eye.* Philadelphia: WB Saunders.

Hogg N, Browning J, Howard T, Winterford C, Fitzpatrick D & Gobe G. (1999) Apoptosis in vascular endothelial cells caused by serum deprivation, oxidative stress and transforming growth factor-beta. *Endothelium* **7**(1): 35-49.

Hollyfield JG, Fliesler SJ, Rayborn ME & Bridges CD. (1985) Rod photoreceptors in the human retina synthesize and secrete interstitial retinol-binding protein. *Prog Clin Biol Res* **190**: 141-9.

Honma Y, Nishida K, Sotozono C & Kinoshita S. (1997) Effect of transforming growth factor-beta1 and -beta2 on in vitro rabbit corneal epithelial cell proliferation promoted by epidermal growth factor, keratinocyte growth factor, or hepatocyte growth factor. *Exp Eye Res* **65**(3): 391-6.

Hu DN, McCormick SA, Lin AY & Lin JY. (1998) TGF-beta2 inhibits growth of uveal melanocytes at physiological concentrations. *Exp Eye Res* **67**(2): 143-50.

Huff KR & Schreier W. (1989) Fibroblast growth factor pretreatment reduces epidermal growth factor-induced proliferation in rat astrocytes. *Life Sci* **45**(17): 1515-20.

Huff KR & Schreier W. (1990) Fibroblast growth factor inhibits epidermal growth factor-induced responses in rat astrocytes. *Glia* **3**(3): 193-204.

Hunter KE, Sporn MB & Davies AM. (1993) Transforming growth factor-betas inhibit mitogen-stimulated proliferation of astrocytes. *Glia* **7**(3): 203-11.

Hutchings H, Maitre-Boube M, Tombran-Tink J & Plouet J. (2002) Pigment epithelium-derived factor exerts opposite effects on endothelial cells of different phenotypes. *Biochem Biophys Res Commun* **294**(4): 764-9.

Huxlin KR, Sefton AJ & Furby JH. (1992) The origin and development of retinal astrocytes in the mouse. *J Neurocytol* **21**(7): 530-44.

Hyman KM, Seghezzi G, Pintucci G, Stellari G, Kim JH, Grossi EA, Galloway AC & Mignatti P. (2002) Transforming growth factor-beta1 induces apoptosis in vascular endothelial cells by activation of mitogen-activated protein kinase. *Surgery* **132**(2): 173-9.

Ignotz RA & Massague J. (1986) Transforming growth factor-beta stimulates the expression of fibronectin and collagen and their incorporation into the extracellular matrix. *J Biol Chem* **261**(9): 4337-45.

Ijichi A, Sakuma S & Tofilon PJ. (1995) Hypoxia-induced vascular endothelial growth factor expression in normal rat astrocyte cultures. *Glia* **14**(2): 87-93.

Ikeda T, Homma Y, Nisida K, Hirase K, Sotozono C, Kinoshita S & Puro DG. (1998) Expression of transforming growth factor-beta s and their receptors by human retinal glial cells. *Curr Eye Res* **17**(5): 546-50.

Ikeda T & Puro DG. (1995) Regulation of retinal glial cell proliferation by antiproliferative molecules. *Exp Eye Res* **60**(4): 435-43.

Ishihara A, Saito H & Abe K. (1994) Transforming growth factor-beta 1 and -beta 2 promote neurite sprouting and elongation of cultured rat hippocampal neurons. *Brain Res* **639**(1): 21-5.

Isner JM, Kalka C, Kawamoto A & Asahara T. (2001) Bone marrow as a source of endothelial cells for natural and iatrogenic vascular repair. *Ann N Y Acad Sci* **953**: 75-84.

Itoh S, Itoh F, Goumans MJ & Ten Dijke P. (2000) Signaling of transforming growth factor-beta family members through Smad proteins. *Eur J Biochem* **267**(24): 6954-67.

Jacobson B, Basu PK & Hasany SM. (1984) Vascular endothelial cell growth inhibitor of normal and pathologic human vitreous. *Arch Ophthalmol* **102**(10): 1543-5.

Jakobiec FA, Ozanics, V. (1982) General topographic anatomy of the eye. *Arch Ophthalmol* **1**: 1.

Jampel HD, Roche N, Stark WJ & Roberts AB. (1990) Transforming growth factor-beta in human aqueous humor. *Curr Eye Res* **9**(10): 963-9.

Javelaud D & Mauviel A. (2004) Mammalian transforming growth factor-betas: Smad signaling and physio-pathological roles. *Int J Biochem Cell Biol* **36**(7): 1161-5.

Jetten AM, Shirley JE & Stoner G. (1986) Regulation of proliferation and differentiation of respiratory tract epithelial cells by TGF beta. *Exp Cell Res* **167**(2): 539-49.

Jhappan C, Geiser AG, Kordon EC, Bagheri D, Hennighausen L, Roberts AB, Smith GH & Merlino G. (1993) Targeting expression of a transforming growth factor beta 1 transgene to the pregnant mammary gland inhibits alveolar development and lactation. *Embo J* **12**(5): 1835-45.

Jiang B, Bezhadian MA & Caldwell RB. (1995) Astrocytes modulate retinal vasculogenesis: effects on endothelial cell differentiation. *Glia* **15**(1): 1-10.

Johns LD, Babcock G, Green D, Freedman M, Sriram S & Ransohoff RM. (1992) Transforming growth factor-beta 1 differentially regulates proliferation and MHC class-II antigen expression in forebrain and brainstem astrocyte primary cultures. *Brain Res* **585**(1-2): 229-36.

Kaartinen V, Cui XM, Heisterkamp N, Groffen J & Shuler CF. (1997) Transforming growth factor-beta3 regulates transdifferentiation of medial edge epithelium during palatal fusion and associated degradation of the basement membrane. *Dev Dyn* **209**(3): 255-60.

Kaartinen V, Voncken JW, Shuler C, Warburton D, Bu D, Heisterkamp N & Groffen J. (1995) Abnormal lung development and cleft palate in mice lacking TGF-beta 3 indicates defects of epithelial-mesenchymal interaction. *Nat Genet* **11**(4): 415-21.

Kalka C, Masuda H, Takahashi T, Gordon R, Tepper O, Gravereaux E, Pieczek A, Iwaguro H, Hayashi SI, Isner JM & Asahara T. (2000a) Vascular endothelial growth factor(165) gene transfer augments circulating endothelial progenitor cells in human subjects. *Circ Res* **86**(12): 1198-202.

Kalka C, Tehrani H, Laudenberg B, Vale PR, Isner JM, Asahara T & Symes JF. (2000b) VEGF gene transfer mobilizes endothelial progenitor cells in patients with inoperable coronary disease. *Ann Thorac Surg* **70**(3): 829-34.

Kane CJ, Hebda PA, Mansbridge JN & Hanawalt PC. (1991) Direct evidence for spatial and temporal regulation of transforming growth factor beta 1 expression during cutaneous wound healing. *J Cell Physiol* **148**(1): 157-73.

Khalil N. (1999) TGF-beta: from latent to active. *Microbes Infect* **1**(15): 1255-63.

Khaliq A, Patel B, Jarvis-Evans J, Moriarty P, McLeod D & Boulton M. (1995) Oxygen modulates production of bFGF and TGF-beta by retinal cells in vitro. *Exp Eye Res* **60**(4): 415-23.
Kim HS, Shang T, Chen Z, Pflugfelder SC & Li DQ. (2004) TGF-beta1 stimulates production of gelatinase (MMP-9), collagenases (MMP-1, -13) and stromelysins (MMP-3, -10, -11) by human corneal epithelial cells. *Exp Eye Res* **79**(2): 263-74.
Kim KJ, Li B, Winer J, Armanini M, Gillett N, Phillips HS & Ferrara N. (1993) Inhibition of vascular endothelial growth factor-induced angiogenesis suppresses tumour growth in vivo. *Nature* **362**(6423): 841-4.
Kingsley DM. (1994) The TGF-beta superfamily: new members, new receptors, and new genetic tests of function in different organisms. *Genes Dev* **8**(2): 133-46.
Kirby MA & Steineke TC. (1996) Morphogenesis of retinal ganglion cells: a model of dendritic, mosaic, and foveal development. *Perspect Dev Neurobiol* **3**(3): 177-94.
Kirschfeld K. (1982) Carotenoid pigments: their possible role in protecting against photooxidation in eyes and photoreceptor cells. *Proc R Soc Lond B Biol Sci* **216**(1202): 71-85.
Knisely TL, Bleicher PA, Vibbard CA & Granstein RD. (1991) Production of latent transforming growth factor-beta and other inhibitory factors by cultured murine iris and ciliary body cells. *Curr Eye Res* **10**(8): 761-71.
Kniss DA & Burry RW. (1988) Serum and fibroblast growth factor stimulate quiescent astrocytes to re-enter the cell cycle. *Brain Res* **439**(1-2): 281-8.
Kokawa N, Sotozono C, Nishida K & Kinoshita S. (1996) High total TGF-beta 2 levels in normal human tears. *Curr Eye Res* **15**(3): 341-3.
Kolb H, Fernandez E, Schouten J, Ahnelt P, Linberg KA & Fisher SK. (1994) Are there three types of horizontal cell in the human retina? *J Comp Neurol* **343**(3): 370-86.
Kolb H, Linberg KA & Fisher SK. (1992) Neurons of the human retina: a Golgi study. *J Comp Neurol* **318**(2): 147-87.
Kolb H, Mariani A & Gallego A. (1980) A second type of horizontal cell in the monkey retina. *J Comp Neurol* **189**(1): 31-44.
Kolb H, Nelson R & Mariani A. (1981) Amacrine cells, bipolar cells and ganglion cells of the cat retina: a Golgi study. *Vision Res* **21**(7): 1081-114.
Koontz MA & Hendrickson AE. (1993) Comparison of immunolocalization patterns for the synaptic vesicle proteins p65 and synapsin I in macaque monkey retina. *Synapse* **14**(4): 268-82.
Krieglstein K, Farkas L & Unsicker K. (1998a) TGF-beta regulates the survival of ciliary ganglionic neurons synergistically with ciliary neurotrophic factor and neurotrophins. *J Neurobiol* **37**(4): 563-72.
Krieglstein K, Henheik P, Farkas L, Jaszai J, Galter D, Krohn K & Unsicker K. (1998b) Glial cell line-derived neurotrophic factor requires transforming growth factor-beta for exerting its full neurotrophic potential on peripheral and CNS neurons. *J Neurosci* **18**(23): 9822-34.
Krieglstein K, Reuss B, Maysinger D & Unsicker K. (1998c) Short communication: transforming growth factor-beta mediates the neurotrophic effect of fibroblast growth factor-2 on midbrain dopaminergic neurons. *Eur J Neurosci* **10**(8): 2746-50.
Krieglstein K, Richter S, Farkas L, Schuster N, Dunker N, Oppenheim RW & Unsicker K. (2000) Reduction of endogenous transforming growth factors beta prevents ontogenetic neuron death. *Nat Neurosci* **3**(11): 1085-90.
Krieglstein K & Unsicker K. (1994) Transforming growth factor-beta promotes survival of midbrain dopaminergic neurons and protects them against N-methyl-4-phenylpyridinium ion toxicity. *Neuroscience* **63**(4): 1189-96.
Labourdette G, Janet T, Laeng P, Perraud F, Lawrence D & Pettmann B. (1990) Transforming growth factor type beta 1 modulates the effects of basic

fibroblast growth factor on growth and phenotypic expression of rat astroblasts in vitro. *J Cell Physiol* **144**(3): 473-84.
Lagna G, Hata A, Hemmati-Brivanlou A & Massague J. (1996) Partnership between DPC4 and SMAD proteins in TGF-beta signalling pathways. *Nature* **383**(6603): 832-6.
Laiho M, Saksela O & Keski-Oja J. (1986) Transforming growth factor beta alters plasminogen activator activity in human skin fibroblasts. *Exp Cell Res* **164**(2): 399-407.
Laping NJ, Morgan TE, Nichols NR, Rozovsky I, Young-Chan CS, Zarow C & Finch CE. (1994) Transforming growth factor-beta 1 induces neuronal and astrocyte genes: tubulin alpha 1, glial fibrillary acidic protein and clusterin. *Neuroscience* **58**(3): 563-72.
Larisch S, Yi Y, Lotan R, Kerner H, Eimerl S, Tony Parks W, Gottfried Y, Birkey Reffey S, de Caestecker MP, Danielpour D, Book-Melamed N, Timberg R, Duckett CS, Lechleider RJ, Steller H, Orly J, Kim SJ & Roberts AB. (2000) A novel mitochondrial septin-like protein, ARTS, mediates apoptosis dependent on its P-loop motif. *Nat Cell Biol* **2**(12): 915-21.
Larsson J, Goumans MJ, Sjostrand LJ, van Rooijen MA, Ward D, Leveen P, Xu X, ten Dijke P, Mummery CL & Karlsson S. (2001) Abnormal angiogenesis but intact hematopoietic potential in TGF-beta type I receptor-deficient mice. *Embo J* **20**(7): 1663-73.
Laterra J, Guerin C & Goldstein GW. (1990) Astrocytes induce neural microvascular endothelial cells to form capillary-like structures in vitro. *J Cell Physiol* **144**(2): 204-15.
La Vail MM, Rapaport DH, Rakic P. (1991) Cytogenesis in the monkey retina. *J Comp Neurol* **309**(1):86-114.
Lawrence DA. (1996) Transforming growth factor-beta: a general review. *Eur Cytokine Netw* **7**(3): 363-74.
Lee LG, Connell CR & Bloch W. (1993) Allelic discrimination by nick-translation PCR with fluorogenic probes. *Nucleic Acids Res* **21**(16): 3761-6.
Lee MS, Gu D, Feng L, Curriden S, Arnush M, Krahl T, Gurushanthaiah D, Wilson C, Loskutoff DL, Fox H & et al. (1995) Accumulation of extracellular matrix and developmental dysregulation in the pancreas by transgenic production of transforming growth factor-beta 1. *Am J Pathol* **147**(1): 42-52.
Leeson TS. (1968) The outer layer of the optic cup and associated tissues. *Can J Ophthalmol* **3**(1): 77-96.
Leschey KH, Hackett SF, Singer JH & Campochiaro PA. (1990) Growth factor responsiveness of human retinal pigment epithelial cells. *Invest Ophthalmol Vis Sci* **31**(5): 839-46.
Leung DW, Cachianes G, Kuang WJ, Goeddel DV & Ferrara N. (1989) Vascular endothelial growth factor is a secreted angiogenic mitogen. *Science* **246**(4935): 1306-9.
Leutz A & Schachner M. (1981) Epidermal growth factor stimulates DNA-synthesis of astrocytes in primary cerebellar cultures. *Cell Tissue Res* **220**(2): 393-404.
Levine EM & Green ES. (2004) Cell-intrinsic regulators of proliferation in vertebrate retinal progenitors. *Semin Cell Dev Biol* **15**(1): 63-74.
Liesi P. (1985) Laminin-immunoreactive glia distinguish regenerative adult CNS systems from non-regenerative ones. *Embo J* **4**(10): 2505-11.
Linberg KA & Fisher SK. (1990) A burst of differentiation in the outer posterior retina of the eleven-week human fetus: an ultrastructural study. *Vis Neurosci* **5**(1): 43-60.
Lindholm D, Castren E, Kiefer R, Zafra F & Thoenen H. (1992) Transforming growth factor-beta 1 in the rat brain: increase after injury and inhibition of astrocyte proliferation. *J Cell Biol* **117**(2): 395-400.
Ling TL, Mitrofanis J & Stone J. (1989) Origin of retinal astrocytes in the rat: evidence of migration from the optic nerve. *J Comp Neurol* **286**(3): 345-52.

Ling TL & Stone J. (1988) The development of astrocytes in the cat retina: evidence of migration from the optic nerve. *Brain Res Dev Brain Res* **44**(1): 73-85.
Liu F, Ventura F, Doody J & Massague J. (1995) Human type II receptor for bone morphogenic proteins (BMPs): extension of the two-kinase receptor model to the BMPs. *Mol Cell Biol* **15**(7): 3479-86.
Lopez-Casillas F, Cheifetz S, Doody J, Andres JL, Lane WS & Massague J. (1991) Structure and expression of the membrane proteoglycan betaglycan, a component of the TGF-beta receptor system. *Cell* **67**(4): 785-95.
Lovicu FJ, Schulz MW, Hales AM, Vincent LN, Overbeek PA, Chamberlain CG & McAvoy JW. (2002) TGFbeta induces morphological and molecular changes similar to human anterior subcapsular cataract. *Br J Ophthalmol* **86**(2): 220-6.
Lutjen-Drecoll E. (2005) Morphological changes in glaucomatous eyes and the role of TGFbeta2 for the pathogenesis of the disease. *Exp Eye Res* **81**(1): 1-4.
Lutty G, Ikeda K, Chandler C & McLeod DS. (1991) Immunohistochemical localization of transforming growth factor-beta in human photoreceptors. *Curr Eye Res* **10**(1): 61-74.
Lutty GA, Mello RJ, Chandler C, Fait C, Bennett A & Patz A. (1985) Regulation of cell growth by vitreous humour. *J Cell Sci* **76**: 53-65.
Lutty GA, Merges C, Threlkeld AB, Crone S & McLeod DS. (1993) Heterogeneity in localization of isoforms of TGF-beta in human retina, vitreous, and choroid. *Invest Ophthalmol Vis Sci* **34**(3): 477-87.
Lutty GA, Thompson DC, Gallup JY, Mello RJ, Patz A & Fenselau A. (1983) Vitreous: an inhibitor of retinal extract-induced neovascularization. *Invest Ophthalmol Vis Sci* **24**(1): 52-6.
Lyons RM, Keski-Oja J & Moses HL. (1988) Proteolytic activation of latent transforming growth factor-beta from fibroblast-conditioned medium. *J Cell Biol* **106**(5): 1659-65.
MacConell LA, Leal AM & Vale WW. (2002) The distribution of betaglycan protein and mRNA in rat brain, pituitary, and gonads: implications for a role for betaglycan in inhibin-mediated reproductive functions. *Endocrinology* **143**(3): 1066-75.
Madri JA, Pratt BM & Tucker AM. (1988) Phenotypic modulation of endothelial cells by transforming growth factor-beta depends upon the composition and organization of the extracellular matrix. *J Cell Biol* **106**(4): 1375-84.
Majack RA, Cook SC & Bornstein P. (1985) Platelet-derived growth factor and heparin-like glycosaminoglycans regulate thrombospondin synthesis and deposition in the matrix by smooth muscle cells. *J Cell Biol* **101**(3): 1059-70.
Majima K. (1997) Presence of growth factor in human vitreous. *Ophthalmologica* **211**(4): 226-8.
Mandriota SJ, Menoud PA & Pepper MS. (1996) Transforming growth factor beta 1 down-regulates vascular endothelial growth factor receptor 2/flk-1 expression in vascular endothelial cells. *J Biol Chem* **271**(19): 11500-5.
Mann I. (1964) *The Development of the Human Eye.* New York: Grune and Stratton.
Manning G, Whyte DB, Martinez R, Hunter T & Sudarsanam S. (2002) The protein kinase complement of the human genome. *Science* **298**(5600): 1912-34.
Marneros AG, Fan J, Yokoyama Y, Gerber HP, Ferrara N, Crouch RK & Olsen BR. (2005) Vascular endothelial growth factor expression in the retinal pigment epithelium is essential for choriocapillaris development and visual function. *Am J Pathol* **167**(5): 1451-9.
Martin KA & Perry VH. (1988) On seeing a butterfly: the physiology of vision. *Sci Prog* **72**(286 Pt 2): 259-80.
Martinez-Morales JR, Del Bene F, Nica G, Hammerschmidt M, Bovolenta P & Wittbrodt J. (2005) Differentiation of the vertebrate retina is coordinated by an FGF signaling center. *Dev Cell* **8**(4): 565-74.
Martinez-Morales JR, Rodrigo I & Bovolenta P. (2004) Eye development: a view from the retina pigmented epithelium. *Bioessays* **26**(7): 766-77.

Mascarelli F, Tassin J & Courtois Y. (1991) Effect of FGFs on adult bovine Muller cells: proliferation, binding and internalization. *Growth Factors* **4**(2): 81-95.
Maslim J, Valter K, Egensperger R, Hollander H & Stone J. (1997) Tissue oxygen during a critical developmental period controls the death and survival of photoreceptors. *Invest Ophthalmol Vis Sci* **38**(9): 1667-77.
Massague J. (1996) TGFbeta signaling: receptors, transducers, and Mad proteins. *Cell* **85**(7): 947-50.
Massague J. (1998) TGF-beta signal transduction. *Annu Rev Biochem* **67**: 753-91.
Massague J. (2000) How cells read TGF-beta signals. *Nat Rev Mol Cell Biol* **1**(3): 169-78.
Massague J, Blain SW & Lo RS. (2000) TGFbeta signaling in growth control, cancer, and heritable disorders. *Cell* **103**(2): 295-309.
Massague J, Cheifetz S, Boyd FT & Andres JL. (1990) TGF-beta receptors and TGF-beta binding proteoglycans: recent progress in identifying their functional properties. *Ann N Y Acad Sci* **593**: 59-72.
Massague J & Chen YG. (2000) Controlling TGF-beta signaling. *Genes Dev* **14**(6): 627-44.
Massague J & Weis-Garcia F. (1996) Serine/threonine kinase receptors: mediators of transforming growth factor beta family signals. *Cancer Surv* **27**: 41-64.
Matsubara T, Pararajasegaram G, Wu GS & Rao NA. (1999) Retinal microglia differentially express phenotypic markers of antigen-presenting cells in vitro. *Invest Ophthalmol Vis Sci* **40**(13): 3186-93.
McAvoy JW, Chamberlain CG, de Iongh RU, Hales AM & Lovicu FJ. (2000) Peter Bishop Lecture: growth factors in lens development and cataract: key roles for fibroblast growth factor and TGF-beta. *Clin Experiment Ophthalmol* **28**(3): 133-9.
McDonald NQ & Hendrickson WA. (1993) A structural superfamily of growth factors containing a cystine knot motif. *Cell* **73**(3): 421-4.
McPherson J, Sage H & Bornstein P. (1981) Isolation and characterization of a glycoprotein secreted by aortic endothelial cells in culture. Apparent identity with platelet thrombospondin. *J Biol Chem* **256**(21): 11330-6.
Merwin JR, Anderson JM, Kocher O, Van Itallie CM & Madri JA. (1990) Transforming growth factor beta 1 modulates extracellular matrix organization and cell-cell junctional complex formation during in vitro angiogenesis. *J Cell Physiol* **142**(1): 117-28.
Merwin JR, Newman W, Beall LD, Tucker A & Madri J. (1991a) Vascular cells respond differentially to transforming growth factors beta 1 and beta 2 in vitro. *Am J Pathol* **138**(1): 37-51.
Merwin JR, Roberts A, Kondaiah P, Tucker A & Madri J. (1991b) Vascular cell responses to TGF-beta 3 mimic those of TGF-beta 1 in vitro. *Growth Factors* **5**(2): 149-58.
Mi H, Haeberle H & Barres BA. (2001) Induction of astrocyte differentiation by endothelial cells. *J Neurosci* **21**(5): 1538-47.
Michaelson IC. (1948) The mode of development of the vascular system of the retina, with some observations on its significance for certain retinal diseases. *Transactions of the Ophthalmological Society of the UK.* **68**: 137-81.
Michaelson IC. (1954) *Retinal Circulation in Man and Animals.* Springfield, Illinois: Charles C. Thomas.
Michaelson IC, Herz N, Lewkowitz E & Kertesz D. (1954) Effect of increased oxygen on the development of the retinal vessels; an experimental study. *Br J Ophthalmol* **38**(10): 577-87.
Mignatti P, Tsuboi R, Robbins E & Rifkin DB. (1989) In vitro angiogenesis on the human amniotic membrane: requirement for basic fibroblast growth factor-induced proteinases. *J Cell Biol* **108**(2): 671-82.
Milenkovic I, Weick M, Wiedemann P, Reichenbach A & Bringmann A. (2003) P2Y receptor-mediated stimulation of Muller glial cell DNA synthesis: dependence

on EGF and PDGF receptor transactivation. *Invest Ophthalmol Vis Sci* **44**(3): 1211-20.
Millauer B, Shawver LK, Plate KH, Risau W & Ullrich A. (1994) Glioblastoma growth inhibited in vivo by a dominant-negative Flk-1 mutant. *Nature* **367**(6463): 576-9.
Miller MW. (2003) Expression of transforming growth factor-beta in developing rat cerebral cortex: effects of prenatal exposure to ethanol. *J Comp Neurol* **460**(3): 410-24.
Mishima H, Nakamura M, Murakami J, Nishida T & Otori T. (1992) Transforming growth factor-beta modulates effects of epidermal growth factor on corneal epithelial cells. *Curr Eye Res* **11**(7): 691-6.
Mita T, Yamashita H, Kaji Y, Obata H, Yamada H, Kato M, Hanyu A, Suzuki M & Tobari I. (1998) Effects of transforming growth factor beta on corneal epithelial and stromal cell function in a rat wound healing model after excimer laser keratectomy. *Graefes Arch Clin Exp Ophthalmol* **236**(11): 834-43.
Mitsuhiro MR, Eguchi S & Yamashita H. (2003) Regulation mechanisms of retinal pigment epithelial cell migration by the TGF-beta superfamily. *Acta Ophthalmol Scand* **81**(6): 630-8.
Mittl PR, Priestle JP, Cox DA, McMaster G, Cerletti N & Grutter MG. (1996) The crystal structure of TGF-beta 3 and comparison to TGF-beta 2: implications for receptor binding. *Protein Sci* **5**(7): 1261-71.
Miyazono K. (2000) Positive and negative regulation of TGF-beta signaling. *J Cell Sci* **113 (Pt 7)**: 1101-9.
Miyazono K, Hellman U, Wernstedt C & Heldin CH. (1988) Latent high molecular weight complex of transforming growth factor beta 1. Purification from human platelets and structural characterization. *J Biol Chem* **263**(13): 6407-15.
Miyazono K, Ten Dijke P, Ichijo H & Heldin CH. (1994) Receptors for transforming growth factor-beta. *Adv Immunol* **55**: 181-220.
Moon LD & Fawcett JW. (2001) Reduction in CNS scar formation without concomitant increase in axon regeneration following treatment of adult rat brain with a combination of antibodies to TGFbeta1 and beta2. *Eur J Neurosci* **14**(10): 1667-77.
Moore KL. (1988) *The Developing Human.* Philadelphia: WB Saunders.
Morganti-Kossmann MC, Kossmann T, Brandes ME, Mergenhagen SE & Wahl SM. (1992) Autocrine and paracrine regulation of astrocyte function by transforming growth factor-beta. *J Neuroimmunol* **39**(1-2): 163-73.
Morita M, Ohneda O, Yamashita T, Takahashi S, Suzuki N, Nakajima O, Kawauchi S, Ema M, Shibahara S, Udono T, Tomita K, Tamai M, Sogawa K, Yamamoto M & Fujii-Kuriyama Y. (2003) HLF/HIF-2alpha is a key factor in retinopathy of prematurity in association with erythropoietin. *Embo J* **22**(5): 1134-46.
Morrison TB, Weis JJ & Wittwer CT. (1998) Quantification of low-copy transcripts by continuous SYBR Green I monitoring during amplification. *Biotechniques* **24**(6): 954-8, 60, 62.
Morse LS, Terrell J & Sidikaro Y. (1989) Bovine retinal pigment epithelium promotes proliferation of choroidal endothelium in vitro. *Arch Ophthalmol* **107**(11): 1659-63.
Moses MA, Marikovsky M, Harper JW, Vogt P, Eriksson E, Klagsbrun M & Langer R. (1996) Temporal study of the activity of matrix metalloproteinases and their endogenous inhibitors during wound healing. *J Cell Biochem* **60**(3): 379-86.
Mudhar HS, Pollock RA, Wang C, Stiles CD & Richardson WD. (1993) PDGF and its receptors in the developing rodent retina and optic nerve. *Development* **118**(2): 539-52.
Mulder KM. (2000) Role of Ras and Mapks in TGFbeta signaling. *Cytokine Growth Factor Rev* **11**(1-2): 23-35.

Muller G, Behrens J, Nussbaumer U, Bohlen P & Birchmeier W. (1987) Inhibitory action of transforming growth factor beta on endothelial cells. *Proc Natl Acad Sci U S A* **84**(16): 5600-4.

Mummery CL. (2001) Transforming growth factor beta and mouse development. *Microsc Res Tech* **52**(4): 374-86.

Mund ML, Rodrigues MM & Fine BS. (1972) Light and electron microscopic observations on the pigmented layers of the developing human eye. *Am J Ophthalmol* **73**(2): 167-82.

Munger JS, Harpel JG, Gleizes PE, Mazzieri R, Nunes I & Rifkin DB. (1997) Latent transforming growth factor-beta: structural features and mechanisms of activation. *Kidney Int* **51**(5): 1376-82.

Mustoe TA, Pierce GF, Thomason A, Gramates P, Sporn MB & Deuel TF. (1987) Accelerated healing of incisional wounds in rats induced by transforming growth factor-beta. *Science* **237**(4820): 1333-6.

Mustonen T & Alitalo K. (1995) Endothelial receptor tyrosine kinases involved in angiogenesis. *J Cell Biol* **129**(4): 895-8.

Nabel EG, Shum L, Pompili VJ, Yang ZY, San H, Shu HB, Liptay S, Gold L, Gordon D, Derynck R & et al. (1993) Direct transfer of transforming growth factor beta 1 gene into arteries stimulates fibrocellular hyperplasia. *Proc Natl Acad Sci U S A* **90**(22): 10759-63.

Neuhardt T, May CA, Wilsch C, Eichhorn M & Lutjen-Drecoll E. (1999) Morphological changes of retinal pigment epithelium and choroid in rd-mice. *Exp Eye Res* **68**(1): 75-83.

Nickla DL, Wildsoet C & Wallman J. (1998) The circadian rhythm in intraocular pressure and its relation to diurnal ocular growth changes in chicks. *Exp Eye Res* **66**(2): 183-93.

Nilhausen K. (1958) The vasoformative tissue in the foetal retina with particular reference to the histochemical demonstration of its alkaline phosphatase activity. *Acta Ophthalmologica* **36**: 65-70.

Nishida K, Kinoshita S, Yokoi N, Kaneda M, Hashimoto K & Yamamoto S. (1994) Immunohistochemical localization of transforming growth factor-beta 1, -beta 2, and -beta 3 latency-associated peptide in human cornea. *Invest Ophthalmol Vis Sci* **35**(8): 3289-94.

Nishida K, Ohashi Y, Nezu E, Yamamoto S, Kinoshita S & Fujita K. (1993) [Transforming growth factor-beta (TGF-beta) inhibits epithelial wound healing of organ-cultured rabbit cornea]. *Nippon Ganka Gakkai Zasshi* **97**(8): 899-905.

Nishida K, Sotozono C, Adachi W, Yamamoto S, Yokoi N & Kinoshita S. (1995) Transforming growth factor-beta 1, -beta 2 and -beta 3 mRNA expression in human cornea. *Curr Eye Res* **14**(3): 235-41.

Nishimura T, Toda S, Mitsumoto T, Oono S & Sugihara H. (1998) Effects of hepatocyte growth factor, transforming growth factor-beta1 and epidermal growth factor on bovine corneal epithelial cells under epithelial-keratocyte interaction in reconstruction culture. *Exp Eye Res* **66**(1): 105-16.

Nishimura Y & Rakic P. (1987) Development of the rhesus monkey retina: II. A three-dimensional analysis of the sequences of synaptic combinations in the inner plexiform layer. *J Comp Neurol* **262**(2): 290-313.

Nomura M, Yamagishi S, Harada S, Hayashi Y, Yamashima T, Yamashita J & Yamamoto H. (1995) Possible participation of autocrine and paracrine vascular endothelial growth factors in hypoxia-induced proliferation of endothelial cells and pericytes. *J Biol Chem* **270**(47): 28316-24.

Nork TM, Wallow IH, Sramek SJ & Anderson G. (1987) Muller's cell involvement in proliferative diabetic retinopathy. *Arch Ophthalmol* **105**(10): 1424-9.

Nuovo GJ. (1996) *PCR In Situ Hybridisation: Protocols and Applications.* New York: Raven Press.

O'Kane S & Ferguson MW. (1997) Transforming growth factor beta s and wound healing. *Int J Biochem Cell Biol* **29**(1): 63-78.

O'Rahilly R. (1975) The prenatal development of the human eye. *Exp Eye Res* **21**(2): 93-112.
O'Reilly MS. (1997) Angiostatin: an endogenous inhibitor of angiogenesis and of tumor growth. *Exs* **79**: 273-94.
O'Reilly MS, Boehm T, Shing Y, Fukai N, Vasios G, Lane WS, Flynn E, Birkhead JR, Olsen BR & Folkman J. (1997) Endostatin: an endogenous inhibitor of angiogenesis and tumor growth. *Cell* **88**(2): 277-85.
O'Reilly MS, Holmgren L, Shing Y, Chen C, Rosenthal RA, Cao Y, Moses M, Lane WS, Sage EH & Folkman J. (1994) Angiostatin: a circulating endothelial cell inhibitor that suppresses angiogenesis and tumor growth. *Cold Spring Harb Symp Quant Biol* **59**: 471-82.
Obata H, Kaji Y, Yamada H, Kato M, Tsuru T & Yamashita H. (1999) Expression of transforming growth factor-beta superfamily receptors in rat eyes. *Acta Ophthalmol Scand* **77**(2): 151-6.
Ogata N, Ando A, Uyama M & Matsumura M. (2001) Expression of cytokines and transcription factors in photocoagulated human retinal pigment epithelial cells. *Graefes Arch Clin Exp Ophthalmol* **239**(2): 87-95.
Oh SP, Seki T, Goss KA, Imamura T, Yi Y, Donahoe PK, Li L, Miyazono K, ten Dijke P, Kim S & Li E. (2000) Activin receptor-like kinase 1 modulates transforming growth factor-beta 1 signaling in the regulation of angiogenesis. *Proc Natl Acad Sci U S A* **97**(6): 2626-31.
Okada M, Erickson A & Hendrickson A. (1994) Light and electron microscopic analysis of synaptic development in Macaca monkey retina as detected by immunocytochemical labeling for the synaptic vesicle protein, SV2. *J Comp Neurol* **339**(4): 535-58.
Olofsson A, Miyazono K, Kanzaki T, Colosetti P, Engstrom U & Heldin CH. (1992) Transforming growth factor-beta 1, -beta 2, and -beta 3 secreted by a human glioblastoma cell line. Identification of small and different forms of large latent complexes. *J Biol Chem* **267**(27): 19482-8.
Oppenheim RW. (1991) Cell death during development of the nervous system. *Annu Rev Neurosci* **14**: 453-501.
Orlidge A & D'Amore PA. (1987) Inhibition of capillary endothelial cell growth by pericytes and smooth muscle cells. *J Cell Biol* **105**(3): 1455-62.
Oshima M, Oshima H & Taketo MM. (1996) TGF-beta receptor type II deficiency results in defects of yolk sac hematopoiesis and vasculogenesis. *Dev Biol* **179**(1): 297-302.
Otani A, Dorrell MI, Kinder K, Moreno SK, Nusinowitz S, Banin E, Heckenlively J & Friedlander M. (2004) Rescue of retinal degeneration by intravitreally injected adult bone marrow-derived lineage-negative hematopoietic stem cells. *J Clin Invest* **114**(6): 765-74.
Otani A, Kinder K, Ewalt K, Otero FJ, Schimmel P & Friedlander M. (2002) Bone marrow-derived stem cells target retinal astrocytes and can promote or inhibit retinal angiogenesis. *Nat Med* **8**(9): 1004-10.
Ozaki H, Yu AY, Della N, Ozaki K, Luna JD, Yamada H, Hackett SF, Okamoto N, Zack DJ, Semenza GL & Campochiaro PA. (1999) Hypoxia inducible factor-1alpha is increased in ischemic retina: temporal and spatial correlation with VEGF expression. *Invest Ophthalmol Vis Sci* **40**(1): 182-9.
Ozanics V, Rayborn ME & Sagun D. (1978) Observations on the ultrastructure of the developing primate choroid coat. *Exp Eye Res* **26**(1): 25-45.
Packer O, Hendrickson AE, Curcio CA. (1989) Photoreceptor topography of the retina in the adult pigtail macaque (Macaca nemestrina). *J Comp Neurol* **288**(1): 165-83
Padgett RW. (1999a) Intracellular signaling: Fleshing out the TGFbeta pathway. *Curr Biol* **9**(11): R408-11.
Padgett RW. (1999b) TGFbeta signaling pathways and human diseases. *Cancer Metastasis Rev* **18**(2): 247-59.

Pasquale LR, Dorman-Pease ME, Lutty GA, Quigley HA & Jampel HD. (1993) Immunolocalization of TGF-beta 1, TGF-beta 2, and TGF-beta 3 in the anterior segment of the human eye. *Invest Ophthalmol Vis Sci* **34**(1): 23-30.

Passaniti A, Taylor RM, Pili R, Guo Y, Long PV, Haney JA, Pauly RR, Grant DS & Martin GR. (1992) A simple, quantitative method for assessing angiogenesis and antiangiogenic agents using reconstituted basement membrane, heparin, and fibroblast growth factor. *Lab Invest* **67**(4): 519-28.

Patterson GI & Padgett RW. (2000) TGF beta-related pathways. Roles in Caenorhabditis elegans development. *Trends Genet* **16**(1): 27-33.

Patz A. (1966) In Vascular Disorders of the Eye. 16-27.

Patz A, Lutty G, Bennett A & Coughlin WR. (1978) Inhibitors of neovascularization in relation to diabetic and other proliferative retinopathies. *Trans Am Ophthalmol Soc* **76**: 102-7.

Pelton RW, Saxena B, Jones M, Moses HL & Gold LI. (1991) Immunohistochemical localization of TGF beta 1, TGF beta 2, and TGF beta 3 in the mouse embryo: expression patterns suggest multiple roles during embryonic development. *J Cell Biol* **115**(4): 1091-105.

Pena JD, Taylor AW, Ricard CS, Vidal I & Hernandez MR. (1999) Transforming growth factor beta isoforms in human optic nerve heads. *Br J Ophthalmol* **83**(2): 209-18.

Penfold PL, Provis JM & Liew SC. (1993) Human retinal microglia express phenotypic characteristics in common with dendritic antigen-presenting cells. *J Neuroimmunol* **45**(1-2): 183-91.

Pepper MS. (1997) Transforming growth factor-beta: vasculogenesis, angiogenesis, and vessel wall integrity. *Cytokine Growth Factor Rev* **8**(1): 21-43.

Pepper MS, Belin D, Montesano R, Orci L & Vassalli JD. (1990) Transforming growth factor-beta 1 modulates basic fibroblast growth factor-induced proteolytic and angiogenic properties of endothelial cells in vitro. *J Cell Biol* **111**(2): 743-55.

Pepper MS, Ferrara N, Orci L & Montesano R. (1991) Vascular endothelial growth factor (VEGF) induces plasminogen activators and plasminogen activator inhibitor-1 in microvascular endothelial cells. *Biochem Biophys Res Commun* **181**(2): 902-6.

Pepper MS, Sappino AP, Stocklin R, Montesano R, Orci L & Vassalli JD. (1993) Upregulation of urokinase receptor expression on migrating endothelial cells. *J Cell Biol* **122**(3): 673-84.

Peress NS & Perillo E. (1994) TGF-beta 2 and TGF-beta 3 immunoreactivity within the ciliary epithelium [corrected]. *Invest Ophthalmol Vis Sci* **35**(2): 453-7.

Perillan PR, Chen M, Potts EA & Simard JM. (2002) Transforming growth factor-beta 1 regulates Kir2.3 inward rectifier K+ channels via phospholipase C and protein kinase C-delta in reactive astrocytes from adult rat brain. *J Biol Chem* **277**(3): 1974-80.

Pfaffl MW. (2001) A new mathematical model for relative quantification in real-time RT-PCR. *Nucleic Acids Res* **29**(9): e45.

Pfeffer BA, Flanders KC, Guerin CJ, Danielpour D & Anderson DH. (1994) Transforming growth factor beta 2 is the predominant isoform in the neural retina, retinal pigment epithelium-choroid and vitreous of the monkey eye. *Exp Eye Res* **59**(3): 323-33.

Phillips GD, Whitehead RA & Knighton DR. (1992) Inhibition by methylprednisolone acetate suggests an indirect mechanism for TGF-B induced angiogenesis. *Growth Factors* **6**(1): 77-84.

Phillips GD, Whitehead RA, Stone AM, Ruebel MW, Goodkin ML & Knighton DR. (1993) Transforming growth factor beta (TGF-B) stimulation of angiogenesis: an electron microscopic study. *J Submicrosc Cytol Pathol* **25**(2): 149-55.

Picht G, Welge-Luessen U, Grehn F & Lutjen-Drecoll E. (2001) Transforming growth factor beta 2 levels in the aqueous humor in different types of glaucoma and

the relation to filtering bleb development. *Graefes Arch Clin Exp Ophthalmol* **239**(3): 199-207.
Pierce DF, Jr., Johnson MD, Matsui Y, Robinson SD, Gold LI, Purchio AF, Daniel CW, Hogan BL & Moses HL. (1993) Inhibition of mammary duct development but not alveolar outgrowth during pregnancy in transgenic mice expressing active TGF-beta 1. *Genes Dev* **7**(12A): 2308-17.
Pierce EA, Avery RL, Foley ED, Aiello LP & Smith LE. (1995) Vascular endothelial growth factor/vascular permeability factor expression in a mouse model of retinal neovascularization. *Proc Natl Acad Sci U S A* **92**(3): 905-9.
Pierce EA, Foley ED & Smith LE. (1996) Regulation of vascular endothelial growth factor by oxygen in a model of retinopathy of prematurity. *Arch Ophthalmol* **114**(10): 1219-28.
Polans AS, Altman LG & Papermaster DS. (1986) Immunocytochemical binding of anti-opsin N-terminal-specific antibodies to the extracellular surface of rod outer segment plasma membranes. Fixation induces antibody binding. *J Histochem Cytochem* **34**(5): 659-64.
Polyak SL. (1941) *The Retina.* Chicago: University of Chicago Press.
Poulsen KT, Armanini MP, Klein RD, Hynes MA, Phillips HS & Rosenthal A. (1994) TGF beta 2 and TGF beta 3 are potent survival factors for midbrain dopaminergic neurons. *Neuron* **13**(5): 1245-52.
Pratt BM & McPherson JM. (1997) TGF-beta in the central nervous system: potential roles in ischemic injury and neurodegenerative diseases. *Cytokine Growth Factor Rev* **8**(4): 267-92.
Prehn JH, Backhauss C & Krieglstein J. (1993) Transforming growth factor-beta 1 prevents glutamate neurotoxicity in rat neocortical cultures and protects mouse neocortex from ischemic injury in vivo. *J Cereb Blood Flow Metab* **13**(3): 521-5.
Prehn JH & Krieglstein J. (1994) Opposing effects of transforming growth factor-beta 1 on glutamate neurotoxicity. *Neuroscience* **60**(1): 7-10.
Presta M, Moscatelli D, Joseph-Silverstein J & Rifkin DB. (1986) Purification from a human hepatoma cell line of a basic fibroblast growth factor-like molecule that stimulates capillary endothelial cell plasminogen activator production, DNA synthesis, and migration. *Mol Cell Biol* **6**(11): 4060-6.
Prockop DJ. (1997) Marrow stromal cells as stem cells for nonhematopoietic tissues. *Science* **276**(5309): 71-4.
Proetzel G, Pawlowski SA, Wiles MV, Yin M, Boivin GP, Howles PN, Ding J, Ferguson MW & Doetschman T. (1995) Transforming growth factor-beta 3 is required for secondary palate fusion. *Nat Genet* **11**(4): 409-14.
Provis JM. (1987) Patterns of cell death in the ganglion cell layer of the human fetal retina. *J Comp Neurol* **259**(2): 237-46.
Provis JM. (2001) Development of the primate retinal vasculature. *Prog Retin Eye Res* **20**(6): 799-821.
Provis JM, Diaz CM & Dreher B. (1998) Ontogeny of the primate fovea: a central issue in retinal development. *Prog Neurobiol* **54**(5): 549-80.
Provis JM, Diaz CM & Penfold PL. (1996) Microglia in human retina: a heterogeneous population with distinct ontogenies. *Perspect Dev Neurobiol* **3**(3): 213-22.
Provis JM, Leech J, Diaz CM, Penfold PL, Stone J & Keshet E. (1997) Development of the human retinal vasculature: cellular relations and VEGF expression. *Exp Eye Res* **65**(4): 555-68.
Provis JM & Penfold PL. (1988) Cell death and the elimination of retinal axons during development. *Prog Neurobiol* **31**(4): 331-47.
Provis JM, Penfold PL, Cornish EE, Sandercoe TM & Madigan MC. (2005) Anatomy and development of the macula: specialisation and the vulnerability to macular degeneration. *Clin Exp Optom* **88**(5): 269-81.

Provis JM, Penfold PL, Edwards AJ & van Driel D. (1995) Human retinal microglia: expression of immune markers and relationship to the glia limitans. *Glia* **14**(4): 243-56.

Provis JM, Sandercoe T & Hendrickson AE. (2000) Astrocytes and blood vessels define the foveal rim during primate retinal development. *Invest Ophthalmol Vis Sci* **41**(10): 2827-36.

Provis JM & van Driel D. (1985) Retinal development in humans: the roles of differential growth rates, cell migration and naturally occurring cell death. *Aust N Z J Ophthalmol* **13**(2): 125-33.

Provis JM, van Driel D, Billson FA & Russell P. (1985) Development of the human retina: patterns of cell distribution and redistribution in the ganglion cell layer. *J Comp Neurol* **233**(4): 429-51.

Rabchevsky AG, Weinitz JM, Coulpier M, Fages C, Tinel M & Junier MP. (1998) A role for transforming growth factor alpha as an inducer of astrogliosis. *J Neurosci* **18**(24): 10541-52.

Rakic P. (1977) Prenatal development of the visual system in rhesus monkey. *Philos Trans R Soc Lond B Biol Sci* **278**(961): 245-60.

Rapaport DH, Rakic P & LaVail MM. (1996) Spatiotemporal gradients of cell genesis in the primate retina. *Perspect Dev Neurobiol* **3**(3): 147-59.

Rapaport DH & Stone J. (1982) The site of commencement of maturation in mammalian retina: observations in the cat. *Brain Res* **281**(3): 273-9.

RayChaudhury A & D'Amore PA. (1991) Endothelial cell regulation by transforming growth factor-beta. *J Cell Biochem* **47**(3): 224-9.

Reichenbach A, Faude, F., Enzmann, V., Bringmann, A., Pannicke, T., Francke, M., Biedermann, B., Kuhrt, H., Stolzenburg, J.U., Skatchkov, S.N., Heinemann, U., Wiedemann, P. and Reichelt, W. (1997) The Müller (glial) cell in normal and diseased retina: a case for single-cell electrophysiology. *Ophthalmic Research.* **29**: 326-40.

Reilly J, Maher P & Kumari V. (1998) Regulation of astrocyte GFAP expression by TGF-beta 1 and FGF-2. *Glia* **22**(2): 202-10.

Reyes M, Dudek A, Jahagirdar B, Koodie L, Marker PH & Verfaillie CM. (2002) Origin of endothelial progenitors in human postnatal bone marrow. *J Clin Invest* **109**(3): 337-46.

Rhodes RH. (1979) A light microscopic study of the developing human neural retina. *Am J Anat* **154**(2): 195-209.

Rich JN, Zhang M, Datto MB, Bigner DD & Wang XF. (1999) Transforming growth factor-beta-mediated p15(INK4B) induction and growth inhibition in astrocytes is SMAD3-dependent and a pathway prominently altered in human glioma cell lines. *J Biol Chem* **274**(49): 35053-8.

Richardson WD, Pringle N, Mosley MJ, Westermark B & Dubois-Dalcq M. (1988) A role for platelet-derived growth factor in normal gliogenesis in the central nervous system. *Cell* **53**(2): 309-19.

Risau W. (1997) Mechanisms of angiogenesis. *Nature* **386**(6626): 671-4.

Rizzino A. (1988) Transforming growth factor-beta: multiple effects on cell differentiation and extracellular matrices. *Dev Biol* **130**(2): 411-22.

Roberts AB. (1998) Molecular and cell biology of TGF-beta. *Miner Electrolyte Metab* **24**(2-3): 111-9.

Roberts AB, Flanders KC, Heine UI, Jakowlew S, Kondaiah P, Kim SJ & Sporn MB. (1990a) Transforming growth factor-beta: multifunctional regulator of differentiation and development. *Philos Trans R Soc Lond B Biol Sci* **327**(1239): 145-54.

Roberts AB, Heine UI, Flanders KC & Sporn MB. (1990b) Transforming growth factor-beta. Major role in regulation of extracellular matrix. *Ann N Y Acad Sci* **580**: 225-32.

Roberts AB & Sporn MB. (1989) Regulation of endothelial cell growth, architecture, and matrix synthesis by TGF-beta. *Am Rev Respir Dis* **140**(4): 1126-8.

Roberts AB & Sporn MB. (1992) Differential expression of the TGF-beta isoforms in embryogenesis suggests specific roles in developing and adult tissues. *Mol Reprod Dev* **32**(2): 91-8.

Roberts AB & Sporn MB. (1993) Physiological actions and clinical applications of transforming growth factor-beta (TGF-beta). *Growth Factors* **8**(1): 1-9.

Roberts AB, Sporn MB, Assoian RK, Smith JM, Roche NS, Wakefield LM, Heine UI, Liotta LA, Falanga V, Kehrl JH & et al. (1986) Transforming growth factor type beta: rapid induction of fibrosis and angiogenesis in vivo and stimulation of collagen formation in vitro. *Proc Natl Acad Sci U S A* **83**(12): 4167-71.

Robinson SD. (1991) *Development of the Mammalian Retina. In: Neuroanatomy of the visual pathways and their development.* London: MacMillan.

Robison WG, Jr., Tillis TN, Laver N & Kinoshita JH. (1990) Diabetes-related histopathologies of the rat retina prevented with an aldose reductase inhibitor. *Exp Eye Res* **50**(4): 355-66.

Rodieck RW. (1988) The Primate Retina. *Comparative Primate Biology* **4**: 203-78.

Rodieck RW, Binmoeller KF & Dineen J. (1985) Parasol and midget ganglion cells of the human retina. *J Comp Neurol* **233**(1): 115-32.

Rohrer B & Stell WK. (1994) Basic fibroblast growth factor (bFGF) and transforming growth factor beta (TGF-beta) act as stop and go signals to modulate postnatal ocular growth in the chick. *Exp Eye Res* **58**(5): 553-61.

Roque RS, Caldwell RB & Behzadian MA. (1992) Cultured Muller cells have high levels of epidermal growth factor receptors. *Invest Ophthalmol Vis Sci* **33**(9): 2587-95.

Roussa E, Farkas LM & Krieglstein K. (2004) TGF-beta promotes survival on mesencephalic dopaminergic neurons in cooperation with Shh and FGF-8. *Neurobiol Dis* **16**(2): 300-10.

Roussa E & Krieglstein K. (2004) Induction and specification of midbrain dopaminergic cells: focus on SHH, FGF8, and TGF-beta. *Cell Tissue Res* **318**(1): 23-33.

Rousseau B, Dubayle D, Sennlaub F, Jeanny JC, Costet P, Bikfalvi A & Javerzat S. (2000) Neural and angiogenic defects in eyes of transgenic mice expressing a dominant-negative FGF receptor in the pigmented cells. *Exp Eye Res* **71**(4): 395-404.

Rousseau B, Larrieu-Lahargue F, Bikfalvi A & Javerzat S. (2003) Involvement of fibroblast growth factors in choroidal angiogenesis and retinal vascularization. *Exp Eye Res* **77**(2): 147-56.

Rubbia-Brandt L, Sappino AP & Gabbiani G. (1991) Locally applied GM-CSF induces the accumulation of alpha-smooth muscle actin containing myofibroblasts. *Virchows Arch B Cell Pathol Incl Mol Pathol* **60**(2): 73-82.

Ryan SJ. (2001) *Retina.* London: Mosby.

Saharinen J & Keski-Oja J. (2000) Specific sequence motif of 8-Cys repeats of TGF-beta binding proteins, LTBPs, creates a hydrophobic interaction surface for binding of small latent TGF-beta. *Mol Biol Cell* **11**(8): 2691-704.

Saika S. (2004) TGF-beta signal transduction in corneal wound healing as a therapeutic target. *Cornea* **23**(8 Suppl): S25-30.

Saika S. (2005) TGFbeta pathobiology in the eye. *Lab Invest* **86**(2): 106-15.

Saika S, Miyamoto T, Kawashima Y, Okada Y, Yamanaka O, Ohnishi Y & Ooshima A. (2000) Immunolocalization of TGF-beta1, -beta2, and -beta3, and TGF-beta receptors in human lens capsules with lens implants. *Graefes Arch Clin Exp Ophthalmol* **238**(3): 283-93.

Saint-Geniez M & D'Amore PA. (2004) Development and pathology of the hyaloid, choroidal and retinal vasculature. *Int J Dev Biol* **48**(8-9): 1045-58.

Saint-Geniez M, Maldonado AE & D'Amore PA. (2006) VEGF expression and receptor activation in the choroid during development and in the adult. *Invest Ophthalmol Vis Sci* **47**(7): 3135-42.

Sakamoto T, Sakamoto H, Murphy TL, Spee C, Soriano D, Ishibashi T, Hinton DR & Ryan SJ. (1995) Vessel formation by choroidal endothelial cells in vitro is

modulated by retinal pigment epithelial cells. *Arch Ophthalmol* **113**(4): 512-20.
Saltis J. (1996) TGF-beta: receptors and cell cycle arrest. *Mol Cell Endocrinol* **116**(2): 227-32.
Sandercoe TM, Geller SF, Hendrickson AE, Stone J & Provis JM. (2003) VEGF expression by ganglion cells in central retina before formation of the foveal depression in monkey retina: evidence of developmental hypoxia. *J Comp Neurol* **462**(1): 42-54.
Sandercoe TM, Madigan MC, Billson FA, Penfold PL & Provis JM. (1999) Astrocyte proliferation during development of the human retinal vasculature. *Exp Eye Res* **69**(5): 511-23.
Sanderson N, Factor V, Nagy P, Kopp J, Kondaiah P, Wakefield L, Roberts AB, Sporn MB & Thorgeirsson SS. (1995) Hepatic expression of mature transforming growth factor beta 1 in transgenic mice results in multiple tissue lesions. *Proc Natl Acad Sci U S A* **92**(7): 2572-6.
Sanes JR. (1989) Extracellular matrix molecules that influence neural development. *Annu Rev Neurosci* **12**: 491-516.
Sanford LP, Ormsby I, Gittenberger-de Groot AC, Sariola H, Friedman R, Boivin GP, Cardell EL & Doetschman T. (1997) TGFbeta2 knockout mice have multiple developmental defects that are non-overlapping with other TGFbeta knockout phenotypes. *Development* **124**(13): 2659-70.
Sato Y, Tsuboi R, Lyons R, Moses H & Rifkin DB. (1990) Characterization of the activation of latent TGF-beta by co-cultures of endothelial cells and pericytes or smooth muscle cells: a self-regulating system. *J Cell Biol* **111**(2): 757-63.
Scherer J & Schnitzer J. (1994) Growth factor effects on the proliferation of different retinal glial cells in vitro. *Brain Res Dev Brain Res* **80**(1-2): 209-21.
Schluesener HJ. (1990) Transforming growth factors type beta 1 and beta 2 suppress rat astrocyte autoantigen presentation and antagonize hyperinduction of class II major histocompatibility complex antigen expression by interferon-gamma and tumor necrosis factor-alpha. *J Neuroimmunol* **27**(1): 41-7.
Schnitzer J. (1987) Retinal astrocytes: their restriction to vascularized parts of the mammalian retina. *Neurosci Lett* **78**(1): 29-34.
Schober A, Hertel R, Arumae U, Farkas L, Jaszai J, Krieglstein K, Saarma M & Unsicker K. (1999) Glial cell line-derived neurotrophic factor rescues target-deprived sympathetic spinal cord neurons but requires transforming growth factor-beta as cofactor in vivo. *J Neurosci* **19**(6): 2008-15.
Schulick AH, Taylor AJ, Zuo W, Qiu CB, Dong G, Woodward RN, Agah R, Roberts AB, Virmani R & Dichek DA. (1998) Overexpression of transforming growth factor beta1 in arterial endothelium causes hyperplasia, apoptosis, and cartilaginous metaplasia. *Proc Natl Acad Sci U S A* **95**(12): 6983-8.
Schulz MW, Chamberlain CG & McAvoy JW. (1996) Inhibition of transforming growth factor-beta-induced cataractous changes in lens explants by ocular media and alpha 2-macroglobulin. *Invest Ophthalmol Vis Sci* **37**(8): 1509-19.
Schuster N, Bender H, Rossler OG, Philippi A, Dunker N, Thiel G & Krieglstein K. (2003) Transforming growth factor-beta and tumor necrosis factor-alpha cooperate to induce apoptosis in the oligodendroglial cell line OLI-neu. *J Neurosci Res* **73**(3): 324-33.
Schuster N, Dunker N & Krieglstein K. (2002) Transforming growth factor-beta induced cell death in the developing chick retina is mediated via activation of c-jun N-terminal kinase and downregulation of the anti-apoptotic protein Bcl-X(L). *Neurosci Lett* **330**(3): 239-42.
Schuster N & Krieglstein K. (2002) Mechanisms of TGF-beta-mediated apoptosis. *Cell Tissue Res* **307**(1): 1-14.
Sellheyer K. (1990) Development of the choroid and related structures. *Eye* **4 (Pt 2)**: 255-61.

Sellheyer K & Spitznas M. (1988) The fine structure of the developing human choriocapillaris during the first trimester. *Graefes Arch Clin Exp Ophthalmol* **226**(1): 65-74.

Semenza GL. (2000) HIF-1: using two hands to flip the angiogenic switch. *Cancer Metastasis Rev* **19**(1-2): 59-65.

Seoane J, Le HV, Shen L, Anderson SA & Massague J. (2004) Integration of Smad and forkhead pathways in the control of neuroepithelial and glioblastoma cell proliferation. *Cell* **117**(2): 211-23.

Shalaby F, Rossant J, Yamaguchi TP, Gertsenstein M, Wu XF, Breitman ML & Schuh AC. (1995) Failure of blood-island formation and vasculogenesis in Flk-1-deficient mice. *Nature* **376**(6535): 62-6.

Shapley R. (1982) Parallel pathways in the mammalian visual system. *Ann N Y Acad Sci* **388**: 11-20.

Shi XH, He SZ & Zhao SH. (2004) [Expression and signification of pigment epithelium-derived factor in experimental choroidal neovascularization of rat]. *Zhonghua Yan Ke Za Zhi* **40**(6): 404-8.

Shi Y & Massague J. (2003) Mechanisms of TGF-beta signaling from cell membrane to the nucleus. *Cell* **113**(6): 685-700.

Shih SC, Ju M, Liu N, Mo JR, Ney JJ & Smith LE. (2003) Transforming growth factor beta1 induction of vascular endothelial growth factor receptor 1: mechanism of pericyte-induced vascular survival in vivo. *Proc Natl Acad Sci U S A* **100**(26): 15859-64.

Shima DT, Adamis AP, Ferrara N, Yeo KT, Yeo TK, Allende R, Folkman J & D'Amore PA. (1995) Hypoxic induction of endothelial cell growth factors in retinal cells: identification and characterization of vascular endothelial growth factor (VEGF) as the mitogen. *Mol Med* **1**(2): 182-93.

Shull MM & Doetschman T. (1994) Transforming growth factor-beta 1 in reproduction and development. *Mol Reprod Dev* **39**(2): 239-46.

Shweiki D, Itin A, Soffer D & Keshet E. (1992) Vascular endothelial growth factor induced by hypoxia may mediate hypoxia-initiated angiogenesis. *Nature* **359**(6398): 843-5.

Siegel PM & Massague J. (2003) Cytostatic and apoptotic actions of TGF-beta in homeostasis and cancer. *Nat Rev Cancer* **3**(11): 807-21.

Siegenthaler JA & Miller MW. (2004) Transforming growth factor beta1 modulates cell migration in rat cortex: effects of ethanol. *Cereb Cortex* **14**(7): 791-802.

Sigelman J, Ozanics, V. (1982) *Retina. In: Ocular Anatomy, Embryology, and Teratology.* Philadelphia: Harper and Row.

Silberstein GB & Daniel CW. (1987) Reversible inhibition of mammary gland growth by transforming growth factor-beta. *Science* **237**(4812): 291-3.

Simpson DA, Feeney S, Boyle C & Stitt AW. (2000) Retinal VEGF mRNA measured by SYBR green I fluorescence: A versatile approach to quantitative PCR. *Mol Vis* **6**: 178-83.

Smith JR, Choi D, Chipps TJ, Pan Y, Zamora DO, Davies MH, Babra B, Powers MR, Planck SR & Rosenbaum JT. (2007) Unique gene expression profiles of donor-matched human retinal and choroidal vascular endothelial cells. *Invest Ophthalmol Vis Sci* **48**(6): 2676-84.

Snodderly DM. (1995) Evidence for protection against age-related macular degeneration by carotenoids and antioxidant vitamins. *Am J Clin Nutr* **62**(6 Suppl): 1448S-61S.

Snodderly DM, Weinhaus RS & Choi JC. (1992) Neural-vascular relationships in central retina of macaque monkeys (Macaca fascicularis). *J Neurosci* **12**(4): 1169-93.

Sousa Vde O, Romao L, Neto VM & Gomes FC. (2004) Glial fibrillary acidic protein gene promoter is differently modulated by transforming growth factor-beta 1 in astrocytes from distinct brain regions. *Eur J Neurosci* **19**(7): 1721-30.

Sporn MB & Roberts AB. (1992) Transforming growth factor-beta: recent progress and new challenges. *J Cell Biol* **119**(5): 1017-21.

Sporn MB, Roberts AB, Shull JH, Smith JM, Ward JM & Sodek J. (1983) Polypeptide transforming growth factors isolated from bovine sources and used for wound healing in vivo. *Science* **219**(4590): 1329-31.

Sporn MB, Roberts AB, Wakefield LM & de Crombrugghe B. (1987) Some recent advances in the chemistry and biology of transforming growth factor-beta. *J Cell Biol* **105**(3): 1039-45.

Spranger J, Meyer-Schwickerath R, Klein M, Schatz H & Pfeiffer A. (1999) Deficient activation and different expression of transforming growth factor-beta isoforms in active proliferative diabetic retinopathy and neovascular eye disease. *Exp Clin Endocrinol Diabetes* **107**(1): 21-8.

Springer AD. (1999) New role for the primate fovea: a retinal excavation determines photoreceptor deployment and shape. *Vis Neurosci* **16**(4): 629-36.

Springer AD & Hendrickson AE. (2004a) Development of the primate area of high acuity. 1. Use of finite element analysis models to identify mechanical variables affecting pit formation. *Vis Neurosci* **21**(1): 53-62.

Springer AD & Hendrickson AE. (2004b) Development of the primate area of high acuity. 2. Quantitative morphological changes associated with retinal and pars plana growth. *Vis Neurosci* **21**(5): 775-90.

Springer AD & Hendrickson AE. (2005) Development of the primate area of high acuity, 3: temporal relationships between pit formation, retinal elongation and cone packing. *Vis Neurosci* **22**(2): 171-85.

Sprugel KH, McPherson JM, Clowes AW & Ross R. (1987) Effects of growth factors in vivo. I. Cell ingrowth into porous subcutaneous chambers. *Am J Pathol* **129**(3): 601-13.

Srinivasan Y, Lovicu FJ & Overbeek PA. (1998) Lens-specific expression of transforming growth factor beta1 in transgenic mice causes anterior subcapsular cataracts. *J Clin Invest* **101**(3): 625-34.

Steinle JJ & Granger HJ. (2003) Nerve growth factor regulates human choroidal, but not retinal, endothelial cell migration and proliferation. *Auton Neurosci* **108**(1-2): 57-62.

Steinle JJ, Pierce JD, Clancy RL, Smith PG. (2002) Increased ocular blood vessel numbers in sizes following chronic sympathectomy in rat. *Exp Eye Res* **74**:761-768.

Steinle JJ & Smith PG. (2002) Role of adrenergic receptors in vascular remodelling of the rat choroid. *Br J Pharmacol* **136**(5): 730-4.

Steinle JJ, Zamora DO, Rosenbaum JT & Granger HJ. (2005) Beta 3-adrenergic receptors mediate choroidal endothelial cell invasion, proliferation, and cell elongation. *Exp Eye Res* **80**(1): 83-91.

Stone J & Dreher Z. (1987) Relationship between astrocytes, ganglion cells and vasculature of the retina. *J Comp Neurol* **255**(1): 35-49.

Stone J, Itin A, Alon T, Pe'er J, Gnessin H, Chan-Ling T & Keshet E. (1995) Development of retinal vasculature is mediated by hypoxia-induced vascular endothelial growth factor (VEGF) expression by neuroglia. *J Neurosci* **15**(7 Pt 1): 4738-47.

Stone J, Maslim J, Valter-Kocsi K, Mervin K, Bowers F, Chu Y, Barnett N, Provis J, Lewis G, Fisher SK, Bisti S, Gargini C, Cervetto L, Merin S & Peer J. (1999) Mechanisms of photoreceptor death and survival in mammalian retina. *Prog Retin Eye Res* **18**(6): 689-735.

Stone J, Maslim, J. (1997) Mechanisms of Retinal Angiogenesis. *Progress in Retinal and Eye Research* **16**: 157-81.

Stone J, Sandercoe, T., Provis, J.P. (2006) *Mechanisms of the Formations and Survival of Retinal Blood Vessels in Ocular Angiogenesis.* Totowa, New Jersey.: Humana Press.

Sueishi K, Hata Y, Murata T, Nakagawa K, Ishibashi T & Inomata H. (1996) Endothelial and glial cell interaction in diabetic retinopathy via the function of vascular endothelial growth factor (VEGF). *Pol J Pharmacol* **48**(3): 307-16.

Tanaka T, Saika S, Ohnishi Y, Ooshima A, McAvoy JW, Liu CY, Azhar M, Doetschman T & Kao WW. (2004) Fibroblast growth factor 2: roles of regulation of lens cell proliferation and epithelial-mesenchymal transition in response to injury. *Mol Vis* **10**: 462-7.

Tanihara H, Yoshida M, Matsumoto M & Yoshimura N. (1993) Identification of transforming growth factor-beta expressed in cultured human retinal pigment epithelial cells. *Invest Ophthalmol Vis Sci* **34**(2): 413-9.

ten Dijke P, Geurts van Kessel AH, Foulkes JG & Le Beau MM. (1988) Transforming growth factor type beta 3 maps to human chromosome 14, region q23-q24. *Oncogene* **3**(6): 721-4.

Ten Dijke P, Goumans MJ, Itoh F & Itoh S. (2002) Regulation of cell proliferation by Smad proteins. *J Cell Physiol* **191**(1): 1-16.

ten Dijke P & Hill CS. (2004) New insights into TGF-beta-Smad signalling. *Trends Biochem Sci* **29**(5): 265-73.

ten Dijke P, Miyazono K & Heldin CH. (2000) Signaling inputs converge on nuclear effectors in TGF-beta signaling. *Trends Biochem Sci* **25**(2): 64-70.

Tolsma SS, Stack MS & Bouck N. (1997) Lumen formation and other angiogenic activities of cultured capillary endothelial cells are inhibited by thrombospondin-1. *Microvasc Res* **54**(1): 13-26.

Toru-Delbauffe D, Baghdassarian-Chalaye D, Gavaret JM, Courtin F, Pomerance M & Pierre M. (1990) Effects of transforming growth factor beta 1 on astroglial cells in culture. *J Neurochem* **54**(3): 1056-61.

Tripathi BJ, Tripathi, R.C., Livingston, A.M. (1991) The role of growth factors in the embryogenesis and differentiation of the eye. *Am J Anat* (192): 442.

Tripathi RC, Chan WF, Li J & Tripathi BJ. (1994a) Trabecular cells express the TGF-beta 2 gene and secrete the cytokine. *Exp Eye Res* **58**(5): 523-8.

Tripathi RC, Li J, Chan WF & Tripathi BJ. (1994b) Aqueous humor in glaucomatous eyes contains an increased level of TGF-beta 2. *Exp Eye Res* **59**(6): 723-7.

Tsukazaki T, Chiang TA, Davison AF, Attisano L & Wrana JL. (1998) SARA, a FYVE domain protein that recruits Smad2 to the TGFbeta receptor. *Cell* **95**(6): 779-91.

Unsicker K & Krieglstein K. (2000) Co-activation of TGF-ss and cytokine signaling pathways are required for neurotrophic functions. *Cytokine Growth Factor Rev* **11**(1-2): 97-102.

Unsicker K, Meier C, Krieglstein K, Sartor BM & Flanders KC. (1996) Expression, localization, and function of transforming growth factor-beta s in embryonic chick spinal cord, hindbrain, and dorsal root ganglia. *J Neurobiol* **29**(2): 262-76.

Valderrama-Carvajal H, Cocolakis E, Lacerte A, Lee EH, Krystal G, Ali S & Lebrun JJ. (2002) Activin/TGF-beta induce apoptosis through Smad-dependent expression of the lipid phosphatase SHIP. *Nat Cell Biol* **4**(12): 963-9.

van Driel D, Provis JM & Billson FA. (1990) Early differentiation of ganglion, amacrine, bipolar, and Muller cells in the developing fovea of human retina. *J Comp Neurol* **291**(2): 203-19.

Vaughan JM & Vale WW. (1993) Alpha 2-macroglobulin is a binding protein of inhibin and activin. *Endocrinology* **132**(5): 2038-50.

Vergeli M, mazzanti B, Ballerini C, Gran B, Amaducci L & Massacesi L. (1995) Transforming growth factor-beta 1 inhibits the proliferation of rat astrocytes induced by serum and growth factors. *J Neurosci Res* **40**(1): 127-33.

Wahl SM. (1992) Transforming growth factor beta (TGF-beta) in inflammation: a cause and a cure. *J Clin Immunol* **12**(2): 61-74.

Wahl SM, Hunt DA, Wakefield LM, McCartney-Francis N, Wahl LM, Roberts AB & Sporn MB. (1987) Transforming growth factor type beta induces monocyte chemotaxis and growth factor production. *Proc Natl Acad Sci U S A* **84**(16): 5788-92.

Waid DK & McLoon SC. (1995) Immediate differentiation of ganglion cells following mitosis in the developing retina. *Neuron* **14**(1): 117-24.

Wakefield LM, Winokur TS, Hollands RS, Christopherson K, Levinson AD & Sporn MB. (1990) Recombinant latent transforming growth factor beta 1 has a longer plasma half-life in rats than active transforming growth factor beta 1, and a different tissue distribution. *J Clin Invest* **86**(6): 1976-84.

Walcott JC & Provis JM. (2003) Muller cells express the neuronal progenitor cell marker nestin in both differentiated and undifferentiated human foetal retina. *Clin Experiment Ophthalmol* **31**(3): 246-9.

Wald G. (1945) Human Vision and the Spectrum. *Science* **101**(2635): 653-8.

Walicke PA & Baird A. (1988) Neurotrophic effects of basic and acidic fibroblast growth factors are not mediated through glial cells. *Brain Res* **468**(1): 71-9.

Wassle H, Dacey DM, Haun T, Haverkamp S, Grunert U & Boycott BB. (2000) The mosaic of horizontal cells in the macaque monkey retina: with a comment on biplexiform ganglion cells. *Vis Neurosci* **17**(4): 591-608.

Wassle H, Grunert U, Martin PR & Boycott BB. (1994) Immunocytochemical characterization and spatial distribution of midget bipolar cells in the macaque monkey retina. *Vision Res* **34**(5): 561-79.

Watanabe T & Raff MC. (1988) Retinal astrocytes are immigrants from the optic nerve. *Nature* **332**(6167): 834-7.

West H, Richardson WD & Fruttiger M. (2005) Stabilization of the retinal vascular network by reciprocal feedback between blood vessels and astrocytes. *Development* **132**(8): 1855-62.

Wieser R, Wrana JL & Massague J. (1995) GS domain mutations that constitutively activate T beta R-I, the downstream signaling component in the TGF-beta receptor complex. *Embo J* **14**(10): 2199-208.

Wilson SE, He YG, Weng J, Zieske JD, Jester JV & Schultz GS. (1994) Effect of epidermal growth factor, hepatocyte growth factor, and keratinocyte growth factor, on proliferation, motility and differentiation of human corneal epithelial cells. *Exp Eye Res* **59**(6): 665-78.

Wittwer CT, Ririe KM, Andrew RV, David DA, Gundry RA & Balis UJ. (1997) The LightCycler: a microvolume multisample fluorimeter with rapid temperature control. *Biotechniques* **22**(1): 176-81.

Wormstone IM, Tamiya S, Anderson I & Duncan G. (2002) TGF-beta2-induced matrix modification and cell transdifferentiation in the human lens capsular bag. *Invest Ophthalmol Vis Sci* **43**(7): 2301-8.

Wrana JL. (1998) TGF-beta receptors and signalling mechanisms. *Miner Electrolyte Metab* **24**(2-3): 120-30.

Wrana JL & Attisano L. (2000) The Smad pathway. *Cytokine Growth Factor Rev* **11**(1-2): 5-13.

Wrana JL, Attisano L, Carcamo J, Zentella A, Doody J, Laiho M, Wang XF & Massague J. (1992) TGF beta signals through a heteromeric protein kinase receptor complex. *Cell* **71**(6): 1003-14.

Wrana JL, Attisano L, Wieser R, Ventura F & Massague J. (1994) Mechanism of activation of the TGF-beta receptor. *Nature* **370**(6488): 341-7.

Wujek JR, Haleem-Smith H, Yamada Y, Lipsky R, Lan YT & Freese E. (1990) Evidence that the B2 chain of laminin is responsible for the neurite outgrowth-promoting activity of astrocyte extracellular matrix. *Brain Res Dev Brain Res* **55**(2): 237-47.

Wyss-Coray T, Feng L, Masliah E, Ruppe MD, Lee HS, Toggas SM, Rockenstein EM & Mucke L. (1995) Increased central nervous system production of extracellular matrix components and development of hydrocephalus in transgenic mice overexpressing transforming growth factor-beta 1. *Am J Pathol* **147**(1): 53-67.

Xiao BG, Bai XF, Zhang GX & Link H. (1997) Transforming growth factor-beta1 induces apoptosis of rat microglia without relation to bcl-2 oncoprotein expression. *Neurosci Lett* **226**(2): 71-4.

Xiao M & Hendrickson A. (2000) Spatial and temporal expression of short, long/medium, or both opsins in human fetal cones. *J Comp Neurol* **425**(4): 545-59.

Yamanaka R, Ogata N, Yamamoto C, Matsushita M, Matsuzaki K, Uyama M & Matsumura M. (2002) Expression of transforming growth factor-beta receptors in normal rat retina and experimental choroidal neovascularization. *Jpn J Ophthalmol* **46**(5): 525-32.

Yamashita H, ten Dijke P, Franzen P, Miyazono K & Heldin CH. (1994) Formation of hetero-oligomeric complexes of type I and type II receptors for transforming growth factor-beta. *J Biol Chem* **269**(31): 20172-8.

Yang EY & Moses HL. (1990) Transforming growth factor beta 1-induced changes in cell migration, proliferation, and angiogenesis in the chicken chorioallantoic membrane. *J Cell Biol* **111**(2): 731-41.

Yang XJ. (2004) Roles of cell-extrinsic growth factors in vertebrate eye pattern formation and retinogenesis. *Semin Cell Dev Biol* **15**(1): 91-103.

Yeh HJ, Ruit KG, Wang YX, Parks WC, Snider WD & Deuel TF. (1991) PDGF A-chain gene is expressed by mammalian neurons during development and in maturity. *Cell* **64**(1): 209-16.

Yi X, Mai LC, Uyama M & Yew DT. (1998) Time-course expression of vascular endothelial growth factor as related to the development of the retinochoroidal vasculature in rats. *Exp Brain Res* **118**(2): 155-60.

Yoshimura N, Matsumoto M, Shimizu H, Mandai M, Hata Y & Ishibashi T. (1995) Photocoagulated human retinal pigment epithelial cells produce an inhibitor of vascular endothelial cell proliferation. *Invest Ophthalmol Vis Sci* **36**(8): 1686-91.

Young RW. (1985) Cell proliferation during postnatal development of the retina in the mouse. *Brain Res* **353**(2): 229-39.

Zhang X, Hachida M, Lu H, Hoshi H & Koyanagi H. (1999) Effect of 15-deoxyspergualine on coronary arteriosclerosis and platelet-derived growth factor-A mRNA expression in the transplanted heart. *Transplant Proc* **31**(3): 1706-9.

Zhang XM & Yang XJ. (2001) Temporal and spatial effects of Sonic hedgehog signaling in chick eye morphogenesis. *Dev Biol* **233**(2): 271-90.

Zhang Y, Feng X, We R & Derynck R. (1996) Receptor-associated Mad homologues synergize as effectors of the TGF-beta response. *Nature* **383**(6596): 168-72.

Zhang Y, Feng XH & Derynck R. (1998) Smad3 and Smad4 cooperate with c-Jun/c-Fos to mediate TGF-beta-induced transcription. *Nature* **394**(6696): 909-13.

Zhang Y & Stone J. (1997) Role of astrocytes in the control of developing retinal vessels. *Invest Ophthalmol Vis Sci* **38**(9): 1653-66.

Zhao S & Overbeek PA. (1999) Tyrosinase-related protein 2 promoter targets transgene expression to ocular and neural crest-derived tissues. *Dev Biol* **216**(1): 154-63.

Zhao S & Overbeek PA. (2001a) Elevated TGFbeta signaling inhibits ocular vascular development. *Dev Biol* **237**(1): 45-53.

Zhao S & Overbeek PA. (2001b) Regulation of choroid development by the retinal pigment epithelium. *Mol Vis* **7**: 277-82.

Zhou L, Dey CR, Wert SE & Whitsett JA. (1996) Arrested lung morphogenesis in transgenic mice bearing an SP-C-TGF-beta 1 chimeric gene. *Dev Biol* **175**(2): 227-38.

Zhu M, Madigan MC, van Driel D, Maslim J, Billson FA, Provis JM & Penfold PL. (2000a) The human hyaloid system: cell death and vascular regression. *Exp Eye Res* **70**(6): 767-76.

Zhu Y, Roth-Eichhorn S, Braun N, Culmsee C, Rami A & Krieglstein J. (2000b) The expression of transforming growth factor-beta1 (TGF-beta1) in hippocampal neurons: a temporary upregulated protein level after transient forebrain ischemia in the rat. *Brain Res* **866**(1-2): 286-98.

Zubilewicz A, Hecquet C, Jeanny JC, Soubrane G, Courtois Y & Mascarelli F. (2001) Two distinct signalling pathways are involved in FGF2-stimulated proliferation of choriocapillary endothelial cells: a comparative study with VEGF. *Oncogene* **20**(12): 1403-13.